2007

FUNCTIONALIZED POLYMERIC MEMBRANES FOR BIOSEPARATION AND BIOCATALYSIS

Saurav Datta
University of Kentucky, sdatt0@engr.uky.edu

STUDENT AGREEMENT:

I represent that my thesis or dissertation and abstract are my original work. Proper attribution has been given to all outside sources. I understand that I am solely responsible for obtaining any needed copyright permissions. I have obtained needed written permission statement(s) from the owner(s) of each third-party copyrighted matter to be included in my work, allowing electronic distribution (if such use is not permitted by the fair use doctrine) which will be submitted to UKnowledge as Additional File.

I hereby grant to The University of Kentucky and its agents the irrevocable, non-exclusive, and royalty-free license to archive and make accessible my work in whole or in part in all forms of media, now or hereafter known. I agree that the document mentioned above may be made available immediately for worldwide access unless an embargo applies.

I retain all other ownership rights to the copyright of my work. I also retain the right to use in future works (such as articles or books) all or part of my work. I understand that I am free to register the copyright to my work.

REVIEW, APPROVAL AND ACCEPTANCE

The document mentioned above has been reviewed and accepted by the student's advisor, on behalf of the advisory committee, and by the Director of Graduate Studies (DGS), on behalf of the program; we verify that this is the final, approved version of the student's thesis including all changes required by the advisory committee. The undersigned agree to abide by the statements above.

Saurav Datta, Student

Dr. D. Bhattacharyya, Major Professor

Dr. B. Knutson, Director of Graduate Studies

ABSTRACT OF DISSERTATION

Saurav Datta

The Graduate School

University of Kentucky

2007

FUNCTIONALIZED POLYMERIC MEMBRANES FOR BIOSEPARATION AND BIOCATALYSIS

ABSTRACT OF DISSERTATION

A dissertation submitted in partial fulfillment of the
requirements for the degree of Doctor of Philosophy in the
College of Engineering
at the University of Kentucky

By
Saurav Datta

Lexington, Kentucky

Director: Dr. Dibakar Bhattacharyya, Alumni Professor of Chemical Engineering

Lexington, Kentucky

2007

ABSTRACT OF DISSERTATION

FUNCTIONALIZED POLYMERIC MEMBRANES
FOR BIOSEPARATION AND BIOCATALYSIS

Functionalized polymeric membrane based techniques are becoming increasingly popular in biotechnology, food and pharmaceutical industries due to their versatility and hydrodynamic benefits over traditional materials and methods. This research work has been directed towards the development of functionalized polymeric membranes, extensive experimental and theoretical analyses of some of the fundamental aspects of accessibility, membrane fouling and enzyme catalysis, and applications in affinity based bioseparation and biocatalysis. In this research work, the impact of different types of functionalization techniques, such as functionalization of different membrane materials, covalent and electrostatic immobilization, on interaction of various biomolecules and active sites in membrane has been studied in detail.

Avidin was used as model biomolecule, and covalently immobilized within acyl anhydride derivatized nylon based membrane. Quantification of the accessibility of covalently immobilized avidin sites was carried out by model biotinylated probe molecules, such as biotin 4-amidobenzoic acid and biotinylated-BSA. This study has been further extended to separate and purify a target protein, HIV-Tat, from a complex mixture of proteins (97-99 % unwanted protein) using avidin-biotin affinity interaction. It has been demonstrated that covalent immobilization of avidin in membranes reduces the accessibility of active sites for probe molecules. Accessibility decreases further for the biotinylated target protein present in the mixture of other unwanted proteins. Affinity based membrane separation of proteins is also associated with decrease in permeate flux due to fouling in membrane structure. Fouling in the membrane has been discussed by analyzing the characteristics of adsorbed protein layer in membrane.

In order to improve the accessibility and fouling behavior of affinity separation of Tat protein, a pre-filtration step has been introduced prior to affinity separation. Significant enhancement in accessibility and reduction in fouling has been observed for pre-filtered cases as it removes unwanted proteins prior to affinity interaction. Contribution of the pre-filtration step in reduction of fouling has been elucidated by

simple model equations. Improvement in accessibility and fouling behavior reflects in higher separation efficiency (protein recovery) and lower processing time for the pre-filtered cases. Quality of membrane purified Tat protein was examined by different analytical techniques, such as SDS-PAGE, Western Blot and biotin analysis, and then compared with that purified by traditional packed-bead column chromatography. It has been demonstrated that membrane based technique was able to isolate superior quality of pure monomeric Tat protein compare to column chromatographic technique.

The other study carried out as a part of this dissertation, has involved development of high capacity, highly active, stable and reusable functionalized membrane domains for electrostatic immobilization of enzymes. Glucose oxidase (GOX) was used as a model enzyme to study the oxidation of glucose to gluconic acid and hydrogen peroxide under convective flow condition. Two different approaches of functionalization of membranes have been presented. In the first approach, alternative electrostatic attachment of cationic and anionic polyelectrolytes was carried out using Layer-By-Layer (LBL) assembly technique within a functionalized nylon based membrane. In the second one, a hydrophobic PVDF membrane was functionalized by in-situ polymerization of acrylic acid. Kinetics of glucose oxidation, effect of pH and flow rate on the activity of GOX was discussed. A comparative study was presented between the activity of free GOX, electrostatically immobilized GOX and covalently immobilized GOX, along with the advantage of convective mode of operation over soaking mode. A novel study has also been conducted on detachment and reattachment of GOX in the same membrane matrix.

Further study has been directed towards implementation of the above mentioned immobilized enzymatic system for oxidative dechlorination of chloro-organics. A first time attempt was made to use a 2-stack functionalized membranes system for simultaneous enzymatic production of hydrogen peroxide in first membrane, and oxidative dechlorination of 2, 4, 6-trichlorophenol (TCP) in the Fe^{+2} immobilized (by ion exchange) second membrane by Fenton reaction. The technique was efficient in destruction of TCP as evident from the overall dechlorination of 70-80 %. This technique provides additional benefit of reusing the same membrane matrices by reattaching fresh GOX and Fe^{+2}.

KEYWORDS: Functionalized Membranes, Affinity Based Bioseparation, HIV-TAT Protein, Biocatalysis, Glucose Oxidase

SAURAV DATTA

12/13/2007

FUNCTIONALIZED POLYMERIC MEMBRANES FOR BIOSEPARATION AND BIOCATALYSIS

By

Saurav Datta

DR. D. BHATTACHARYYA

Director of Dissertation

DR. B. KNUTSON

Director of Graduate Studies

12/13/2007

Date

RULES FOR THE USE OF DISSERTATIONS

Unpublished dissertations submitted for the Doctor's degree and deposited in the University of Kentucky Library are as a rule open for inspection, but are to be used only with due regard to the rights of the authors. Bibliographical references may be noted, but quotations or summaries of parts may be published only with the permission of the author, and with the usual scholarly acknowledgements.

Extensive copying or publication of the dissertation in whole or in part also requires the consent of the Dean of the Graduate School of the University of Kentucky.

A library that borrows this dissertation for use by its patrons is expected to secure the signature of each user.

Name	Date

DISSERTATION

Saurav Datta

The Graduate School

University of Kentucky

2007

FUNCTIONALIZED POLYMERIC MEMBRANES FOR BIOSEPARATION AND BIOCATALYSIS

DISSERTATION

A dissertation submitted in partial fulfillment of the
requirements for the degree of Doctor of Philosophy in the
College of Engineering
at the University of Kentucky

By
Saurav Datta

Lexington, Kentucky

Director: Dr. Dibakar Bhattacharyya, Alumni Professor of Chemical Engineering

Lexington, Kentucky

2007

ACKNOWLEDGEMENTS

I would like to express heartfelt gratitude to my advisor Prof. Dibakar Bhattacharyya for his guidance, support and motivation during my PhD research studies. His ingenious ideas, unending passion and dedication to the field of membrane science & biotechnology have left an indelible impression in me. Thanks to my PhD dissertation committee members, Prof. A. Butterfield, Prof. B. Knutson, Dr. C. Crofcheck and Dr. J. Zack Hilt for their technical inputs.

A special thanks to our DGS, Prof. Knutson for her invaluable help in transferring my wife from Colorado State University.

I would also like to express my gratitude to all of the faculty members at University of Calcutta and Indian Institute of Technology, Kanpur for giving me the basic knowledge of Chemical Engineering and for motivating me to pursue higher study.

I would like to thank Philip D. Ray, Research Analyst, Department of Anatomy and Neurobiology and John May, Research Analyst, Environmental Research and Training Laboratory (ERTL) for their help in different analyses. Special thanks to Dr. Sumita Raha and Ms. Robin Ehrick for helping in SDS-PAGE and Western Blot analyses.

I would like to thank my colleagues in DB's lab, Aaron, Abhay, Ajay, Andrew, Dave, Deepak, Jian, Morgan, Noah, Peter, Scott, Tee, Vasile and Yongchao for their support and maintaining nice working atmosphere. Thanks to Caitlyn Cecil and Melody Morris for their respective experimental contributions as a part of NSF-REU program. I would also like to thank Mr. Bruce Cole and Mr. Jerome Vice for their help. Thanks to all of my friends for making my stay at Lexington memorable.

I would also like to mention the contributions of my wife, Gargi, my mother, Namita Datta, my father, Late Sankar Datta, my elder brother, Sudip Datta and all of my other family members in the form of their unconditional love and support.

Finally, I would like to acknowledge Dr. A. Nath, Johns Hopkins University, Dr. Michal J. Toborek, Department of Surgery, University of Kentucky, and National Institute of Health (NIH) for financial support in the bioseparation project. I would also like to acknowledge National Institute of Environmental Health Science (NIEHS-SBRP) for financial support in the biocatalysis project.

Table of Contents

ACKNOWLEDGEMENTS iii
Table of Contents iv
List of Tables viii
List of Figures x
List of Files xvii
Chapter 1 Introduction 1
1.1 Functionalized membranes for affinity based bio-separation: research objectives 1
1.2 Functionalized membranes for enzymatic catalysis: research objectives 3
Chapter 2 Background 5
2.1 Membrane and membrane based processes 5
2.2 Functionalized membranes 9
2.2.1 Development of functionalized polymeric membranes 9
2.2.2 Further attachment of groups/molecules 14
2.2.3 Applications of functionalized membranes 18
2.3 Bioseparation 19
2.3.1 Proteins 19
2.3.2 TAT protein 20
2.3.3 Column chromatographic separation of proteins 22
2.3.4 Membrane based separation of proteins 25
2.4 Biocatalysis 33
2.4.1 Enzyme 33
2.5 Concluding remarks 38
Chapter 3 Experimental and Analytical Procedures 39
3.1 Equipments 39
3.2 Materials 39
3.2.1 Membranes 39
3.2.2 Chemicals 40
3.3 Analytical procedures 41
3.4 Functionalization of membranes 43

3.4.1 Covalent immobilization of avidin in anhydride activated nylon membrane 43
3.4.2 Functionalization of anhydride activated nylon membranes based on LBL technique for electrostatic immobilization of GOX..... 45
3.4.3 Functionalization of PVDF membrane by in-situ polymerization of acrylic acid for electrostatic immobilization of GOX 48
3.4.4 Functionalization of other unactivated base membranes 50
3.5 Separation and purification of HIV-Tat protein in avidin functionalized membranes 55
3.5.1 Accessibility of covalently immobilized avidin sites in nylon membrane by biotin moieties present in different species..... 55
3.5.2 Affinity separation of HIV-Tat protein from bacterial lysate (BL) 56
3.6 Effect of pre-filtration on affinity membrane separation of Tat 63
3.6.1 Pre-filtration..... 63
3.6.2 Affinity membrane separation of Tat from pre-filtered BL feed..... 63
3.7 Enzymatic oxidation of glucose by electrostatically immobilized GOX in LBL assembled nylon membrane and functionalized PVDF membrane.. 64
3.7.1 Activity study of electrostatically immobilized GOX in LBL functionalized nylon membrane..... 64
3.7.2 Activity study of electrostatically immobilized GOX in functionalized PVDF membrane 66
Chapter 4 Functionalization of Membranes 68
4.1 Results and discussion 68
4.1.1 Covalently immobilized avidin in anhydride activated nylon membrane 68
4.1.2 Electrostatically immobilized GOX in LBL assembled nylon membrane and functionalized PVDF membrane..... 69
4.1.3 Determination of extent of functionalization in other membranes (RC, CA, nylon) 81
4.2 Conclusions..... 84
Chapter 5 Affinity Based Separation of HIV-TAT Protein: Analysis of Accessibility of Avidin Sites and Fouling in Membranes 85
5.1 Results and discussion 86
5.1.1 Accessibility of covalently immobilized avidin sites 86
5.1.2 Study of associated fouling in avidin immobilized nylon membrane..... 103
5.1.3 Separation and purification of Tat 118
5.2 Conclusions..... 130

Chapter 6 Enzymatic Oxidation of Glucose to Gluconic Acid and H_2O_2 by Electrostatically Immobilized Glucose Oxidase in Functionalized Membranes 132
6.1 Results and discussion 132
6.1.1 Steady state experiment 132
6.1.2 Importance of O_2 134
6.1.3 Kinetics of glucose oxidation by GOX 134
6.1.4 Effect of residence time, i.e., flow rate 145
6.1.5 Effect of pH 148
6.1.6 Stability 150
6.1.7 Reusability of membrane matrix by detachment and reattachment of GOX 150
6.2 Conclusions 152
Chapter 7 Oxidative Dechlorination of Trichlorophenol (TCP) by Functionalized 2-Stack Membranes Containing Electrostatically Immobilized GOX and Fe^{+2} 153
7.1 Introduction and background studies 153
7.2 Experimental and analytical procedures 154
7.2.1 Equipment and materials 154
7.2.2 Analytical procedures 155
7.2.3 Electrostatic immobilization of GOX in functionalized PVDF membrane 156
7.2.4 Immobilization of Fe^{+2} in functionalized PVDF membrane by ion exchange 156
7.2.5 Experimental procedure for dechlorination of TCP 157
7.3 Results and discussions 157
7.3.1 Electrostatically immobilized GOX in functionalized PVDF membrane 157
7.3.2 Fe^{+2} in functionalized PVDF membrane 158
7.3.3 Dechlorination of TCP 158
7.4 Conclusions 164
Chapter 8 Conclusions 165
8.1 Overall scientific and technological advancements 165
8.2 Specific accomplishments 166
8.2.1 Functionalized membranes for affinity based bioseparation 166
8.2.2 Functionalized membranes for biocatalysis 167
Nomenclature 168

References.. 173
Vita... 202

List of Tables

Table 2.1 A comparative study of types of solid matrix used and kinetic parameters obtained for different GOX immobilization techniques reported in literature. MUDA = mercaptoundecanoic acid, EDC = N-ethyl-N'-(3-dimethylaminopropyl) carbodiimide, NHS = N-hydroxysuccinimide, PMMA = poly(methylmethacrylate), PSt = poly(styrene), GMA = Glycidolmethacrylate, APTES = 3-aminopropyltrimethoxysilane, PAA = poly(acrylic acid), PVDF = polyvinylidene fluoride, AAc = acrylic acid, CA = cellulose acetate 37

Table 4.1 Characterization of LBL assembled nylon membrane by calculating the amount of repeat units immobilized in subsequent layers. Molecular weight of repeat units of different polyelectrolytes is as follows: PLL 164.5, PSS 206, and PAH 93.5. External membrane area = 13.2 cm^2, Membrane thickness = 165 μm, pH = 6 72

Table 4.2 Characterization of functionalized PVDF membrane by calculating the amount of repeat units immobilized in subsequent domains. Molecular weight of repeat units of different polyelectrolytes / polymers is as follows: PAH 93.5 and PAA 72. External membrane area = 13.2 cm^2, Membrane thickness = 165 μm, pH = 6 75

Table 4.3 Amount of active groups attached for functionalization of different base membranes, such as regenerated cellulose (RC), cellulose acetate (CA) and nylon. ECH = epichlorohydrin, BDDE = 1, 4-butanediol diglycidol ether, CDI = 1, 1'-carbonyldiimidazole, PABA = para-aminobenzoic acid 82

Table 5.1 Accessibility of avidin sites for the permeation of biotin 4-amidobenzoic acid (BABA) through avidin immobilized nylon membrane (Pore dia. = 0.45 μm) at 0.34 bar. Single membrane was used for this case..... 90

Table 5.2 Accessibility of avidin sites for permeation of biotinylated-BSA (BBSA), BBSA + Gamma Globulin (GG, Non-biotinylated) and Tat in unfiltered bacterial lysate (UNF BL) through avidin immobilized nylon membrane (Pore dia. = 0.45 μm) at 0.34 bar. Single membrane was used for BBSA and BBSA+GG, whereas, 4-stack membranes were used for Tat in BL 94

Table 5.3 Effect of pre-filtration (UF and MF) on BL feed. Concentration of total protein in pre-filtration feed = 1120 μg/ml. Concentration of total biotin (exposed + entangled) in pre-filtration feed = 3.8 x 10^{-3} μmole/ml (i.e. 32 μg/ml Tat). UF: 100 KDa MWCO regenerated cellulose membrane, ΔP = 1.36 bar, MF: 0.1 μm pore size hydrophilized PVDF membrane, ΔP = 0.34 bar 98

Table 5.4 Effect of pre-filtration on accessibility of avidin sites for BL permeation. For proper comparison, results of Table 5.2 are reproduced here along with the MF BL and UF BL results. Single membrane was used for BBSA and BBSA+GG, whereas, 4-stack membranes were used for Tat in BL..... 102

Table 5.5 Calculated resistance and thickness of protein layer formed due to the permeation of BSA, Biotinylated-BSA (BBSA), BBSA + Gamma Globulin (GG) and UNF BL feed through avidin immobilized membrane (Pore dia. = 0.45 μm) at 0.34 bar. R_P = Resistance of protein layer, δ_p= Effective thickness of protein layer 105

List of Figures

Figure 2.1 Different operating streams involved in a typical membrane separation process 6

Figure 2.2 Filtration spectrum describing the classification of membrane processes based on diameter of the pore of membrane. Figure also indicates the proper choice of membrane process in order to separate some common molecules, based solely on size. RO = Reverse osmosis, NF = nanofiltration, UF = ultrafiltration, MF = microfiltration... 7

Figure 2.3 Chemical structures of building blocks of different membranes used in this research study..... 11

Figure 2.4 Different schemes of immobilization of biomolecules in membrane 15

Figure 2.5 Primary structure of HIV-Tat_{1-72} protein showing the amino acid residues. Figure also indicates the salient features of Tat in terms of structure, isolation and further therapeutic applications 21

Figure 2.6 Different types of column chromatographic separation of proteins..... 23

Figure 2.7 Classification of membrane separation of proteins based on size, charge and interaction 26

Figure 2.8 (a) Structure of biotin and (b) partial primary structure of avidin showing the tryptophan (Trp) amino acid residues. 29

Figure 2.9 Enzymatic oxidation of glucose to gluconolactone by Glucose Oxidase (GOX). Gluconolactone immediately converts to gluconic acid. Cofactor of GOX, FAD, first converts to reduced form, $FADH_2$, and then oxidized to FAD by O_2 35

Figure 3.1 Reaction scheme for covalent immobilization of primary amine group containing molecule ($:NH_2\text{-}R'$) in activated nylon membrane. ($:NH_2\text{-}R''$) could be avidin or poly(L-Lysine) or GOX..... 44

Figure 3.2 Schematic of formation of 7-layers of polyelectrolytes inside an anhydride activated nylon based membrane using Layer-By-Layer (LBL) technique followed by electrostatic immobilization of GOX..... 46

Figure 3.3 Schematic of functionalized PVDF membrane by PAA (shown here as a single chain for illustration purposes) and electrostatic attachment of PAH, followed by electrostatic immobilization of GOX..... 49

Figure 3.4 Reaction schemes showing functionalization of unactivated base membranes by different active groups. CA: Cellulose Acetate, RC: Regenerated Cellulose, ECH:

Epichlorohydrin, CDI: 1, 1'-carbonyldiimidazole, BDDE: 1, 4-butanediol diglycidol ether 51

Figure 3.5 Reaction of carbonyl, carbonyl imidazole and epoxide activated membranes with primary amine containing molecules ($R\text{-}NH_2$), such as PABA, avidin, PAH, etc. .. 53

Figure 3.6 Schematics of basic steps involved in affinity based membrane separation of a target protein from mixture of proteins..... 57

Figure 3.7 Schematic of separation of Tat protein from bacterial lysate using avidin-biotin interaction in a functionalized membrane pore. Biotinylated-Tat (Bio-F-Tat) forms a complex (Tat-F-Bio-Av-Mem) with avidin immobilized membrane (Av-Mem). Tat is then isolated by cleaving the Tat-Fusion protein bond with Factor X_a 59

Figure 3.8 Experimental steps for the separation and purification of Tat from Bacterial Lysate (BL) using avidin-biotin interaction in functionalized stacked membranes. In few experiments, a pre-filtration step (shown as a dotted box) was introduced to remove unwanted proteins and impurities prior to the affinity separation 60

Figure 4.1 Calculated cumulative thickness of layers after electrostatic immobilization of polyelectrolytes inside nylon membrane pore. Hagen Poiseuiile's equation was used to calculate layer thickness. Inset Figure shows the decrease in permeability due to formation of layers inside membrane pores. Pore radius of pure nylon membrane = 225 nm, water permeability of pure nylon membrane = 570×10^{-4} cc/cm^2-s-bar, permeability after GOX immobilization = 52×10^{-4} cc/cm^2-s-bar, external membrane area = 13.2 cm^2, membrane thickness = 165 μm, pH of water used for permeability measurement = 6, NaCl concentration used to form layers = 0.25 M..... 73

Figure 4.2 Effect of functionalization on PVDF membrane as depicted by the permeate flux vs pressure curve. Pore radius of pure PVDF membrane = 225 nm, pore radius of PVDF-PAA-PAH-GOX membrane = 100 nm. Water (pH 6) permeability values for different steps of functionalized membrane are given by the slope of the curves. External membrane area = 13.2 cm^2, membrane thickness = 125 μm 77

Figure 4.3 Effect of pH on permeate water flux for PAA-functionalized PVDF membrane in Na-form. Flux was normalized with maximum flux for this experiment (330×10^{-4} cc/cm^2-s) at a pH of 2.5 and pressure of 1.38 bar. Pore radius of pure PVDF membrane = 225 nm, pore radius of PVDF-PAA-PAH-GOX membrane = 100 nm, external membrane area = 13.2 cm^2, membrane thickness = 125 μm 78

Figure 4.4 SEM images of cross section of (a) unmodified PVDF membrane and (b) PAA-functionalized PVDF membrane with immobilized Fe^{+2}. The figure also shows SEM-EDX analysis of different elements present in (c) virgin PVDF membrane and (d) PAA-functionalized PVDF membrane with immobilized Fe^{+2} 80

Figure 5.1 Schematic of different ways of attachment of avidin molecules in functionalized membranes and its effect on interaction with biotin moieties. (a) avidin in homogeneous phase. Four sites are available for biotin, (b) covalently immobilized avidin in membrane, (c) multiple attachment of avidin molecules by different amine groups, (d) blockage of avidin sites by next layer of immobilized avidin due to protein-protein interaction, and (e) blockage of avidin sites by big molecules of protein (biotinylated as well as non-biotinylated)..... 87

Figure 5.2 Comparison of breakthrough curves for permeation of different biotin 4-amidobenzoic acid (BABA) solutions through avidin immobilized (3.8×10^{-2} - 5.1×10^{-2} μmoles / ml bed volume) single nylon membrane (Pore dia. = 0.45 μm) at 0.34 bar. Avidin functionalized membrane permeability = 4×10^{-3}- 7×10^{-3} cm^3/cm^2.s.bar. C_P = conc. of biotin in permeate, C_f = conc. of biotin in feed 88

Figure 5.3 Comparison of breakthrough curves for permeation of different biotinylated-BSA (BBSA) solutions through avidin immobilized (3.8×10^{-2} - 5.1×10^{-2} μmoles/ml bed volume) single nylon membrane (Pore dia. = 0.45 μm) at 0.34 bar. Avidin functionalized membrane permeability = 5×10^{-3} – 7×10^{-3} cm^3/cm^2.s.bar. C_P = Conc. of biotin in permeate, C_f = Conc. of biotin in feed 92

Figure 5.4 Comparison of accessibility of the avidin sites (3.8×10^{-2} - 5.1×10^{-2} μmoles/ml bed volume) immobilized in single nylon membrane (Pore dia. = 0.45 μm) for different biotinylated-BSA (BBSA) solutions at 0.34 bar. Avidin functionalized membrane permeability = 5×10^{-3} - 7×10^{-3} cm^3/cm^2.s.bar 93

Figure 5.5 Comparison of normalized accessibility vs. biotin permeated for biotin 4-amidobenzoic acid (BABA), biotinylated-BSA (BBSA) and BBSA + Gamma Globulin (GG, non-biotinylated protein) through avidin immobilized (3.8×10^{-2} - 5.1×10^{-2} μmoles/ml bed volume) single nylon membrane (0.45 μm) at 0.34 bar. Avidin functionalized membrane permeability = 4×10^{-3} - 5×10^{-3} cm^3/cm^2.s.bar 96

Figure 5.6 Normalized flux vs cumulative volume for pre-filtration experiments. UF: 100KDa MWCO regenerated cellulose membrane, ΔP = 1.36 bar, Permeability = 4×10^{-3} cm^3/cm^2-s-bar. MF: 0.1 μm pore size hydrophilized PVDF membrane, ΔP = 0.34 bar, Permeability = 20×10^{-3} cm^3/cm^2-s-bar. Dotted curves represent trend lines for experimental data. Volume of pre-filtration feeds = 300 cm^3 99

Figure 5.7 SDS-PAGE images of feed and permeate streams of pre-filtration experiments prior to affinity separation. Total protein concentration in pre-filtration feed (UF/MF F) = 1120 μg/ml, in microfiltration permeate (MF P) = 465 ± 10 μg/ml, and in ultrafiltration permeate (UF P) = 155 ± 5 μg/ml..... 100

Figure 5.8 Comparison of normalized flux (J_v/J_{v0}) for permeation of BSA, BBSA, BBSA + gamma globulin (GG) and bacterial lysate (BL) through avidin immobilized nylon membranes (pore dia. = 0.45 μm) at 0.34 bar. Normalized flux = ratio of flux at any time of permeation to initial flux. J_{v0} = 14×10^{-4} – 24×10^{-4} cm^3/cm^2.s..... 104

Figure 5.9 Comparison of effective thickness of protein layer formed within the membrane while permeating BSA, BBSA, BBSA + Gamma Globulin (GG) and bacterial lysate (BL) through avidin immobilized nylon membranes (Pore dia. = 0.45 μm) at 0.34 bar 109

Figure 5.10 SEM images (6K magnification) of the surface of the nylon based MF membranes (Pore dia. = 0.45 μm). (a) Bare Immunodyne membrane, (b) Topmost membrane of the 4-stack nylon membranes matrix through which UNF BL1, wash buffer and cleavage buffer were permeated at 0.34 bar..... 110

Figure 5.11 Schematic of adsorption of protein (a) both within the pores and on the external surface of the membranes: combined model, and (b) only within the pores of the membranes: standard model. The thickness of adsorbed protein layer formed at a distance r from the center of pore at any time interval of Δt is Δr 112

Figure 5.12 Kinetics of total protein adsorption for UNF BL2 feed. The solid curves represent the best fitted values according to Equation 5.13 for total adsorption and according to Equation 5.14 for surface adsorption, respectively..... 114

Figure 5.13 Normalized flux vs cumulative permeate volume for the affinity separation of different BL feeds through avidin-immobilized 4-stack Immunodyne membranes at 0.34 bar. The solid curves represent the Standard Blocking Model calculated values according to Equation 5.18, whereas, the broken curve represents the Combined Model calculated values according to Equation 5.11. UNF BL2 = Unfiltered BL2, UF BL = Ultrafiltered BL, MF BL = Microfiltered BL..... 117

Figure 5.14 Effect of dilution on free available Tat by diluting bacterial lysate with 0.1 M (0.1×10^3 μmoles/ml) NaCl..... 119

Figure 5.15 Effect of ionic strength on free available Tat by diluting bacterial lysate (dilution factor = 10) with different concentrations of NaCl..... 120

Figure 5.16 Characteristic flux vs. time curve for permeation of unfiltered bacterial lysate (UNF BL2), wash buffer 1 (WB 1), wash buffer 2 (WB 2) and cleavage buffer (CB) through avidin immobilized 4-stack functionalized membranes. Permeate flux is normalized by dividing with initial flux through avidin immobilized 4-stack membranes. 122

Figure 5.17 Concentration of total protein in permeate for different solution streams in affinity separation of Tat from UNF BL2 feed through 4-stack avidin immobilized functionalized membranes. UNF BL2 = unfiltered bacterial lysate with 1120 μg/ml total protein concentration in feed, WB 1 = wash buffer 1, WB 2 = wash buffer 2 and CB = cleavage buffer..... 123

Figure 5.18 SDS-PAGE images of different streams for the separation of Tat from bacterial lysate (UNF BL2) using avidin-biotin interaction in avidin immobilized 4-stack

nylon membranes (F = Feed, P = Permeate, R = Retentate, WB = wash buffer, CB = cleavage buffer, E = Tat eluate). Conc. of total protein in feed = 1120 μg/ml 124

Figure 5.19 SDS-PAGE images of purified Tat eluates separated from bacterial lysate (BL) using different techniques. E = Tat eluate, UNF BL1 = unfiltered BL 1, UNF BL2 = unfiltered BL 2, MF BL = microfiltered BL, UF BL = ultrafiltered BL, CC = column chromatography, RC ECH = Tat separated using RC-ECH functionalized membrane . 126

Figure 5.20 Western Blot analysis of different purified Tat eluates from bacterial lysate (BL). E = Tat eluates, UNF BL1 = unfiltered BL 1, UNF BL2 = unfiltered BL 2, MF BL = microfiltered BL, UF BL = ultrafiltered BL, CC = column chromatography 127

Figure 5.21 Comparison of total processing time for unfiltered BL feed (UNF BL2 feed), microfiltered BL feed (MF BL feed) and ultrafiltered BL feed (UF BL feed) in separation and purification of Tat from BL. For all cases, external membrane area = 33.2 cm^2, volume of BL feed = 250 cm^3 with 95 % permeate water recovery; Amount of biotinylated-Tat fed = 0.55 μmole, maximum possible Tat recovery = 0.18 μmole (1500 μg) 129

Figure 6.1 Determination of the steady state concentration of H_2O_2 produced in LBL assembled nylon membrane for fixed flow rate and substrate concentration. Two different substrate concentrations, 15 mM and 75 mM glucose, were studied. Amount of GOX immobilized = 1.5 mg, permeate flux = 140 x 10^{-4} cc/cm^2.s, residence time = 0.6 s, pore radius of LBL assembled nylon membrane = 125 nm, external membrane area = 13.2 cm^2, membrane thickness = 165 μm, pH = 5.5, Temperature = 25 ^{0}C 133

Figure 6.2 Importance of O_2 in enzymatic oxidation of glucose by GOX immobilized in LBL assembled nylon membrane. Activity is calculated based on concentration of H_2O_2 produced, and normalized by dividing with maximum activity for this experiment, which is $[H_2O_2]$ / $[H_2O_2]_{max}$. Concentration of glucose fed = 0.75 mM, Amount of GOX immobilized = 1.5 mg, permeate flux = 140 x 10^{-4} cc/cm^2.s, residence time = 0.6 s, pore radius of LBL assembled nylon membrane = 125 nm, external membrane area = 13.2 cm^2, membrane thickness = 165 μm, pH = 5.5, temperature = 25 ^{0}C 135

Figure 6.3 Rate (v) vs substrate concentration (s) for free GOX in homogeneous phase batch reaction. Concentration of glucose solution = 0.75 - 75 mM, reactor volume = 25 cm^3, amount of GOX = 0.25 mg, temperature = 25 ^{0}C, pH of NaOAc-HCl buffer = 5.5 137

Figure 6.4 Lineweaver-Burke plot for free GOX in homogeneous phase batch reaction. Concentration of glucose solution = 0.75-75 mM (1/s = 1.33 - 0.013 mM^{-1}), reactor volume = 25 cm^3, amount of GOX = 0.25 mg, temperature = 25 ^{0}C, pH of NaOAc-HCl buffer = 5.5 138

Figure 6.5 Schematic diagram of electrostatically immobilized GOX in polyelectrolyte / polymer domain for both LBL-GOX and PVDF-GOX membranes. There are two distinct

regions; one containing GOX and the other devoid of GOX. The first region is responsible for the catalytic action of the membrane, whereas, the latter one is associated with core leakage 140

Figure 6.6 Rate of oxidation of glucose as a function of substrate concentration for different GOX immobilization experiments. Amount of GOX immobilized = 1.8 mg, 1.5 mg and 1 mg for PVDF membrane, LBL membrane and covalent immobilization, respectively. Residence time for all experiments were around 0.6 s, temperature = 25 ^{0}C, pH of NaOAc-HCl buffer = 5.5 142

Figure 6.7 Lineweaver-Burke plot for GOX immobilized in functionalized LBL (LBL-GOX-convective) and PVDF (PVDF-GOX-convective) membranes. Concentration of glucose solution = 0.75 - 75 mM (1/s = 1.33 - 013 mM^{-1}), amount of GOX immobilized = 1.5 and 1.8 mg for LBL and PVDF membranes, respectively, temperature = 25 ^{0}C, pH of NaOAc-HCl buffer = 5.5. Inset figure shows Lineweaver-Burke plot for the substrate concentration range of 15 - 75 mM (1/s = 0.067 - 0.013 mM^{-1})..... 144

Figure 6.8 Effect of flow rate, i.e. residence time, on conversion of glucose and rate of formation of H_2O_2 for 15 mM glucose solution fed in LBL assembled nylon membrane. Rate and conversions are calculated from equations (6.3) and (6.5). Model values are calculated based on equation of PFR (equation 6.4). Amount of GOX immobilized = 1.5 mg, volume of LBL membrane reactor 0.122 cm^3, pH = 5.5, temperature = 25 ^{0}C, permeate flux = (75 - 265) x 10^{-4} cm^3/cm^2-s, residence time = 0.4 - 1.25 s 146

Figure 6.9 Effect of flow rate, i.e. residence time, on conversion of glucose and rate of formation of H_2O_2 for 15 mM glucose solution fed in functionalized PVDF membrane. Rate and conversions are calculated from equations (6.3) and (6.5). Model values are calculated based on equation of PFR (equation 6.4). Amount of GOX immobilized = 1.8 mg, volume of PVDF membrane reactor = 0.1 cm^3, pH = 5.5, temperature = 25 ^{0}C, permeate flux = (60 - 200) x 10^{-4} cm^3/cm^2-s, residence time varied from 0.4 - 1.25 s... 147

Figure 6.10 Effect of pH on activity for both free GOX and immobilized GOX in LBL assembled membrane. Activity is calculated based on concentration of H_2O_2 in permeate and is normalized by dividing with maximum activity, i.e., $(C_{PH2O2})/ (C_{PH2O2})_{max}$. Amount of GOX immobilized = 1.5 mg, volume of LBL membrane reactor = 0.122 cm^3, permeate flux = 140 x 10^{-4} cc/cm^2.s, residence time = 0.6 s, external membrane area = 13.2 cm^2, membrane thickness = 165 μm, pH = 5.5, Temperature = 25 ^{0}C, concentration of glucose fed = 0.75 - 75 mM..... 149

Figure 6.11 Stability of GOX immobilized in LBL assembled nylon membrane as well as PVDF-PAA-PAH membrane based on the change in activity over a period of time. The stability is compared with that reported (Ahuja 2006; Ozyilmaz et al. 2005) for free GOX. Activity is calculated based on concentration of H_2O_2 and is normalized by dividing with the activity on first day of immobilization at pH = 5.5..... 151

Figure 7.1 Schematic of formation of 2-stack functionalized membranes system for oxidative dechlorination of TCP by Fenton reaction. Membrane 1 and 2 were functionalized with electrostatically immobilized GOX and Fe^{+2}, respectively 159

Figure 7.2 Breakthrough curve for H_2O_2 in the permeate of 2-stack functionalized-PVDF membranes system used for dechlorination of TCP. Y-axis represents the ratio of concentration of H_2O_2 in permeate at time t ($[H_2O_2]_P$) to the concentration of H_2O_2 produced in first membrane under steady state condition ($[H_2O_2]_{ss}$). Inset figure represents the breakthrough curve of TCP for the same experiment. Y-axis of inset figure represents the ratio of concentration of TCP in permeate ($[TCP]_P$) at time t to the concentration of TCP in feed ($[TCP]_F$). $[H_2O_2]_{ss}$ = 0.1 mM, $[TCP]_F$ = 0.07 mM (15 ppm), Fe loading = 0.09 mmole, residence time in the first membrane = 2.7 s, residence time in the second membrane = 2 s 161

Figure 7.3 The conversion of TCP during the dechlorination reaction as a function of cumulative amount of TCP permeated. Conversion of TCP is the ratio of cumulative amount of TCP dechlorinated at any time to cumulative amount of TCP permeated at that time. Steady state concentration of H_2O_2 from the first membrane is around 0.1 mM, Fe loading = 0.09 mmole, residence time in the first membrane = 2.7 s, residence time in the second membrane = 2 s 162

Figure 7.4 Total amount of Cl^- formed as a function of total amount of TCP converted during the dechlorination reaction. The dotted line is constructed by considering 1 mole of TCP conversion corresponds to maximum of 3 mole of chloride formation. Slope of the solid lines represent experimentally obtained ratio of chloride formed to TCP converted. Steady state concentration of H_2O_2 from the first membrane is around 0.1 mM, Fe loading = 0.09 mmole, residence time in the first membrane = 2.7 s, residence time in the second membrane = 2 s 163

List of Files

Saurav Dissertation.pdf ……2 MB

Chapter 1 Introduction

This section summarizes the contents of the dissertation. The research areas studied in this dissertation are also broadly described along with the objectives. Functionalized polymeric membranes are used in various fields of research, such as, bioseparation, biocatalysis, biosensor, bioremediation, metal capture, etc. This research work has been directed towards the development and applications of functionalized polymeric membranes in bio-separation (affinity based) and bio-catalysis.

Chapter 2 contains background information on different aspects of functionalized membranes and their applications in bioseparation and biocatalysis. All experimental and analytical procedures are described in Chapter 3. Chapter 4 describes the results and discussions of functionalization of different membranes used in this study along with their characterization. Chapter 5 includes the results, discussions and important findings for the research on affinity based separation of HIV-TAT protein, using functionalized membranes, and effect of pre-filtration on the affinity separation. Accessibility of covalently immobilized avidin sites and fouling in the membrane are highlighted. Chapter 6 contains the details of the research on enzymatic oxidation of glucose with the enzyme, glucose oxidase (GOX), electrostatically immobilized in functionalized membranes. Chapter 6 is followed by the description of a practical application of the above mentioned immobilized enzymatic system for dechlorination of a chlorinated organic molecule, in the form of Chapter 7. Finally, all scientific accomplishments of this research work are summarized in Chapter 8.

1.1 Functionalized membranes for affinity based bio-separation: research objectives

Separation and purification of a protein from mixture of proteins require high selectivity, and incur a major part of the total production cost of the protein (Thoemmes and Kula 1995). Conventional packed-bead column chromatography is widely used for this type of separation (Lundberg et al. 2006). However, functionalized polymeric membrane based separation processes are emerging as cost effective and hydrodynamically favorable alternative to conventional column chromatography.

The overall objective of this research study was to improve the efficacy of the affinity membrane separation of proteins by better understanding the fundamental aspects of accessibility of avidin sites and fouling in membrane matrix. In this research work, HIV-Tat protein was used as a model protein. Although avidin is also a protein, now onwards, unless mentioned otherwise, the term "protein" will only be used to denote any biotinylated (BBSA, HIV-Tat) / non-biotinylated (BSA, GG) protein other than avidin. Separation of biotin-tagged Tat protein from a fermentation broth was demonstrated using avidin-biotin affinity interaction in an avidin-immobilized membranes system. The specific objectives were:

- To develop avidin-functionalized membranes system by covalent interaction.
- To determine the accessibility of covalently immobilized avidin sites by biotin moieties present in different species, such as, (i) a small biotinylated-compound, biotin 4-amidobenzoic acid (BABA), (ii) a biotinylated-protein, biotinylated-BSA (BBSA), and (iii) a mixture of BBSA and a non-biotinylated protein, gamma globulin (GG).
- To study the fouling associated with separation of proteins in membranes.
- To study the effect of pretreatment of bacterial lysate (BL) on available free Tat in solution.
- To characterize the membrane purified Tat protein by different analytical techniques, such as SDS-PAGE, Western Blot, ELISA.
- To compare the quality of the membrane purified Tat protein with column chromatographically purified Tat protein.
- To introduce a pre-filtration step to remove unwanted high molecular weight proteins and other impurities from BL feed prior to the affinity separation step.
- To study the effects of pre-filtration step on permeate flux, recovery of protein and processing time.
- To quantify the fouling in the affinity separation step by model equations.
- To quantify Tat protein present in different streams by a simple technique of biotin analysis.

1.2 Functionalized membranes for enzymatic catalysis: research objectives

Bio-catalytic reactions with free enzyme in homogeneous phase possess the advantage of higher activity, but its use is limited due to lower stability and lack of reusability. As a potential alternative, a novel approach has been proposed for the immobilization of enzyme in functionalized (Layer-By-Layer assembled and in-situ polymerized) polymeric membranes using electrostatic interactions.

Two different approaches of functionalization of polymeric membranes based on electrostatic interaction are presented. Glucose oxidase (GOX), which catalyses the oxidation of glucose to gluconic acid and hydrogen peroxide, was used as a model enzyme. A novel study has also been carried out on reusability of the same membrane matrix. Beside these, oxidative dechlorination of a chloro-organic molecule has been performed on 2-stack functionalized PVDF membranes using Fenton reaction.

The overall objective of this bio-catalysis research work was the development of high capacity, highly active, stable and reusable GOX immobilized (electrostatically) polymeric membranes for the oxidation of glucose to gluconic acid and hydrogen peroxide under convective flow condition. The specific objectives were:

- To develop a functionalized membrane system by alternative attachment of cationic and anionic polyelectrolytes based on Layer-By-Layer (LBL) technique inside anhydride activated nylon membrane.
- To develop a functionalized membrane system by in-situ polymerization of acrylic acid inside hydrophobic PVDF membrane.
- To characterize the functionalized domain created inside the membranes by different techniques.
- To immobilize the enzyme, Glucose oxidase (GOX), inside the above mentioned functionalized membranes using electrostatic interaction.
- To study the activity and kinetics of electrostatically immobilized GOX for the oxidation of glucose to gluconic acid and hydrogen peroxide under convective flow condition.
- To compare the activity of GOX present in different attachment forms.

- To study the effect of residence time and pH on the activity of GOX.
- To study the stability of the electrostatically immobilized GOX in the functionalized membranes.
- To detach the used GOX from the membrane matrix, check the activity after detachment, and then reattach it in the same membrane.
- To form a 2-stack functionalized PVDF membranes system with first one containing electrostatically immobilized GOX and the second one containing ferrous iron.
- To apply the above mentioned 2-stack membranes for simultaneous enzymatic production of hydrogen peroxide in first membrane and oxidative dechlorination of trichlorophenol (TCP) in the second membrane by Fenton reaction using hydrogen peroxide and immobilized ferrous ion.

Chapter 2 Background

This chapter contains a comprehensive background study of the research areas related to this dissertation. It starts with a brief history and introduction of the membranes and membrane based processes. Then various aspects of development of functionalized membranes are discussed, followed by their applications in different research fields. Application of functionalized polymeric membranes in protein separation and enzymatic catalysis are described in detail.

2.1 Membrane and membrane based processes

A membrane can be broadly defined as a barrier which allows selective transportation of species under the influence of a certain driving force. The driving force is generally due to the difference in chemical or electrical potential in two sides of the membrane, and is expressed in terms of pressure (ultrafiltration, microfiltration, pervaporation), concentration (osmosis), temperature (membrane distillation) or electrical (electro dialysis) potential gradients (Mulder 1991). Membranes can be made of polymers, metals, inorganic compounds, carbon, ceramic and liquids. Among the polymers, cellulosic materials, nylon, polyether sulfone (PES), polysulfone (PS), polypropylene (PP), polyethylene (PE) and polyvinylidene fluoride (PVDF) are the most popular starting materials for membranes (Kesting 1971).

Figure 2.1 represents different operating streams involved in a typical membrane based process. The streams are: (i) feed, which is fed into the system; (ii) permeate, which is passed through the membrane; and (iii) retentate, which is rejected by the membrane. Membranes can be non-porous or porous. Even the size of the pores varies staring from 10 μm for microfiltration membrane (MF) to 1 nm for nanofiltration membranes (NF) as shown in Figure 2.2. The reverse osmosis (RO) and pervaporation (PV) membranes are considered to be non-porous. Figure 2.2 demonstrates size of the pores of different kinds of membranes along with the sizes of some common molecules.

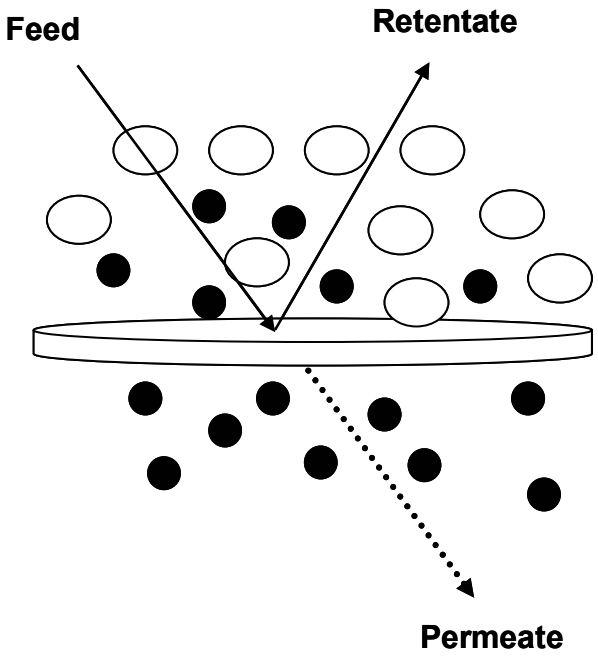

Figure 2.1 Different operating streams involved in a typical membrane separation process

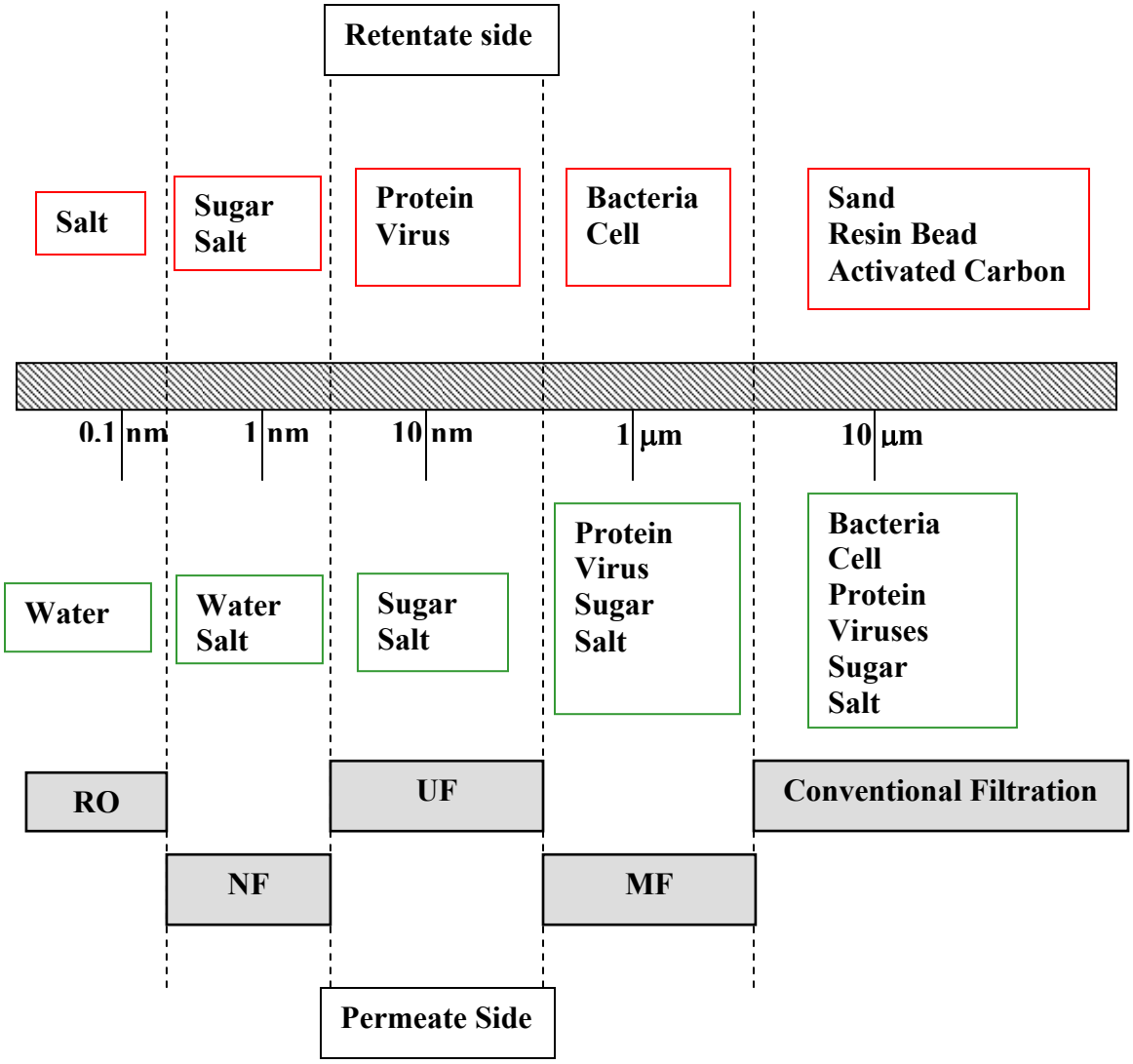

Figure 2.2 Filtration spectrum describing the classification of membrane processes based on diameter of the pore of membrane. Figure also indicates the proper choice of membrane process in order to separate some common molecules, based solely on size. RO = Reverse osmosis, NF = nanofiltration, UF = ultrafiltration, MF = microfiltration

This figure is presented to give an idea about the selection of proper membrane for a separation, based solely on size. For example, in order to separate a protein and salt, a UF membrane, which will reject the protein and permeate the salt, can be used.

The history of application of synthetic polymeric membranes goes back to the beginning of nineteenth century. However, the commercial application of membranes started in late 1960s to early 1970s. One of the most path breaking discoveries in the field of membranes was that of asymmetric membranes by Loeb and Sourirajan (Loeb and Sourirajan 1964). They were the first to introduce the concept of a thin skin layer of separating barrier on the top of a highly porous polymer support. This configuration is associated with a much lower pressure drop than symmetric membranes. After that, membrane based separation techniques gained popularity in different process industries. Membranes have been used extensively in water desalination, waste water treatment, biotechnology, biomedical industries, pharmaceutical industries, food industries and gas separation (Bhattacharyya and Butterfield 2003; Ho and Sirkar 1992; McGregor and Editor 1986; Mohr C. M. 1989; Scott 1995). Membrane based techniques include, but are not limited to, reverse osmosis (RO), pervaporation (PV), nanofiltration (NF), ultrafiltration (UF), microfiltration (MF) and electrodialysis (ED). The main advantage of membrane separation over conventional processes, such as, distillation or evaporation, is the energy efficiency and compact module design.

Earlier, membranes were considered to be a separation media based solely on size (UF, MF) or solubility (RO, PV) of species. However, with the advancement of functionalization chemistry and availability of new materials and technologies, it was realized that membrane has more potential than just being used as a separation media. Then, the concept of functionalized membranes was conceived and researchers started modifying membranes to incorporate various kinds of functionality to use them in different fields of research. This research work involves extensive experimental and theoretical studies with functionalized polymeric membranes. Background studies of the important research areas related to this dissertation are discussed in following sub-sections.

2.2 Functionalized membranes

Functionalized membranes are widely used in various fields, such as, biotechnology, food and pharmaceutical industries. The main advantage of functionalized membrane is the versatility of the active groups. It can be tailor-made to impart the desired functionality from a pool of active groups/molecules/moieties, depending on the applications. For example, to capture a metal ion, a cation exchange group/molecule (sulfonic acid group or polycysteine) (Hestekin et al. 2001; Ritchie et al. 1999; Smuleac et al. 2005); to detect glucose, glucose oxidase enzyme (Zhao and Ju 2006); to isolate an antibody from mixture, antigen of that antibody (Hout and Federspiel 2003); to release a drug, a polyelectrolyte (Grimshaw et al. 1992); is introduced in the functionalized membranes.

Functionalized membranes are created by attaching active groups in the base polymer of the porous membranes (UF or MF membranes). Porous membranes offer two fold benefits over non-porous membranes. Firstly, the functionalization takes place mainly inside the pores of the membranes. Since, pore surface area is much higher than the external surface area of the membrane, the amount of active groups attached inside the pore is much higher. Hence, the capacity of pore functionalized membranes is also higher. Secondly, the molecules of interest in the solution can permeate under convective flow condition. The convective flow through the membrane minimizes the mass transfer resistance and enhances the accessibility. The active groups are either incorporated during the formation of the membrane, or post modification is done on the base membranes to introduce the functionality.

2.2.1 Development of functionalized polymeric membranes

Some well documented literature reviews (Klein 2000; Zeng and Ruckenstein 1999; Zou et al. 2001) and book (Klein 1991) on functionalized membranes, encompassing base materials of membranes, active groups, their respective applications, are available. The chapter on affinity membranes in the book written by Klein deserves special mention because of the detail discussion of the chemistry involved between the

activation reagents and the base materials. The common polymeric membrane materials that are being used to attach active groups in membranes are described below.

Polymeric membrane materials: Researchers have exploited different base materials as the constituent of the starting membrane. Applications of cellulose (Hollman and Bhattacharyya 2002), regenerated cellulose (Liu et al. 2005), cellulose acetate (Hestekin et al. 2001), chitosan (Zeng and Ruckenstein 1998), nylon (Gsell et al. 1988; Hou et al. 1989), PVDF (Ritter 1991b) and polypropylene (Schisla et al. 1995) have been reported. This dissertation deals with cellulose acetate (CA), regenerated cellulose (RC), nylon and PVDF membranes. A brief introduction of these membranes is presented below and the chemical structures of the building blocks are shown in Figure 2.3.

Cellulose acetate (CA): Although pure cellulose is relatively stable, uniform and extremely hydrophilic material, its use is limited because of lower availability of active – CH_2OH groups. CA membranes contain sufficient exposed active groups and can be manufactured by process of phase inversion, but they are associated with lower mechanical and chemical strength (Zou et al. 2001). Activation of CA membranes has been conducted to incorporate aldehyde functionality by hydrolysis, followed by oxidation. These membranes have been used for poly-amino acid attachment for heavy metal recovery (Hestekin et al. 2001).

Regenerated cellulose (RC): Another popular, modified form of pure cellulose is regenerate cellulose (RC). RC membranes have high mechanical and chemical strength along with satisfactory contents of active groups (Zou et al. 2001). RC membranes have been activated with epichlorohydrin for purification of protein (Liu et al. 2005); with 1, 4-butanediol diglycidol ether for purification of enzyme (Ruckenstein and Guo 2004; Suen et al. 2000); with 1, 1'-carbonyldiimidazole for immobilization of enzymes and other affinity ligands (Hearn 1987) and also for the development of immunosensor (Stoellner et al. 2002).

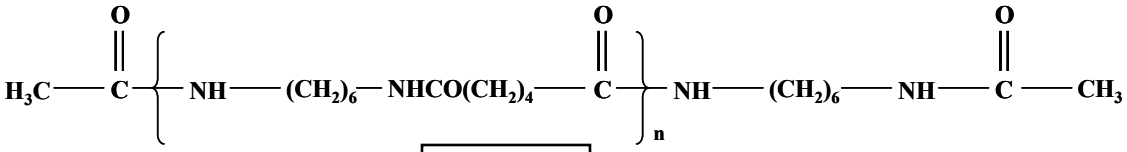

Nylon 6

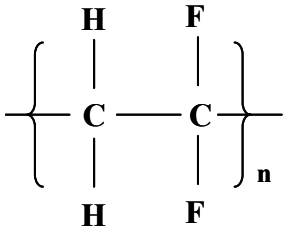

Polyvinylidene fluoride

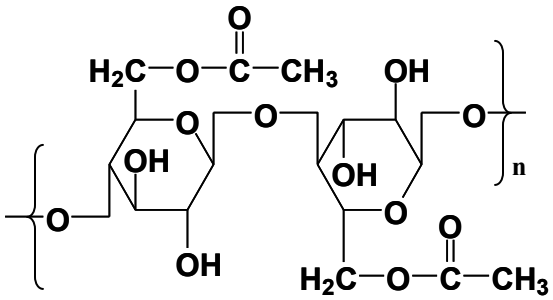

Cellulose Acetate

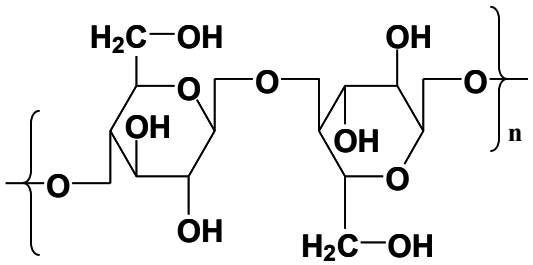

Cellulose

Figure 2.3 Chemical structures of building blocks of different membranes used in this research study

Nylon: Nylon is a polyamide material with high mechanical and chemical strength, but its applications in the process involving biomolecules are restricted due to considerable hydrophobicity and a lower number of exposed amine groups. Research has been conducted to convert nylon to a hydrophilic material by attaching active groups and then applying it for purifying BSA (Briefs and Kula 1992). Nylon membranes are generally hydrolyzed first to expose the primary amine groups (Hendry and Herrmann 1980). Shang and coworkers (Shang et al. 1998) have reported the superiority of 1, 1'-carbonyldiimidazole over other activation agents for binding of histidine in nylon 66 microfiltration membranes.

Polyvinylidene fluoride (PVDF): The repeat unit of PVDF membranes is $–CH_2–CF_2$. These membranes are inherently hydrophobic in nature; however, studies have been carried out to incorporate hydrophilicity into it. Polyacrylic acid (PAA), due to its hydrophilic nature and ion exchange property, has been extensively used for the formation of nanoparticles (Xu et al. 2005), adsorption of non-ionic surfactants (Ladhe et al. 2006) and capture of metal ions (Rivas et al. 2003) in the PVDF membranes. PAA has also been used to functionalize membranes for RO, NF and PV type applications (Dai et al. 2001; Fery et al. 2001; Gabriel and Gillberg 1993). Gabriel and coworker (Gabriel and Gillberg 1993) have reported a method to functionalize hydrophobic PVDF membranes by in-situ polymerization of acrylic acid. This technique has already been used for the formation of nanoparticles (Xu and Bhattacharyya 2007) and immobilization of Fe^{+2} (Li et al. 2007) inside the PVDF membrane pore. A study has also been reported on covalent immobilization of GOX on acrylic acid-graft-copolymerized-PVDF membrane (Ying et al. 2002). However, to the best of our knowledge, PAA-functionalized PVDF membrane has never been used for electrostatic immobilization of GOX.

Chemical activation by covalent attachment: Chemical modification of membrane is done to incorporate either active groups, such as, amine, carboxylic acid, aldehyde, epoxide and thiol or ligands (Blitz et al. 1987; Klein 1991; Zou et al. 2001) for further

applications. Some well known membrane functionalization techniques are described below.

Periodate oxidation: Membranes containing hydroxyl groups (cellulose) can be activated by oxidizing with sodium periodate to form aldehyde group. This aldehyde activated membrane can then react with any primary amine containing molecule, following Schiff's base reaction (Hestekin et al. 2001).

Epoxide activation: Membranes containing hydroxyl or primary amine (nylon) can be activated with epoxide group, by reacting with epichlorohydrin or 1, 4-butanediol diglycidol ether. The resultant epoxide group can react further with any amine containing molecule, such as protein (Liu et al. 2005).

Carbonyldiimidazole activation: Membranes containing hydroxyl and primary amine can again be activated by reacting with 1, 1'-carbonyldiimidazole, which releases its first imidazole group in this reaction. The attached active group further participates in nucleophilic substitution with any primary amine containing molecule, such as protein, to release its second imidazole group and form very stable amide linkage (Klein 1991).

Triazine activation: Another approach of activating membranes containing hydroxyl and primary amine is known as triazine activation. In this technique, 2, 4, 6-trichlorotriazine (cyanuric chloride) is reacted with the membrane to attach it in the solid matrix by releasing highly reactive first chlorine. Since, the second and third chlorines are now attached with the membrane and available for substitution, this forms a highly reactive system (Klein 2000).

Carbodiimide coupling: Carbodiimide coupling is the most widely used technique to form an amide bond between the amine group of the membrane and carboxylic acid group of the ligand, or vice-versa (Klein 1991). The carbodiimide reacts with the carboxyl group to form an active intermediate, which reacts further with amine group to form an amide bond and urea (Smuleac et al. 2004).

Radiation grafted activation: In this technique the inert base polymer of the membrane is irradiated with UV radiation or electron beam to generate free radicals. These free radicals then react with the monomers of activation reagent to incorporate it into the membrane matrix. The advantage of this technique is that the inert polymeric support of the membrane can be activated with virtually any polymer desired. Modification of PP (Ulbricht and Yang 2005), PVDF (Tarvainen et al. 2000) and PS with PAA (Ulbricht and Riedel 1998); PE with glycidylmethacrylate (Iwata et al. 1991) and nylon with glycidylmethacrylate (Hou et al. 2007) using this technique have been reported.

Activation during synthesizing the membrane: Sometimes in order to simplify the step of functionalization, the active monomer is copolymerized with the base polymer while casting the membrane. Incorporation of acrylic acid into PVDF (Ying 2002), acrolein-co-hydroxyethyl methacrylate into PES (Pemawansa 1993), hydroxyalkyl methacrylate into acrylonitrile (Klein and Silva 1991), various reactive groups containing copolymer into nylon (Degen et al. 1986; Gsell et al. 1988) and acrolein into acrylonitrile (Wolpert 1997) have been successfully carried out. Incorporation of particles, containing certain types of activity, into the casting monomer solution has also been reported (Avramescu et al. 2003; Lensmeyer et al. 1995; Lingeman and Hoekstra-Oussoren 1997).

2.2.2 Further attachment of groups/molecules

Once the base membrane is activated, further attachment of groups/molecules depends on the application of the membrane. Since this research study mainly deals with biomolecules, further discussion is restricted to those molecules only. Various techniques of biomolecules immobilization into solid support have been well documented in literature (Ratner et al. 2004; Woodward and Editor 1985). A schematic diagram showing different types of interactions is presented in Figure 2.4.

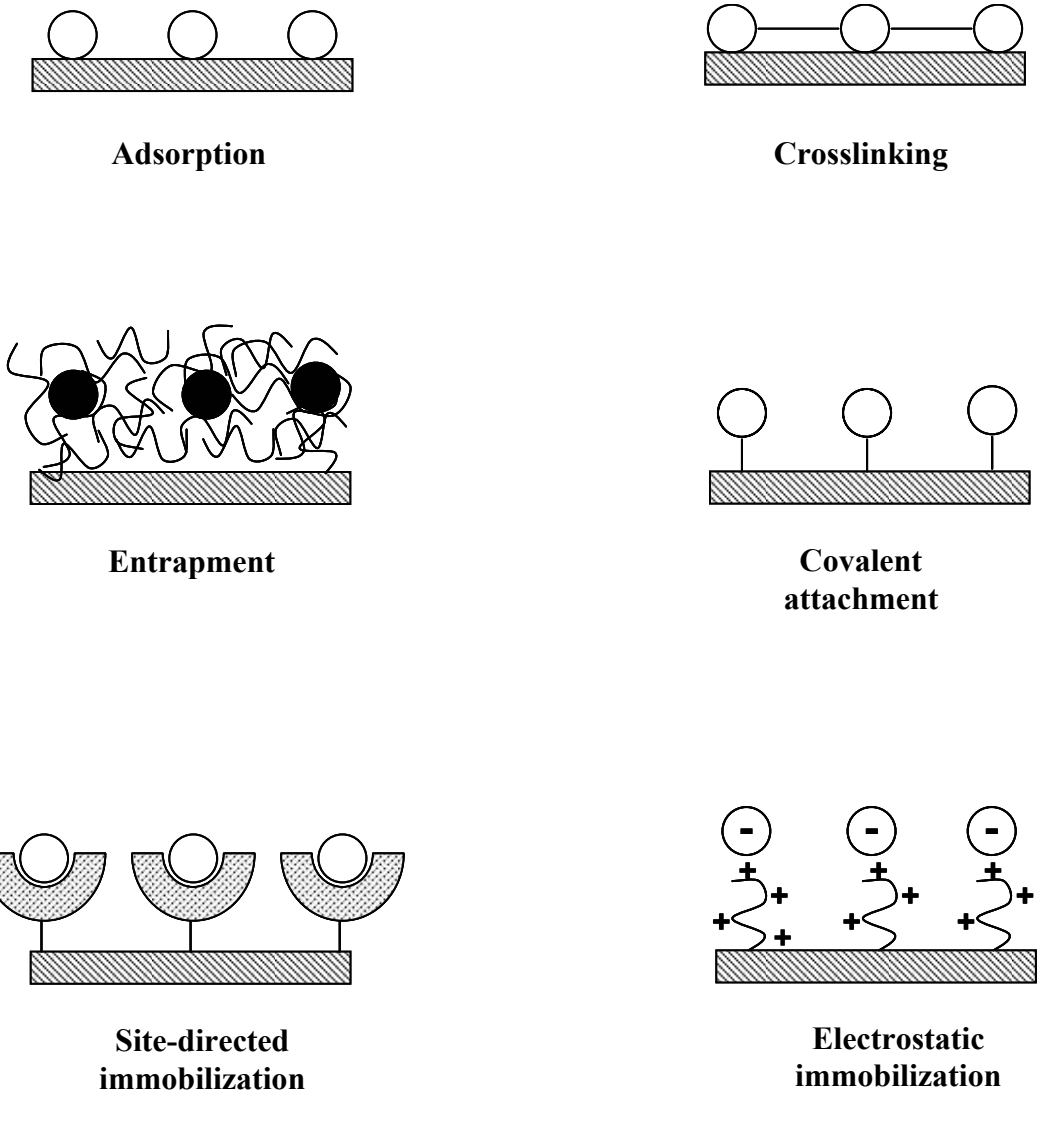

Figure 2.4 Different schemes of immobilization of biomolecules in membrane

Adsorption: Biomolecules are physically adsorbed on the membrane materials. Adsorption takes place due to hydrophobic, van der Waals, and other interactions. This technique is very simple, but stability is a matter of concern.

Crosslinking: Sometimes to incorporate stability in the adsorption mode of immobilization, adsorption is followed by crosslinking of the biomolecules. This technique is associated with loss of active properties of immobilized biomolecules.

Entrapment: In this technique, a network is created inside the pores of the membrane, and then biomolecules are entrapped in that. Networks are generally created by polymers or polyelectrolytes. The mode of interaction is same as adsorption. Although the immobilization is much more stable than adsorption, blockage of membrane pore due to network formation is a problem in this technique.

Covalent attachment: Protein molecules are covalently attached with the active groups, such as amine, epoxide, anhydride and carboxylic acid present in the membrane. Advantage of covalent immobilization is the very stable attachment; however, the biggest disadvantage is the alterations in the active sites of the biomolecules due to proximity to the solid polymeric support (Datta et al. 2006).

Site-directed attachment: Site-directed immobilization technique retains the activity of the biomolecule along with the benefits of traditional covalent bonding. It possess several advantages over random covalent immobilization (Butterfield and Bhattacharyya 2003; Butterfield et al. 2001). Although, this technique is very specific and provides high activity, it is associated with complex methods and is expensive.

Electrostatic attachment: A protein molecule becomes positively charged at any pH below its isoelectric point (P_I) and negatively charged at any pH above its P_I. Protein molecules are electrostatically immobilized on a charged membrane by using the net opposite charge on protein. Similarly, polyelectrolytes (both cationic and anionic) are also attached in a charged membrane by manipulating the pH. A sophisticated approach

of immobilization of biomolecules by electrostatic interaction has been demonstrated in this research study. This approach is known as Layer-By-Layer (LBL) technique.

Layer-By-Layer (LBL) technique: Alternative attachment of polycations and polyanions by LBL is a simple but robust technique to create layers in a solid support with high capacity and versatile functionality. In our laboratory Bhattacharyya and Hollman (Hollman and Bhattacharyya 2004) first developed this technique for membrane applications. The technique was first conceived by Decher (Decher 1997; Decher and Hong 1991; Decher et al. 1994), based on a study indicating the possibility of existence of such a technique by Iler (Iler and Colloid 1966). A detailed literature review covering the mechanisms of layers formation, applications in various fields and scope of future studies has been published recently (Ariga et al. 2007). LBL technique is used to create functional domain containing various kinds of species, such as, polyelectrolytes (Chen and McCarthy 1997; Dai et al. 2001; Nguyen et al. 2003; Smuleac et al. 2006), proteins (Caruso et al. 1998b; He et al. 2004; Lvov et al. 1995), dyes (Tang et al. 2006; Tedeschi et al. 2000), nanoparticles (Dotzauer et al. 2006; Ko et al. 2005; Kotov et al. 1995; Zhang et al. 2003), thiols (Chun and Stroeve 2001), metal ions (Khopade and Caruso 2002; Krass et al. 2003), virus (Lvov et al. 1994) and lipids (Ichinose et al. 1996). It is also used in different fields of applications, such as, separation (Jain et al. 2007; Krasemann and Tieke 1998; Liu and Bruening 2004; Malaisamy and Bruening 2005), biosensors (Hoshi et al. 2007; Zhao and Ju 2006; Zhou and Arnold 1995) and bio-catalysis (Matsuno et al. 2007; Onda et al. 1996; Smuleac et al. 2006; Su et al. 2005). One of the most intriguing studies has been carried out by Caruso et al. (Caruso et al. 1998a, 1999) to create “hollow capsules” based on LBL technique. This study has been further extended to encapsulate solid microparicles of GOX, utilizing LBL technique, for applications as biosensor (Trau and Renneberg 2003). A high concentration of salt solution has been used to preserve the solid state of GOX in aqueous solution. Attempts have also been made to characterize the layers (Caruso et al. 1998b).

2.2.3 Applications of functionalized membranes

Functionalized membranes have a wide spectrum of applications in water treatments, energy related research work, heavy metal recovery, bioseparation and biocatalysis. A few of them, relevant to this research, are mentioned below.

Alternative to traditional RO/PV type applications: Traditional RO or PV membranes selectively separate a component from other, but the associated flux is very low as non-porous membranes are used. Polyelectrolyte functionalized NF or UF membranes are an exciting alternative to those processes. Due to comparatively larger pore size of UF/NF membranes, the permeate flux is very high and the selectivity is also retained because of the involvement of charge exclusion of ions. Polyelectrolyte assembled functionalized membranes have been used for separation of salt from seawater under RO and NF conditions (Jin W. 2003; Toutianoush et al. 2005) as well as for the separation of ethanol-water mixture by pervaporation (Krasemann et al. 2001). It has also been used for controlled water permeability and charge based ion exclusion by changing the conformation of attached polyelectrolytes (Hollman and Bhattacharyya 2002; Smuleac et al. 2004). Size based selective transport of uncharged molecules, such as, glucose, sucrose methanol, has also been reported (Liu and Bruening 2004).

Heavy metal recovery: Functionalized membranes have also been used for heavy metal recovery. Ritchie and co-workers (Ritchie et al. 1999) and Hestekin and co-workers (Hestekin et al. 2001) have reported the use of polyamino acid functionalized silica and cellulose membranes for the capture of Cd and Pb, respectively. Smuleac and co-workers (Smuleac et al. 2005) have implemented polythiol functionalized alumina membrane for Hg capture, whereas, Makkuni and co-workers (Makkuni et al. 2007) have used organic sulfide modified iron-copper nanoparticle aggregates for sorption of vapor phase Hg.

This research work has been directed towards development and applications of functionalized polymeric membranes for bioseparation and biocatalysis. Therefore, background studies of these two research areas are presented below.

2.3 Bioseparation

Various biomolecules, such as, protein, nucleic acid and virus are isolated from mixtures using their characteristic properties like size, charge, interaction with other molecules, etc. Among the above mentioned biomolecules, protein is the primary focus of interest in biotechnology, biomedical and pharmaceutical community as it is the most fundamental biomolecules present in leaving cells and responsible for majority of intra-cellular as well as extra-cellular functions. In-vitro, it is used as catalyst, therapeutic agents, biomarkers and sensors, to name a few (Lehninger 1977; Voet et al. 2004).

2.3.1 Proteins

Amino acids are the building blocks of protein molecules. Twenty amino acids are available, and each contains a carboxylic acid group (α-carboxylic acid), a terminal primary amine group (α-amine), a hydrogen atom and a side chain group (R-group) attached to the central α-carbon atom. The R-group is the key factor in determining the identity of an amino acid. For example, the R-group is CH_3 and $(CH_2)_4$-NH_2 for alanine and lysine amino acids, respectively. α-carboxylic acid group of one amino acid reacts with the α-primary amine group of other to form an amide bond, which is known as peptide bond in biotechnology. Genetically encoded sequence of peptide bonds in different combinations, from a choice of 20 amino acids, are the basis of formation of proteins. Examples of some common proteins are serum albumin, hemoglobin, insulin, fibrinogen, etc. (Lehninger 1977). In this research work, a regulatory protein of Human Immunodeficiency Virus type 1 (HIV-1), known as TAT (Trans-Activator of Transcription or Trans-Activating Transduction) has been purified using affinity based membrane separation. A brief background study of TAT protein is presented later.

Function of a protein is strictly dependent on its structure. The straight chain amino acid sequence of a protein is its primary structure. The secondary structure (α-helix, β-sheet) is the spatial arrangement of only the polypeptide backbones (not the side chains) under the main influence of hydrogen bonding. Tertiary and quaternary structures involve protein folding, and are arrangements of a complete polypeptide and more than one polypeptide chains, respectively (Voet et al. 2004). Different process parameters,

such as pH and temperature have significant effects on structure of proteins. Shielding effect of salt on charge, well known as salting-in and salting-out, has strong influence on solubility of proteins. Additional interactions, such as hydrophobic interaction, influence the conformation change of protein molecules. Proteins also demonstrate variation in size, shape and charge depending on the amino acid residues and existing circumstances. All these variations in properties and conformations are used to separate proteins from mixtures by different techniques. Traditional column chromatography is the most popular technique used for protein separation and is discussed later.

2.3.2 TAT protein

TAT (Trans-Activator of Transcription or Trans-Activating Transduction) is an extra-cellular regulatory protein of human immunodeficiency virus type 1 (HIV-1) and is critical for viral replication (Jeang et al. 1999; Ma and Nath 1997; Rusnati et al. 1997; Stauber and Pavlakis 1998). Tat protein is formed from two exons. The first one is responsible for coding initial 72 amino acid residues (Tat_{1-72}), whereas, the second one codes for remaining 14-32 residues. This study deals with only first 1-72 polypeptide sequence of Tat, and hence, in this dissertation, Tat_{1-72} is always referred as Tat. Primary structure of Tat showing the amino acid residues, along with the salient features of Tat, is represented in Figure 2.5. The primary role of Tat is to magnify the HIV gene expression (Fisher et al. 1986) by regulating transcription. Tat activates the transcription by interacting with an RNA element, known as TAR (Trans Activation Response), which is located close to the promoter region of HIV-1 gene, termed as long terminal repeat (LTR) (Dingwall et al. 1989; Long and Crothers 1999; Rosen et al. 1988).

The failure of available retro-viral therapies to exterminate HIV has been implicated to the extra-cellular secretion of Tat by the HIV-infected cells (de Mareuil et al. 2005; Ramratnam et al. 2000). Moreover, Tat has several deleterious effects on immune and nervous systems (Nath and Chauhan 2005; Nath and Geiger 1998; Prendergast et al. 2002). Tat is thus an excellent target for AIDS related vaccine and drug development (Gallo 1999).

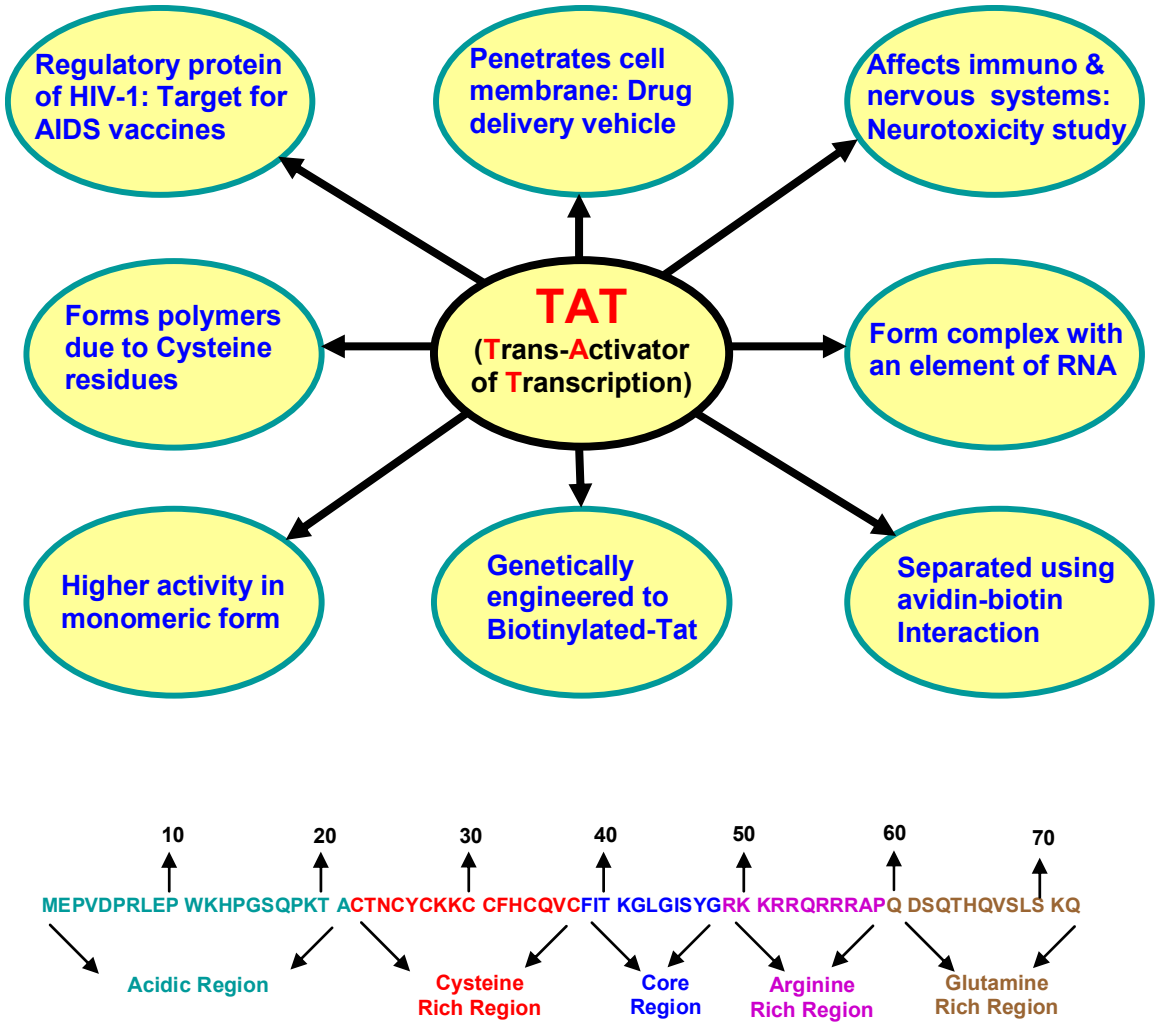

Figure 2.5 Primary structure of HIV-Tat_{1-72} protein showing the amino acid residues. Figure also indicates the salient features of Tat in terms of structure, isolation and further therapeutic applications

Although Tat is an extra-cellular protein, it has a unique ability to translocate across the cell membrane. This unique feature of Tat has been first reported by Frankel and Pabo (Frankel and Pabo 1988). After that Tat protein or Tat derived peptide sequences have been utilized as novel delivery vehicles for internalization of wide varieties of "cargo molecules" inside the living cells. The cargo molecules include nanoparticles (Lewin et al. 2000), quantum dots (Ruan et al.), DNA (Abu-Amer et al. 2001), enzymes (Schwarze et al. 1999), liposomes (Torchilin et al. 2001), proteins (Caron et al. 2001), small molecules of drugs (Polyakov et al. 2000) etc. The excellent delivery efficiency of Tat has facilitated the trans-cellular transduction of active therapeutic agents (Brooks et al. 2005; Wadia and Dowdy 2003; Zorko and Langel 2005) for the treatment of different diseases, such as, cancer (Wadia and Dowdy 2005).

It is important to mention here that Tat is functional in monomeric form only; not in dimeric or polymeric forms (Jeang et al. 1999). Hence, in order to carry out all of the above mentioned research studies, isolation of monomeric Tat is necessary. However, the isolation of monomeric Tat protein presents several challenges. Tat includes a cysteine-rich region, a hydrophobic core sequence, a highly basic region, and a glutamine-rich region (Bayer et al. 1995; Ruben et al. 1989; Stauber and Pavlakis 1998) as shown in Figure 2.5. It binds to different cellular proteins, and also due to cysteine rich region tends to form large complex polymers. The basic region of Tat has a strong interaction with TAR region of RNA to form complex (Stauber and Pavlakis 1998).

2.3.3 Column chromatographic separation of proteins

In all the column chromatographic techniques, the mixture of proteins is present in a liquid phase (mobile phase) and percolated through a column containing solid matrix (stationary phase). As the mixture flows through the column, different components of the mixture interact to different extent with the solid matrix and fractionate (Regnier 1987a) as shown in Figure 2.6. The type and extent of interaction depends on the nature of solid matrix as well as on the proteins. Column chromatographic techniques can be broadly classified into four categories depending on the mode of fractionation as demonstrated in Figure 2.4.

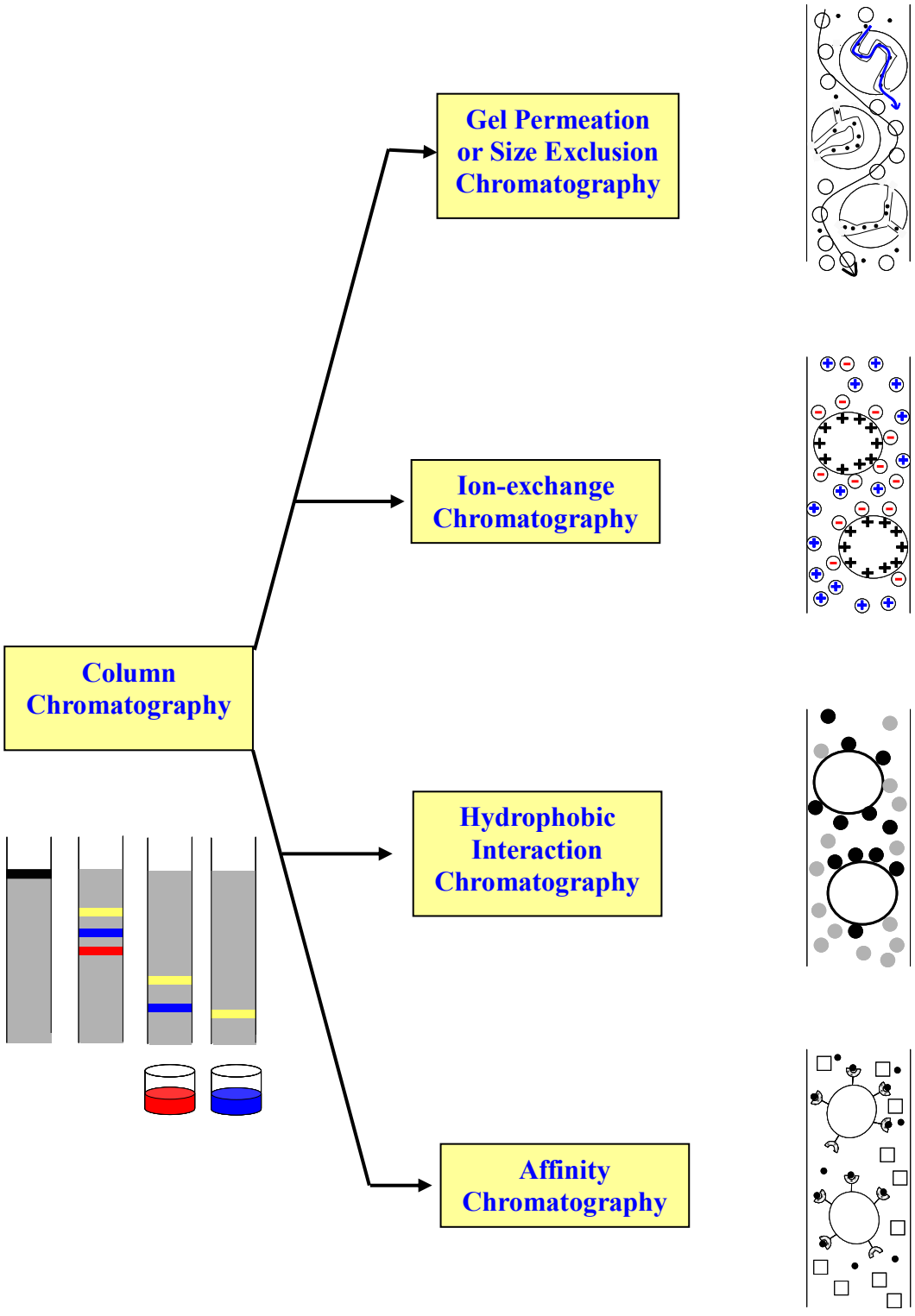

Figure 2.6 Different types of column chromatographic separation of proteins

Gel-permeation / Size exclusion chromatography (size-based): This fractionation technique is based solely on the size of the protein molecules (Porath and Flodin 1959). The column is packed with porous gel beads (e.g. polysaccharide). Small protein molecules penetrate through the beads and retarded, whereas, the larger proteins can not enter the porous structure of the beads and elute first. A schematic diagram of this technique is presented in Figure 2.6. Different kinds of proteins, including antibodies, have been separated using this technique (Barth et al. 1994). Size exclusion chromatography has also been used for the estimation of molecular weight of proteins (Irvine 1997).

Ion exchange chromatography (charge-based): This chromatographic technique fractionates proteins by electrostatic interaction based on charge of the molecules (Levison 2003) as shown in Figure 2.6. It can differentiate between oppositely charged species as well as species with different amount of charges. pH and ionic strength of the mobile phase is manipulated to achieve the desired difference in electrical properties between the molecules. Both cation (Torres and Peterson 1990) and anion (Peterson 1978) exchange columns are used for protein separation by this technique. Often, diethylaminoethyl or quaternary ammonium salts are used as anion exchange and carboxymethyl is used as cation exchange groups (Amesham Biosciences).

Hydrophobic interaction chromatography (hydrophobic interaction-based): In this technique, stationary phase is loaded with hydrophobic groups, such, as phenyl, butyl, etc. Proteins containing higher hydrophobic side chains interact with the stationary phase and retarded, whereas, less hydrophobic proteins are eluted first (Fausnaugh et al. 1984b). Sometimes, to increase the selectivity, mobile phase with high ionic strength is used. Reverse phase chromatography (RPC) based on hydrophobic interaction is also used. High-performance liquid chromatography (HPLC), based on RPC, is most widely used protein separation technique (Regnier 1987b). It speeds up the separation by applying pressure to the mobile phase using a pump. However, there are some basic differences in the separation principles of HIC and RPC (Fausnaugh et al. 1984a).

Affinity chromatography: This kind of chromatography is associated with highest level of selectivity as specific biological interactions are commonly used (Riggin et al. 1991; Voet et al. 2004). In this technique, a ligand, that has specific interaction with the target protein, is immobilized into the stationary phase. When mixture of proteins percolates through the column, only the target protein is captured. In next step, the target protein is eluted by changing the pH or applying high salt concentration or applying a protease. A detailed review article has been published by Varilova and co-workers (Varilova et al. 2006) describing various kinds of solid matrix used for affinity chromatography of proteins, including beads and membranes. Some well known protein-ligand interactions are enzyme-substrate and antibody-antigen. Additionally, tagged proteins are also isolated using this technique. Target protein is tagged previously with an active group/molecule that has specific interaction with the ligand attached to the stationary phase, and then separated using affinity chromatography. Histidine-tagged proteins are separated by this technique using Ni^{+2} as the ligand (Lechtken et al. 2006). Chromatographic technique, involving immobilized metal ions as affinity ligand (Chaga 2001), is well known as immobilized metal affinity chromatography (IMAC).

2.3.4 Membrane based separation of proteins

Membrane based separation of proteins are well known in biotechnology, food and pharmaceutical industries. Membrane based protein separation techniques can be broadly classified in three types, depending on size, charge and affinity of the molecules as shown in Figure 2.7.

Size based membrane separation of proteins: Traditional membrane separation techniques, such as ultrafiltration (UF) and microfiltration (MF), fall under size based separations. In UF and MF, proteins are separated based on their molecular weight, using particular molecular-weight-cut-off (MWCO) membranes. However, selectivity of proteins with moderately different molecular weights is poor by ordinary UF or MF.

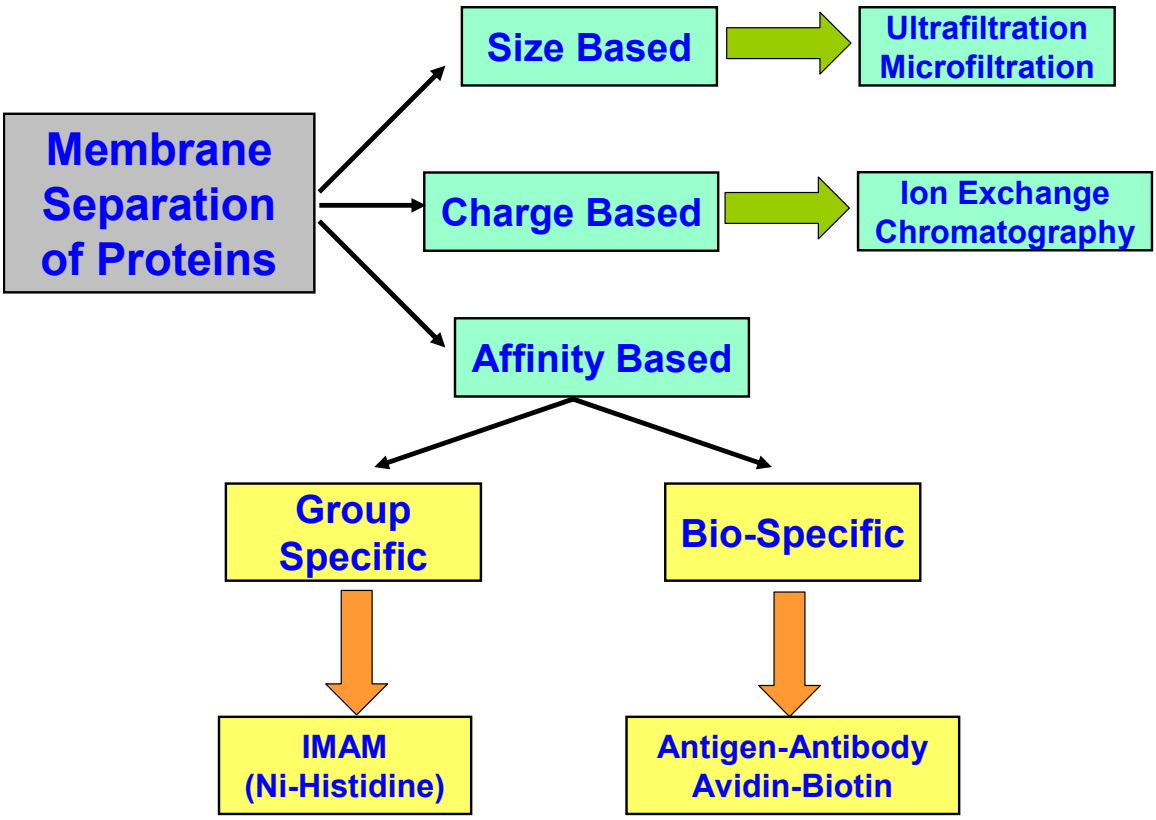

Figure 2.7 Classification of membrane separation of proteins based on size, charge and interaction

Sometimes, moderately different molecular weight proteins are separated by manipulating the operating conditions, such as pH, ionic strength, etc (Nystrom et al. 1998; Saksena and Zydney 1994; van Eijndhoven et al. 1995). Stacked ultrafiltration membranes have also been used to separate proteins, closer in size, from mixture with higher selectivity (Feins and Sirkar 2004). Occasionally, to increase the selectivity, UF is followed by diafiltration (van Eijndhoven et al. 1995).

Charge based membrane separation of proteins: Ion exchange membranes separate protein based on charge interaction (Avramescu et al. 2003; Yang et al. 2002). This technique is generally applied when the mixture of proteins is such that the isoelectric point (P_I) of the target protein is significantly different than that of unwanted proteins. The pH of the solution is adjusted to induce a charge to the target protein and then it is separated using an ion exchange membrane containing oppositely charged groups. The target protein is eluted by changing the pH again. A positively charged chitosan membrane, cross linked with glycol diglycidyl ether, has been used to separate ovalbumin ($P_I = 4.6$) from a mixture with lysozyme ($P_I = 11$), and human serum albumin ($P_I = 4.8$) from a mixture with cytochrome c ($P_I = 10.6$) (Zeng and Ruckenstein 1998).

Affinity based membrane separation of proteins: Affinity based separation using functionalized membranes has opened a new horizon for selective isolation of proteins from mixtures in the downstream processing of biotechnological and pharmaceutical industries. Two types of interactions are generally being used; group-specific interaction and bio-specific (biological) interaction. Group specific interaction is associated with higher capacity, but lower selectivity. Immobilized metal ion affinity membranes (IMAM), such as Ni^{+2} or Cu^{+2} immobilized membranes, for separation of histidine-tagged proteins is well known example of group specific interaction in membranes. A comprehensive review article on IMAM containing types of membrane matrices, chelating agents, metal ions and membrane modules is available (Suen et al. 2003).

This dissertation focuses on affinity membrane separation of proteins based on biological interaction. Affinity separation, involving very specific interaction based on biological properties, is more attractive among the biotechnologists (Brandt et al. 1988;

Charcosset 1998; Datta et al. 2007; Datta et al. 2006; Hollman et al. 2005; Jain et al. 2007; Klein 2000; Roper and Lightfoot 1995; Thoemmes and Kula 1995; Zou et al. 2001). Background study of affinity membrane separation is discussed in detail below.

Some commonly used interactions are avidin-biotin, antigen-antibody, enzyme-substrate or oligonucleotide-protein binding (Klein 2000; Zou et al. 2001). Among the above mentioned interactions, avidin-biotin interaction is widely used (Green 1975; Jahraus et al. 1998) because of the high association constant of 10^{15} M^{-1}. This is much higher than that detected for strongest known antigen-antibody interaction of 10^{6}-10^{9} M^{-1} (Piramowicz et al. 2006). In fact, avidin-biotin is the strongest known non-covalent biological interaction, which remains unaffected up to 132 ^{0}C and pH of 2-13 (Savage 1992).

Biotin is a vitamin that is abundant in living cells of liver and kidney. It has a molecular weight of around 244 and isoelectric point of 3.5. Structure of biotin is given in Figure 2.8. Avidin is a tetrameric protein with combined molecular weight of 67,000 and isoelectric point of 10 (Savage 1992). Four subunits are identical and each has strong interaction with biotin. Thus, one mole of tetrameric avidin in ideal situation could bind four moles of biotin (Green 1965; Green 1975; Piramowicz et al. 2006). The mechanism of association between avidin and biotin is not clear yet. van der Waals force and hydrogen bonding network between the biotin and amino acid residues of avidin, mainly the Tryptophan (Trp) and Lysine (Lys) residues, are suspected to have principle roles in the interaction (Grubmuller et al. 1996; Livnah et al. 1993). Avidin-biotin interaction has been used by many researchers to immobilize enzymes on a membrane (Amounas et al. 2000; Bhardwaj et al. 1996; Butterfield et al. 2001). It has also been used for creating biomaterials (Zheng Liu 2004), assay elements (J.-L. Guesdon 1979), sensors (T. Hoshi 1995) and bioseparations (Datta et al. 2006).

Affinity membrane separation is also known as membrane chromatography or recognition based membrane separation. Membrane chromatography, as introduced first by Brandt et al., could combine capture and purification steps for the processing of large amount of protein at a shorter processing time (Brandt et al. 1988).

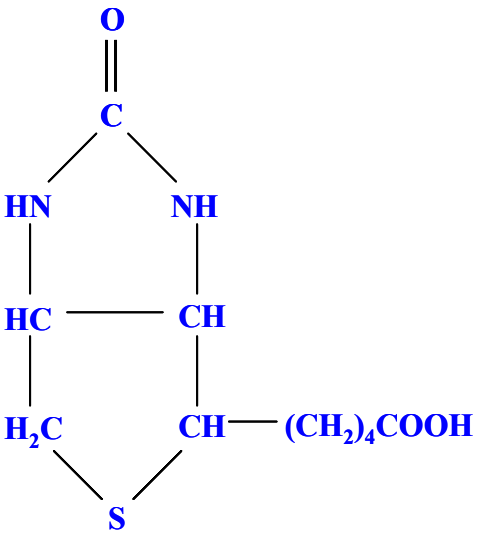

(a)

-{ }-Lys-Trp-Thr-{ }-Asn-Trp-Lys-{ }-Met-Trp-Leu-{ }-Asp-Trp-Lys-{ }-
9 10 11 69 70 71 96 97 98 109 110 111

(b)

Figure 2.8 (a) Structure of biotin and (b) partial primary structure of avidin showing the tryptophan (Trp) amino acid residues.

Thoemmes and Kula (Thoemmes and Kula 1995) in their review article have specifically highlighted several hydrodynamic advantages of membrane chromatography over conventional column chromatography. Due to convective flow within the membrane, mass transfer resistance is reduced; resulting in shorter cycle time, thereby minimizing the protein denaturation, whereas, in column chromatography the hydrodynamics are controlled by diffusion. Therefore, affinity based separation in membranes has the ability to obtain superior quality of purified protein in a substantially lower processing time than the conventional column chromatographic separation. Again, the thinner module of membranes enables a lesser pressure drop in comparison to column chromatography. Beside that, it is also easy to scale up membrane processes to large-scale processes. Charcosset (Charcosset 1998) in his review article, has described the ligand and membrane material performances. They categorized the applications of membrane chromatography based on the nature of the ligand used. The ligands mentioned were amino acids, antigen-antibody, dye, metal affinity and other biomolecules. Klein (Klein 2000) has described the types of membranes and modules that can be used for affinity based membrane separation, the kinetics of the affinity based separation and the applications.

Development and applications of functionalized membranes for affinity separation of proteins have been studied extensively (Zeng and Ruckenstein 1999; Zou et al. 2001). So far functionalized membranes have been used for affinity separation of lysozyme from egg white using chitin membrane (Ruckenstein and Zeng 1997); BSA using the antibody anti-BSA in flat sheet of RC membrane (Kugel et al. 1992) as well as hollow fiber module containing RC membrane (Hout and Federspiel 2003); IgG using protein A/G in composite cellulose membrane (Mandaro R. M. 1987; Ritter 1991a) as well as functionalized PVDF membrane (Ritter 1991b); pyruvate decarboxylase using cibacron blue F3GA dye in nylon membrane (Champluvier and Kula 1991); fibronectin using gelatin in modified PES-poly(ethylene) oxide membrane (Brandt et al. 1988), the enzyme horseradish peroxidase using concanavalin A in cellulose membrane (Guo and Ruckenstein 2003) and hormone 17-β-estradiol using its antibody (Urmenyi et al. 2005).

Mathematical analyses of affinity based membrane separation of proteins have been studied, considering different perspectives of transport and interaction of

biomolecules within the membrane (Boi et al. 2007; Briefs and Kula 1992; Hout and Federspiel 2003; Suen and Etzel 1992). Effects of the variation in different process parameters, such as, diffusivities and reaction rate constants, have been critically examined.

Fouling: The most severe problem associated with the practical application of membrane processes to protein solutions are the decrease in permeate flux with time due to fouling of the membrane surface and pores. In fact, the applicability of UF and MF processes in protein separation is limited by protein-membrane and protein-protein interactions that lead to irreversible alteration or fouling of the membrane surface and pore structure (Bowen et al. 1995; Bowen and Gan 1991; Hlavacek and Bouchet 1993; Ho and Zydney 2000; Kelly and Zydney 1995; Marshal et al. 1993; Palacio et al. 2003; Tracy and Davis 1994; Velasco et al. 2003). To minimize the protein-membrane interactions, and hence to improve the separation efficiency, the membrane material needs to be hydrophilic and resistant to the prevailing experimental conditions.

Marshall et al. (Marshal et al. 1993) have presented an extensive literature review on protein fouling in UF and MF. They described the effects of feed properties (concentration, pH, ionic strength and nature of components), membrane materials (hydrophobicity, pore size and charge), and operating conditions (transmembrane pressure and cross flow velocity) on the permeate flux, protein retention and selectivity. They suggested a three step mechanism of fouling, which consists of an initial flux drop due to concentration polarization, a decline in flux due to the formation of monolayer of protein by deposition, followed by a slow decline in flux due to further deposition of protein molecules. They have also pointed out the difference between the compaction, concentration polarization and fouling. Effect of different process parameters, such as, pH and ionic strength, on thickness of adsorbed foulant layer has also been studied (Zeman 1983).

Ho and co-worker (Ho and Zydney 2006) have presented a review article on overview of fouling, highlighting the modeling approaches based on classical blocking mechanisms. In general, the phenomenon of flux decline due to membrane fouling can be described in terms of four blocking mechanisms (Bowen et al. 1995):

1. In the *standard blocking model*, it is assumed that reduction in effective radii occurs due to the adsorption of molecules in pore walls.

2. In the *complete blocking model*, each molecule is assumed to block a pore.

3. In the *intermediate blocking model*, some molecules are assumed to block the pores and some attached to nonporous surface.

4. Finally, in the *cake filtration model*, a protein layer (cake) is assumed to cover the active membrane face.

For all of the blocking mechanisms common mathematical expression is

$$-\frac{dJ_v}{dt} = \alpha J_v^{(3-\beta)}$$

Where, J_v = Permeate flux; and α and β are the model parameters whose values are dependent on specific blocking mechanism.

Many researchers have tried to analyze their experimental data of flux decline for the same protein with a single fouling mechanism, but they differ in finding out the most appropriate mechanism to be applicable for that protein (Ho and Zydney 2000). Bowen and Gan (Bowen and Gan 1991) have used standard blocking mechanism to analyze their data of fouling of capillary pore aluminium oxide membranes by BSA, whereas, Hlavacek and Bouchet (Hlavacek and Bouchet 1993) used intermediate blocking mechanism, and Kelly and Zydney (Kelly and Zydney 1995) used a modified complete blocking model to satisfactorily explain the flux decline for BSA. Tracey and coworker (Tracy and Davis 1994) and Bowen and coworkers (Bowen et al. 1995) showed the transition of fouling mechanism with respect to time. They observed that at short times the fouling follows a particular mechanism, which at longer times shifted to another mechanism. This has suggested the involvement of complex theories of fouling, which could not be explained by a single fouling mechanism. Ho and Zydney (Ho and Zydney 2000) were the first to develop a mathematical model, which incorporates both the initial fouling by complete blocking mechanism and subsequent fouling by cake filtration mechanism. In this way, they have eliminated the need of using two different equations to describe fouling in two time domains. Their model predicted flux showed excellent agreement with the experimental data obtained for the permeation of BSA through polycarbonate MF membrane throughout the course of the experiment. Later, Zydney and

coworkers (Palacio et al. 2003) studied the fouling behavior for protein mixtures, BSA-lysozyme and BSA-pepsin. They have used the previously described combined model to predict the flux and to evaluate the effect of mixture composition on protein aggregates. The predicted results were in good agreement with the experimental data, which proved the applicability of this model for mixture of proteins.

Chan and co-worker (Chan and Chen 2004) reviewed the phenomenon of fouling on the perspective of different techniques used for the characterization of nature of foulants and morphology of fouled membranes. They described electron para-magnetic resonance spectroscopy (EPRS), scanning electron microscopy (SEM), atomic force microscopy (AFM), attenuated total reflection-Fourier transform infrared spectroscopy (ATR-FTIR), ellipsometry, small angle neutron scattering (SANS), confocal microscopy and matrix-assisted laser desorption ionization-mass spectrometry (MALDI-MS) as characterization tools.

2.4 Biocatalysis

Biocatalytic reactions involving enzyme and substrate are extremely important and a very promising area of research. In fact, the whole metabolism of human body is controlled by biocatalytic reactions involving different enzymes. Enzymes are also extensively used in food, pharmaceutical and biotechnological industries (McGregor and Editor 1986). A brief introduction of enzymes, highlighting the enzyme Glucose oxidase, their immobilization techniques in solid support and kinetic studies are presented below.

2.4.1 Enzyme

Enzymes are a special group of proteins that act as catalysts in a very selective manner. The reaction involving enzymes is known as biocatalysis and the reactant that is being catalyzed with a high degree of specificity is called the substrate (s). The high degree of specificity of an enzyme for a substrate can be attributed to the complementary geometric and electronic structure of the binding sites of the enzyme and substrate (Voet et al. 2004). Some enzymes do require a non-covalently bound small group/moiety to

show their activity. This small group/moiety is known as a cofactor. Cofactors may be metal ions, such as, Cu^{+2}, Fe^{+3}. When an organic molecule acts as cofactor then it is called coenzyme, such as flavin. Enzymes are widely used in food industries. For example use of amylase in brewing, lactase in stabilization of milk, lipase in cheese making, glucose oxidase in removal of O_2 and/or glucose from beer and cheese are well documented (Whitaker 1994). Among these enzymes, glucose oxidase (GOX) is one of the most popular, and has been used in our research related to biocatalysis. Additional background information about GOX is provided below.

Glucose oxidase (GOX): Glucose oxidase (GOX) is a well known enzyme from nineteenth century since Müllar has reported its activity in *Aspergillus Niger* (Muller 1928). GOX is very specific to the substrate β-D Glucose (Johnson et al. 2002) and catalyzes the oxidation of β-D glucose to δ-gluconolactone and hydrogen peroxide in a two step mechanism, known as Ping Pong Bi Bi mechanism (Figure 2.9). In first step, the co-factor of the enzyme, flavin adenine dinucleotide (FAD) oxidizes glucose to δ-gluconolactone and itself converts to the reduced form ($FADH_2$). In the second step, $FADH_2$ is oxidized back to FAD by O_2, which itself reduces to H_2O_2. δ-gluconolactone is an unstable compound, and immediately forms gluconic acid. The mechanism and kinetics of glucose oxidation by GOX has been extensively studied by several researchers (Duke et al. 1969; Gibson et al. 1964; Weibel and Bright 1971) and summarized in the literature (Leskovac et al. 2005). The structure of GOX has also been studied (Hecht et al. 1993). GOX is a dimeric protein consisting of two subunits of molecular weight 80 KDa each and connected by disulfide bond. Each subunit contains a non-covalently attached FAD and a ferrous iron (Wong and Editor 1995). There are three amino acid residues in the proximity of the active sites, namely, two histidine and one glutamic acid residues (Leskovac et al. 2005). Factors affecting the kinetics of glucose oxidation by GOX, such as pH (Bright and Appleby 1969; Chen and Weng 1986; Li et al. 1998), temperature (Li et al. 1998) and inhibition by product H_2O_2 (Bao et al. 2003) has been demonstrated thoroughly. Mathematical modeling of the kinetics of immobilized GOX has also been reported (Parker and Schwartz 1987).

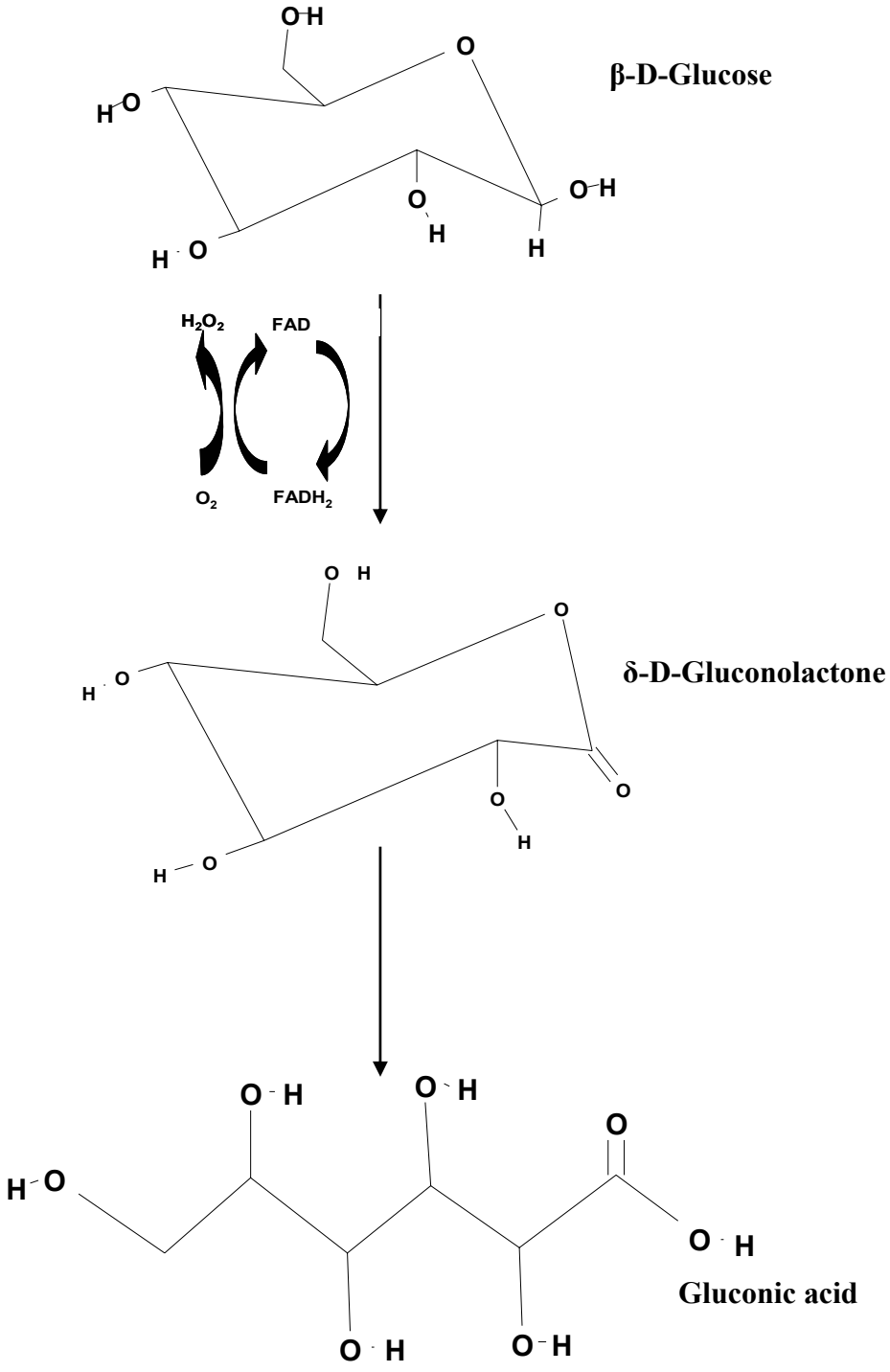

Figure 2.9 Enzymatic oxidation of glucose to gluconolactone by Glucose Oxidase (GOX). Gluconolactone immediately converts to gluconic acid. Cofactor of GOX, FAD, first converts to reduced form, $FADH_2$, and then oxidized to FAD by O_2

Immobilization of GOX in solid support: The activity of traditional covalently immobilized GOX in solid matrix is significantly low. The lower activity can be attributed to the conformation change of the enzyme in contact with solid support and also to the mass transfer resistances. To improve the situation, researchers have explored different new techniques of GOX immobilization. Table 2.1 summarizes some of the recent approaches adopted by the researchers along with the result of the kinetic study.

One approach has been to keep the mode of attachment the same (i.e. covalent) but modify the solid matrix. For example, covalent attachment of GOX in different activated beads/particles (Ahuja et al. 2007; Hou et al. 2007; Ozyilmaz et al. 2005), nanoparticles (Pandey et al. 2007), membranes (Rauf et al. 2006; Ying et al. 2002) and films (Li et al. 1998) have been reported in literature. The other approach is the non-covalent attachment of GOX on the solid matrix. Electrochemical polymerization (Ekinci et al. 2007), Layer-By-Layer deposition along with gold nanoparticles (Hoshi et al. 2007), electrostatic immobilization on anionic polystyrene beads (Tomotani and Vitolo 2007), electrostatic immobilization on LBL assembled nylon membrane (Smuleac et al. 2006) and LBL assembly along with multiwall carbon nanotubes on gold electrode (Zhao and Ju 2006) are to mention a few. Site-directed immobilization (Ahuja 2006) of GOX has also been studied. Although extensive studies were carried out to solve the problem of conformation change by proper immobilization, the issue of mass transfer resistance acquired less attention. Our research group has addressed this issue and used convective flow instead of diffusion (Smuleac et al. 2006).

Kinetic study of GOX: The kinetics of free and immobilized enzymes are generally studied and compared by the well known Michaelis-Menten equation, which is discussed elaborately in Chapter 6. Two important kinetic parameters of Michaelis-Menten equation are v_{max} and K_m. v_{max} is the maximum attainable rate at an imaginary substrate concentration of infinity, whereas K_m is the substrate concentration at which rate becomes half of v_{max}. Both parameters, in combination, indicate the affinity of the enzyme towards the substrate. One would expect higher value of v_{max} and lower value of K_m for homogeneous phase compared to immobilized phase.

Table 2.1 A comparative study of types of solid matrix used and kinetic parameters obtained for different GOX immobilization techniques reported in literature. MUDA = mercaptoundecanoic acid, EDC = N-ethyl-N'-(3-dimethylaminopropyl) carbodiimide, NHS = N-hydroxysuccinimide, PMMA = poly(methylmethacrylate), PSt = poly(styrene), GMA = Glycidolmethacrylate, APTES = 3-aminopropyltrimethoxysilane, PAA = poly(acrylic acid), PVDF = polyvinylidene fluoride, AAc = acrylic acid, CA = cellulose acetate

References	**Types of solid matrix**	**Mode of GOX immobilization**	**Kinetics Study**			
			Free GOX		**Immobilized GOX**	
			K_m (mM)	**v_{max} (mmole/min-mg)**	**K_m (mM)**	**v_{max} (mmole/min-mg)**
Ekinci et al. 2007	Pt-electrode coated with copolymer of Pyrrole and Polystyrene	Entrapment	3.0	0.68 (μmole/min-ml)	11.8	0.04 (μmole/min-ml)
Tomotani and Vitolo 2007	Anioinic polystyrene beads+UF membrane	Electrostatic	-	$57x10^{-4}$	-	$34x10^{-4}$
Ahuja et al. 2007	Polystyrene beads activated with hydrazide + Glutaraldehyde	Site-directed	25	0.273	29	0.248
Ahuja et al. 2007	Polystyrene beads activated with hydrazide + Glutaraldehyde	Covalent	25	0.273	39.3	0.052
Pandey et al. 2007	Au nanoparticle+MUDA+EDC-NHS	Covalent	5.85	$2.5x10^{-4}$	3.74	$14.2x10^{-4}$
Rauf et al. 2006	CA-PMMA membrane+Glutaraldehyde	Covalent	17.42	1.34 mM/min	41.65	1.17 mM/min
Hou et al. 2007	PSt-GMA Microsphere	Covalent	23.3	21.65 mM/mg-min	35.2	15.5 mM/mg-min
Ozyilmaz et al. 2005	Magnesium silicate + APTES	Covalent	68.2	0.435	259	0.217
Ying et al. 2002	Grafted PAA on PVDF membrane	Covalent	4.9	$48x10^{-4}$	10.5	$14x10^{-4}$
Li et al. 1998	Grafted AAc on Polyaniline film	Covalent	45	0.78 mM/min	80.6	0.62 mM/min

However, the reverse trend is not impossible, and has already been reported for in the literature (Pandey et al. 2007) as shown in Table 2.1. The activity of an enzyme depends on its conformation under existing conditions. Pandey and co-workers have carried out circular dichroism studies, which revealed a favorable conformational change of GOX due to binding upon thiolated gold nanoparticles. It was also mentioned that, secondary and tertiary structures of free GOX may restrict the active site accessibility. Additionally, the accessibility could be reduced due to aggregation in homogeneous phase by protein-protein interaction.

2.5 Concluding remarks

From the detailed background study of the research areas relevant to this dissertation, the following interesting observations can be made.

Affinity based membrane separation of proteins: Various studies have been reported with avidin-biotin interaction, but, quantification of the immobilized avidin sites within membranes by biotinylated probe molecules has never been done. Affinity separation of Tat has already been demonstrated by our research group (Hollman et al. 2005); however, attempt has not been made to improve the accessibility, processing time and fouling of the membranes by incorporating a prefiltration step.

Immobilized enzymatic catalysis: Researchers have exploited various solid matrices for enzyme immobilization; however, major studies are based on covalent attachment. The research works involving electrostatic immobilization have paid less attention to the reusability of the matrix. Enzyme immobilization by LBL assembly is a comparatively new technique, and is yet to be explored properly. Although, PVDF membranes have been used for covalent attachment of GOX, it has never been used for electrostatic immobilization of GOX.

Chapter 3 Experimental and Analytical Procedures

This chapter describes the experimental methods and the analytical techniques used in this dissertation for functionalized membrane based bioseparation and biocatalysis. The equipments and materials involved are also presented here.

3.1 Equipments

A stirred membrane cell purchased from Millipore Corporation (Product number XFUF07601) was used for all the experiments related to the bioseparation project. To ensure complete mixing in the cell, mixtures were stirred with a magnetic stirrer. The effective external surface area of the membranes in this cell was 33.2 cm^2.

For the biocatalysis part of the dissertation, all the experiments were carried out in a stainless steel membrane cell from Osmonics. The effective external surface area of the membranes in this cell was 13.2 cm^2.

3.2 Materials

3.2.1 Membranes

The acyl-anhydride functionalized nylon based microfiltration (MF) membranes (Immunodyne ABC, pore diameter 0.45 μm, thickness 165 μm, porosity 80 % as supplied by manufacturer) used in all affinity separation experiments were purchased from Pall Corporation. 100KDa MWCO regenerated cellulose membranes were used for ultrafiltration (UF) experiments and hydrophilized PVDF membranes (Pore size 0.1 μm) were used for MF experiments. These two types of membranes were purchased from Millipore Corp.

The nylon based acyl-anhydride activated Immunodyne membranes were again used for the Layer-By-Layer (LBL) experiments for biocatalysis. Hydrophobic PVDF membranes (pore diameter 0.45 μm, thickness 125 μm, porosity 75 % as supplied by manufacturer), used for the rest of the biocatalysis experiments, were purchased from Millipore Corporation.

Unactivated regenerated cellulose (RC), nylon and cellulose acetate (CA) membranes were activated using different techniques. CA (pore diameter = 0.45 μm, thickness = 125 μm) and RC (pore diameter = 0.2 μm, thickness = 125 μm) membranes were purchased from Sartorius. Nylon membranes (pore diameter = 0.2 μm, thickness = 165 μm) were purchased from Pall Corp.

3.2.2 Chemicals

Biotinylated-bovine serum albumin (BBSA), Factor X_a and Biotin Quantification Kit were purchased from Pierce Biotechnology. Gamma Globulin (GG) and the reagents for Bradford protein assay were purchased from Bio-Rad Laboratories. Unless specified otherwise, all other chemicals used in the bioseparation project were purchased from Sigma Corporation. The bacterial lysate supernatant was prepared in the Department of Anatomy and Neurobiology, University of Kentucky.

The enzyme Glucose Oxidase from *Aspergillus Niger* (GOX, Product No. G0543, MWt. 160000), β-D (+) Glucose (Product No. G5250, MWt. 180) and Poly-L-Lysine-hydrochloride (PLL, Product No. P9404, MWt. 105500, MWt. of repeat units 164.5) were purchased from Sigma. Poly(sodium 4-styrenesulfonate) (PSS, Product No. 243051, MWt. 70000, MWt. of repeat units 206), Poly(allylamine-hydrochloride) (PAH, Product No. 283223, MWt. 56000, MWt. of repeat units 93.5), 15 % solution of Titanium Oxysulfate in dilute H_2SO_4 (Product No. 495379), Benzoyl Peroxide (Product No. 179981), Trimethylolpropane triacrylate (TMPTA, Product No. 246808), Anhydrous Toluene (Product No. 244511) and Acrylic Acid (Product No. 147230, MWt. 72) were purchased from Aldrich. Epichlorohydrin (ECH), 1, 4-butanediol diglycidol ether (BDDE), 1, 1'-carbonyldiimidazole (CDI), Sodium Periodate ($NaIO_4$), and para-amino benzoic acid (PABA) were purchased from Sigma-Aldrich.

Unless mentioned otherwise, rest of the chemicals, including the de-ionized ultra filtered water (DIUF), were purchased from Fisher Scientific.

3.3 Analytical procedures

All spectrophotometric measurements in the UV and visible range were done by UV-VIS Spectrophotometer (Varian, Cary 300).The concentrations of BABA were determined by measuring the absorbance directly at 264 nm. Amount of immobilization of avidin was determined by measuring the concentration in the feed and permeate using the well known Bradford Protein Assay technique (Bradford 1976) at 595 nm. The same procedure was followed for measuring pure BBSA concentrations. The salt-wash solutions were also analyzed by the Bradford Assay to quantify the reversibly adsorbed species (avidin, BABA, BBSA). BBSA in mixture with GG was quantified by measuring the biotin content of BBSA using HABA ((2-(4´-Hydroxyazobenzene) Benzoic Acid)-avidin complex method (Green 1965). The linear range of detection for BABA was 0.1-25 μg/ml and the analytical error was less than 1 % for 10-25 μg /ml, 1-5 % for 1-10 μg /ml and 5-15 % for 0.1-1 μg /ml. The linear range of total protein analyses by Bradford Protein Assay was 1-24 μg /ml and the analytical error was less than 1 % for 2-24 μg /ml and 1-10 % for 1-2 μg /ml of protein solutions in this research work. The lower limit of detection of biotin for HABA-avidin complex method was 5 x 10^{-4} μmoles/ml of biotin with analytical error of 5 %. To check the reproducibility, the analyses were triplicated.

Qualitative analyses of Tat protein was conducted by Sodium Dodecyl Sulfate-Polyacrylamide Gel Electrophoresis (SDS-PAGE) and Western Blot analysis as described below. Quantification of total protein in bacterial lysate (BL) was carried out by Bradford Assay, and that of Tat protein was carried out by Enzyme-Linked-Immuno-Sorbent-Assay (ELISA). One of the additional goals of this research was to quantify the biotinylated-Tat present in different solutions of pre-filtered BL feed by an easy analysis of biotin. This has enabled to surpass the requirement of complex analysis of Tat by ELISA. This analysis was not possible for unfiltered BL feed due to the presence of impurities which interferes with the assay. Biotinylated Tat protein present in different streams of pre-filtered affinity separation experiments was quantified by measuring the biotin content using HABA-avidin complex method (Green 1965). Detail of the analytical protocol is mentioned below.

SDS-PAGE: SDS-PAGE was used to carry out qualitative analysis of proteins in different streams of Tat separation experiments, such as, feed, permeate, retentate, wash buffer 1 (WB1), wash buffer (WB2), cleavage buffer (CB) and eluate. SDS, being an anionic surfactant, denatures proteins and induces a uniform mass to charge ratio to all the proteins present in the mixture. So, the migration of proteins through the gel is strictly controlled by the size, i.e. molecular weight of the proteins. Therefore, SDS-PAGE fractionates proteins, and because of the presence of a tracking dye, generates bands in different location for proteins of varying molecular weights. In our case, a 15 % polyacrylamide gel was used under reducing environment of dithiothreitol (DTT). Coomassie blue or bromophenol blue was used as tracking dye.

Western Blot analysis: Western Blot analysis works on the principle of interaction with an antibody to the target protein. Hence, it is very sensitive and selective. Any band that shows up in a Western Blot, irrespective of the location, is due to the target protein. In our case, monoclonal mouse anti-Tat antibody and goat anti-mouse IgG were used as primary and secondary antibodies, respectively. The blot was developed with Amersham ECL kit (GE Healthcare) and exposed on a Kodak Bioquant system.

Biotin analysis: HABA-avidin complex method works on the ability of binding of HABA with avidin to give an absorption band at 500nm. The absorption decreases proportionately as biotin is added to the solution to displace HABA. By measuring the decrease in absorbance at 500nm, the amount of biotin in different solutions was measured. Then amount of Tat protein was calculated considering 1:1 molar ratio of biotin to Tat. Accuracy of the analysis was tested by adding known quantity of biotinylated-BSA in different BL solutions.

For the biocatalysis part of the research, the analytical techniques used were as follows.

Analysis of PAH and PLL: PLL and PAH were quantified with a Total Organic Carbon (TOC) analyzer from Shimadzu (TOC 5000 A) using a calibration curve in the range of 5-100 ppm. The analytical error for this analysis was 5-10 %.

Analysis of PSS: PSS in a layer was quantified by measuring the absorbance in feed, permeate and wash directly at 261 nm using the UV-VIS spectrometer. The linear range of detection for PSS was 1-400 ppm and the analytical error was less than 1 %.

Analysis of GOX: Amount of GOX in a solution was determined by the well known Bradford Protein Assay (Bradford) using a calibration curve prepared from GOX at 595 nm. The linear range of Bradford Protein Assay was 1-24 μg/ml and the analytical error was less than 1 % for 2-24 μg/ml and 1-10 % for 1-2 μg/ml of GOX in this research work.

Analysis of H_2O_2: H_2O_2 in solution was analyzed by a colorimetric method (Clapp et al. 1989) using acidified titanium oxysulfate and measuring the absorbance at 407 nm. The linear range of calibration for H_2O_2 analysis was 0.03-3 mM (1-100 ppm), and the analytical error was less than 5 % for 1-3 mM and 5-10 % for 0.03-1 mM.

3.4 Functionalization of membranes

3.4.1 Covalent immobilization of avidin in anhydride activated nylon membrane

Avidin was covalently immobilized on commercially available anhydride activated nylon membrane by permeating in 0.05 M Na_2HPO_4 buffer (pH 9) at room temperature (25 ^{0}C) and 0.68 bar (10 psi) pressure with constant stirring at 300 rpm. Pressure in the cell was maintained by N_2 gas. Avidin molecules became covalently attached with the acyl-anhydride groups present in the membrane following the reaction scheme shown in Figure 3.1. The avidin solution was recycled twice to attain the saturation capacity. After immobilization of avidin, the membrane matrix was washed with 50 ml of 0.25 M NaCl solution to remove the reversibly adsorbed molecules from the membrane.

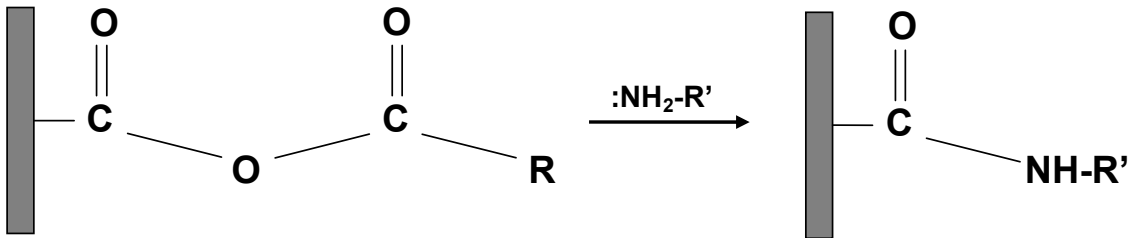

Figure 3.1 Reaction scheme for covalent immobilization of primary amine group containing molecule ($:NH_2\text{-}R^{'}$) in activated nylon membrane. ($:NH_2\text{-}R^{''}$) could be avidin or poly(L-Lysine) or GOX

3.4.2 Functionalization of anhydride activated nylon membranes based on LBL technique for electrostatic immobilization of GOX

Development of LBL assembly in activated nylon membrane: Layers of polyelectrolytes, mainly within the membrane pores, was assembled by alternative electrostatic attachment of cationic and anionic polyelectrolytes under convective flow and constant stirring conditions (Figure 3.2). For all layer formation steps, convective flow was maintained by applying pressure using N_2 gas. Convective flow was applied to achieve the functionalization mainly within the membrane pores. Membrane pores were preferred because of higher pore surface area over external membrane surface area. The immobilization was non-stoichiometric. In order to ensure non-stoichiometric attachment of subsequent layers, all layer formation steps were carried out in presence of 0.25 M NaCl solution. The shielding effect of salt increases the availability of free charges for the next layer.

In order to impart stability in subsequent layers, the first layer of PLL was attached covalently in the membrane matrix. This was done by the reaction between the terminal amine group of PLL and anhydride group of the membrane (Figure 3.1). The first layer of PLL was attached by permeating 100 ml of 40 ppm PLL solution (4mg or 0.039 μmole PLL) in DIUF at 0.07 bar (1 psi) pressure, pH 9.3. The solution was recirculated once. After that, the membrane was washed to get rid off the loosely adsorbed molecules. The recirculation and washing steps were followed for all other layer formation steps as well. As the first layer, PLL was preferred over PAH, because the difference of pK_a between the terminal amine group ($pK_a \sim 9$) and amine groups in the side chains ($pK_a \sim 10.5$) of PLL is precisely known. Hence, at a pH of around 9.3, the terminal amine group is uncharged, and therefore, forms covalent attachment preferentially over the side chain amine groups, which are positively charged at that pH. This has enhanced the probability of single point attachment of the first layer, rather than multipoint attachment through the side chain amine groups. The side chain amine groups provide free positive charges available for the next layer formation step. Layer formation on surface was minimized by high stirring and never allowing the feed side volume to go below 20 ml.

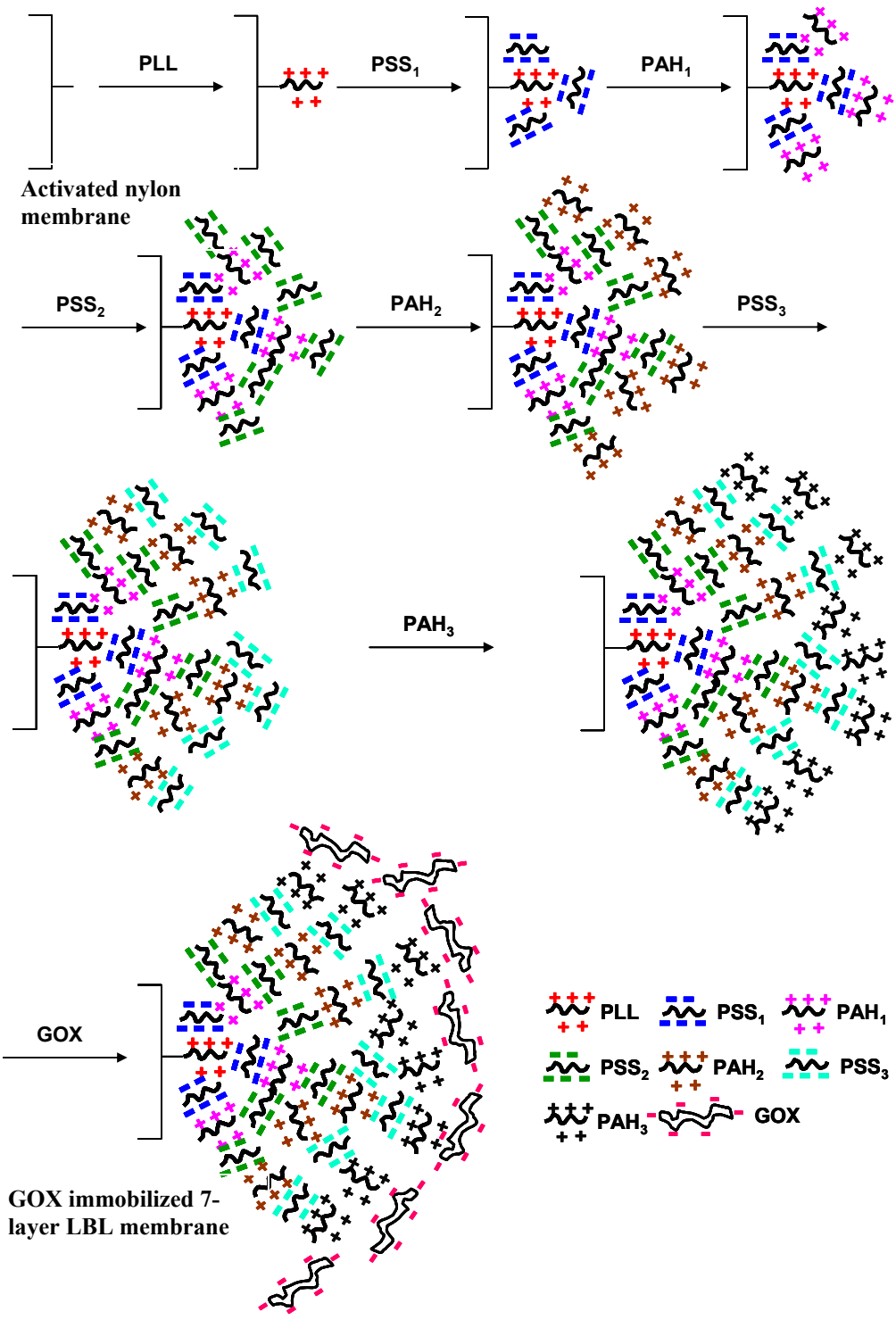

Figure 3.2 Schematic of formation of 7-layers of polyelectrolytes inside an anhydride activated nylon based membrane using Layer-By-Layer (LBL) technique followed by electrostatic immobilization of GOX

The second layer of PSS was attached by electrostatic interaction between the side chain amine groups of PLL and sulfonic acid groups (pK_a ~2.0-2.5) of PSS. 100 ml of ~400 ppm solution (40 mg PSS, 0.2 mmole of negative charges based on repeat units) of PSS was permeated in DIUF at pH 6. At working pH of 6, the net charge on amine groups of PLL is positive, whereas, the net charge on sulfonic acid groups of PSS is negative. So, they easily interact with each other.

The third layer of PAH was formed similarly by the electrostatic interaction between the negatively charged sulfonic acid groups of PSS and positively charged amine groups of PAH. PAH was attached by permeating 100 ml of 300 ppm solution (30 mg PAH, 0.3 mmole of negative charges based on repeat units) in DIUF at pH 6. In this case, PAH is preferred over PLL as it does the same function at a lower cost.

After this, two more bi-layers of PSS and PAH were attached in the membrane matrix to obtain PLL-$(PSS\text{-}PAH)_3$ as shown in Figure 3.2. In an earlier study (Smuleac et al. 2006) only 3 layers were assembled to study GOX activity. In current research, more layers have been introduced to increase the enzyme loading and also to decrease the core leakage (discussed later in Chapter 6) of the substrate molecules. The goal was to synthesize a net positively charged membrane in the working pH (i.e. ~6) so that GOX (P_I 4.2) can be attached using its negative charges. GOX was attached electrostatically in the absence of salt so that all the charges on membrane matrix could be neutralized by it.

Stability of each layer was checked by permeating solutions of varying pH, ranging from 2.7-9. The data of pure water flux as a function of pressure was obtained after the formation of each layer.

Electrostatic immobilization of GOX in LBL assembled membrane: After formation of PLL-$(PSS\text{-}PAH)_3$ layers, GOX was immobilized electrostatically by permeating 100 ml of 25 ppm solution (2.5 mg) in DIUF at pH 6. Then, the system was washed with DIUF. Feed, permeate and wash solutions were analyzed for GOX. The GOX functionalized LBL membrane was preserved at 4 ^{0}C. For comparison, covalent attachment of GOX was carried out by the reaction of the amine group of it with the anhydride groups in the Immunodyne membrane (Figure 3.1).

3.4.3 Functionalization of PVDF membrane by in-situ polymerization of acrylic acid for electrostatic immobilization of GOX

Functionalization of PVDF membrane: A method reported in literature (Gabriel and Gillberg 1993) was adopted to functionalize hydrophobic PVDF membrane with PAA by in-situ polymerization of acrylic acid monomer. The polymerization solution consists of 70 % toluene, 30 % acrylic acid, 0.5 % benzoyl peroxide and 1.2 % TMPTA by weight. Benzoyl peroxide was used as the initiator. To increase the stability and density of the polymer network inside the membrane matrix, TMPTA was used as the cross-linker. The membrane was dipped into polymerization solution for 30 sec, and then it was sandwiched between two Teflon plates and clipped tightly. It was then inserted into an oven at 90 ^{0}C for 4 hrs under constant N_2 environment. After that, the membrane was washed with copious amount of DIUF water under convective flow condition to remove impurities. The membrane obtained at this point was functionalized with hydrogen form (H-form) of PAA. It was converted to Na-form by permeating 200 ml of 0.1 M NaOH solution. Na-form helps resisting any drastic change in pH that generally occurs in H-form, for the following ion exchange steps. Flux of water and effect of pH on water flux through PAA-functionalized PVDF (PVDF-PAA) membrane was studied.

Electrostatic immobilization of GOX in PAA functionalized PVDF membrane: In order to electrostatically immobilize GOX in PAA-functionalized PVDF membrane, it was converted to a positively charged membrane. This was achieved by attaching a layer of PAH using same principle of electrostatical interaction (Figure 3.3) as used for PSS-PAH layer in LBL membrane. 100 ml of 300 ppm solution of PAH (30 mg PAH, 0.3 mmole of negative charges based on repeat units) in DIUF water at pH 6 was permeated through the PVDF-PAA membrane. The carboxylate anions of PAA have a pK_a of around 4.7. So, at pH 6, these groups interact with positively charged amine groups of PAH. After that, GOX was immobilized on PAH layer as demonstrated in Figure 3.3. The stability of the system was checked frequently by analyzing leakage of GOX in permeate. The GOX immobilized PVDF membrane was stored at 4 ^{0}C and reused.

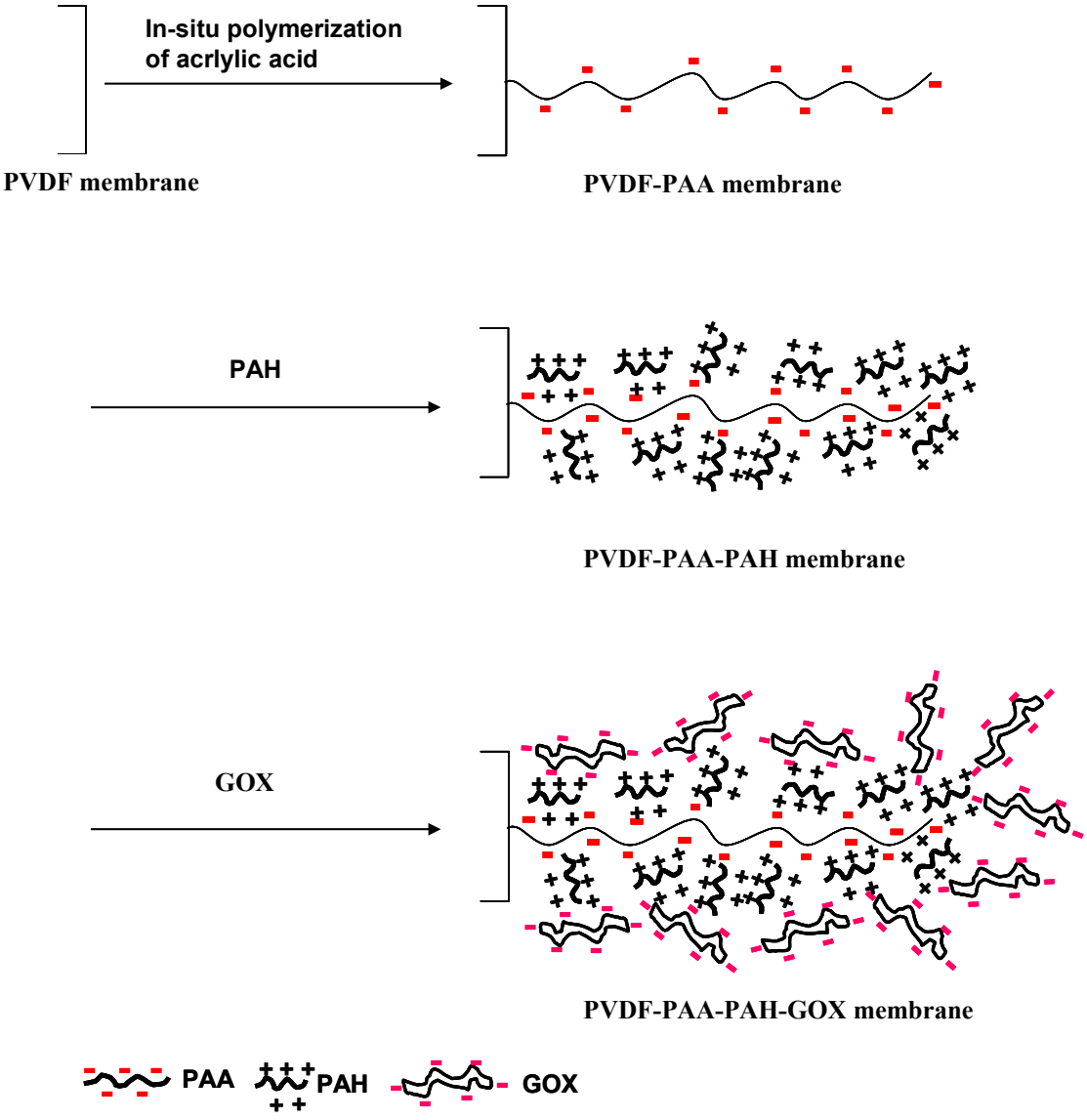

Figure 3.3 Schematic of functionalized PVDF membrane by PAA (shown here as a single chain for illustration purposes) and electrostatic attachment of PAH, followed by electrostatic immobilization of GOX

3.4.4 Functionalization of other unactivated base membranes

In this section, experimental procedure for functionalization of three base membranes, namely, CA, nylon and RC, with four different kinds of functional groups in different combinations, are described (Figure 3.4). The functional groups were carbonyl (for CA), epoxide (for all three), carbonyl imidazole (for nylon and RC) and di-epoxide (for RC). The activation reagents used were $NaIO_4$ (for CA), ECH (for all three), CDI (for nylon and RC) and BDDE (for RC). Functionalized membranes were developed in such a way that facilitates the immobilization of primary amine groups in the form of either a probe molecule (PABA) or a protein (avidin) or poly(allylamine hydrochloride).

Cellulose acetate (CA): CA membranes were functionalized using two different approaches. For both approaches, the acetate groups of the membranes were first hydrolyzed to hydroxyl groups by permeating 200 ml of 1:1 mixture of 0.01 M NaOH and 0.1 M NH_4OH. In the first case, the hydrolyzed cellulose membranes were treated with 5 g/l of $NaIO_4$ for 90 min to oxidize the hydroxyl groups to carbonyl groups. In another case, 5 % by volume solution of epichlorohydrin (ECH) in hot (50 ^{0}C), 0.5 M NaOH was permeated through the hydrolyzed cellulose membrane to attach the epoxide ring in the membrane matrix by forming an ether bond. This reaction is commonly known as base catalyzed Williamson synthesis of ether. The reaction schemes of functionalization of all base membranes are represented in Figure 3.4 along with the important conditions used.

Nylon: Nylon membranes were treated with 0.1 M HCl to expose its amine groups followed by attachment of epoxide groups by reacting with ECH. Reaction between the amine groups of nylon membrane and ECH is an example of base catalyzed nucleophilic substitution of the 2nd type (S_{N2}). In this reaction mechanism, the nucleophile attacks the less hindered primary carbon. In another approach, nylon membranes were functionalized by reacting with 1, 1'-carbonyldiimidazome (CDI). CDI was dissolved in anhydrous acetone and then permeated through the membrane. Since, CDI is prone to hydrolysis by even trace amount of water present in the solution, anhydrous acetone was used.

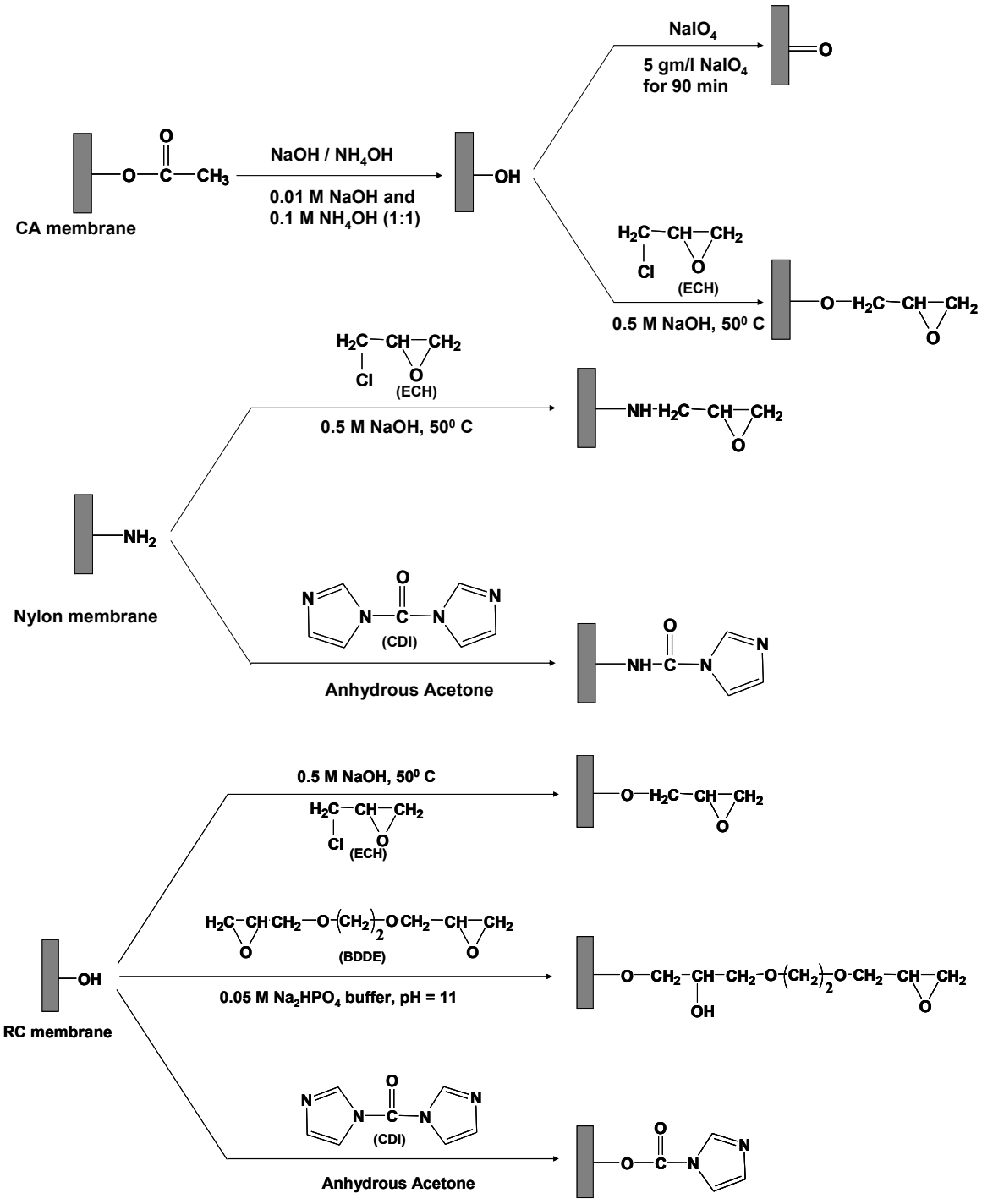

Figure 3.4 Reaction schemes showing functionalization of unactivated base membranes by different active groups. CA: Cellulose Acetate, RC: Regenerated Cellulose, ECH: Epichlorohydrin, CDI: 1, 1'-carbonyldiimidazole, BDDE: 1, 4-butanediol diglycidol ether

CDI reacts with the amine groups of the nylon membranes to form a carbonyl diamide by releasing one of the imidazole rings as shown in Figure 3.4. This intermediate diamide is sufficiently stable in aqueous solution (Hearn 1987). CDI activated membranes react readily with primary amine containing compounds, such as, proteins to release the other imidazole ring and form a very stable urea bond.

Regenerated cellulose (RC): RC membranes were functionalized using three different techniques as described in Figure 3.4. For all of them, the commercially purchased RC membranes were first washed with 2 % by volume aqueous solution of glycerol. Then, in the first two techniques, RC membranes were treated with ECH and CDI as described earlier for CA and nylon membranes, respectively. In the third one, it was reacted with BDDE, which contains two epoxide rings at the two ends. The condensation of first epoxide ring with hydroxyl group of RC membrane occurs at pH 11. To achieve that, BDDE was permeated by dissolving in Na_2HPO_4/NaOH buffer of pH 11. The second epoxide ring, which acts as the active functionality, condenses at pH 7-10.

Chemical characterization of functionalized membranes: Functionalized membranes derived from unactivated base membranes were chemically characterized to determine the extent of functionalization. The probe molecule used for this purpose was para-amino benzoic acid (PABA). 100 ppm solution of PABA in Na_2HPO_4 buffer (pH = 9) was permeated, followed by washing with 0.25 M NaCl to remove the adsorbed PABA. PABA in feed, permeate, retentate and wash was analyzed, and amount of active group was determined from amount of PABA attached.

Amine group of PABA, being a strong nucleophile, reacts with different active group present in membrane as demonstrated in Figure 3.5. For carbonyl activated CA, the amine group of PABA was involved in Schiff's base reaction to form C=N, which was then converted to C-N by reducing with $NaBH_4$. On the other hand, for epoxide activated CA, nylon and RC membranes, amine group of PABA was reacted by base catalyzed nucleophilic substitution of the 2nd type, i.e., the S_{N2}, to open the epoxide ring and form a stable C-N bond. During this reaction, the amine group preferred the less hindered primary carbon in the epoxide ring, a typical feature of base catalyzed S_{N2} reaction.

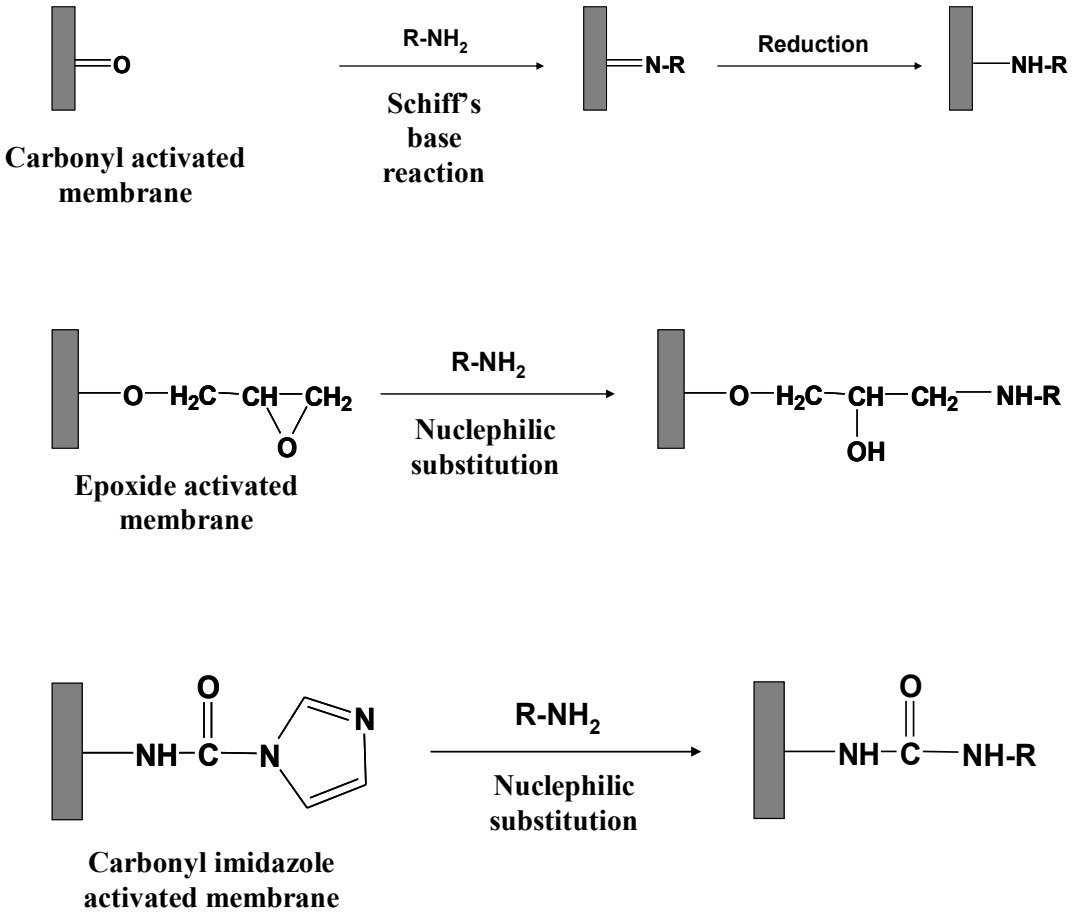

Figure 3.5 Reaction of carbonyl, carbonyl imidazole and epoxide activated membranes with primary amine containing molecules ($R\text{-}NH_2$), such as PABA, avidin, PAH, etc.

For a di-epoxide activated RC membrane, a similar reaction was occurred as mentioned earlier for epoxide activated membrane. For carbonyl imidazole activated nylon and RC membranes, the imidazole group was displaced due to the nucleophilic attack by amine group of PABA, and a highly stable urethane (for RC) or urea (for nylon) bond was formed.

Covalent immobilization of avidin in RC-ECH membrane: From the PABA attachment results and considering some other factors, which have been discussed later, further experiments were carried out with only functionalized RC-ECH membranes. 4.5 x 10^{-2} μmole (3 mg) of avidin was dissolved in 100 ml of 0.05 M Na_2HPO_4 buffer (pH 9) and permeated through the membrane. Avidin molecules became covalently immobilized in the RC-ECH membrane by the reaction between the amine groups of it and the epoxide groups present in membrane (Figure 3.5). Non-specifically adsorbed avidin was removed from the membranes by washing with 0.25 M NaCl solution. Avidin immobilized in the membrane was quantified by analyzing it in feed, permeate, retentate and wash solutions. This membrane was used further for affinity separation of Tat.

Formation of LBL assembly in RC-ECH membrane: Attachment of polyelectrolytes based on LBL technique was carried out in same fashion as mentioned earlier for activated nylon (Immounodyne) membrane. In this case, PAH was attached as the first layer by covalent immobilization of amine group with the epoxide ring present in the membrane (Figure 3.5). In order to establish that LBL technique works satisfactorily in RC-ECH membrane, avidin was used as a model protein. Avidin has an isoelectric point of 10, and hence the final layer of the membrane was kept negative using PSS. Avidin was electrostatically attached, in the negatively charged membrane at pH 6, utilizing the net positive charge at that pH. Amount of avidin attached was quantified using the Bradford Assay. This experiment was done just to demonstrate that functionalized RC-ECH membrane can potentially be used for development of LBL assembly.

3.5 Separation and purification of HIV-Tat protein in avidin functionalized membranes

This section describes the experimental procedures for quantification of covalently immobilized avidin sites by probe biotinylated compounds. Different steps of affinity separation of Tat from BL in avidin functionalized membranes are also discussed in detail along with a brief description of column chromatographic separation of Tat.

3.5.1 Accessibility of covalently immobilized avidin sites in nylon membrane by biotin moieties present in different species

Accessibility of avidin sites by biotin present in homogeneous phase was determined using probe biotinylated molecule, biotin, 4-amidobenzoic acid (BABA, 1mole of BABA is equivalent to 1 mole of biotin). Avidin and BABA was mixed in 0.05 M Na_2HPO_4 buffer (pH = 9). Samples were collected at different time intervals, unreacted BABA was separated from avidin-BABA complex and unreacted avidin using ultrafiltration membrane, followed by analysis of BABA.

Single membrane (diameter 6.5 cm, external surface area 33.2 cm^2, bed volume = external surface area x thickness = 0.55 ml) was used for permeation of (i) BABA (0.6, 3.2 and 9.6 μg/ml), (ii) BBSA (3, 10, 19.3 μg/ml) and (iii) 10 μg/ml BBSA in mixture with a non-biotinylated protein, Gamma Globulin (GG). BABA and BBSA solutions were prepared in 0.05 M Na_2HPO_4 buffer (pH 9) and permeated at room temperature and 0.34 bar (5 psi) pressure with constant stirring at 300 rpm. It was observed that accessibility of avidin sites by biotin is independent of number of membranes present. Therefore, a single membrane was used for accessibility studies, whereas a 4-stack membranes system was used for Tat separation experiments. Volumetric flow rate and cumulative volume of permeates were measured as a function of time. After permeating BABA, BBSA and BBSA+GG, the membrane matrix was washed with 100 ml of 0.25 M NaCl solution to remove the reversibly adsorbed molecules from the membrane.

Total protein present in membrane can be classified into two categories: (i) specifically attached proteins (avidin-biotin interaction) and (ii) non-specifically adsorbed

proteins (protein-membrane and protein-protein interaction), which consisted of reversibly and irreversibly adsorbed proteins. Reversibly adsorbed proteins were quantified as stated earlier. To quantify the irreversibly adsorbed proteins for BBSA, separate permeation experiments were carried out with non-biotinylated protein (BSA) under the same conditions and concentrations. While calculating the accessibility of avidin sites, non-specifically adsorbed protein quantity was deducted from the total proteins in membrane to estimate the specifically attached proteins. To analyze the formation of protein layers in the membranes, pure water flow rate was measured through bare membranes, after immobilization of avidin and after permeation of protein.

3.5.2 Affinity separation of HIV-Tat protein from bacterial lysate (BL)

Affinity based membrane separation of a specific protein from mixture of proteins is achieved using the knowledge of molecular biology and membrane technology. It consists of the following steps (Figure 3.6): (i) immobilization of a ligand, which has specific affinity towards the target protein, on the pore walls of membrane, (ii) selective attachment of the target protein from a mixture to the membrane by ligand-protein interaction, (iii) purification of the attached protein by removing the impurities and (iv) elution of target protein from membrane by disrupting protein-ligand interaction. The activity of the immobilized ligand depends on the method of immobilization in the membranes. The membrane allows the protein molecules to permeate through the pores. While permeating through the pores, target protein molecules have easy convective access to the immobilized ligands. Besides that, the bigger pores facilitate a wide range of ligand immobilization techniques without hindering the flow of the permeate significantly.

Production of biotinylated-Tat: To isolate Tat protein based on avidin-biotin interaction, it is genetically engineered to introduce biotin structure by gene fusion while cloning in the cell of *E.Coli*. vector. It is expressed in *E. Coli.*, followed by lysing of the bacterial cells using French pressure cell press (SLM Amimco). Then, the fermentation broth was centrifuged at 10000g rpm to remove cell debris and precipitates.

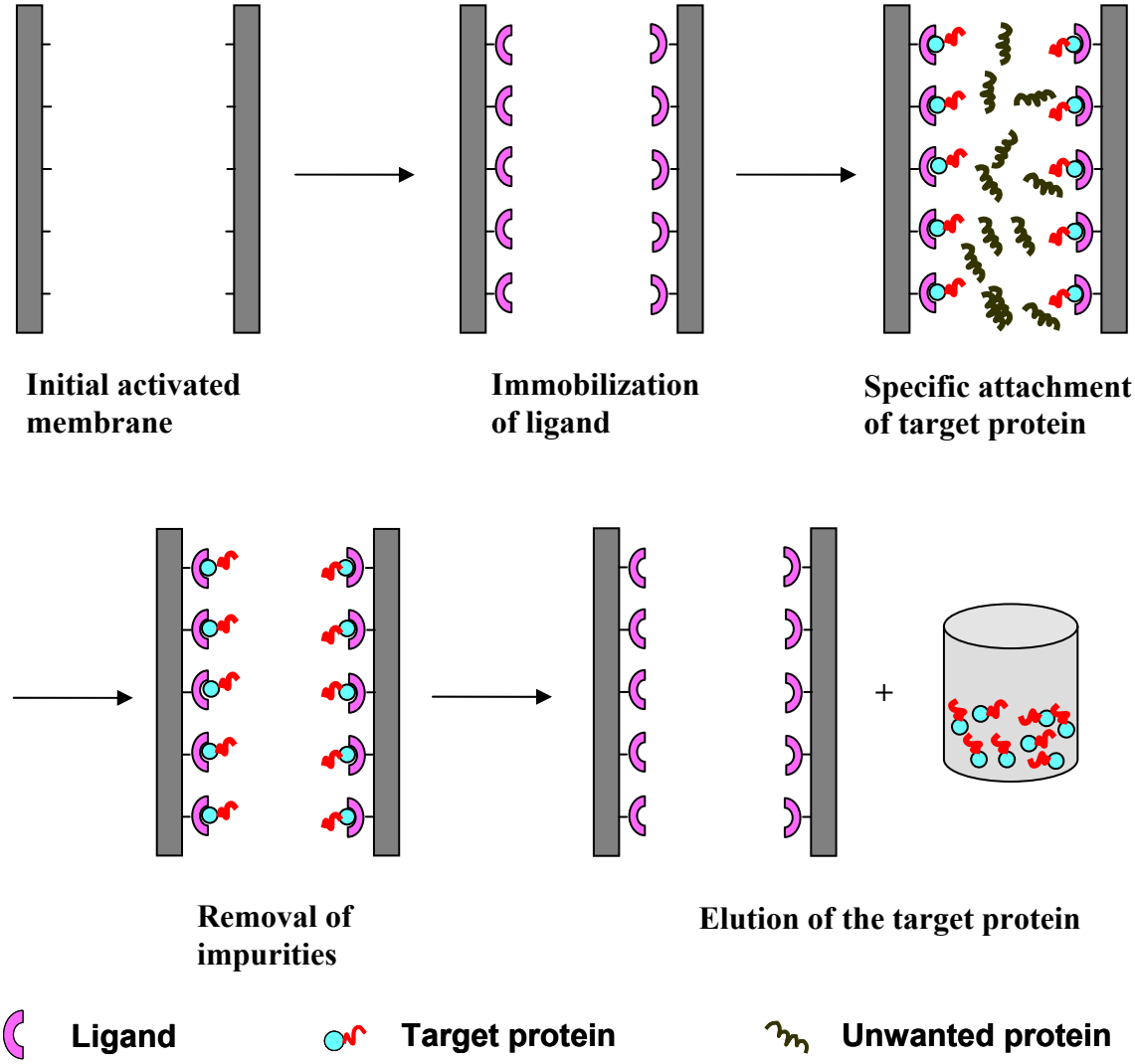

Figure 3.6 Schematics of basic steps involved in affinity based membrane separation of a target protein from mixture of proteins

The supernatant, containing biotinylated-Tat (1-3 %) along with other proteins, is known as bacterial lysate (BL).Genetically engineered Tat contains a fusion protein, which bridges between the biotin moiety and the protein as shown in Figure 3.7. BL supernatant, containing biotinylated-Tat along with other proteins and impurities, was then treated separately by membrane and conventional packed-bead chromatography to obtain pure Tat.

A. Affinity membrane separation of Tat: The experimental steps for the pretreatment, separation and purification of Tat from BL are presented in Figure 3.8.

Pretreatment of bacterial lysate (BL): BL supernatant contains exposed biotinylated Tat, which are available for binding with avidin. It also contains biotinylated Tat, which are entangled within other protein aggregates due to non-specific protein-protein interactions. Formation of these aggregates depends on the nature of the solution (dilution and ionic strength). The entangled Tat never comes in contact with avidin as shown in Figure 3.7. Pre-treatment (dilution and addition of chemicals) of BL supernatant was necessary to disentangle Tat from those protein aggregates in order to maximize the exposed biotinylated Tat. The primary objective of bacterial lysate pretreatment was to mitigate protein-protein and Tat-RNA interactions to increase the quantity of free Tat in solution.

It was observed that by diluting BL and applying a higher salt concentration, the aggregate formation between proteins can be reduced, thereby increasing the available free Tat in the BL (Hollman et al. 2005). To study the effect of dilution and salt concentration on the amount of available free Tat in BL, two separate experiments were carried out. In one experiment, 1 ml of stock BL was diluted by varying dilution factor in the range of 1-1000 with 0.1 M (0.1×10^3 μmoles/ml) NaCl. In another experiment, 1 ml of BL was diluted (dilution factor 10) with 0, 0.1, 0.25 and 0.5 M NaCl solutions. ELISA was carried out to measure the amount of Tat in solutions. The results of these experiments are discussed later in Chapter 5; however, it is worth mentioning here that amount of available free Tat in BL was found to increase with increase in dilution factor up to around 150. After that it remained constant.

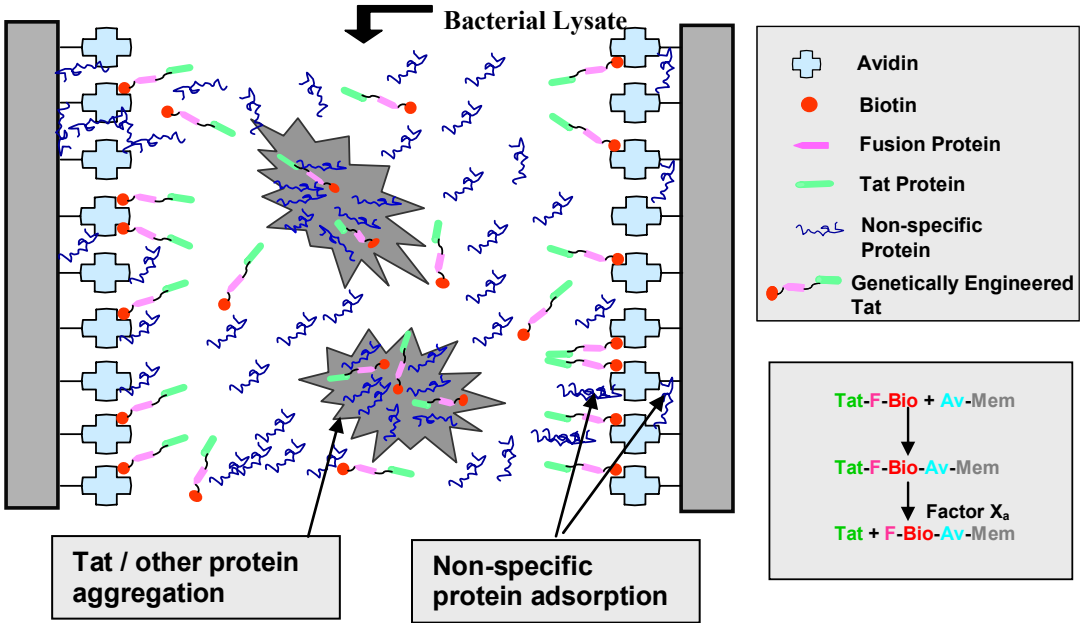

Figure 3.7 Schematic of separation of Tat protein from bacterial lysate using avidin-biotin interaction in a functionalized membrane pore. Biotinylated-Tat (Bio-F-Tat) forms a complex (Tat-F-Bio-Av-Mem) with avidin immobilized membrane (Av-Mem). Tat is then isolated by cleaving the Tat-Fusion protein bond with Factor X_a

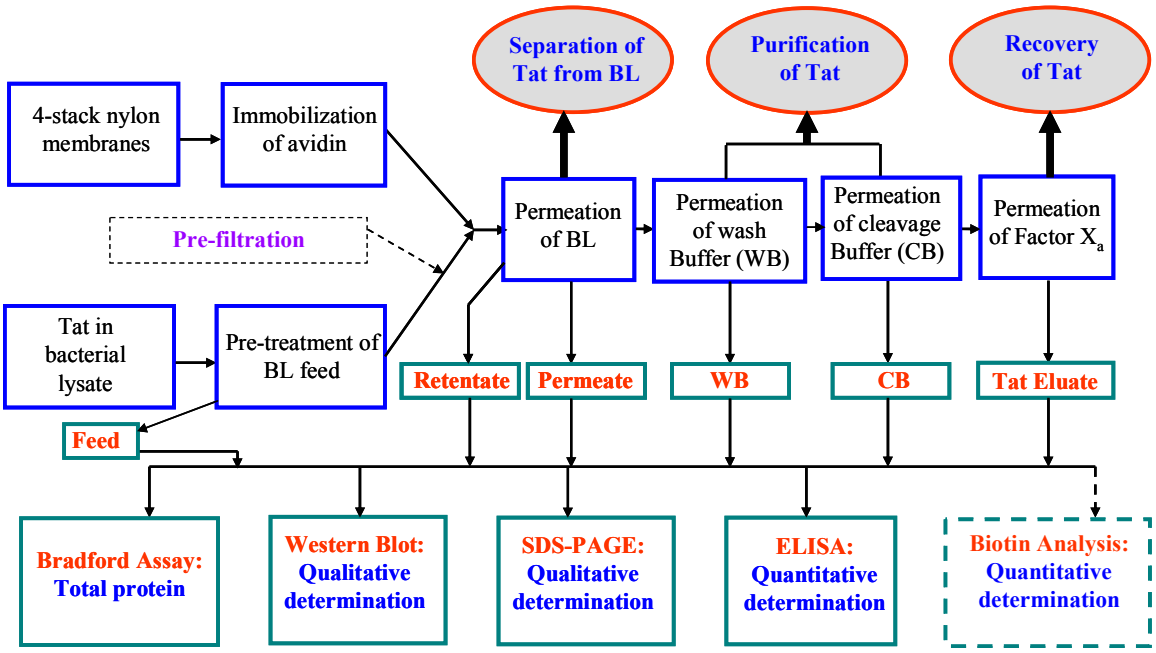

Figure 3.8 Experimental steps for the separation and purification of Tat from Bacterial Lysate (BL) using avidin-biotin interaction in functionalized stacked membranes. In few experiments, a pre-filtration step (shown as a dotted box) was introduced to remove unwanted proteins and impurities prior to the affinity separation

On the other hand, amount of available free Tat was observed to increase linearly in the range of NaCl concentration studied. Therefore, the feed for affinity separation was prepared by diluting BL supernatant in desired ratio with 0.5 M NaCl.

Further, it was observed that the basic region of Tat protein has a high affinity to form a Tat-RNA complex (Rana and Jeang 1999), which alters the binding affinity of Tat with the immobilized avidin due to steric hindrance. Hence, 25 μg RNAse per ml of BL was added to degrade RNA and eradicate the formation of Tat-RNA complex. Other than these, dithiothreitol (DTT) was added as antioxidant and phenylmethylsulphonylfluoride (PMSF) was added as protease inhibitor.

Separation of Tat**:** Biotinylated-Tat present in BL was separated by permeating through an avidin immobilized nylon membranes matrix. Membrane matrix consisted of 4 membrane sheets arranged in stacked configuration to provide greater internal surface area for avidin immobilization. While permeating through the membrane, Biotinylated Tat interacted with avidin and attached to the membrane matrix, while other proteins present in the mixture permeated through (Figure 3.7). Some non-biotinylated proteins were also adsorbed into the membrane due to non-specific protein-membrane interaction.

In this dissertation, results obtained from two different dilution factor experiments are discussed. In one experiment 10 ml and in another 15 ml of BL was diluted to 300 ml with 0.5 M NaCl. Diluted BL solution was then permeated at 0.34 bar pressure, and the permeate flow rate and cumulative volume were measured at different time intervals.

In order to demonstrate that avidin immobilized RC-ECH membrane can also be used for affinity separation of Tat; separate experiments were carried out with stack of 4 avidin immobilized RC-ECH membranes. All other steps of were identical as affinity separation of Tat using avidin immobilized nylon membranes.

Purification and isolation of Tat: After separating Tat from other proteins, the membrane module was treated with suitable wash solutions to remove the non-specifically adsorbed proteins. 75 ml of wash buffer 1 (WB1; 0.05 M Tris HCl pH 8, 0.1 M NaCl, 1.6×10^{-5} M Triton X-100, and 0.031 M NaN_3, 30 μl 1 M DTT, 20 μl PMSF) containing both PMSF and DTT was permeated first, followed by permeation of wash buffer 2 (WB 2) devoid of

PMSF. The system was then preconditioned for cleavage with 100 ml cleavage buffer (CB; 0.05 M Tris HCl pH 8, 0.10 M NaCl, 0.001 M $CaCl_2$, and 0.031 M NaN_3, 30 µl 1 M DTT) containing DTT, but no PMSF. Purified Tat was then eluted by disrupting the fusion protein-Tat bond from the membrane module using 20 µg Factor X_a (cleavage protease) per ml of cleavage buffer. Restriction protease, Factor X_a, has a specific cleavage location after arginine residue in the sequence of Ile-[Glu or Asp]-Gly-Arg (Nagai and Thøgersen 1984).

Characterization of purified Tat: Before analyzing the isolated Tat, it was desalted using size-based packed-bead (polyacrylamide) column chromatography, followed by endotoxin removal in an affinity column containing Polymixin B beads (Pierce Biotechnology). The purified protein obtained in this research was characterized by SDS-PAGE, Western Blot Analysis, and ELISA. Fouling within the membranes was characterized by Scanning Electron Microscopy (SEM). SDS-PAGE and Western Blot analysis were carried out to qualitatively determine, and ELISA was done to quantitatively determine Tat in BL feed, permeate, retentate, WB permeate, CB permeate and the eluate. For BL permeation, to analyze the protein layer formed in the membranes, pure water flow rate through the 4-stack membrane matrix was measured before and after the permeation of BL as done for other protein solutions.

B. Column chromatographic affinity separation of Tat: Packed-bead column chromatographic separation of Tat was conducted in the Department of Anatomy and Neurobiology, University of Kentucky. Separation of biotinylated Tat was achieved by equilibrating BL supernatant with 5 ml of avidin containing agarose beads (Ultralink Immobilized NeutrAvidin from Pierce Biotechnology) in 30 ml of cell lysing buffer for 2 hours. The binding capacity of the beads was $5 \times 10^{-2} - 8 \times 10^{-2}$ µmoles biotin/ml of beads. The purification and elution steps followed the same protocols; however, the major difference in principle was the use of diffusive mode instead of convective mode.

3.6 Effect of pre-filtration on affinity membrane separation of Tat

3.6.1 Pre-filtration

A pre-filtration step was incorporated just after the pre-treatment step and prior to affinity separation step as shown in Figure 3.8. The pre-treated (30 times dilution, 0.5 M NaCl, 25 μg RNAse/ml BL, 30 μl DTT, 20 μl PMSF) BL supernatant was subjected to UF in one case and MF in other. All pre-filtration experiments were carried out at 25 ^{0}C with constant stirring at 300 rpm. The trans-membrane pressure for UF was 1.36 bar (20 psi) and for MF was 0.34 bar (5 psi). Pressure in the cell was maintained by N_2 gas. To study the effect of pre-filtration on BL feed, biotin analysis and total protein analysis were carried out on pre-filtration feed and permeate. Since, the pre-filtration feed (i.e. diluted BL supernatant) contained significant amount of impurities, direct measurement of biotin was erroneous. In order to get accurate measure of total biotin, the feed was digested with 10 % by volume of 6N HCl at 120 ^{0}C for 12 hrs until all proteins hydrolyze, but biotin structure remains same. Then, biotin analysis was carried out to obtain total biotin (exposed + entangled) present. For pre-filtration permeate, both direct analysis of biotin and analysis of biotin from the digested fraction of permeate were carried out. SDS-PAGE images were obtained to observe the effect of pre-filtration on BL feed. Characteristic flux decline behavior was also studied for pre-filtration experiments. Permeate of pre-filtration experiments were used directly as BL feed (UF BL feed and MF BL feed) in affinity separation experiments.

3.6.2 Affinity membrane separation of Tat from pre-filtered BL feed

Tat protein was separated from BL feed following exact same procedure as described in sub-section 3.5.2. The only difference was the use of pre-filtered BL feed instead of unfiltered BL feed to the affinity membrane system. After that, biotin analysis was carried out on different streams to quantify biotinylated Tat. Then material balance was done on biotinylated Tat present in different streams to determine the amount of Tat separated by membrane based affinity separation. From that the normalized accessibility of avidin sites was calculated and discussed later in Chapter 5. Due to specific cleavage

location of restriction protease, Factor X_a, purified Tat eluate ideally should not contain any biotin. But, for column chromatographically purified Tat eluate, biotin impurities have been identified by HABA-avidin complex analysis. Hence the same analysis was also carried out for membrane purified Tat eluate. SDS-PAGE and Western Blot analysis were also carried out to check the purity of the membrane purified Tat and compare with column chromatographically purified Tat. The results obtained for pre-filtered BL feed (both MF BL and UF BL) are also compared with that obtained for unfiltered BL feed.

3.7 Enzymatic oxidation of glucose by electrostatically immobilized GOX in LBL assembled nylon membrane and functionalized PVDF membrane

This section describes the experimental protocols of the enzymatic oxidation of glucose using electrostatically immobilized GOX in LBL functionalized nylon membrane and functionalized PVDF membrane. Detachment of GOX from membrane matrix and reattachment of the detached GOX are also stated.

3.7.1 Activity study of electrostatically immobilized GOX in LBL functionalized nylon membrane

All the activity measurement experiments were performed in 50 mM sodium acetate-HCl buffer (NaOAC-HCl buffer) saturated with O_2, and under constant pressure of air. NaOH and HCl were used to adjust the pH of the solution. Activity was determined by measuring the concentration of H_2O_2 in permeate. Permeate glucose solutions were tested frequently to determine any GOX leakage from the system. β-D (+) Glucose is referred as glucose in the text.

Steady state determination: Oxidation of glucose by GOX, in this case, was a biocatalytic reaction carried out in a constant flow reactor. Hence, condition of steady state prevails. In order to get an idea about the time needed to reach the steady state, experiments were conducted with 15 and 75 mM glucose solution at constant flow rate through the GOX-LBL membrane. Permeates were collected as a function of time.

Importance of O_2: Oxygen is very important in the second step of the two step reaction mechanism of catalytic oxidation of glucose. Monitoring the effect of variation of O_2 on the reaction was out of scope of this research work. In fact, in order to ensure excess O_2 in the media throughout the reaction, the system was designed with oxygen saturated buffer and also kept under constant pressure of air. However, to study the consequences of depletion of O_2 from the reaction media, constant flow rate experiment was carried out with initial air purging. After certain time air supply was replaced by supply of N_2, which gradually started removing O_2 from the solution. Then again, air supply was re-established. Activity of GOX was observed as a function of time through out the reaction.

Kinetic study: Activity of free GOX in homogeneous phase reaction was studied as a function of time in a batch reactor at pH 5.5. The concentration of glucose was varied from 0.15-75 mM. For all experiments O_2 saturated buffer was used and air was purged into the reactor continuously. Samples were collected at different time intervals and activity was determined by analyzing H_2O_2 formed.

For electrostatically immobilized GOX in LBL membrane (LBL-GOX-convective), glucose concentration was varied from 0.15-75 mM for different experiments, while flow rate was adjusted such that the condition of equal residence time prevails for all the kinetic experiments. In order to study the kinetics of the same GOX immobilized LBL membrane in diffusive mode (LBL-GOX-soaking), experiments were carried out by soaking the membrane in glucose solution and measuring the activity of GOX in reaction mixture as a function of time. Kinetics of covalently attached GOX was studied under convective mode and represented as covalent-GOX-convective.

Effect of residence time i.e., flow rate: Effect of residence time on the activity of GOX was studied by varying permeate flow rate for a fixed concentration of glucose solution at pH 5.5. Flow rate was varied from 2-25 ml/min by changing the pressure from 0.34-3.4 bar (5-50 psi).

Effect of pH: Effect of pH on the activity of GOX was studied by varying pH from 4.5-7, for a fixed concentration of glucose solution at a constant flow rate. Homogeneous phase experiments for free GOX were also carried out with pH varying in the same range.

Stability of GOX immobilized in LBL membrane: Stability of GOX, immobilized in LBL assembled membrane, was studied by measuring the activity after every 7 days for a total of 28 days. While not including, the membrane was stored at 4 ^{0}C. A 15 mM glucose solution at pH 5.5 was used for all stability studies.

Detachment and re-attachment of GOX in the same LBL functionalized membrane: Immobilized GOX, activity of which has already been studied, was detached from the membrane matrix by permeating 50 ml DIUF water of pH 3 at 10-15 psi. After detachment, the pH of the solution was immediately adjusted to 5.5. Activity of any undetached GOX in the membrane matrix was determined by permeating glucose solution at pH 5.5. Amount of detached GOX was quantified by analyzing the solution using the Bradford Assay. The activity of the detached GOX in free form was determined by homogeneous phase batch reaction at pH 5.5. The rest of the detached GOX was then reattached in the same membrane matrix using principle of electrostatic interaction. The activity of the reattached GOX in the membrane was determined as earlier. The steps of detachment and reattachment were repeated. Attachment of fresh GOX in the same membrane matrix was also performed followed by the activity study.

3.7.2 Activity study of electrostatically immobilized GOX in functionalized PVDF membrane

Kinetic study of immobilized GOX in functionalized PVDF membrane (PVDF-GOX-convective) and effect of residence time i.e., flow rate, on activity were studied similarly as carried out for LBL membrane.

Reusability of GOX immobilized PVDF membrane: The functionalized PVDF membranes were reused for GOX immobilization. When, the activity of GOX went below the acceptable value, the system was regenerated by detaching the used GOX and attaching fresh GOX in the same PVDF-PAA membrane. This was done by permeating DIUF water of pH 4 at convective flow mode. However, there was a fundamental difference in regeneration of this membrane matrix with LBL membrane matrix. The pK_a of amine groups of PAH is 9.5 and the P_I of GOX is 4.2. Hence, in order to nullify the electrostatic interaction and detach GOX, the pH of the detaching solution should be less than 4.2. But, at that pH the interaction between PAH and PAA also vanishes as the pKa of carboxylic acid groups of PAA is around 4.7. Thus, the detaching solution dislocates the whole PAH-GOX domain from the PVDF-PAA matrix. To reattach fresh GOX in the same membrane, PAH layer was re-introduced as stated earlier, followed by electrostatic immobilization of GOX. Stability of the domain and activity of fresh GOX were tested.

Chapter 4 Functionalization of Membranes

This Chapter deals with functionalization of different membranes carried out for various applications.

4.1 Results and discussion

In this section, results obtained for random covalent immobilization of avidin in acyl-anhydride activated nylon membranes are presented. Electrostatic immobilization of GOX in Layer-By-Layer (LBL) functionalized nylon membrane (LBL-GOX) and polyacrylic acid (PAA) functionalized PVDF membrane (PVDF-GOX) are described. Characterization of these two types of membranes is also demonstrated. Additionally, the extent of functionalization of unactivated membranes (CA, nylon and RC) are presented in terms of probe molecule, para-aminobenzoic acid (PABA). This is followed by a brief discussion of covalent immobilization of avidin in RC-ECH membrane and electrostatic immobilization of avidin in LBL assembly developed within the RC-ECH membrane.

4.1.1 Covalently immobilized avidin in anhydride activated nylon membrane

To study the variation in the amount of avidin immobilized, both single membranes and 4-stack membranes matrices were tested. Based on the information supplied by the manufacturer, the acylanhydride groups present in a membrane (bed volume 0.55 ml, external membrane area 33.2 cm^2) could covalently immobilize 2.4 x 10^{-2} - 3.3 x 10^{-2} μmoles of avidin/ml bed volume, when spot loaded with 4000 μg/ml avidin solution in PBS buffer and allowed to react for 15 min at pH 7-9. However in our research, for the single membranes, immobilization of avidin was 3.8 x 10^{-2} – 5.1 x 10^{-2} μmoles/ml bed volume (6.3 x 10^{-4} – 8.5 x 10^{-4} μmole/cm^2 external membrane area). This corresponds to a biotin binding capacity (based on biotin : avidin = 3.6 : 1) of 13.7 x 10^{-2} – 18.4 x 10^{-2} μmoles /ml bed volume. The avidin to biotin ratio of 1:3.6 is obtained from homogeneous phase avidin-biotin interaction experiment. Due to convective flow within the membrane pores, the avidin molecules could easily access the acylanhydride groups,

and therefore the amount of avidin immobilized was significantly higher for these experiments. The variation in the amount of avidin immobilized was due to the presence of different amount of acylanhydride groups in different membranes and multiple attachment of single molecule of avidin with their different amine groups. For 4-stack membranes matrices (bed volume = 4 x 0.55 = 2.2 ml), the immobilization of avidin varied from 2.2 x 10^{-2} μmoles avidin / ml bed volume (corresponding to biotin binding capacity of 7.9 x 10^{-2} μmoles / ml bed volume) to 4.5 x 10^{-2} μmoles avidin / ml bed volume (corresponding to biotin binding capacity of 16.2 x 10^{-2} μmoles /ml bed volume).

The effective thickness of the covalently immobilized avidin layer in the membranes, δ_{avidin}, was calculated (applying Hagen-Poiseuille's equation) using the water flow rate data obtained before and after permeating avidin solution. Depending on the amount of avidin immobilized, calculated δ_{avidin} varied within 9 - 13 nm. The calculation of δ_{avidin} is discussed in detail later while explaining the results of fouling in Chapter 5. Due to immobilization of avidin, 15-20 % decrease in water flux was observed for all the membranes. The initial flux through the avidin-immobilized membranes (J_{v0}) was 14 x 10^{-4} - 24 x 10^{-4} $cm^3/cm^2.s$ (corresponds to a flow rate of 3 - 5 ml/min) at 0.34 bar. Based on the initial flux through avidin-immobilized membrane and the porosity determined from water sorption experiment, the approximate initial linear velocity through the pores was calculated to be 370 - 620 cm/h. At this linear velocity the residence time through a 4-stack membranes system would be 1.6 - 2.6 sec.

4.1.2 Electrostatically immobilized GOX in LBL assembled nylon membrane and functionalized PVDF membrane

Bio-catalytic reactions with free enzyme in homogeneous phase possess the advantage of higher activity, but its use is limited due to lower stability, inhibition from product and lack of reusability. As an alternative, enzyme is immobilized covalently in a solid matrix and then used as a catalyst. The advantages of immobilized enzyme over free enzyme are; (i) stability due to the protective action of the solid matrix, (ii) reusability as it is confined in the solid support and (iii) ease of operating under continuous flow mode. However, the biggest disadvantage is the lower activity of the immobilized enzyme.

Sometimes, the activity is as low as 10 % of the activity of free enzyme (Cheryan M. 1986). The lower activity can be attributed to the proximity of the active sites of enzyme to the solid matrix. The solid matrix reduces the accessibility of active sites, causes a conformational change of the enzyme and offers diffusional resistance. Membrane is a common solid support for enzyme immobilization. Diffusional resistance is minimized by permeating the substrate solution under convective flow condition. Researchers have studied site-directed immobilization of enzymes to restrict conformation change, and hence, increase the accessibility (Butterfield and Bhattacharyya 2003; Liu et al. 2001). However, site-directed immobilization requires complicated techniques, and it is considerably expensive.

A simple, but efficient alternative to traditional covalent immobilization of enzymes in solid matrix is to create a charged domain of polyelectrolytes inside the membrane pore, and then immobilize the enzyme using electrostatic interaction (Smuleac et al. 2006). This technique combines the benefits of activity of free enzyme in homogeneous phase along with the stability and reusability of the immobilized enzyme. The higher activity compare to covalent binding is due to the fact that the enzyme is loosely bound to the polymer matrix and away from the solid support. Hence, the chances of conformation change and the accessibility problem due to the proximity to the solid support are significantly less. There also exists a possibility of reusing the membrane matrix by detaching (eluting) the used enzyme, when needed, and attaching fresh enzyme.

For electrostatic immobilization of GOX, the functionalized membrane domain was positively charged and GOX was attached using its negative charges primarily from the carboxylic acid side chains of glutamic acid and aspartic acid residues. It is important to note the existence of one glutamic acid residue near the active site of GOX (Frederick et al. 1990; Hecht et al. 1993). This particular glutamic acid residue can play an important role in determining the activity of electrostatically immobilized GOX. It can also be observed from the sequence of amino acid residues of GOX (Frederick et al. 1990) that its negative charges are well distributed through out the structure. Hence, immobilizing it electrostatically means extending it in coil form and then attaching it loosely with the polymer domain at almost regular intervals. This conformation will expose its active sites.

Electrostatically immobilized GOX in LBL assembled nylon membrane

Characterization of LBL assembled nylon membrane: The amount of repeat units of polyelectrolyte attached in each layer was determined from different analytical procedures and represented in Table 4.1. A single repeat unit of all the polyelectrolytes contains a unit charge. Based on that, net charges in the subsequent layers are calculated and represented in the same Table. Since, the addition of layers were non-stoichiometric, there is no particular correlation between the amounts of polyelectrolytes attached in each layer.

However, it is important to note here, that each layer was associated with excess net opposite charges compare to the previous layer. This has governed the electrostatic attachment of next layer. The attachment of excess opposite charges was possible due to non-stoichiometric addition of polyelectrolytes in presence of salt. The net charge after the 7th layer of polyelectrolyte (PAH_3) mentioned in this dissertation was (+) ve.

Cumulative thickness of n-th layer (δ_n) is calculated by applying Hagen-Poiseuille's equation (Ho and Sirkar 1992) on water flux through the virgin membrane (Q_{w0}) and after attachment of the n-th layer (Q_{wn}) as shown below.

$$r_n = r_0\left(\frac{Q_{wn}}{Q_{w0}}\right)^{0.25} \tag{4.1}$$

$$\delta_n = r_0 - r_n \tag{4.2}$$

Permeability after n-th layer (P_n) in cc/cm^2-s-bar is calculated as follows:

$$P_n = \frac{Q_{wn}}{A_m \Delta P} \tag{4.3}$$

where, Q terms are volumetric flow rate in cm^3/min, r terms are radius of pore in cm, A_m is the external area of membrane = 13.2 cm^2, ΔP = transmembrane pressure in bar.

The calculated cumulative thicknesses of layers are plotted in Figure 4.1, along with the calculated water permeability values. It can be observed that cumulative thickness of layers increases as subsequent layers are assembled in the membrane pores. Final cumulative thickness of functionalized domain after GOX immobilization is 100 nm, which corresponds to 44 % reduction in pore radius. Hence, the radius of functionalized pore after GOX immobilization was 125 nm.

Table 4.1 Characterization of LBL assembled nylon membrane by calculating the amount of repeat units immobilized in subsequent layers. Molecular weight of repeat units of different polyelectrolytes is as follows: PLL 164.5, PSS 206, and PAH 93.5. External membrane area = 13.2 cm^2, Membrane thickness = 165 μm, pH = 6

Layer	**Amount of repeat units immobilized x 10^3, mmole**	**Net charge x 10^3, mmole**
PLL	2.1	(+) 2.1
PSS_1	6.9	(-) 4.8
PAH_1	9.1	(+) 4.3
PSS_2	10.4	(-) 6.1
PAH_2	13.1	(+) 7.0
PSS_3	8.2	(-) 1.2
PAH_3	2.5	(+) 1.3
GOX	1.1	-

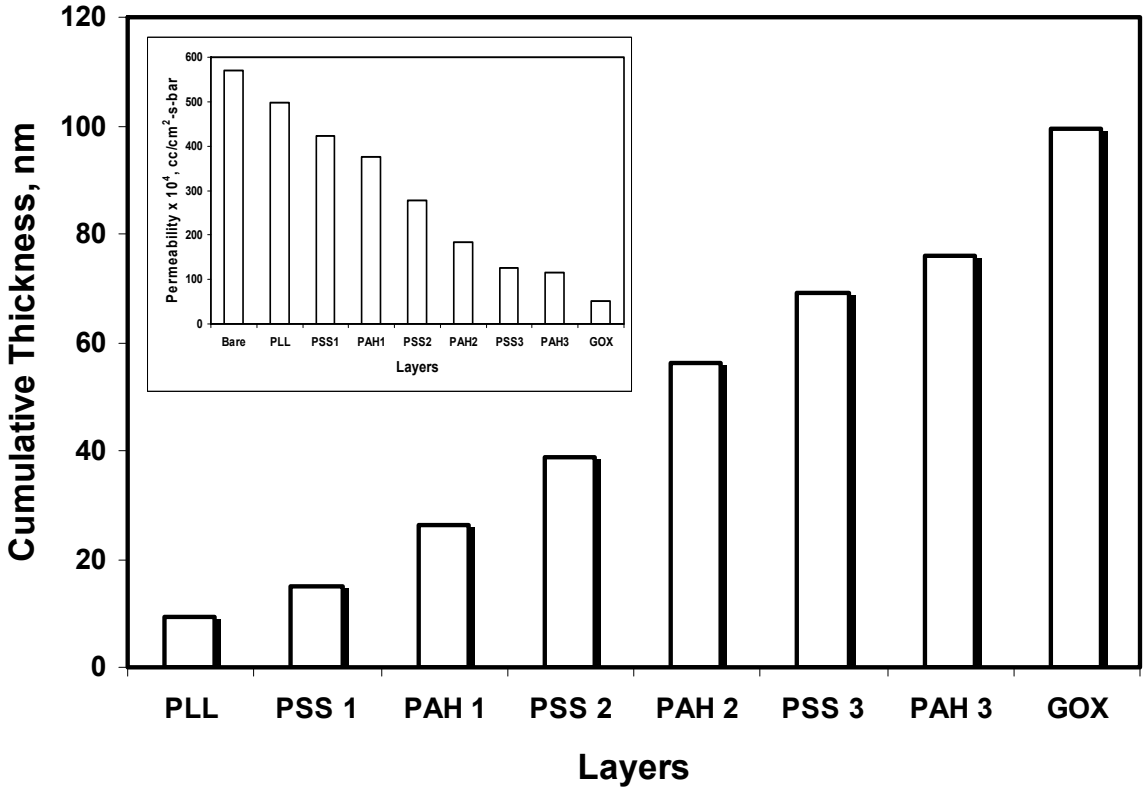

Figure 4.1 Calculated cumulative thickness of layers after electrostatic immobilization of polyelectrolytes inside nylon membrane pore. Hagen Poiseuiile's equation was used to calculate layer thickness. Inset Figure shows the decrease in permeability due to formation of layers inside membrane pores. Pore radius of pure nylon membrane = 225 nm, water permeability of pure nylon membrane = 570 x 10^{-4} cc/cm^2-s-bar, permeability after GOX immobilization = 52 x 10^{-4} cc/cm^2-s-bar, external membrane area = 13.2 cm^2, membrane thickness = 165 μm, pH of water used for permeability measurement = 6, NaCl concentration used to form layers = 0.25 M

The inset of Figure 4.1 represents the decrease in water permeability of the membrane due to decrease in pore radius with addition of each layer. Water permeability of nylon membrane before any functionalization was 570 x 10^{-4} cc/cm^2-s-bar. At the end of GOX immobilization the water permeability decreases to 52 x 10^{-4} cc/cm^2-s-bar, which is 4 % of the permeability of pure nylon membrane. This shows that addition 7-layers of polyelectrolytes and one layer of GOX affect the water permeability of the membrane significantly.

Immobilization of GOX in LBL assembled nylon membrane: The amount of GOX immobilized electrostatically on the 7 layers assembled nylon membrane was 1.5 ± 0.2 mg (9.37 x 10^{-5} ± 1.25 x 10^{-5} mmole). In another set of experiments, the amount of GOX immobilized was 1.1 ± 0.1 mg for 3 layers of assembled membrane. Comparison of above results suggests that 4 additional layers did not increase the amount of immobilized GOX substantially. However, the additional layers contributed significantly in reducing the core leakage of reaction mixture through the center region of membrane pore. The results discussed in this dissertation are associated with 7-layers membrane system. Amount of covalently immobilized GOX was 1 ± 0.1 mg (6.25 x 10^{-6} mmole or 5 x 10^{-7} mmole/cm^2). In a previous study, the amount of covalent immobilization of avidin in Immunodyne membranes was 8 x 10^{-7} mmole/cm^2 (subsection 4.1.1). Considering the fact that GOX is bulkier than avidin, these results show that our experiments with covalently immobilized protein in Immunodyne membrane are consistent.

Electrostatically immobilized GOX within functionalized PVDF membrane:

Characterization of functionalized PVDF domain: Characterization of polyacrylic acid (PAA) functionalized PVDF membranes was carried out by determining the amount of repeat units incorporated into the membrane (Table 4.2), and then, by calculating the thickness of the functionalized domain as done earlier for LBL membrane using Hagen-Poiseuille's equation. Amount of repeat units of polyallylamine hydrochloride (PAH) attached in PVDF-PAA membrane was determined to be 0.13 mmole. This corresponds to similar amount of positive charges.

Table 4.2 Characterization of functionalized PVDF membrane by calculating the amount of repeat units immobilized in subsequent domains. Molecular weight of repeat units of different polyelectrolytes / polymers is as follows: PAH 93.5 and PAA 72. External membrane area = 13.2 cm^2, Membrane thickness = 165 μm, pH = 6

Domain	**Amount of repeat units immobilized x 10^3, mmole**	**Net charge x 10^3, mmole**
PAA	128.7	(-) 128.7
PAH	130	(+) 1.3
GOX	1.3	-

Since direct analysis of PAA attachment was not possible, the amount of PAA attached was determined by knowing the amount of GOX immobilized, as explained later. The cumulative thickness of functionalized domains of PVDF-PAA-PAH-GOX membrane was calculated to be 125 nm, i.e., the effective radius of pore became 100 nm.

Effect of functionalization on water flux was studied for subsequent layers in PVDF-PAA-PAH-GOX membrane. Figure 4.2 shows the behavior of pure water flux (pH 6) as a function of pressure at different stages of functionalization. The slope of each curve plotted in Figure 4.2 is the permeability of water x 10^4 through the membrane at that particular stage of functionalization. It can be observed that water permeability decreases dramatically from PVDF membrane before functionalization (596 x 10^{-4} cc/cm^2-s-bar) to PVDF-PAA membrane (82 x 10^{-4} cc/cm^2-s-bar). This observation can be attributed to the formation of highly dense PAA network inside the membrane pore. Also, at pH 6, carboxylic acid groups of PAA become ionized and start repelling each other. This leads to an elongated conformation of PAA as explained in next paragraph and causes a substantial decrease in pore radius. Permeability further decreases as PVDF-PAA membrane was converted to PVDF-PAA-PAH membrane (permeability = 50 x 10^{-4} cc/cm^2-s-bar) and PVDF-PAA-PAH-GOX membrane (permeability = 24 x 10^{-4} cc/cm^2-s-bar), subsequently.

Variation in water flux as a function of pH is demonstrated in Figure 4.3. It can be observed, that staring from 2.5, as pH increases, water flux remains constant till around 4.5, and then it starts decreasing sharply. At pH 5.5 the flux reduces to 40 % and at pH 7 the flux reduces to 20 % of the initial value. After pH 7, again it becomes constant. This indicates that between pH 4.5 to 7 some kind of conformational change of PAA structure takes place. For a layer of PAA immobilized in a solid matrix, this kind of phenomenon is referred as “helix-to coil transition” (Hollman and Bhattacharyya 2004). However, PAA in this case, forms a network structure inside the PVDF membrane pore, and the existence of helical or coil conformations are unlikely. Hence, although the fundamental science behind the observation is identical, the same terminology would be a misnomer. It can be stated that through out this pH range PAA transforms from retracted to elongated form.

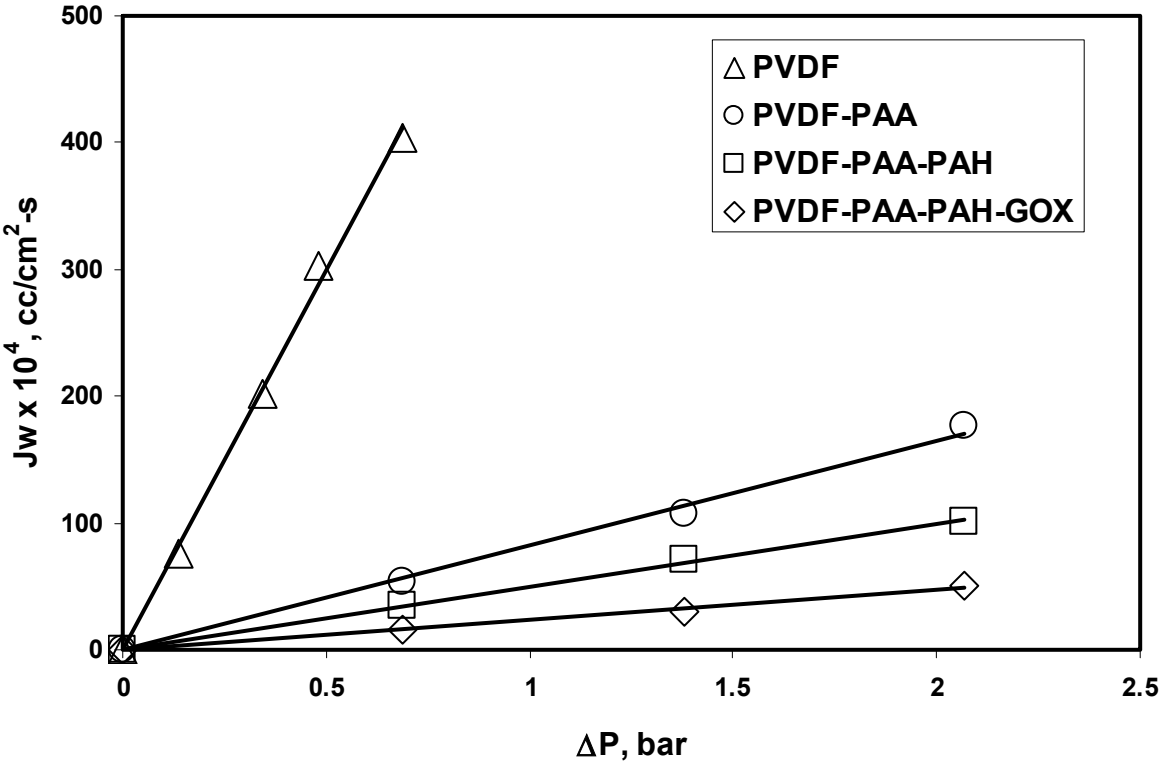

Figure 4.2 Effect of functionalization on PVDF membrane as depicted by the permeate flux vs pressure curve. Pore radius of pure PVDF membrane = 225 nm, pore radius of PVDF-PAA-PAH-GOX membrane = 100 nm. Water (pH 6) permeability values for different steps of functionalized membrane are given by the slope of the curves. External membrane area = 13.2 cm^2, membrane thickness = 125 μm

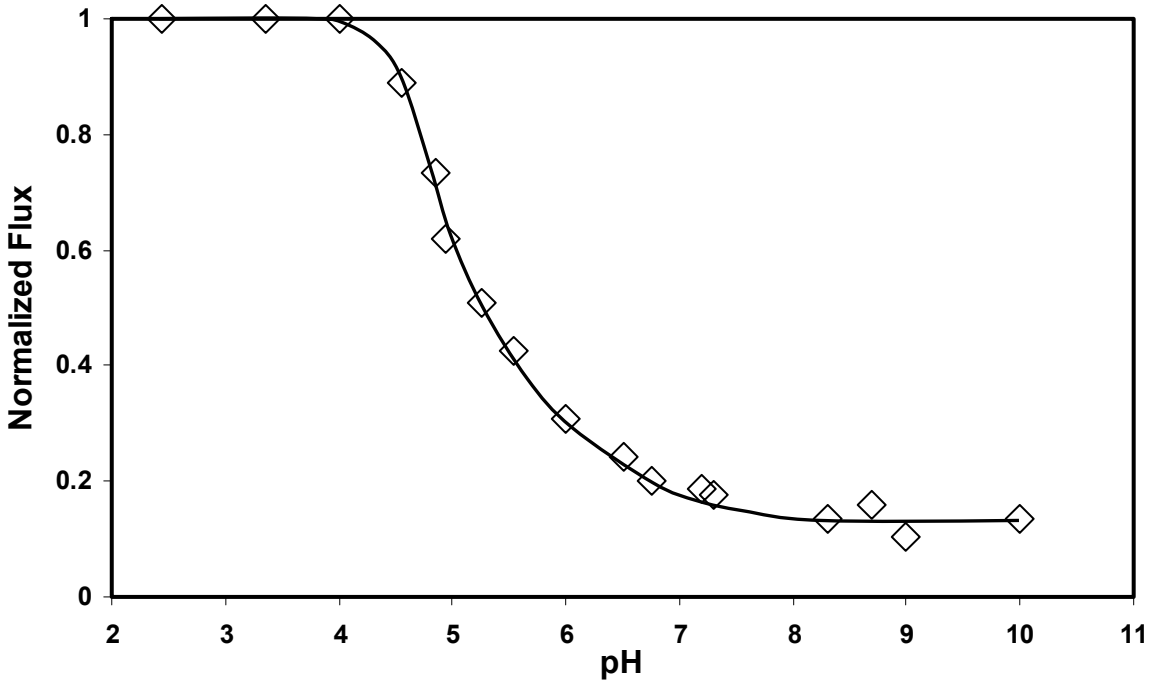

Figure 4.3 Effect of pH on permeate water flux for PAA-functionalized PVDF membrane in Na-form. Flux was normalized with maximum flux for this experiment (330 x 10^{-4} cc/cm^2-s) at a pH of 2.5 and pressure of 1.38 bar. Pore radius of pure PVDF membrane = 225 nm, pore radius of PVDF-PAA-PAH-GOX membrane = 100 nm, external membrane area = 13.2 cm^2, membrane thickness = 125 μm

Below pH 4.5, PAA remains totally protonated and hence retracted. With increase in pH it starts de-protonating, and above pH 7 all of its acid groups become de-protonated and fully elongated. A slight hysteresis was observed (not shown in Figure) as the same experiment was repeated in a reverse manner, i.e. starting from pH 10 and going to pH 2.5. At pH 6, the normalized flux was 0.31, which corresponds to water permeability value of 74 x 10^{-4} cc/cm^2-s-bar.

Functionalization within the membrane was also characterized by Scanning Electron Microscope (SEM) images and Energy Dispersive X-ray (EDX) analysis of the elements present in the membrane before and after functionalization. Comparison of SEM images (Figure 4.4a and 4.4b) of cross section of the membranes before and after functionalization clearly indicates attachment of polymer inside the PVDF membrane. SEM-EDX analysis diagram shows a peak corresponding to the element oxygen for PVDF-PAA membrane (Figure 4.4d) in addition to the other elemental picks (carbon and fluorine) present for virgin PVDF membrane (Figure 4.4c). This also demonstrates PAA functionalization within the pores of PVDF membrane. The pick corresponding to the element Fe is obtained as the analysis was carried out with Fe-immobilized PVDF-PAA membrane. This shows immobilization of Fe in the ion exchange step as discussed later in Chapter 7. The picks for Au and Pd are observed because the samples were sputtered with Au-Pd before the SEM-EDX characterization to increase the conductivity.

Immobilization of GOX in functionalized PVDF membrane: The amount of GOX attached electrostatically on the functionalized PVDF membrane was 1.8 ± 0.1 mg. This corresponds to about 1.12 x 10^{-5} mmole GOX or 1.33 x 10^{-3} mmole negative charges, considering one mole of GOX is equivalent to approximately 118 moles of negative charge (calculated from the number of aspartic and glutamic acid residues present in GOX). Assuming, for the present membrane system, this is the saturation capacity of GOX attachment by electrostatic immobilization, the excess positive charges of PAH that was neutralized by PAA = 0.13-1.33 x 10^{-2} mmole = 0.1287 mmole. This corresponds to an attachment of 0.1287 mmole or 9.3 mg of repeat units of PAA, i.e., acrylic acid.

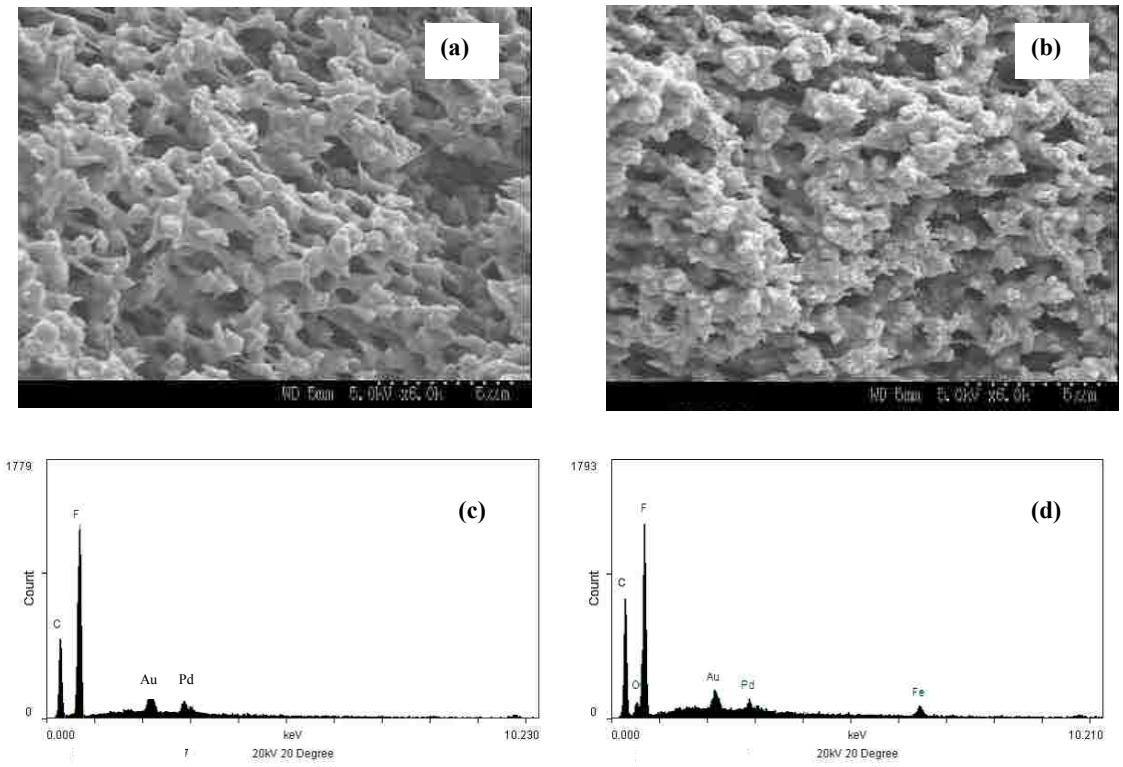

Figure 4.4 SEM images of cross section of (a) unmodified PVDF membrane and (b) PAA-functionalized PVDF membrane with immobilized Fe^{+2}. The figure also shows SEM-EDX analysis of different elements present in (c) virgin PVDF membrane and (d) PAA-functionalized PVDF membrane with immobilized Fe^{+2}

4.1.3 Determination of extent of functionalization in other membranes (RC, CA, nylon)

Amount of active groups attached in membranes were determined from amount of PABA attached. The values are shown in Table 4.3. As can be seen from the Table, all methods were able to functionalize active groups in the membrane, however, the amount attached were different. Due to limitations of time and scope, a particular type of membrane was chosen for further study mentioned in this dissertation; however, all others are also capable of being used as effective functionalized membranes system.

For CA membrane, oxidation was observed to be a better way than reacting with ECH. The base structure of CA gets affected under extreme reaction conditions, such as during the oxidation by $NaIO_4$ or reaction of ECH in presence of hot NaOH. This causes stability and reproducibility problems with CA membranes. The extent of functionalization values obtained for same lot of CA membranes varied a lot (~ 30 %) as given in Table 4.3. Therefore, although CA is a very hydrophilic membrane, it was not considered for further studies related to immobilization of avidin.

For nylon membranes, both ECH and CDI techniques were efficient. The extent of immobilization of active groups was significantly higher than functionalized CA membranes as shown in Table 4.3. The value of active groups attached for nylon membranes were satisfactorily reproducible. Nylon membranes are substantially robust; however, since they are comparatively more hydrophobic than RC membranes, they were not used for further attachment of avidin in this study.

As can be seen from Table 4.3, functionalization of active groups by all three different techniques was satisfactory for RC membranes. In spite of the same pore size, RC membranes were functionalized with more active groups than nylon membranes, probably because the amount of reactive groups were more in RC (hydroxyl) than nylon (amine). Among the three different techniques used for RC, the ECH activation was found to be superior to other two in terms of the capacity as well as reproducibility. RC is hydrophilic membrane with good mechanical and chemical strength. Hence, among all the choices of membranes, RC-ECH functionalized membranes were selected for separation of Tat as well as formation of LBL assembly.

Table 4.3 Amount of active groups attached for functionalization of different base membranes, such as regenerated cellulose (RC), cellulose acetate (CA) and nylon. ECH = epichlorohydrin, BDDE = 1, 4-butanediol diglycidol ether, CDI = 1, 1'-carbonyldiimidazole, PABA = para-aminobenzoic acid. Variation in results are represented as standard deviation

Membranes (Pore dia. in μm)	**Methods used for functionalization**	**PABA attachment i.e. amount of active group functionalized (μmole x 10^2/cm^2 external surface area)**
RC (0.2)	ECH	8.5 ± 0.6
	BDDE	6.0 ± 0.2
	CDI	5.5 ± 0.5
CA (0.45)	ECH	2.0 ± 0.6
	Oxidation	3.5 ± 0.7
Nylon (0.2)	ECH	4.5 ± 0.5
	CDI	5.2 ± 0.2

Covalent immobilization of avidin in RC-ECH membrane for separation of Tat: Amount of avidin immobilized covalently in a 13.2 cm^2 RC-ECH membrane was $2 \pm 0.2 \times 10^{-2}$ μmole (1.35 ± 0.15 mg), which corresponds to $1.5 \pm 0.15 \times 10^{-3}$ μmole of avidin/cm^2 of external area. The immobilization was significantly lower for larger molecule of avidin in compare to smaller molecule of PABA (Table 4.3). For commercially available anhydride functionalized nylon membranes (Immunodyne ABC), maximum amount of covalently immobilized avidin was 8.5×10^{-4} μmole/cm^2 external area. So, it can be observed that the RC-ECH functionalized membranes created as a part of this dissertation was of higher capacity than the commercially available Immunodyne membranes.

Amount of biotin attachment obtained in the RC-ECH-Avidin membrane was around 3.6×10^{-2} μmole for 10 μg/ml BBSA (1.3×10^{-3} μmole of biotin/ml) feed. This corresponds to an avidin to biotin ratio of 1:1.8, whereas, the avidin to biotin ratio was only 1:1.3 for the same case in Immunodyne membrane. This clearly demonstrates that accessibility of avidin sites is higher for functionalized RC membranes compare to Immunodyne membranes. This can probably be attributed to the higher hydrophilicity of RC over nylon membranes.

Formation of LBL in RC-ECH membrane: Four layers of polyelectrolytes in the sequence of PAH_1-PSS_1-PAH_2-PSS_2 were attached in functionalized RC-ECH membrane following the principle of electrostatic immobilization as described earlier. Only PSS layers were quantified. The amount of PSS immobilization was 16×10^{-3} mmole and 10×10^{-3} mmole for PSS_1 and PSS_2, respectively. For Immunodyne membranes, maximum amount of immobilization of PSS was 10.5×10^{-3} mmole. This demonstrates that RC-ECH membranes could be efficiently used for layer-by-layer attachment of polyelectrolytes. The amount of avidin immobilized electrostatically in the negatively charged RC-ECH-LBL membrane was 6×10^{-2} μmole (4 mg). Hence, it can be hypothesized, that functionalized RC-ECH-LBL membrane can also be potentially used for enzyme immobilization.

4.2 Conclusions

Covalent immobilization of avidin molecules was successfully carried out in commercially available anhydride activated nylon membranes. The amount of avidin immobilization under convective mode was higher than that mentioned by the manufacturer under soaking mode.

Enzyme Glucose Oxidase (GOX) was successfully immobilized in two different kinds of charged functionalized membrane domains by electrostatic interaction. In one case, the domain was created by alternative Layer-By-Layer (LBL) deposition of anionic and cationic polyelectrolytes on nylon based membrane, whereas, in other, the domain was created by in-situ polymerization of acrylic acid in hydrophobic PVDF membrane. Functionalized membranes were characterized in terms of permeate flux and attached domains. For PVDF membrane, functionalization was also demonstrated by SEM images. Functionalized domains in both cases were observed to be stable under tested conditions.

RC, CA and nylon membranes were activated by covalent attachment of active groups. Attachment was quantified by a probe molecule para-aminobenzoic acid (PABA). From capture of PABA and considering some other facts, epoxide activated RC membranes (RC-ECH) were selected for further studies. Avidin immobilized RC-ECH membranes were created for potential use in affinity based separation of HIV-Tat protein. Amount of avidin attached per unit membrane area was higher for RC-ECH than commercially available nylon membrane. RC-ECH membrane was also used for development of polyelectrolyte functionalized membrane based on Layer-By-Layer (LBL) technique. Attachment of layers was satisfactory as shown by the capture of avidin based on electrostatic interaction. This study has demonstrated the fact that base membranes can be modified to create initial activated membranes for applications in bioseparation and biocatalysis. However, since it is out of scope of this research work, further experiments were mainly conducted using commercially available activated nylon membrane and PVDF membrane.

Chapter 5 Affinity Based Separation of HIV-TAT Protein: Analysis of Accessibility of Avidin Sites and Fouling in Membranes

This chapter addresses two fundamental aspects of affinity based membrane separation of proteins; the accessibility of covalently immobilized active sites and fouling of the membranes. Avidin was covalently immobilized in the anhydride activated nylon membrane. Attempt was made to quantify the accessibility of avidin sites with biotin moieties present in a small probe molecule, biotin 4-amidobenzoic acid (BABA), as well as in a protein, biotinylated-BSA (BBSA). Further studies were extended to separation and purification of a target protein, HIV-Tat, from a complex fermentation broth (bacterial lysate, BL) using very specific interaction between the biotinylated-Tat protein and the avidin-functionalized membrane matrix. Fouling in the membranes was studied by critically examining the flux decline behavior and calculating the thickness of adsorbed protein layers inside the membrane.

It was hypothesized, that to make the technique more efficient, increase in separation efficiency (recovery of Tat per unit amount of avidin immobilized), increase in permeate flux and decrease in processing time are essential. Separation efficiency of Tat could be increased by enhancing the accessibility of the immobilized avidin sites. Permeate flux, and hence processing time could be improved by reducing the fouling. Incidentally, both accessibility and fouling are governed by the presence of unwanted high molecular weight proteins and other impurities in the BL.

Therefore, a pre-filtration step was introduced to remove unwanted high molecular weight proteins and other impurities from BL feed prior to affinity membrane separation. Two types of pre-filtration were studied; Ultrafiltration (UF) and Microfiltration (MF). Pre-filtered BL feed containing biotinylated Tat was then subjected to affinity based membrane separation. Effects of pre-filtration on the permeate flux, separation efficiency and processing time is discussed in detail. A comparative study is presented between the pre-filtered and unfiltered affinity separation. The flux decline during affinity separation is described by model equations and the calculated flux values are compared with the experimental values. The quality of purified Tat protein isolated

from unfiltered BL feed as well as from pre-filtered BL feed was analyzed by different analytical techniques and compared with that obtained for column chromatographic separation.

5.1 Results and discussion

In order to check the reproducibility of the results, all experiments were triplicated. The error bars shown in different figures represent standard deviations.

5.1.1 Accessibility of covalently immobilized avidin sites

From homogeneous phase avidin-biotin interaction experiments, it was determined that 1 mole of avidin, in homogeneous phase, could bind 3.6 mole of biotin present in BABA, which is close to 4 mole that has been reported in literature (Savage 1992).

Biotin moieties present in biotin 4-amidobenzoic acid (BABA): In homogeneous phase, because of the ease of accessibility (Figure 5.1 (a)), 4 moles of biotin uptake was possible by the active sites of one mole of avidin. However, within the membrane pores, the biotin uptake by the immobilized avidin sites would be less because of the associated hindrance to accessibility. In this research, BABA was used as a probe molecule to determine the maximum accessible sites of avidin, immobilized covalently within membrane pores.

Breakthrough curves obtained for different concentration of BABA solutions are presented in Figure 5.2. Concentration is represented in terms of biotin. As expected, the breakthrough curve is steeper for higher concentration of BABA solutions due to higher amount of biotin permeated. It is also observed that C_p / C_f is never zero at time > 0 (initially pores were filled with buffer) for any of the solutions.

Due to bigger pores (~0.42-0.43 μm) of avidin-immobilized MF membranes and convective flow of permeate, significant amount of biotin has permeated through central region of the pores without even interacting with the avidin sites. This phenomenon is known as “Core Leakage” (Datta et al. 2006).

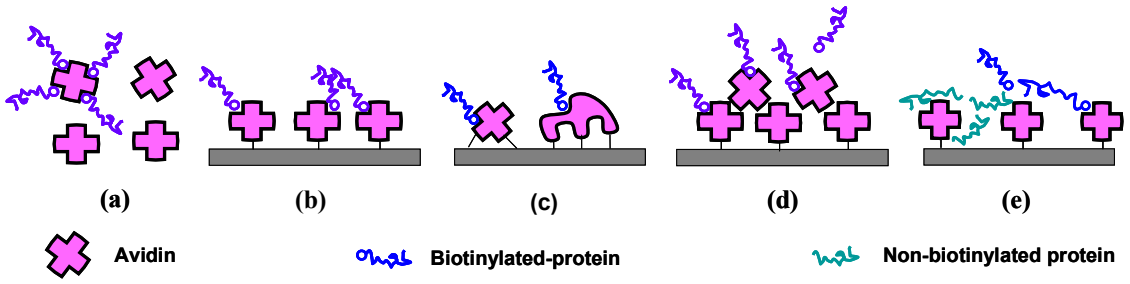

Figure 5.1 Schematic of different ways of attachment of avidin molecules in functionalized membranes and its effect on interaction with biotin moieties. (a) avidin in homogeneous phase. Four sites are available for biotin, (b) covalently immobilized avidin in membrane, (c) multiple attachment of avidin molecules by different amine groups, (d) blockage of avidin sites by next layer of immobilized avidin due to protein-protein interaction, and (e) blockage of avidin sites by big molecules of protein (biotinylated as well as non-biotinylated)

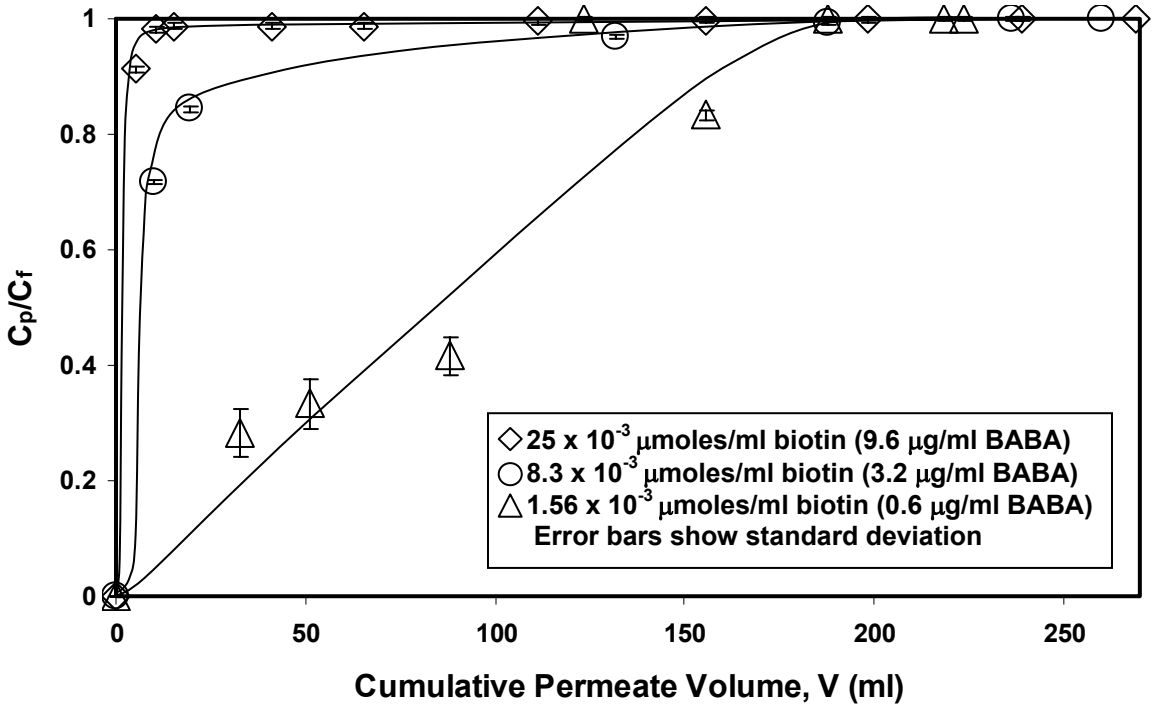

Figure 5.2 Comparison of breakthrough curves for permeation of different biotin 4-amidobenzoic acid (BABA) solutions through avidin immobilized (3.8×10^{-2} - 5.1×10^{-2} μmoles / ml bed volume) single nylon membrane (Pore dia. = 0.45 μm) at 0.34 bar. Avidin functionalized membrane permeability = 4×10^{-3}- 7×10^{-3} cm^3/cm^2.s.bar. C_P = conc. of biotin in permeate, C_f = conc. of biotin in feed

It was observed, that even for this small biotinylated-compound, BABA, the amount of biotin capture (Table 5.1) by the covalently immobilized avidin sites in the membrane was only half of the biotin capture capacity of the same amount of avidin in homogeneous phase. Similar kind of observation has already been reported in literature (Hollman et al. 2005). This signifies that only half of the total active sites of covalently immobilized avidin, in this type of membrane, were accessible by BABA. Thus, saturation biotin capture by covalently immobilized avidin in this membrane (Immunodyne) was considered to be equal to that obtained for BABA, i.e. by considering biotin : avidin = 1.8 : 1. Based on that, for all other biotinylated solutions used, normalized accessibility of the covalently immobilized avidin sites is defined as follows:

$$Normalized\ Accessibility = \frac{Actual\ amount\ of\ biotin\ capture\ from\ biotinylated\text{–}species}{Saturation\ biotin\ capture\ based\ on\ BABA}$$

$$= \frac{Actual\ amount\ of\ biotin\ capture\ from\ biotinylated\text{–}species}{Biotin\ capture\ based\ on\ avidin : biotin = 1:1.8}$$

The normalized accessibility is very specific for a particular type of membrane as the saturation biotin capture by avidin can vary with membrane.

The possible explanations of lower accessibility of immobilized avidin sites by BABA are; (i) blockage of avidin sites near the walls of the membrane pores as shown in Figure 5.1 b, (ii) multiple attachment of single molecule of avidin by different amine groups as shown in Figure 5.1 c, (iii) blockage of avidin sites by next layer of immobilized avidin molecules (Figure 5.1 d), and/or (iv) conformation change on the wall of membrane pores by protein-polymer interaction. It is interesting to notice in Table 5.1, that accessibility values are same for all BABA solutions irrespective of the concentration of biotin in feed BABA. The non-dependency of accessibility on concentration suggests that the small molecules of BABA did not offer any steric hindrance to biotin moieties and did not block the avidin sites.

Table 5.1 Accessibility of avidin sites for the permeation of biotin 4-amidobenzoic acid (BABA) through avidin immobilized nylon membrane (Pore dia. = 0.45 μm) at 0.34 bar. A single membrane was used for this case

Avidin immobilized x 10^2 (μmoles)	**Conc. of BABA in feed (μg/ml)**	**Conc. of biotin in feed x 10^3 (μmoles/ml)**	**Biotin uptake capacity of avidin in homogeneous phase x 10^2 (μmoles)**	**Biotin uptake by avidin x 10^2 (μmoles)**	**Normalized accessibility**
2.4	9.6	25.0	8.6	4.3	1
2.1	3.2	8.3	7.6	3.8	1
2.3	0.6	1.56	8.3	4.2	1

Biotin moieties present in biotinylated-BSA (BBSA): Figure 5.3 shows the breakthrough curves for the permeation of different concentrations of BBSA solutions. The concentration of biotin is obtained by considering each mole of BBSA is equivalent to 8 moles of biotin, as specified by the manufacturer. The initial breakthrough curve is steeper for higher concentration of BBSA due to the higher amount of biotin permeated, as observed earlier for BABA. "Core leakage" is also observed for BBSA, as for BABA.

The normalized accessibility values plotted as a function of amount of biotin permeated in Figure 5.4 and presented in Table 5.2, show lower accessibilities for BBSA compare to BABA. It is not trivial to calculate the accessibilities of avidin sites for BBSA, as the location and orientation of 8 biotin moieties present per molecules of BBSA are unknown. It is possible, that the accessibility for BBSA solutions was less because some of the biotin moieties were never exposed to avidin. It is also possible that instead of all 8 biotin moieties, BBSA molecules were attached using few biotin moieties only, making calculations of accessibility more difficult. In our calculations, a simple approach was taken considering a BBSA molecule was always attached with 8 biotin moieties. Figure 5.4 depicts that as biotin moieties permeated through the avidin-immobilized membrane; they interacted with avidin and bound to the membrane matrix. The hindrance in accessibility by large molecules of proteins was two fold. Bulky molecules of BBSA offered substantial steric hindrance to the biotin moieties present in it to access the avidin sites. Additionally, some BBSA molecules blocked nearby avidin sites by non-specific adsorption (Figure 5.1 (d)), thereby reducing the accessibility in comparison to BABA.

It can also be observed from Figure 5.4, that in contrast to BABA, accessibility shows a decreasing trend with increasing BBSA concentration. This can be attributed to the fact that as the concentration of BBSA in the feed increases, the biotin moieties experienced increased steric hindrance from larger number of protein molecules present. The blockage of avidin sites by the molecules of proteins was also higher for the concentrated BBSA solution.

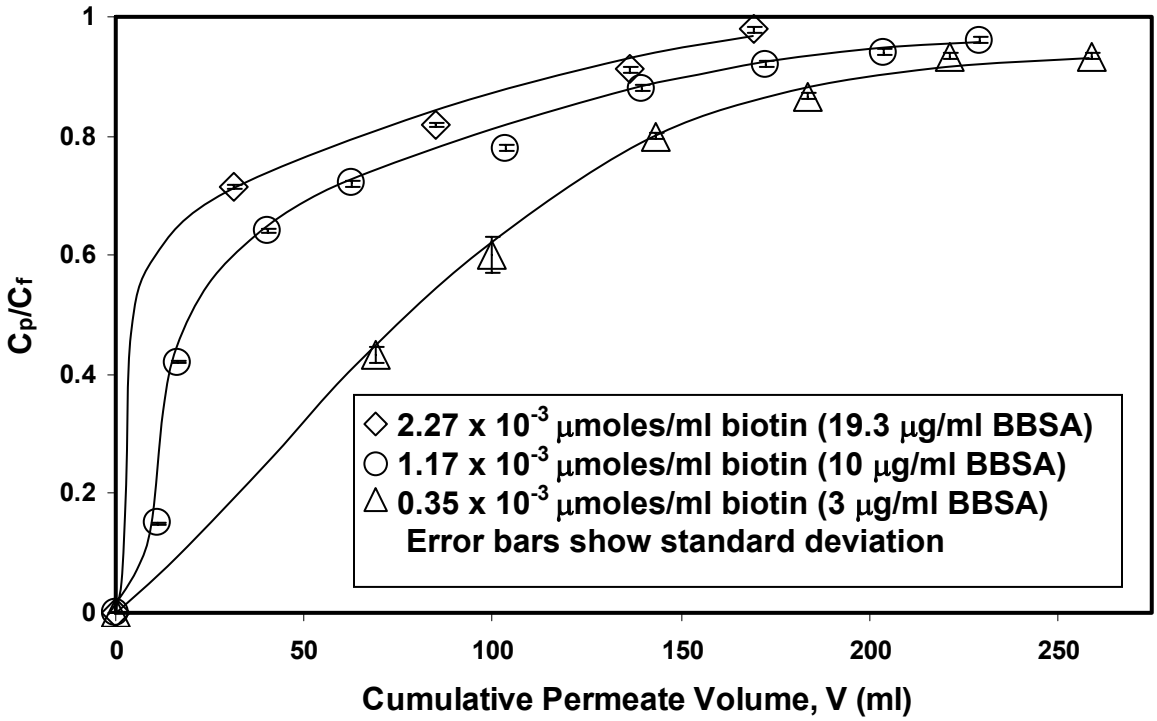

Figure 5.3 Comparison of breakthrough curves for permeation of different biotinylated-BSA (BBSA) solutions through avidin immobilized (3.8 x 10^{-2} - 5.1 x 10^{-2} μmoles/ml bed volume) single nylon membrane (Pore dia. = 0.45 μm) at 0.34 bar. Avidin functionalized membrane permeability = 5 x 10^{-3} – 7 x 10^{-3} cm^3/cm^2.s.bar. C_P = Conc. of biotin in permeate, C_f = Conc. of biotin in feed

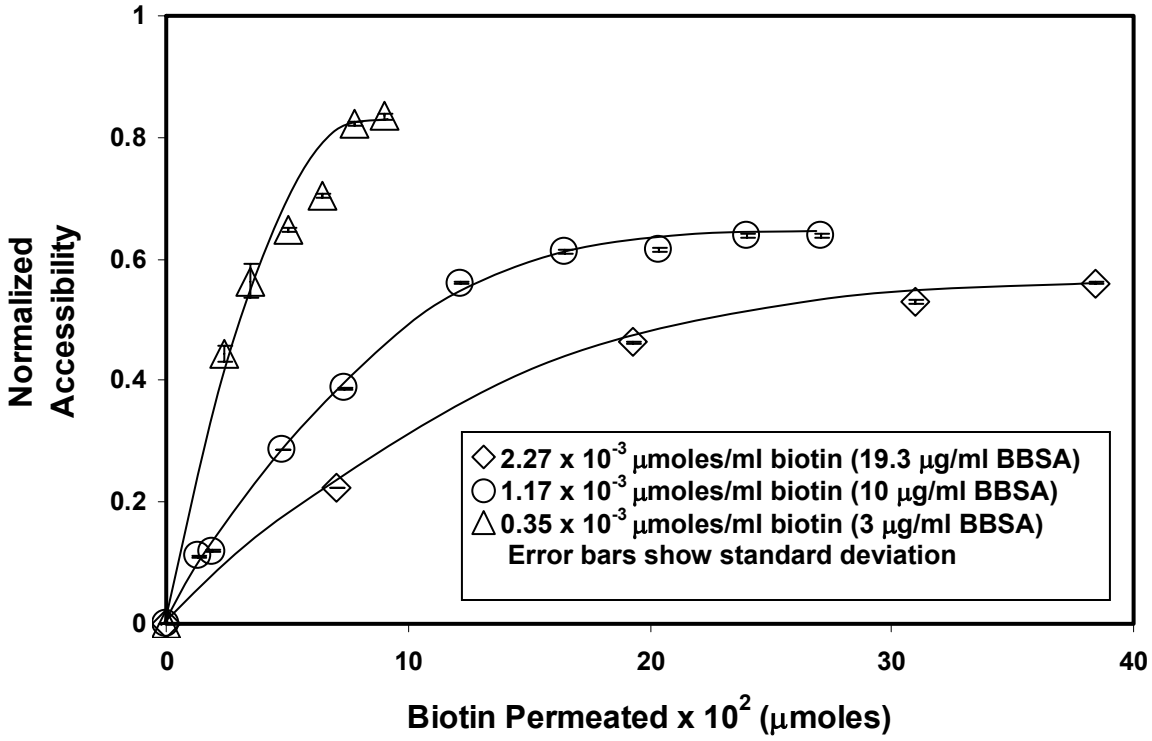

Figure 5.4 Comparison of accessibility of the avidin sites (3.8 x 10^{-2} - 5.1 x 10^{-2} μmoles/ml bed volume) immobilized in single nylon membrane (Pore dia. = 0.45 μm) for different biotinylated-BSA (BBSA) solutions at 0.34 bar. Avidin functionalized membrane permeability = 5 x 10^{-3} - 7 x 10^{-3} cm^3/cm^2.s.bar

Table 5.2 Accessibility of avidin sites for permeation of biotinylated-BSA (BBSA), BBSA + Gamma Globulin (GG, Non-biotinylated) and Tat in unfiltered bacterial lysate (UNF BL) through avidin immobilized nylon membrane (Pore dia. = 0.45 μm) at 0.34 bar. Single membrane was used for BBSA and BBSA+GG, whereas, 4-stack membranes were used for Tat in BL

Avidin immobilized x 10^2 (μmoles)		**Conc. of biotinylated species in feed (μg/ml)**	**Conc. of biotin in feed x 10^3 (μmoles/ml)**	**Biotin capture by avidin x 10^2 (μmoles)**	**Saturation capture of biotin based on BABA x 10^2 (μmoles)**	**Normalized accessibility**
2.8	**BBSA**	19.3	2.27	2.9	5.0	0.58
2.4		10.0	1.17	2.8	4.4	0.64
1.5		3.0	0.35	2.3	2.8	0.83
2.5	**BBSA+GG (13 μg/ml)**	10.0	1.17	2.5	4.5	0.55
5.0	**Tat in UNF BL1 (3864 μg/ml total protein)**	15.0	1.8	3.0	9.0	0.35
10.0	**Tat in UNF BL2 (1120 μg/ml total protein)**	15.0	1.8	3.2	18.0	0.18

Biotin moieties present in BBSA, along with non-biotinylated gamma globulin: The normalized accessibility of avidin sites for BBSA present in a mixture with GG is shown in Table 5.2. The biotin attachment, and hence the accessibility of avidin sites is less than that for pure BBSA with same biotin concentration (1.17×10^{-3} μmoles/ml biotin). In addition to the reasons already stated for BBSA, accessibility decreased further due to the blockage of avidin sites by non-biotinylated protein (GG) present (Figure 5.1 (d)).

Figure 5.5 compares the normalized accessibility as a function of total biotin permeated for three different types of solutions (BABA, BBSA, and BBSA+GG) containing comparable concentration of biotin. The accessibility for BABA was always higher than the other two because of the unhindered access to avidin sites by biotin moieties present in small BABA molecules. However, the accessibility was less for biotin moieties present in complex molecules of proteins as discussed earlier. Between BBSA and BBSA+GG, the initial biotin attachment was the same, probably because the effect of non-biotinylated protein was insignificant initially. But, finally accessibility decreased for BBSA+GG due to the increased steric hindrance and blockage of avidin sites by the non-biotinylated protein.

Biotin moieties present in bacterial lysate (BL): This section contains accessibility results for biotin present as biotinylated-Tat in BL. The effect of pre-filtration on accessibility is also discussed here.

Accessibility for biotinylated-Tat in unfiltered BL (UNF BL) feed: Table 5.2 contains the avidin sites accessibility values for biotinylated Tat present in a complex mixture of proteins (97-99 % unwanted protein). Results for two different sets of unfiltered BL feed, namely UNF BL1 (total protein concentration 3864 μg/ml) and UNF BL2 (total protein concentration 1120 μg/ml) are presented. From Table 5.2 it can be observed that the avidin site accessibility is least for the permeation of both UNF BL1 and UNF BL2. Although the concentration of biotin (biotin : monomeric Tat = 1:1) present in UNF BL was comparable with 0.6 μg/ml of BABA, 10 μg/ml of BBSA and 10 μg/ml of BBSA + 13 μg/ml of GG; the presence of 97-99 wt % of unwanted protein was responsible for the decreasing accessibility.

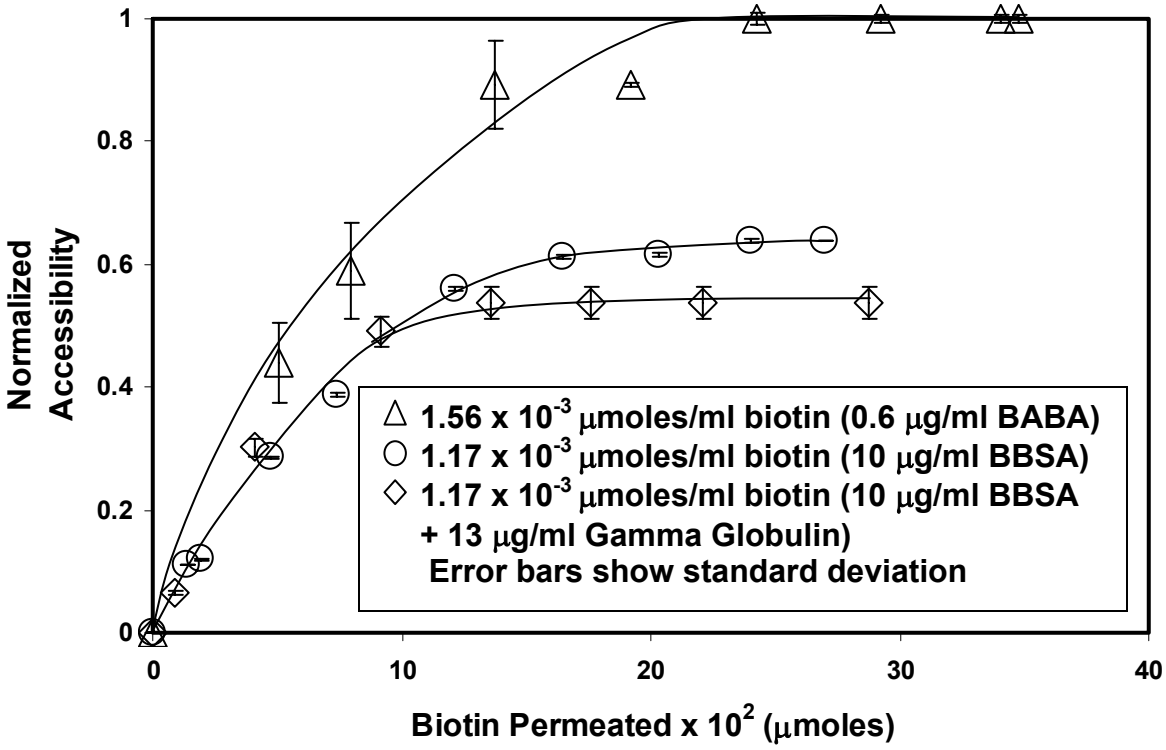

Figure 5.5 Comparison of normalized accessibility vs. biotin permeated for biotin 4-amidobenzoic acid (BABA), biotinylated-BSA (BBSA) and BBSA + Gamma Globulin (GG, non-biotinylated protein) through avidin immobilized (3.8×10^{-2} - 5.1×10^{-2} μmoles/ml bed volume) single nylon membrane (0.45 μm) at 0.34 bar. Avidin functionalized membrane permeability = 4×10^{-3} - 5×10^{-3} $cm^3/cm^2.s.bar$

The difference in accessibility for the two cases of BL, particularly the lower accessibility for dilute solution, is difficult to explain. However, due to the complex nature of the mixture it can be assumed that some other factor, like interactions between proteins present in BL, might have overshadowed the advantage of lower concentration of proteins in solution.

Accessibility for biotinylated-Tat present in pre-filtered BL feed: In order to understand the discussion on accessibility of avidin sites for biotinylated Tat present in pre-filtered BL feed, it is necessary to have an idea of the effects of pre-filtration on BL feed. Hence, the following sub-section is dedicated to study the effects of two different set of pre-filtration experiments; one UF and another MF, on BL feed.

Effect of pre-filtration on BL feed: Results of pre-filtration experiments are summarized in Table 5.3 and Figures 5.6-5.7. Feed to the pre-filtration step had 1120 μg/ml of total protein among which 3 wt % was total (exposed + entangled) biotinylated-Tat protein. It can be observed from Table 5.3 that UF removed 85 ± 5 wt % of the total protein from diluted BL supernatant, and produced UF BL feed (UF permeate) containing the lowest concentration (155 ± 5 μg/ml) of total protein. MF removed 57 ± 5 wt % of the protein, and produced MF BL feed (MF permeate) containing 465 ± 10 μg/ml of total protein.

Fouling in UF and MF is illustrated by flux decline curves in Figure 5.6. Due to higher rejection of proteins by UF membrane, it was associated with gel polarization effect, which has caused higher flux decline compare to MF. Severe flux drop was observed right from the beginning for UF as proteins started depositing on the external surface of the membrane, blocking some of the pores and then eventually formed a cake. The formation of cake is associated with flattening of flux vs time curve as shown in Figure 5.6. For MF, fouling was gradual compare to UF as initially protein adsorption occurred mainly inside the pores. Then, it also started depositing on the external surface due to formation of aggregates and eventually ends up forming cake. Palacio and coworkers have used 0.2 μm polycarbonate membrane to study the fouling behavior of mixture of BSA and pepsin with a total protein concentration of 2000 mg/l.

Table 5.3 Effect of pre-filtration (UF and MF) on BL feed. Concentration of total protein in pre-filtration feed = 1120 μg/ml. Concentration of total biotin (exposed + entangled) in pre-filtration feed = 3.8 x 10^{-3} μmole/ml (i.e. 32 μg/ml Tat). UF: 100 KDa MWCO regenerated cellulose membrane, ΔP = 1.36 bar, MF: 0.1 μm pore size hydrophilized PVDF membrane, ΔP = 0.34 bar

Pre-Filtration	**Protein removed from system, wt %**	**Conc. of total protein in permeate, μg/ml**	**Conc. of total biotin in permeate, μmole/ml (μg Tat/ml)**	**Conc. of exposed biotin in permeate, μmole/ml (μg Tat/ml)**
UF	85 ± 5	155 ± 5	3.0 x 10^{-3} (25)	2.2 x 10^{-3} (18)
MF	57 ± 5	465 ± 10	3.2 x 10^{-3} (27)	2.5 x 10^{-3} (21)

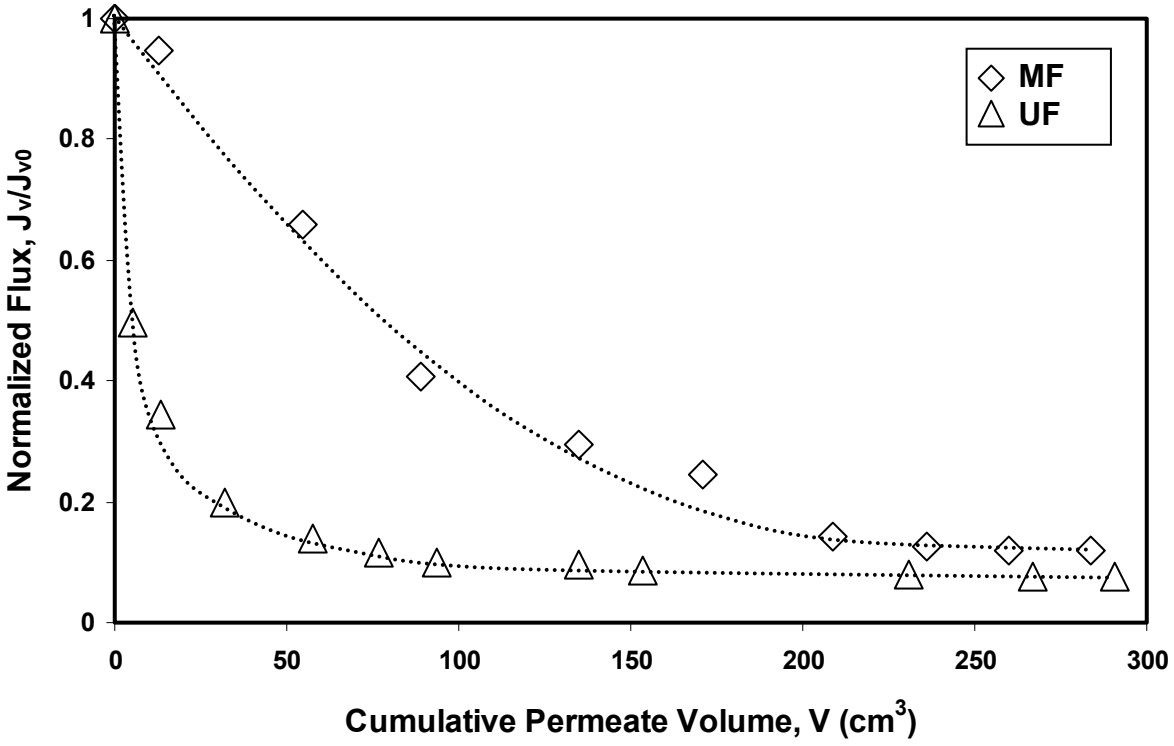

Figure 5.6 Normalized flux vs cumulative volume for pre-filtration experiments. UF: 100KDa MWCO regenerated cellulose membrane, ΔP = 1.36 bar, Permeability = $4x10^{-3}$ cm^3/cm^2-s-bar. MF: 0.1 μm pore size hydrophilized PVDF membrane, ΔP = 0.34 bar, Permeability = 20 x 10^{-3} cm^3/cm^2-s-bar. Dotted curves represent trend lines for experimental data. Volume of pre-filtration feeds = 300 cm^3

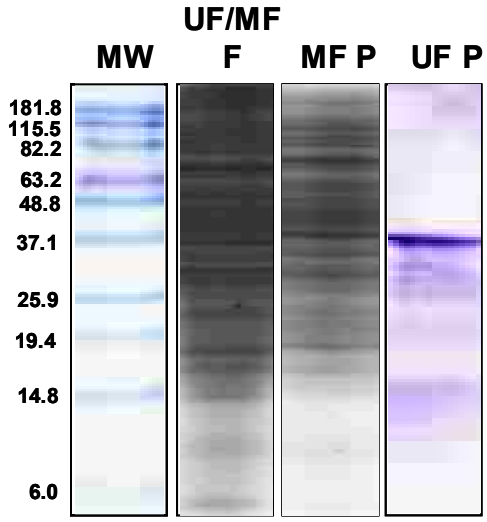

Figure 5.7 SDS-PAGE images of feed and permeate streams of pre-filtration experiments prior to affinity separation. Total protein concentration in pre-filtration feed (UF/MF F) = 1120 μg/ml, in microfiltration permeate (MF P) = 465 ± 10 μg/ml, and in ultrafiltration permeate (UF P) = 155 ± 5 μg/ml

They have also observed similar trend in flux decline behavior due to blockage of pores and formation of cake by the adsorbed proteins (Palacio et al. 2003).

The biotin analysis data presented in Table 5.3 reveal some interesting phenomenon. It can be observed that there is significant difference in concentration of total biotin (obtained from biotin analysis of digested fraction) and exposed biotin (obtained from direct biotin analysis) for both UF and MF permeate. This suggests that although the pre-filtration step was able to remove unwanted proteins from BL feed, it was not able to disentangle all biotinylated-Tat from non-specific aggregates. There also exists a difference between the concentration of biotin in pre-filtration feed and permeate for both UF and MF. This implies that some of the biotinylated-Tat proteins were rejected by the membrane due to entanglement in non-specific protein aggregates and adsorption to membranes. The concentration of exposed biotin was 2.2×10^{-3} and 2.5×10^{-3} μmole/ml for UF and MF permeate, respectively. Since, the exposed biotinylated-Tat was available for binding with avidin; those values were used for further calculations.

Figure 5.7 shows SDS-PAGE images of process streams before and after pre-filtration. It can be observed from the figure that the MF membrane was functional only to partially reject the high molecular weight proteins as the corresponding bands still exist in lesser intensity. In contrast, UF membrane, due to its smaller pore size, was able to reject all of the proteins above 35 KDa molecular weight. Although UF membrane was 100 KDa MWCO, the reason of rejecting proteins below 100 KDa was probably the formation of larger size protein aggregates and non-uniform pore size distribution. Both MF and UF were able to completely reject the other impurities, such as cell debris.

Effect of pre-filtration on accessibility: The focus of this particular sub-section is to understand the effect of pre-filtration on accessibility by discussing the results obtained for 2 different pre-filtered BL permeation experiments (MF BL and UF BL) along with the result obtained for UNF BL2. For proper comparison, the results of Table 5.2 are reproduced in Table 5.4 along with the MF BL and UF BL results.

Table 5.4 Effect of pre-filtration on accessibility of avidin sites for BL permeation. For proper comparison, results of Table 5.2 are reproduced here along with the MF BL and UF BL results. Single membrane was used for BBSA and BBSA+GG, whereas, 4-stack membranes were used for Tat in BL

Avidin immobilized x 10^2 (μmoles)		**Conc. of biotinylated species in feed (μg/ml)**	**Conc. of biotin in feed x 10^3 (μmoles/ml)**	**Biotin capture by avidin x 10^2 (μmoles)**	**Saturation capture of biotin based on BABA x 10^2 (μmoles)**	**Normalized accessibility**
2.8	**BBSA**	19.3	2.27	2.9	5.0	0.58
2.4		10.0	1.17	2.8	4.4	0.64
1.5		3.0	0.35	2.3	2.8	0.83
2.5	**BBSA+GG (13 μg/ml)**	10.0	1.17	2.5	4.5	0.55
5.0	**Tat in BL (3864 μg/ml total protein)**	15.0	1.8	3.0	9.0	0.35
10.0	**Tat in BL (1120 μg/ml total protein)**	32.0	3.8	3.2	18.0	0.18
10.0	**Tat in MF BL (465 μg/ml total protein)**	21.0	2.5	9.0	18.0	0.50
10.0	**Tat in UF BL (155 μg/ml total protein)**	18.0	2.2	12.6	18.0	0.70

Maximum possible capture of biotin by the immobilized avidin (avidin immobilization = 0.1 μmoles or 6000 μg for all 3 cases) was 0.18 μmole (1500 μg of biotinylated-Tat) for all 3 cases. Only 0.032 μmole of biotin (270 μg of biotinylated-Tat) was captured for UNF BL2. On the other hand, 0.1262 μmole of biotin (1050 μg of biotinylated-Tat) and 0.092 μmole of biotin (750 μg of biotinylated-Tat) were captured for UF BL and MF BL, respectively. UF BL has the highest normalized accessibility (0.7) followed by MF BL (0.5), while UNF BL2 has the lowest normalized accessibility (0.18).

Point to be noted that the amount of biotinylated-Tat capture for pre-filtered BL feed was calculated from biotin analysis and material balance. ELISA was also carried out on some samples of purified Tat eluate to make sure that the calculated values of Tat recovery from biotin analysis and material balance were accurate. The obtained values showed ± 12 % standard deviation. Accessibility depends on both blockage of avidin sites and steric hindrance offered to biotin moieties by unwanted proteins. Since, amount and molecular weight of unwanted proteins present was highest in the UNF BL2 feed, accessibility was lowest. On the other hand, lowest amount of unwanted proteins as well as lower molecular weight proteins were present for the UF BL feed compare to others. Hence, it has the highest accessibility. It is also very interesting to observe from Table 5.4, that accessibility of the pre-filtered BL was even higher than most of the BBSA (MWt. 68000) experiments. This can be attributed to the rejection of higher molecular weight proteins from the pre-filtered BL feed.

5.1.2 Study of associated fouling in avidin immobilized nylon membrane

The fouling in the membrane due to permeation of proteins can be observed by the flux decline curves shown in Figure 5.8. Due to the presence of higher amount of protein (attached + adsorbed) in the membrane (Table 5.5), reduction of flux increases as the concentration of protein in feed increases (except 10 μg/ml BSA). For BL (3864 μg/ml total protein) the flux decline (85 %) was highest because of maximum amount of protein in membrane matrix.

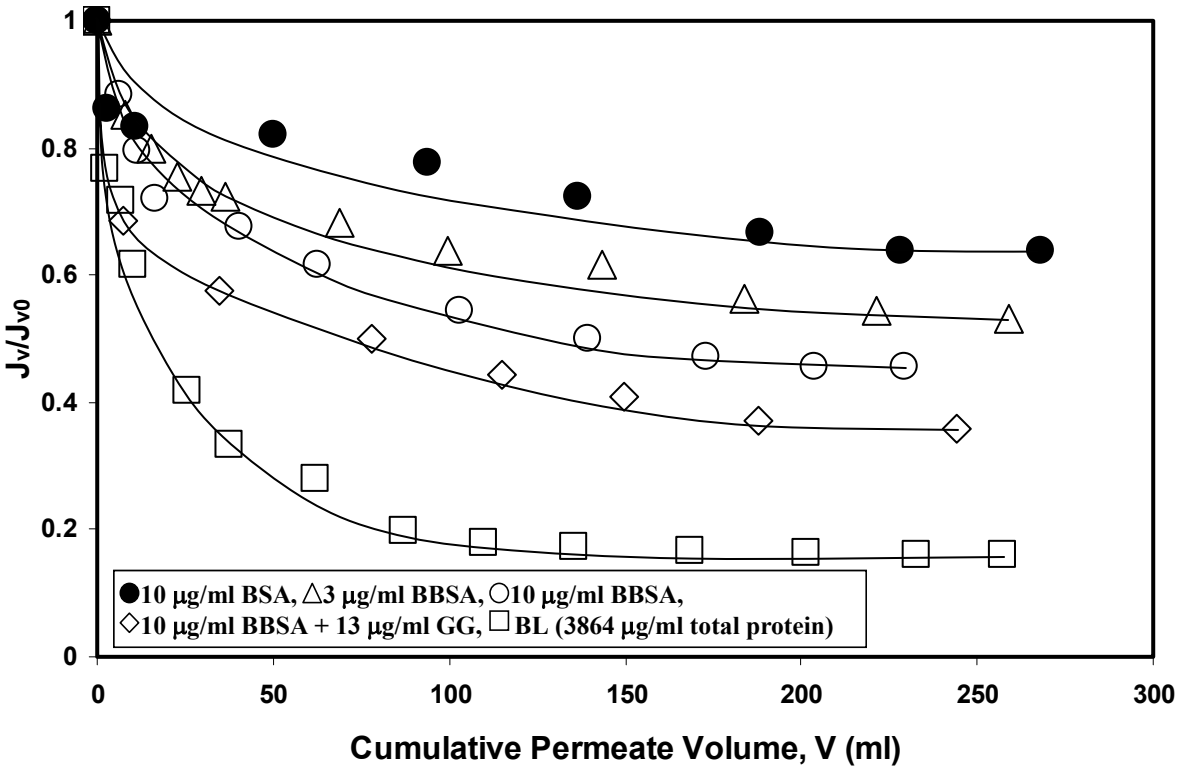

Figure 5.8 Comparison of normalized flux (J_v/J_{v0}) for permeation of BSA, BBSA, BBSA + gamma globulin (GG) and bacterial lysate (BL) through avidin immobilized nylon membranes (pore dia. = 0.45 µm) at 0.34 bar. Normalized flux = ratio of flux at any time of permeation to initial flux. $J_{v0} = 14 \times 10^{-4} - 24 \times 10^{-4}$ $cm^3/cm^2.s$

Table 5.5 Calculated resistance and thickness of protein layer formed due to the permeation of BSA, Biotinylated-BSA (BBSA), BBSA + Gamma Globulin (GG) and UNF BL feed through avidin immobilized membrane (Pore dia. = 0.45 μm) at 0.34 bar. R_P = Resistance of protein layer, δ_p= Effective thickness of protein layer

Conc. of total protein in feed	**Total amount of protein in membrane (μg)**	**R_P x 10^{-10} (cm^{-1})**	**δ_p (nm)**
10 μg/ml BSA	256	1.3	6.0
3 μg/ml BBSA	307	1.53	12.0
10 μg/ml BBSA	493	2.37	15.5
19.3 μg/ml BBSA	653	2.6	20.0
10 μg/ml BBSA+13 μg/ml GG	678	2.75	27.0
3864 μg/ml (UNF BL1)	16251	12.3	68.0
1120 μg/ml (UNF BL2)	15000	8.3	61.0

Membrane pores experience fouling because of the adsorption of proteins due to different interactions (hydrophobic and van der Waals). Some protein molecules form aggregates by protein-protein interaction (e.g., Tat and BSA are rich in cysteine residues, so prone to form aggregates by S-S linkages) and deposited in the pores of the membrane (Kelly and Zydney 1995; Marshal et al. 1993). Reversibly adsorbed molecules were removed by salt washing. However, significant amount of proteins were adsorbed irreversibly, particularly for the higher concentration of protein solution, and hence, permeate flux could not be recovered to the initial value. Based on the initial flux through avidin-immobilized membrane, the flux recovery was 90 % for 10 μg/ml BSA and 70-80 % for 19.3-3 μg/ml BBSA. The flux recovery (25 %) to significant extent was not possible for BL by washing with salt solutions (wash buffer and cleavage buffer), which proves highly irreversible nature of fouling for BL as again discussed later.

Figure 5.8 also reveals that fouling is less for 10 μg/ml BSA than that for 10 μg/ml BBSA, suggesting that fouling is not dependent entirely on total protein in feed, but also depends on the biotin molecules. For BBSA, due to the avidin-biotin interaction the amount of total protein present in membrane is higher than that for BSA (Table 4.3), which has caused the higher flux drop.

Calculation of resistance and thickness of adsorbed protein layer: Assuming all pores in the membrane have the same radius, the volumetric permeate flux (J_{w0}) and the volumetric flow rate (Q_{w0}) of water through a non-fouled avidin-immobilized membrane can be represented by Hagen-Poiseuille's equation as (Mulder 1991):

$$J_{w0} = \frac{\varepsilon r_0^{\,2}}{8\mu\tau l}\Delta P = \frac{\Delta P}{\mu R_m} \tag{5.1}$$

and, $$Q_{w_0} = N_P \frac{\pi r_0^{\,4}\Delta P}{8\mu l} \tag{5.2}$$

where, r_0 = radius of non-fouled avidin-immobilized membrane pore; μ = viscosity of solution; ℓ = thickness of the membrane or length of membrane pore; ΔP = transmembrane pressure drop; τ = tortuousity of the membrane; ε = porosity = 0.8; N_P =

total number of pores in the membrane; A_m = external membrane surface area; intrinsic membrane resistance, $R_m = 8l\tau / \varepsilon r_0^2$.

For permeation of proteins, the volumetric flux, J_v, through the fouled membrane can be described using Darcy's Law as follows (Ho and Sirkar 1992):

$$J_v = \frac{\Delta P}{\mu(R_m + R_P)} \tag{5.3}$$

where, R_P = resistance offered by the layer of proteins present in the membrane.

Rearranging equation (5.1) and (5.3) the expressions for R_m and R_P can be obtained as follows:

$$R_m = \frac{\Delta P}{\mu J_{w_0}} \tag{5.4}$$

$$R_m + R_P = \frac{\Delta P}{\mu J_v} \tag{5.5}$$

Assuming N_P remains same and proteins form an effective uniform thickness of layer throughout the pores of the membrane, equation (5.2) could be reproduced for the volumetric flow rate of pure water through the fouled membrane, Q_w, by substituting the radius of the bare membrane pore (r_0) with the effective radius of the fouled membrane pore (r_P). Now, r_P can be represented similarly as reported in literature (Zeman 1983) by:

$$r_P = r_0 \left(\frac{Q_w}{Q_{w_0}} \right)^{0.25} \tag{5.6}$$

Equation (5.6) can also be used to calculate the effective radius of membrane pores after immobilization of avidin (r_{avidin}), using the water flow rate data obtained after immobilization.

The effective thickness of immobilized avidin layer (δ_{avidin}), the effective thickness of protein layer (δ_p) and the effective thickness of total protein (including avidin) layer (δ_T) can be calculated as:

$$\delta_T = r - r_P,\ \delta_{avidin} = r - r_{avidin}, \text{ and } \delta_P = \delta_T - \delta_{avidin} = r_{avidin} - r_P \tag{5.7}$$

Equation (5.4) and (5.5) are used to calculate the equivalent resistance (R_P) offered by the effective protein layer, and equation (5.6) and (5.7) are used to calculate

the thickness of the protein layer (δ_p) present in the membrane pores after the permeation of protein and salt washing.

Due to the high concentration of proteins in BL, surface fouling occurred to some extent along with the adsorption of proteins within the pores. However, in order to get a rough estimate of the effect of protein layer on the fouling, the same assumption of "formation of an effective uniform thickness of protein layer throughout the pores of the membrane" was followed for BL also. For BL, it was also assumed that 4-stack membranes system obeys resistance-in-series model. Calculated values of R_P and δ_P for different protein solutions are presented in Table 5.5. It can be observed that R_P and δ_p increase with increase in protein concentration in feed, due to the presence of higher amount of protein in the membrane. The R_P and δ_p for both cases of BL are much higher than that for BSA, BBSA and BBSA+GG.

The increase in effective thickness of protein layer during the permeation of BSA, BBSA, BBSA+GG and UNF BL were calculated using same type of correlation as equations (5.6) and (5.7). The calculated values of effective thickness of protein layers are plotted in Figure 5.9 as a function of cumulative permeate volume, V. Starting from zero thickness, the layer built up sharply as protein molecules were attached by avidin-biotin interaction, as well as adsorbed by non-specific protein-avidin interaction on the membrane pores. Later, formation of the adsorbed protein layer was gradual due to the slower rate of attachment and adsorption, and finally it leveled off.

SEM images of the unused Immunodyne membrane and the topmost membrane used in the 4-stack membranes system for UNF BL1 permeation are shown in Figure 5.10. Substantial fouling is observed in some places of the surface of the topmost membrane used for UNF BL1 permeation. So, it can be inferred that the fouling is mainly on the pore of the membrane, along with some surface fouling as shown by SEM image. Deposition of aggregated proteins was the cause of this surface fouling.

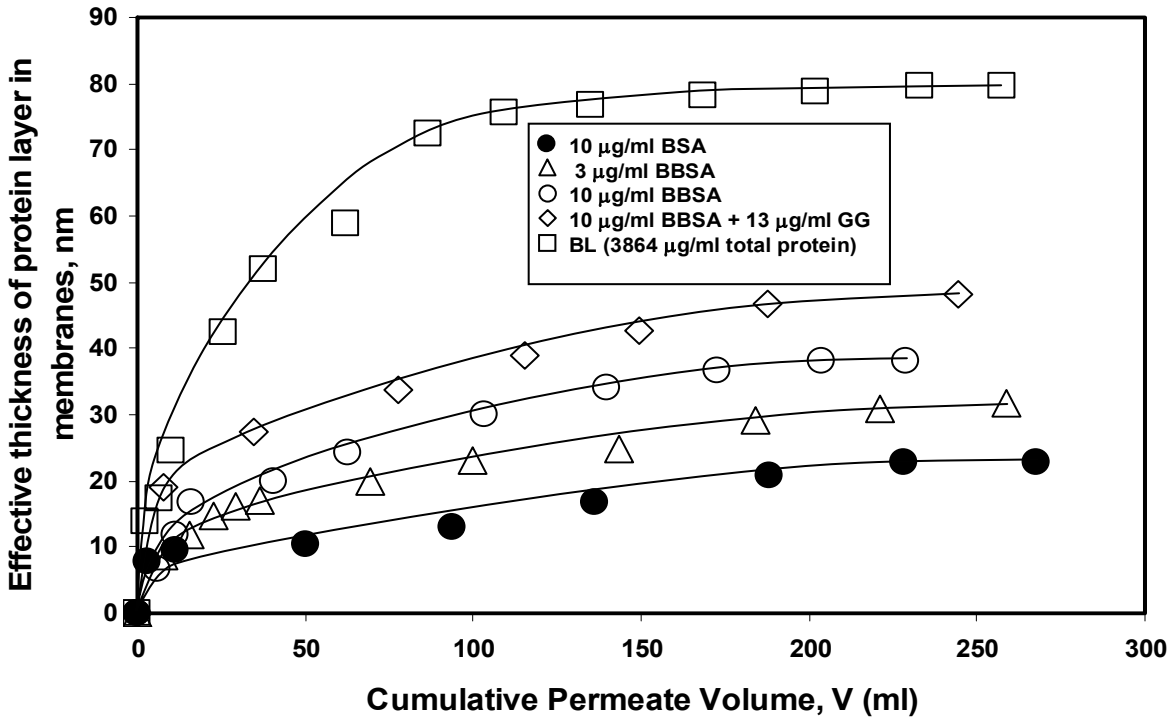

Figure 5.9 Comparison of effective thickness of protein layer formed within the membrane while permeating BSA, BBSA, BBSA + Gamma Globulin (GG) and bacterial lysate (BL) through avidin immobilized nylon membranes (Pore dia. = 0.45 μm) at 0.34 bar

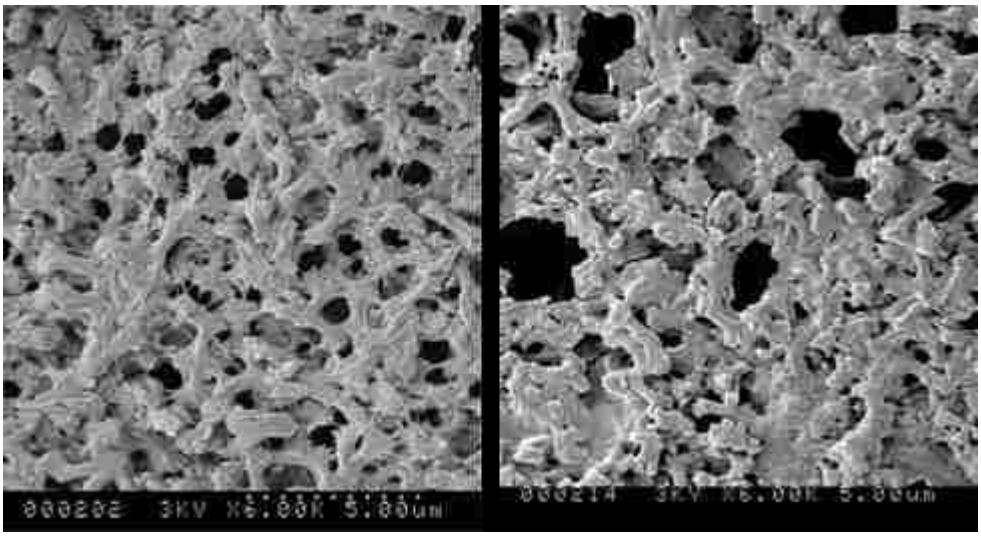

(a) (b)

Figure 5.10 SEM images (6K magnification) of the surface of the nylon based MF membranes (Pore dia. = 0.45 μm). (a) Bare Immunodyne membrane, (b) Topmost membrane of the 4-stack nylon membranes matrix through which UNF BL1, wash buffer and cleavage buffer were permeated at 0.34 bar

Effect of pre-filtration on fouling behavior of affinity separation: Simplified mathematical models are presented to explain the change in fouling behavior of the pre-filtered affinity separation. Two mechanisms of flux decline are considered; combined Model and standard Blocking Model (Bowen and Gan 1991). Combined model is applicable for protein solutions of higher concentration (UNF BL2 feed), where the chances of formation of aggregates are significant. But, standard blocking model describes fouling for lower concentration of protein solutions (UF BL and MF BL feeds).

For both the models, it is assumed that membranes consist of equal numbers of uniform, cylindrical pores and adsorbed protein molecules form a uniform layer of thickness, δ, within all of the pores. It is also assumed that in the 4-stack membranes system, pores are aligned coaxially on top of each other to form a continuous cylindrical channel of length equal to 4 times the length of a single pore.

The schematic of the membrane pore within which mass balance is done to formulate flux decline due to protein adsorption is shown in Figures 5.11 (a) and (b). For the combined model, fouling is assumed to occur both inside the pores and on the external surface of the membrane. As protein molecules permeate through the membrane, some of them adsorb on the pore walls reducing the pore radius from r_0 to r at time t and some of them adsorb on the external surface of the membrane (Figure 5.11 a).

From the protein mass balance, the amount of total adsorption at any time interval can be written as summation of the amount of pore and external surface adsorption as

$$dM_t = N_P\left(-2\pi rL\rho\right)dr + dM_S \tag{5.8}$$

where, N_P = number of pores in avidin-immobilized membrane, which is estimated as

$$N_P = \sqrt{\frac{8\mu\, l\varepsilon Q_w A_m}{\pi^2 r_0^{\,6}\Delta P}} = 2\text{x}10^9 \tag{5.9}$$

A_m = external surface area of membrane = 33.2 cm^2; ε = 0.8 (from manufacturers data); r_0 = radius of avidin-immobilized membrane pore = 215 x 10^{-7} cm (Datta et al. 2006); L = Total length of a cylindrical channel in 4-stack membranes = 4ℓ = 4 x 165 x 10^{-4} cm; ρ = mass of protein adsorbed per unit volume of adsorbed layer inside the pore, μg/ cm^3; M_S = mass of protein adsorbed on the external surface of membrane at t, μg; M_T = mass of total protein adsorbed in membrane (external surface + pore) at t, μg.

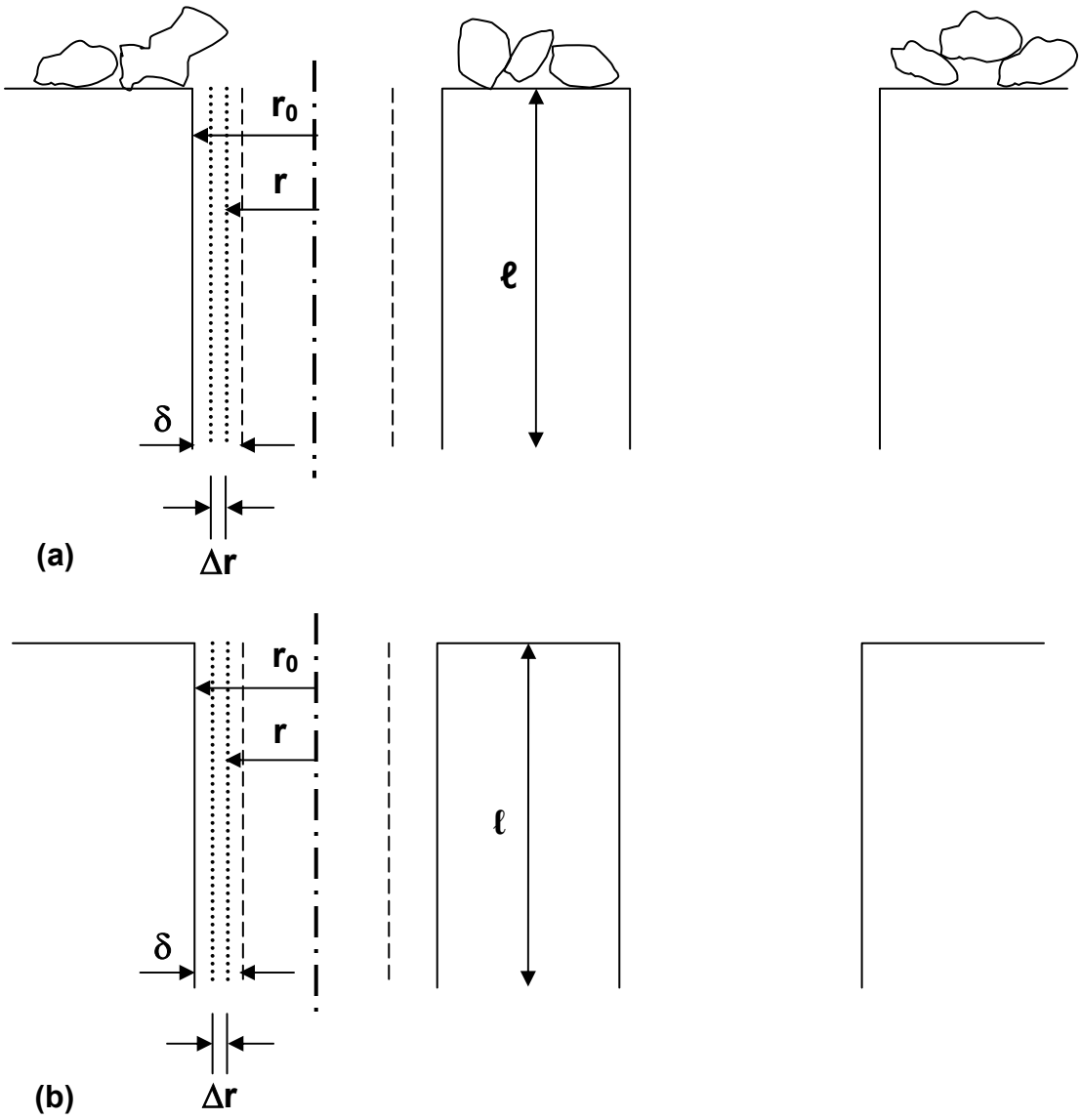

Figure 5.11 Schematic of adsorption of protein (a) both within the pores and on the external surface of the membranes: combined model, and (b) only within the pores of the membranes: standard model. The thickness of adsorbed protein layer formed at a distance r from the center of pore at any time interval of Δt is Δr

Equation 5.8 is integrated with the initial conditions; at t = 0, r = r_0, M_S = 0, M_T = 0, to obtain

$$\pi N_P L \rho r_0^2 \left[1 - \left(\frac{r}{r_0} \right)^2 \right] = M_T - M_S \tag{5.10}$$

Hagen-Poiseuille's equation is used to substitute the ratio r/r_0 with the ratio of permeate volumetric fluxes (J_v/J_{v0}) in Equation 5.10. Rearranging the resulting equation, an expression for the normalized permeate flux is obtained as

$$\frac{J_v}{J_{v0}} = \left[1 - \left(\frac{M_T - M_S}{\pi N_P L \rho r_0^2} \right) \right]^2 \tag{5.11}$$

where, J_v = permeate flux at any time t, cm^3/cm^2-s; J_{v0} = initial permeate flux (i.e. at t = 0), cm^3/cm^2-s; and J_v/J_{v0} = normalized permeate flux.

Determination of M_T and M_S are necessary to calculate permeate flux. For that, equation 5.11 is treated as a semi-empirical model and M_T and M_S are obtained by studying the kinetics of total protein and surface protein adsorption, respectively.

Total protein adsorption data are obtained from the affinity separation experiment of UNF BL2 feed by measuring the concentration of total protein in permeates at different time. It is observed that the amount of adsorbed protein eventually approaches equilibrium. Suki et al. (Suki et al. 1984) studied the adsorption kinetics of BSA and observed similar kind of equilibrium adsorption. Considering the same type of kinetics of adsorption is valid in our case, the rate of adsorption is defined following Suki et al. as:

$$\frac{dM_T}{dt} = K_T \left(M_T^* - M_T \right) \tag{5.12}$$

where, M_T^* = final amount of total protein adsorbed, μg, and K_T = rate constant of the total adsorption, min^{-1}

Integrating equation 5.12 with the initial condition; at t = 0 M_T = 0, one can obtain

$$M_T = M_T^* [1 - e^{-K_T t}] \tag{5.13}$$

The experimental values of M_T are plotted in Figure 5.12 as a function of time and fitted with equation 5.13.

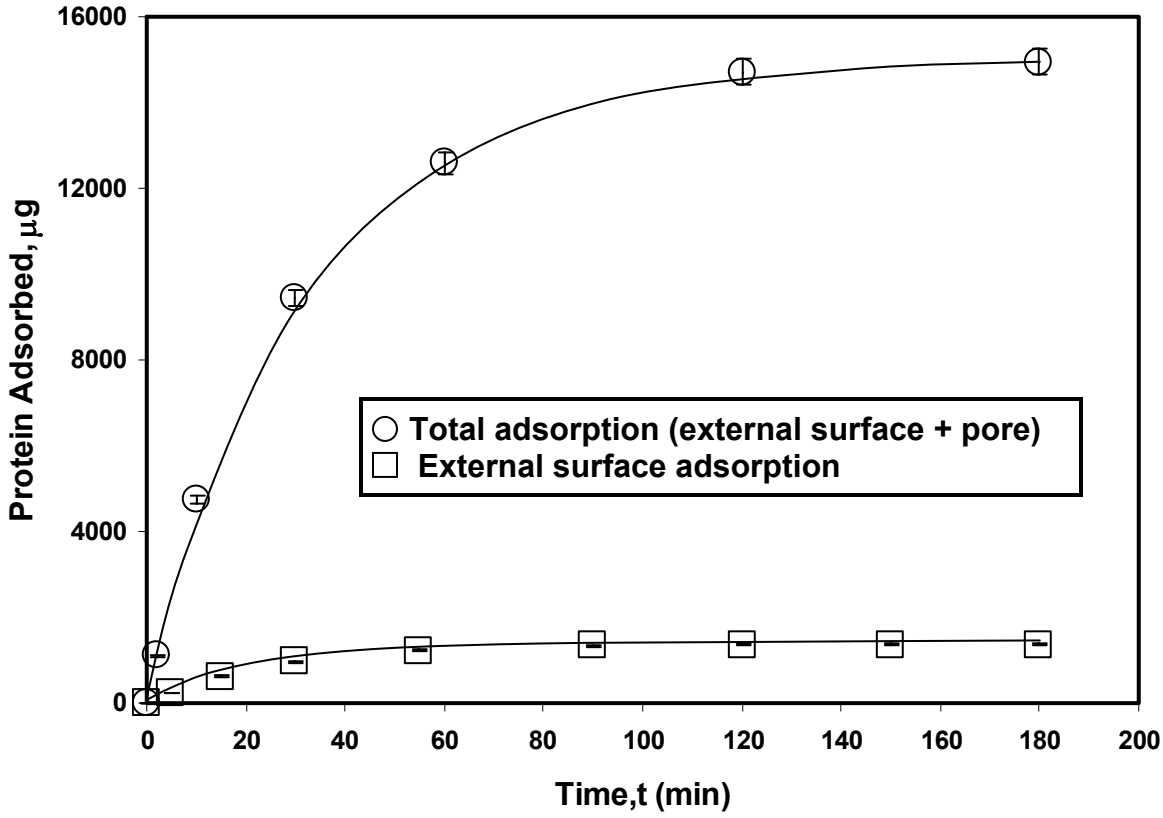

Figure 5.12 Kinetics of total protein adsorption for UNF BL2 feed. The solid curves represent the best fitted values according to Equation 5.13 for total adsorption and according to Equation 5.14 for surface adsorption, respectively

The best fitting value of the total adsorption rate constant, K_T, is determined to be 0.034 min^{-1}, while the value of M_T^* (15000 μg) was known from material balance on total protein present in different streams of affinity separation of UNF BL2 feed.

In order to study the kinetics of surface adsorption, separate batch experiments (no flow condition) were carried out with avidin-immobilized Immunodyne membrane and UNF BL feed containing the same protein concentration as in the affinity separation. The amount of adsorbed protein was determined at different time intervals. Then, similar procedure as total adsorption is followed to obtain

$$M_S = M_S^*[1 - e^{-K_S t}] \tag{5.14}$$

where, M_S^* = final amount of protein adsorbed on surface = 1400 μg (from material balance on total protein present in different streams of batch experiment), and K_S = rate constant of the surface adsorption = 0.04 min^{-1} (best fitting value obtained from Figure 5.12).

The value of ρ is obtained by defining it as $\rho = \frac{\left(M_T^* - M_S^*\right)}{N_P 2\pi r_0 \delta L} = 1.3x10^5\ \mu g / cm^3$

where, δ = calculated thickness of protein layer adsorbed within the pores = 61 nm (Table 5.5). Knowing M_T and M_S from Equation 5.13 and 5.14, respectively, the normalized flux for UNF BL2 can be calculated from Equation 5.11 as a function of time.

Standard blocking model can be applied to dilute solutions of protein. In this case, external surface adsorption is assumed to be negligible and flux decline is described by adsorption of protein molecules only inside the pores of membrane. Equation 5.8 can be simplified assuming negligible external surface adsorption, i.e. the last term of right hand side of Equation 5.8 is assumed to be zero. The simplified equation is written as

$N_P(-2\pi rL)dr = \frac{dM_t}{\rho}$ = change in volume of adsorbed pore layer

The change in volume of adsorbed pore layer, shown in Figure 5.11 (b), can be correlated with the volume of the adsorbed protein as done by Bowen et al (Bowen and Gan 1991).

$$N_P(-2\pi rL)dr = XdV \tag{5.15}$$

where, X = Volume of total protein adsorbed per unit volume of permeate

V = Volume of permeate collected at any time, cm^3

Integrating Equation 5.15 with the condition; at V = 0, r = r_0, and then substituting r/r_0 with J_v/J_{v0}, an expression for the normalized permeate flux is obtained as

$$\frac{J_v}{J_{v0}} = \left[1 - \left(K_X V\right)\right]^2 \tag{5.16}$$

where, $K_X = X/LA_0$, cm^{-3}; A_0 = Initial pore area = $N_P \pi r_0^2$, cm^2.

Integrating Equation 5.16 by substituting $J_v = (dV/dt)/A_m$ and rearranging gives

$$\frac{1}{V} = \frac{1}{J_{v0} A_m t} + K_X \tag{5.17}$$

Substituting the value of V from Equation 5.17 to 5.16 and rearranging gives

$$\frac{J_v}{J_{v0}} = \frac{1}{\left[1 + \left(K_X J_{v0} A_m t\right)\right]^2} \tag{5.18}$$

Equation 5.18 is used to calculate normalized permeate flux of UF BL and MF BL feeds. It is also used to calculate permeate flux of UNF BL2 feed so that comparison can be made between the applicability of two models for UNF BL2 feed. K_X values for all three cases are obtained from the Y-axis intercept of straight line fit (not shown here) of respective affinity separation experimental data ($R^2 > 0.98$) according to Equation 5.17. The K_X values are 0.0064, 0.0032 and 0.0006 cm^{-3} for UNF BL2, MF BL and UF BL, respectively. These values are then used in equation 5.18 to calculate normalized flux (J_v/J_{v0}) values as a function of time.

The combined model calculated J_v/J_{v0} values for UNF BL2 feed as well as the standard model calculated J_v/J_{v0} values for UNF BL2, MF BL and UF BL feed are plotted in Figure 5.13 as a function of cumulative permeate volume (V). The experimental normalized flux values are also plotted in the same figure for comparison. For all of the affinity separation experiments, J_v/J_{v0} decreased with increasing V, however, the extent and nature of the decline are different for different cases. Flux decline for the UNF BL2 feed was highest because of the fouling caused by feed containing highest protein concentration. This was followed by MF BL feed and UF BL feed. It was determined that total protein adsorption at the end of each experiment were 15000, 3000 and 2000 μg for UNF BL, MF BL and UF BL feeds, respectively Similarly, due to the very high rate of fouling the flux decline curve for UNF BL2 feed is steeper than the others.

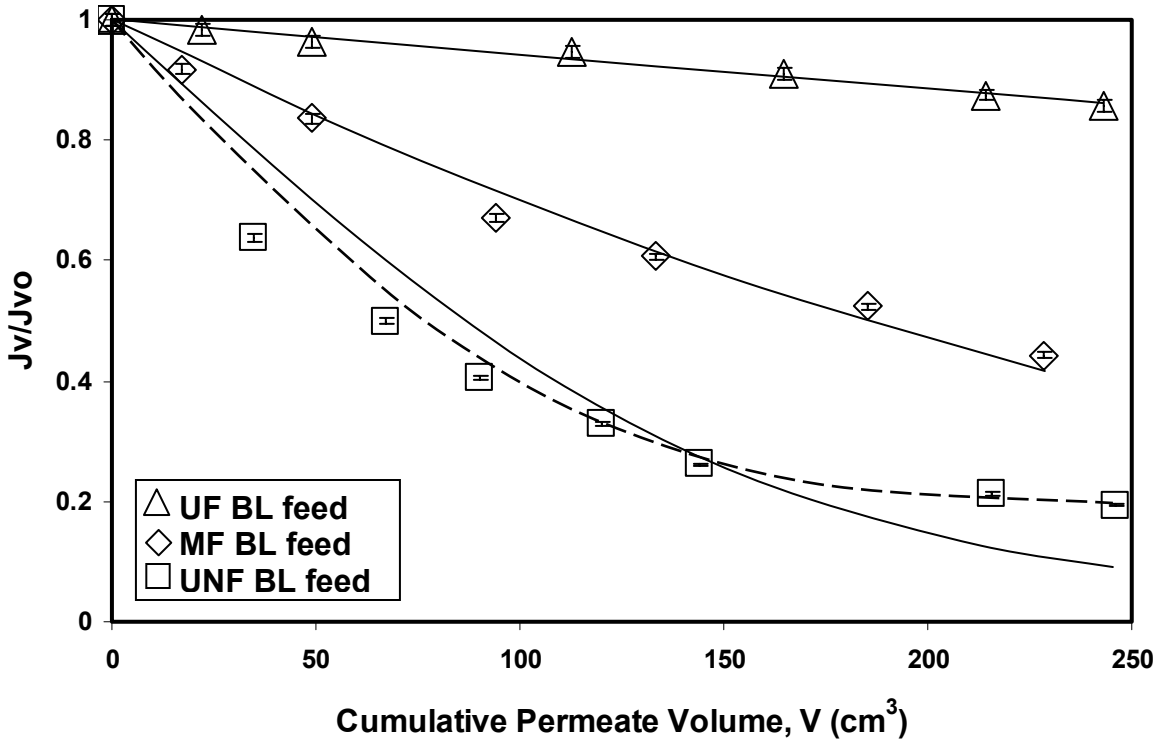

Figure 5.13 Normalized flux vs cumulative permeate volume for the affinity separation of different BL feeds through avidin-immobilized 4-stack Immunodyne membranes at 0.34 bar. The solid curves represent the Standard Blocking Model calculated values according to Equation 5.18, whereas, the broken curve represents the Combined Model calculated values according to Equation 5.11. UNF BL2 = Unfiltered BL2, UF BL = Ultrafiltered BL, MF BL = Microfiltered BL

It is also observed from Figure 5.13 that the standard model calculated J_v/J_{v0} values match very well with the experimental values of UF and MF BL feeds. This proves that the standard blocking mechanism was sufficient to explain fouling for the UF and MF BL feeds. However, for the UNF BL feed the standard blocking mechanism did not provide J_v/J_{v0} values accurately. The deviation between the experimental and the standard model calculated values was due to surface adsorption of proteins in addition to pore adsorption for the UNF BL2 feed. It can be observed from Figure 5.13 that the combined model calculated values describe the experimental flux decline for the UNF BL2 feed more accurately than the standard model. The model calculated values of UF BL, MF BL and UNF BL2 have indicated that pre-filtration step was able to restrict the fouling only within the pore structure for affinity separation step. The deviation noticed in the model predicted and experimental values for UNF BL2 feed in the initial phase of affinity separation was probably due to blockage of some of the pores that was not accounted for in the combined model.

5.1.3 Separation and purification of Tat

Effect of dilution and ionic strength: Figure 5.14 and 5.15 show the effect of dilution and salt concentration on available free Tat as analyzed by ELISA. Normally with dilution the total amount of a component present in a solution remains same (the concentration decreases). In case of Tat in BL, it was observed that the total amount of available free Tat in diluted BL increased with an increase in dilution factor till around 150 as shown in Figure 5.14. After that it became constant eventually. This observation suggests that in undiluted BL supernatant, Tat was entangled within the aggregates formed. As dilution increased, due to decrease in protein-protein interaction Tat was released from the aggregates, resulting in increase in amount of Tat. However, after certain dilution all the entangled Tat was released. In our experiment we have taken conservative approach by diluting BL up to 30 times only. This was done to make sure that the advantage of dilution has been utilized properly. Similarly, due to the shielding effect of ions, the interaction between the proteins decreased at higher salt concentration and more amount of Tat was released in BL as shown in Figure 5.15.

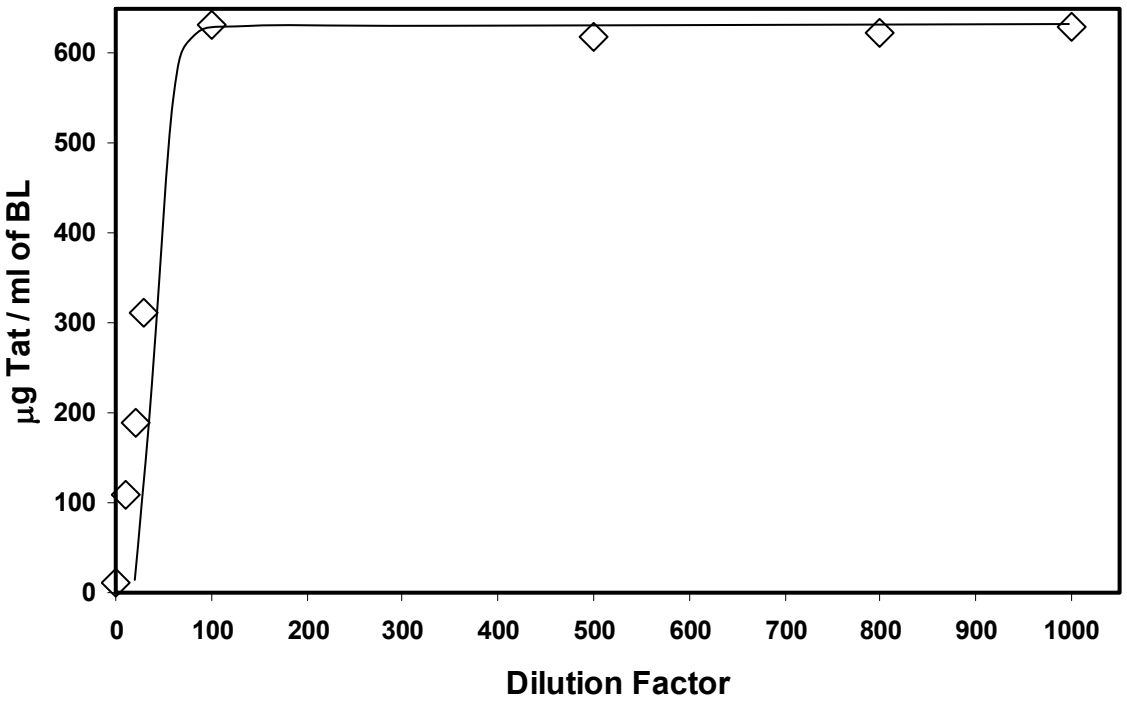

Figure 5.14 Effect of dilution on free available Tat by diluting bacterial lysate with 0.1 M (0.1×10^3 µmoles/ml) NaCl

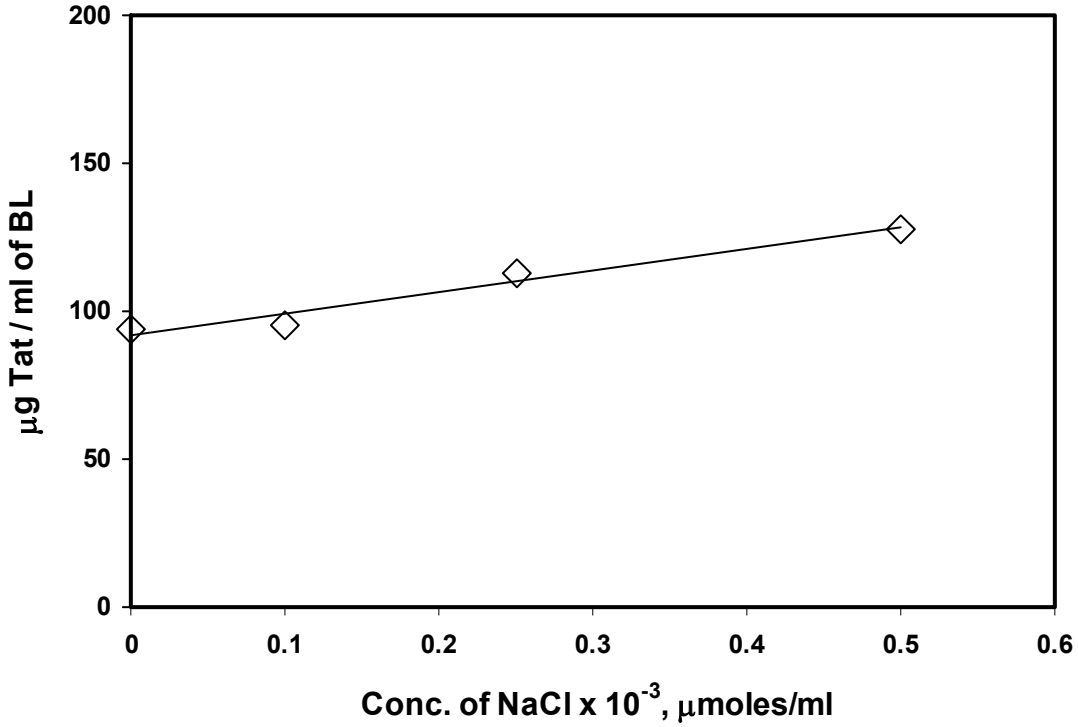

Figure 5.15 Effect of ionic strength on free available Tat by diluting bacterial lysate (dilution factor = 10) with different concentrations of NaCl

Characteristic flux and concentration of protein profiles in permeate of affinity membrane separation of Tat: Figure 5.16 represents characteristic flux decline profile as a function of time for different solutions in affinity separation of Tat from UNF BL2 feed. It can be observed that permeation of BL is associated with dramatic decrease in permeate flux. It decreases to 50 % and 20 % of initial flux after first 10 min and 60 min, respectively. After that it remains almost constant. Even the washing steps (WB 1, WB 2 and CB) were not able to enhance the flux significantly. This shows that the fouling inside the membrane matrix was pre-dominantly irreversible in nature. Some reversibly adsorbed proteins were removed in the washing steps thereby increasing the flux from 20 % to 25 % of the initial value. Figure 5.17 is a semi-logarithmic plot, which demonstrates the concentration of total protein obtained in permeate as different solutions were permeated in the same affinity separation experiment. Concentration of protein in permeate decreases due to adsorption inside the membranes. It reaches a minimum (550 μg/ml) after around 60 min, which also corresponds to maximum decline in the permeate flux. Then, adsorption of protein attains an equilibrium value and almost ceases. After that, concentration of protein in permeate increases and eventually approaches the concentration of protein in feed side. Figure 5.17 also shows that the subsequent washing steps were able to remove the reversibly adsorbed protein molecules from the membrane matrix.

Qualitative analysis of membrane purified Tat protein: Quality of the membrane purified Tat, isolated from unfiltered BL as well as pre-filtered BL feed, was analyzed by SDS-PAGE, Western Blot and Biotin analyses. SDS-PAGE fractionates proteins from a mixture based on their molecular weight and shows specific band for different molecular weight proteins present. Figure 5.18 demonstrates that for a typical Tat separation experiment, feed, permeate and retentate streams were consisted of substantial amount of unwanted proteins along with Tat. The wash buffer and cleavage buffer did not contain Tat protein. The eluate, which is basically the purified Tat stream, has a distinct band near 13-14 kDa molecular weight range.

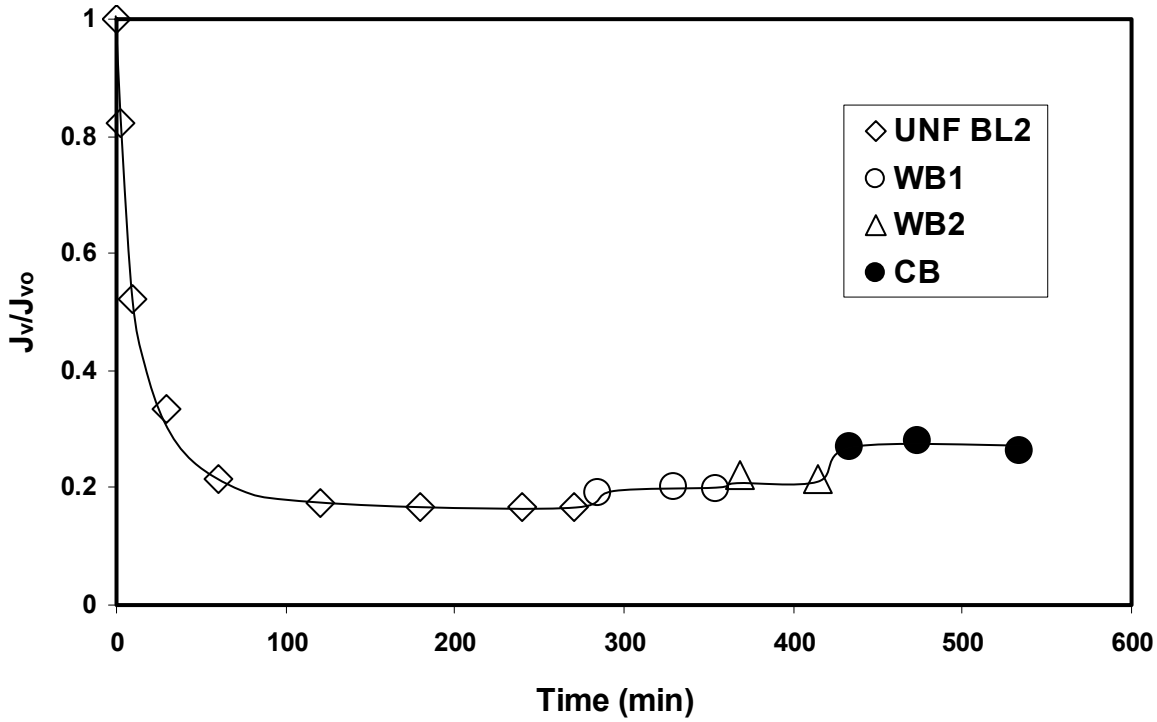

Figure 5.16 Characteristic flux vs. time curve for permeation of unfiltered bacterial lysate (UNF BL2), wash buffer 1 (WB 1), wash buffer 2 (WB 2) and cleavage buffer (CB) through avidin immobilized 4-stack functionalized membranes. Permeate flux is normalized by dividing with initial flux through avidin immobilized 4-stack membranes.

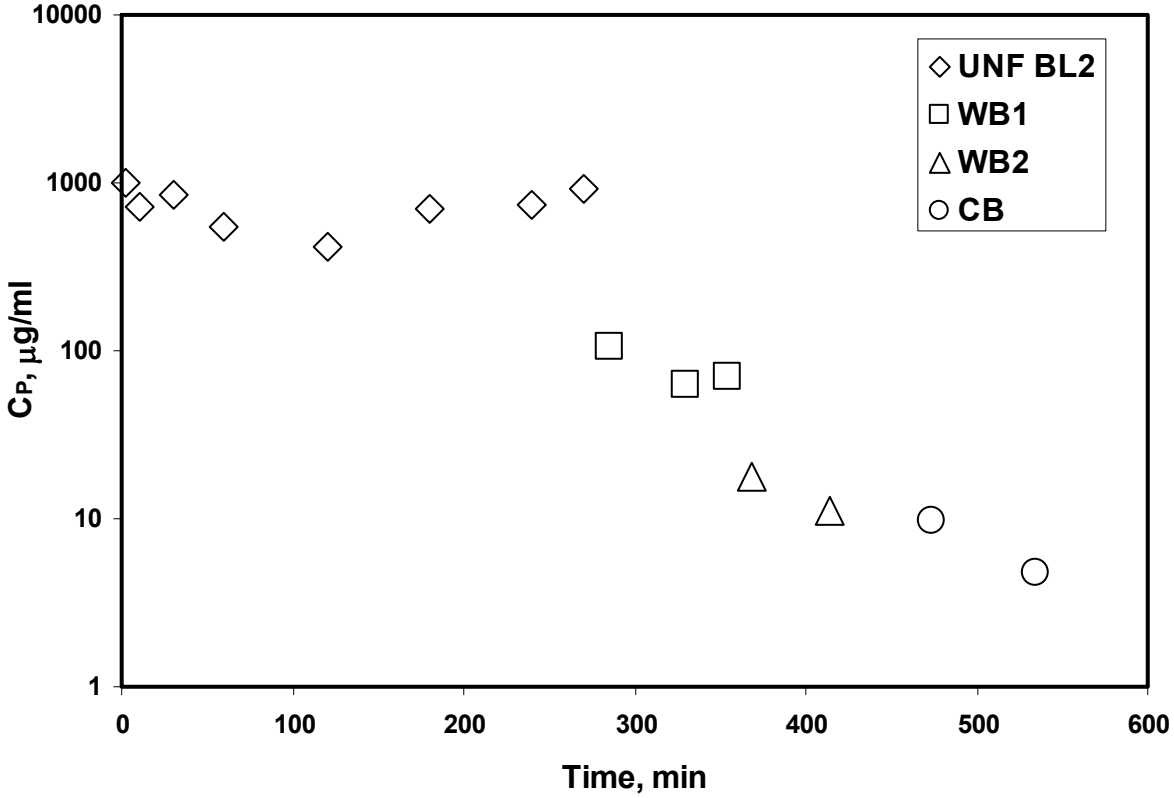

Figure 5.17 Concentration of total protein in permeate for different solution streams in affinity separation of Tat from UNF BL2 feed through 4-stack avidin immobilized functionalized membranes. UNF BL2 = unfiltered bacterial lysate with 1120 µg/ml total protein concentration in feed, WB 1 = wash buffer 1, WB 2 = wash buffer 2 and CB = cleavage buffer

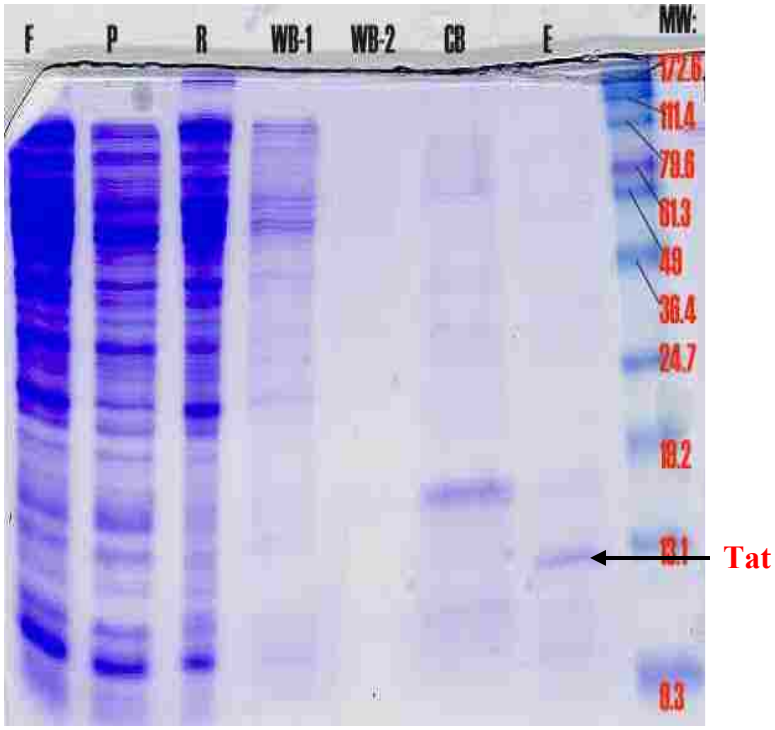

Figure 5.18 SDS-PAGE images of different streams for the separation of Tat from bacterial lysate (UNF BL2) using avidin-biotin interaction in avidin immobilized 4-stack nylon membranes (F = Feed, P = Permeate, R = Retentate, WB = wash buffer, CB = cleavage buffer, E = Tat eluate). Conc. of total protein in feed = 1120 µg/ml

For the ease of comparison, SDS-PAGE and Western Blot analysis images of Tat eluates from UNF BL1, UNF BL2, MF BL and UF BL feed are represented in Figures 5.19 and 5.20 along with the column chromatographically purified Tat. A distinct band near 13-14 KDa can be observed in SDS-PAGE images (Figure 5.19) of all membrane purified Tat eluates along with few additional bands for minor impurities. However, due to the presence of substantial amount of impurities, several other bands are observed for column chromatographically purified Tat eluate. Although molecular weight of Tat monomer is 8335 Da, the band obtained at 13-14 kDa due to the strong interaction between SDS and the highly basic polypeptide sequence of Tat (Hollman et al. 2005).

Western Blot analysis has also been used to compare the purity of Tat protein obtained by membrane and packed-bead column chromatographic separation. Since, a very specific antibody of the protein of interest is utilized to analyze a sample in Western Blot; any band that shows up in the image must be due to the corresponding protein. As seen from Figure 5.20, the purified Tat obtained from membrane separation contains a distinct band near 13 kDa, indicating the presence of pure monomeric form of Tat, whereas the Tat from packed-bead column chromatographic separation contains several other bands ranging from 10-80 kDa, indicating the presence of polymeric forms of Tat, which are unwanted for further therapeutic usages of Tat protein.

Biotin analysis results also proved the presence of impurities in the form of biotin for column chromatographically purified Tat. It was determined that column purified Tat contains impurities equivalent to 17 mole % (0.5 wt %) of biotin, which was substantially high. On the other hand, biotin was not detected (lower limit of detection was found to be 4 mole % of biotin) for membrane purified Tat. The biotin impurities in column chromatographically purified Tat indicates the shortcomings of diffusion mode in washing and cleavage steps. It is speculated that the biotin containing impurities might be due to the uncleaved biotin-fusion protein-Tat or biotin-fusion protein or free biotin.

Total amount of purified Tat for UNF BL1 and UNF BL2 feed were 250 and 270 μg, respectively, as analyzed by ELISA. This corresponds to only 5-6 % recovery of Tat from BL. The % recovery implies that substantial amount of Tat (95 %) is still present in other streams along with the impurities.

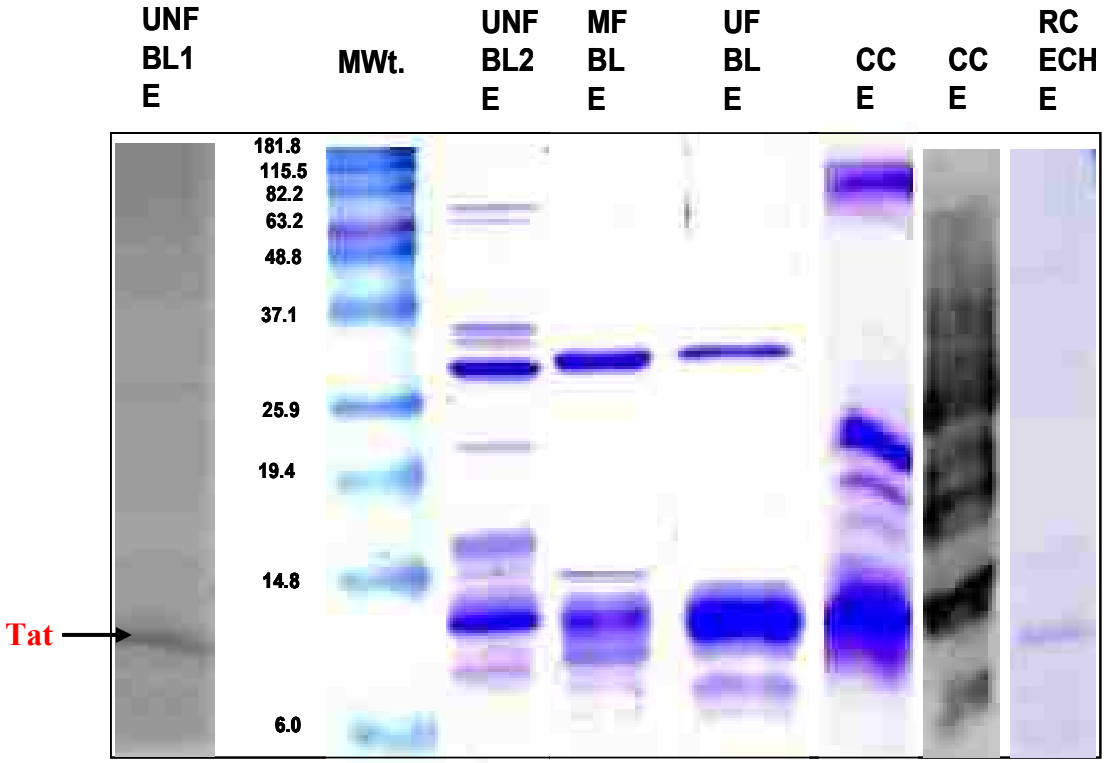

Figure 5.19 SDS-PAGE images of purified Tat eluates separated from bacterial lysate (BL) using different techniques. E = Tat eluate, UNF BL1 = unfiltered BL 1, UNF BL2 = unfiltered BL 2, MF BL = microfiltered BL, UF BL = ultrafiltered BL, CC = column chromatography, RC ECH = Tat separated using RC-ECH functionalized membrane

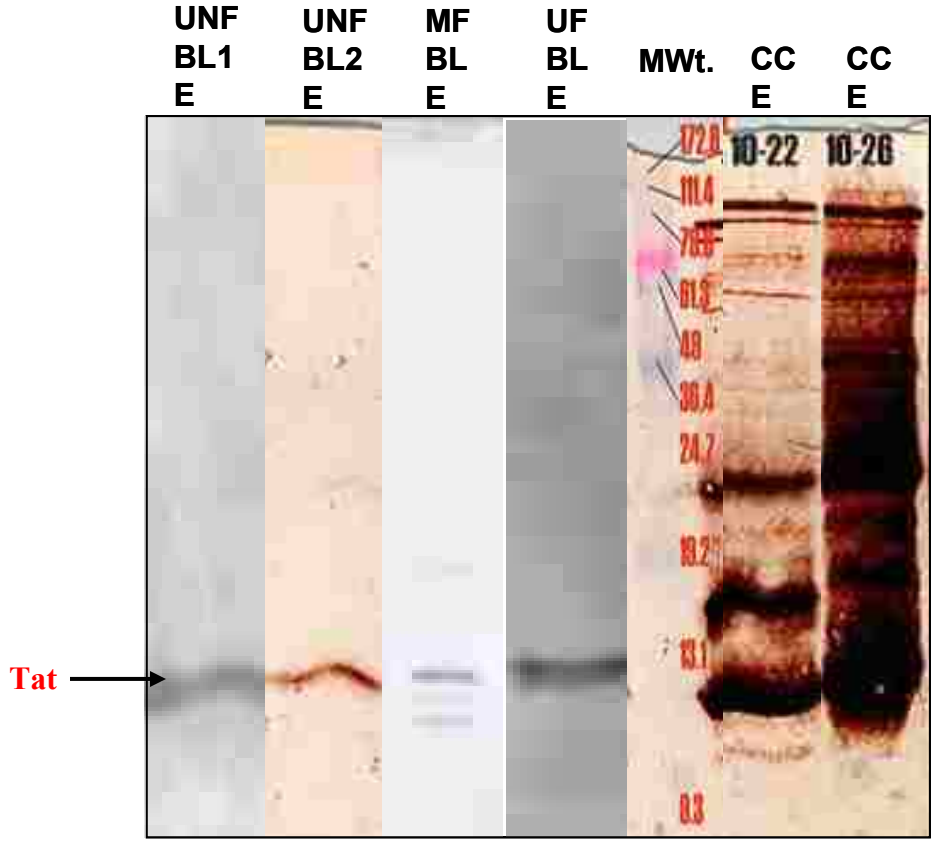

Figure 5.20 Western Blot analysis of different purified Tat eluates from bacterial lysate (BL). E = Tat eluates, UNF BL1 = unfiltered BL 1, UNF BL2 = unfiltered BL 2, MF BL = microfiltered BL, UF BL = ultrafiltered BL, CC = column chromatography

Effect of pre-filtration on processing time and recovery: Pre-filtration has a critical impact on the processing time of not only the affinity separation, but also the overall process, i.e. including the washing and pre-conditioning for cleavage steps. Comparison of processing time for various steps of membrane separation is given in Figure 5.21 for different BL feeds. It can be observed from the Figure that pre-filtration step was able to substantially reduce the overall processing time.

Although pre-filtration step itself has incurred significant time, it has dramatically reduced processing time for affinity separation, two washing cycles and pre-conditioning by cleavage buffer. Time required for affinity separation of pre-filtered feed was less due to overall higher flux (lower fouling). Similarly, time for subsequent wash and cleavage buffers was less due to higher fluxes for the pre-filtered cases. Time for washing cycles was also less because lower amount of wash buffers were sufficient to remove the non-specifically adsorbed proteins. However, the isolation of Tat by Factor X_a required same amount of time for all the three cases as it was dependent on the kinetics of cleavage by the protease.

The amount of Tat recovered was significantly higher for UF BL (1050 μg Tat), followed by MF BL (750 μg Tat), whereas, it was substantially lower for UNF BL2 (270 μg Tat). Amount of biotinylated-Tat fed and avidin immobilized in membranes were same for all the three cases. This shows that pre-filtration step has significantly improved the extent of Tat recovery, i.e., separation efficiency, due to the enhanced accessibility. The processing time to treat 0.55 μmole of biotin in feed has reduced from around 9 hr for unfiltered BL feed to 6.5-7 hr for pre-filtered BL feeds. Point to note that processing time needed to recover 250 μg of Tat by packed-bead column chromatography was almost 11 hr. However, if the processing time is represented in terms of time required per unit amount of Tat isolated then the values obtained are 2.6, 2, 0.5, 0.4 min/μg for column chromatography, unfiltered BL feed, MF BL feed and UF BL feed in membranes, respectively. This demonstrates, that for pre-filtered BL feed, the processing time per unit amount of Tat isolated is five times lower than that for column chromatography.

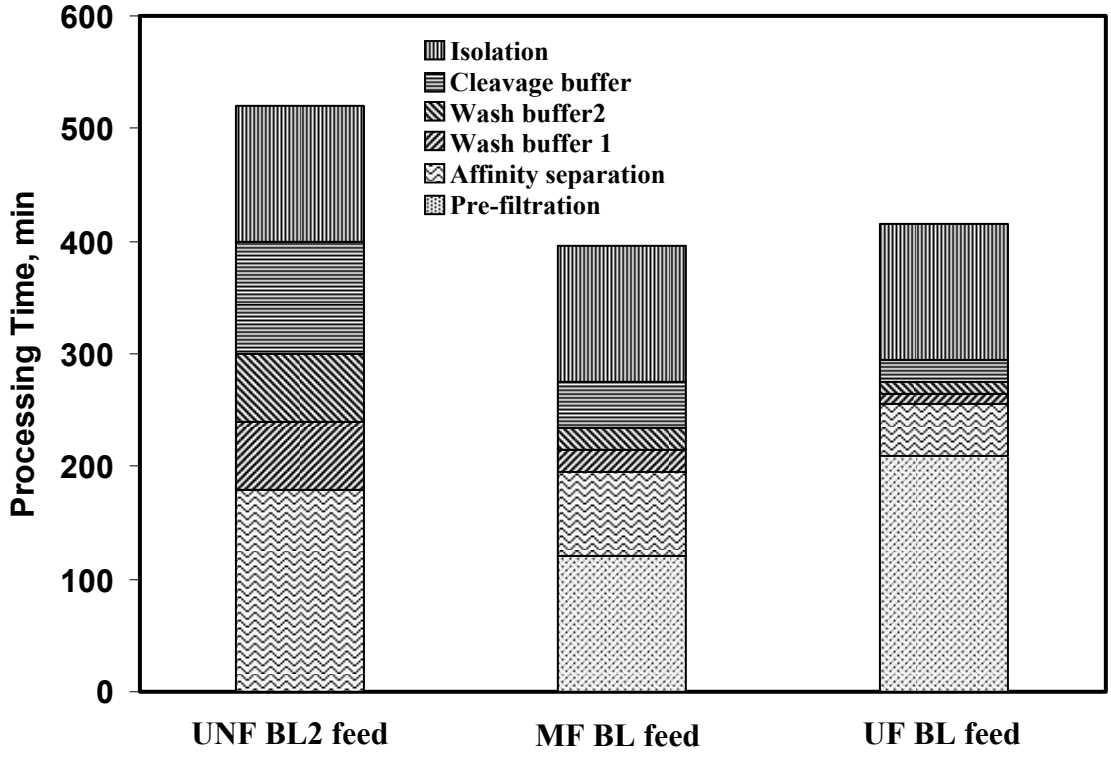

Figure 5.21 Comparison of total processing time for unfiltered BL feed (UNF BL2 feed), microfiltered BL feed (MF BL feed) and ultrafiltered BL feed (UF BL feed) in separation and purification of Tat from BL. For all cases, external membrane area = 33.2 cm^2, volume of BL feed = 250 cm^3 with 95 % permeate water recovery; Amount of biotinylated-Tat fed = 0.55 μmole, maximum possible Tat recovery = 0.18 μmole (1500 μg)

RC-ECH TAT: Tat separation was carried out using 4-stack functionalized RC-ECH-avidin membranes. Since, this is just an initial study showing RC-ECH membranes can be used for separation of Tat protein from BL; all analyses were not done. Only, SDS-PAGE analysis was carried out with the Tat eluate to show that pure Tat is isolated. Figure 5.19 illustrates that this functionalized membranes system was indeed able to isolate satisfactorily pure Tat as confirmed from the distinct band near 13-14 KDa.

5.2 Conclusions

Affinity based separation technique was applied to obtain high quality Tat protein from bacterial lysate (BL) supernatant using avidin-biotin interaction in functionalized stacked MF membranes. Tat protein obtained by this technique was superior in quality than that obtained by conventional packed-bead column chromatographic separation as demonstrated by SDS-PAGE, Western Blot and biotin analyses. Membrane purified Tat was pure and monomeric in nature compare to polymeric Tat obtained for conventional packed-bead column chromatographic separation. The amount of biotin impurities in Tat protein purified by conventional packed-bead column chromatographic separation was 17 mole %, whereas, biotin impurities were not detected for membrane purified Tat.

The major factors associated with this separation are the accessibility of covalently immobilized avidin sites by the biotinylated protein and fouling of the membranes due to permeation of significant quantity of non-biotinylated proteins. In this research, accessibility of avidin sites was quantified using different biotinylated-species. It was observed that in case of covalent immobilization of avidin, only half of the total avidin sites were actually accessible by biotin moiety present in a small biotinylated probe molecule. The accessibility decreases further for pure biotinylated model protein, and becomes least for the target protein, Tat, in bacterial lysate due to the presence of substantial amount of non-biotinylated proteins (97-99 wt %). The avidin immobilized membranes were also susceptible to non-specific protein adsorption causing significant flux drop due to fouling. For permeation of BL, the flux decreased by 80 % of the initial value due to fouling.

In order to improve the efficiency of the technique, a pre-filtration step was introduced. The pre-filtration step was effective in removing high molecular weight proteins and other impurities from BL feed. Accessibility of immobilized avidin sites, and hence the separation efficiency of biotinylated-Tat protein was significantly enhanced for the pre-filtered BL feed (normalized accessibility = 0.5-0.7) compared to unfiltered BL feed (normalized accessibility = 0.18-0.35). Significant improvement was also observed in the flux decline behavior of the pre-filtered BL feed due to reduced fouling. The processing time was also reduced (5 times lower) for the pre-filtered BL feed. The pre-filtered BL feed has also allowed the analysis of biotinylated-Tat content of different process streams of affinity separation directly by HABA-avidin complex method.

Pre-filtration step was able to restrict the fouling only within the pores of the membranes. Hence, under the experimental conditions mentioned in this research work, standard blocking model was sufficient to predict the flux decline due to fouling for the pre-filtered BL feeds in affinity separation. However, a combined model considering adsorption on both external surface and pores of the membrane was necessary to predict fouling behavior of unfiltered BL feed.

Chapter 6 Enzymatic Oxidation of Glucose to Gluconic Acid and H_2O_2 by Electrostatically Immobilized Glucose Oxidase in Functionalized Membranes

Glucose oxidase (GOX) is one of the most widely used enzymes due to its ability to detect glucose, and remove oxygen and glucose from the system by forming gluconic acid and hydrogen peroxide. The focus of this research study was to form high capacity, highly active, stable and reusable GOX-immobilized functionalized polymeric membranes for catalytic oxidation of glucose using Layer-By-Layer (LBL) technique within nylon based membrane and in-situ polymerization of acrylic acid in hydrophobic PVDF membrane. Functionalization of membranes and immobilization of GOX was described in Chapter 4. This Chapter discusses the experimental results obtained for kinetics of enzymatic oxidation of glucose, effects of pH and flow rate on activity of the immobilized GOX under convective flow condition, and some other important observations. One of the major achievements in this research was the reusability of the membranes. To the best of our knowledge, this is the first time that a study has been carried out to detach and reattach enzyme from membranes to explore the reusability.

6.1 Results and discussion

In order to check the reproducibility of the results, all experiments were triplicated. The error bars shown in different figures represent standard deviations.

6.1.1 Steady state experiment

Steady state concentration of H_2O_2 produced as a function of time, for a fixed substrate concentration and flow rate, is represented in Figure 6.1. From the Figure it is evident, that the concentration of H_2O_2 in permeate has reached steady state from the beginning itself for both of the substrate concentrations studied. The variation is within the error range of 5 %. It was also observed that the amount of H_2O_2 produced in the feed side of the membrane was < 5 % after t = 30 minutes for all the cases. This is because the surface immobilization of GOX was insignificant compare to pore immobilization.

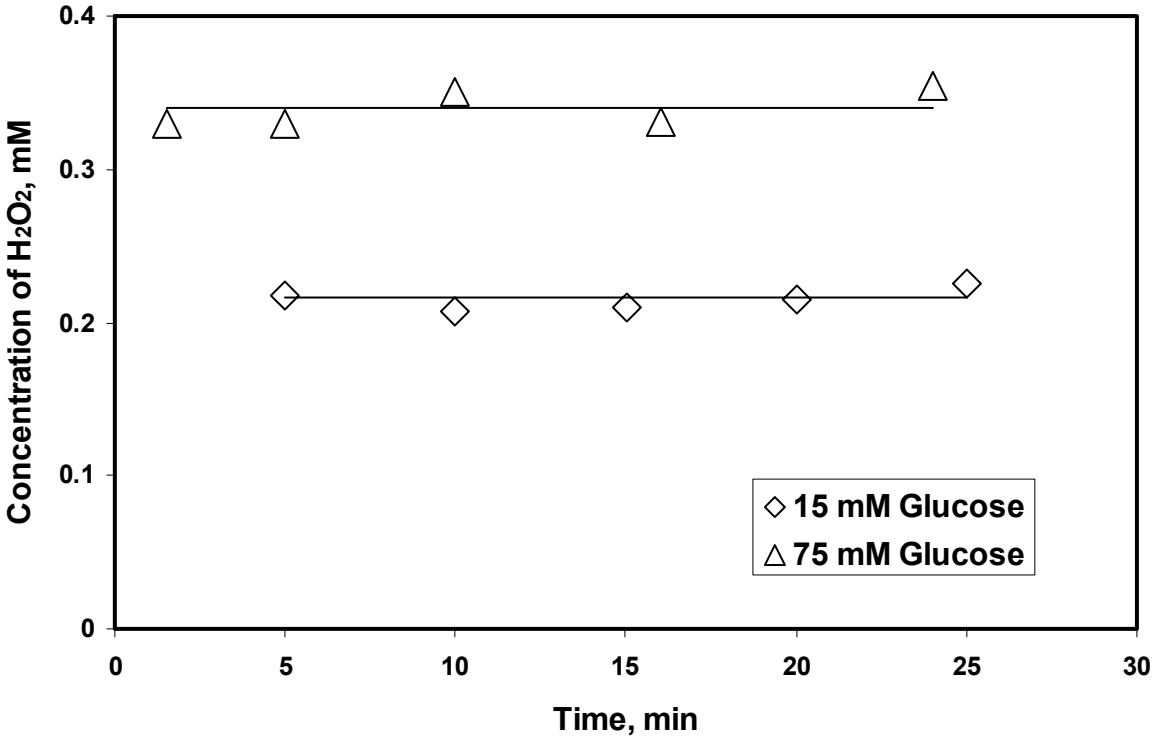

Figure 6.1 Determination of the steady state concentration of H_2O_2 produced in LBL assembled nylon membrane for fixed flow rate and substrate concentration. Two different substrate concentrations, 15 mM and 75 mM glucose, were studied. Amount of GOX immobilized = 1.5 mg, permeate flux = 140 x 10^{-4} cc/cm^2.s, residence time = 0.6 s, pore radius of LBL assembled nylon membrane = 125 nm, external membrane area = 13.2 cm^2, membrane thickness = 165 μm, pH = 5.5, Temperature = 25 ^{0}C

However, if the experiment is carried out for long time, the production of H_2O_2 will be significant as it behaves like a batch reactor on the feed side. Therefore, to avoid production of H_2O_2 on feed side, all activity data were collected within first 5-10 minutes of the experiments.

6.1.2 Importance of O_2

Figure 6.2 represents the normalized activity of immobilized GOX as a function of time for three different regimes; (i) initial phase of air supply, (ii) air supply replaced with N_2, and (iii) re-establishment of air supply. As air was replaced by N_2, activity started dropping dramatically and reached a minimum. Then, with reestablishment of the air supply, the activity increased sharply. This shows that depletion of O_2 from the reaction mixture could severely affect the activity of enzyme. Thus, it was necessary to maintain the saturation condition of O_2 in the reaction mixture for all experiments. Higher activity observed in the latter phase of the experiment was due to the increase in concentration of H_2O_2 in the feed side with time.

6.1.3 Kinetics of glucose oxidation by GOX

Homogeneous phase kinetics: Homogeneous phase catalytic oxidation of glucose was carried out using free GOX. Well known Michaelis-Menten rate equation (Voet et al. 2004) is used to describe the kinetics of homogeneous phase glucose oxidation. The equation expressing the rate, v is as follows

$$v = \frac{v_{max} s}{(K_m + s)} \tag{6.1}$$

where, s is the substrate concentration, v_{max} is the maximum possible rate at an imaginary substrate concentration of infinity, K_m is the Michaelis-Menten rate constant and is defined as the substrate concentration at which rate becomes half of v_{max}.

Equation (6.1) can be manipulated to give

$$\frac{1}{v} = \frac{1}{v_{max}} + \frac{K_m}{v_{max} s} \tag{6.2}$$

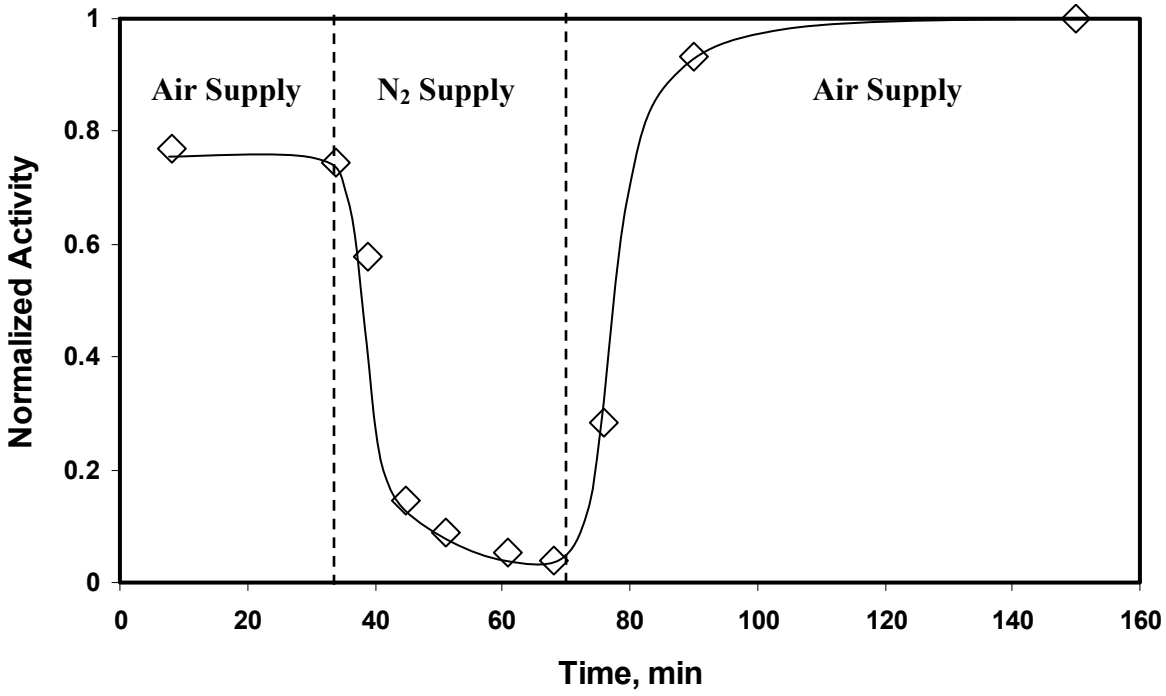

Figure 6.2 Importance of O_2 in enzymatic oxidation of glucose by GOX immobilized in LBL assembled nylon membrane. Activity is calculated based on concentration of H_2O_2 produced, and normalized by dividing with maximum activity for this experiment, which is $[H_2O_2]$ / $[H_2O_2]_{max}$. Concentration of glucose fed = 0.75 mM, Amount of GOX immobilized = 1.5 mg, permeate flux = 140 x 10^{-4} cc/cm^2.s, residence time = 0.6 s, pore radius of LBL assembled nylon membrane = 125 nm, external membrane area = 13.2 cm^2, membrane thickness = 165 μm, pH = 5.5, temperature = 25 ^{0}C

Equation (6.2) is used to determine the kinetic parameters by a straight line plot (Lineweaver-Burke Plot) of 1/v vs. 1/s and then calculating v_{max} and K_m from intercept and slope, respectively.

The rate (v) for a particular substrate concentration is considered to be equal to the initial rate, assuming the conversion is negligible initially. Initial rate were estimated by determining the slope of the activity vs. time data at t = 0 for each substrate concentration (not shown). Then, v is plotted as a function of s and represented in Figure 6.3. It can be observed that v increases sharply with s at lower range of s, then gradually flattens out at higher s (Smuleac et al. 2006). This is a typical behavior of enzymatic reaction kinetics. Rate data are also utilized to determine the Michaelis-Menten kinetic parameters. Lineweaver-Burke Plot for homogeneous phase reaction is demonstrated in Figure 6.4, and then v_{max} and K_m are calculated using equation (6.2). Experimental data were extremely linear in nature as illustrated by the R^2 value of > 0.99 in Figure 6.4. The values of intercept and slopes are around 3.72 and 71.5, respectively. From these, the values of v_{max} and K_m are calculated to be 0.27 mmole/mg-min and 19 mM, respectively. It is very difficult to compare the experimentally obtained value of homogeneous phase v_{max} with the literature values as it varies from μmole to mmole range (Table 2.1). The reported values of homogeneous phase K_m also varies from 3- 70 mM (Table 2.1).

This enormous deviation is probably because of the variations in experimental conditions and set-up. It is also probably due to the fact that GOX is available in different forms and activities from different manufacturers. The experimentally obtained value of homogeneous phase v_{max}, in our case, is close to that has been reported by the manufacturer (0.3 mmole/mg-min). The experimentally obtained value of K_m also matches reasonably well with an earlier reported value (Ahuja et al. 2007). Hence, these experimentally obtained values of v_{max} and K_m for homogeneous phase GOX are used further in this dissertation.

It is worth mentioning here that for free GOX and glucose in homogeneous phase batch reaction the rate must be expressed in the unit of mmole/mg-min, as the volume of reaction mixture used is important. For example, if 75 mM glucose solution is oxidized in presence of GOX in 25 ml reaction mixture, then the initial rate is 8.26 mM/mg-min, whereas, for 50 ml reaction mixture it is 4.13 mM/mg-min.

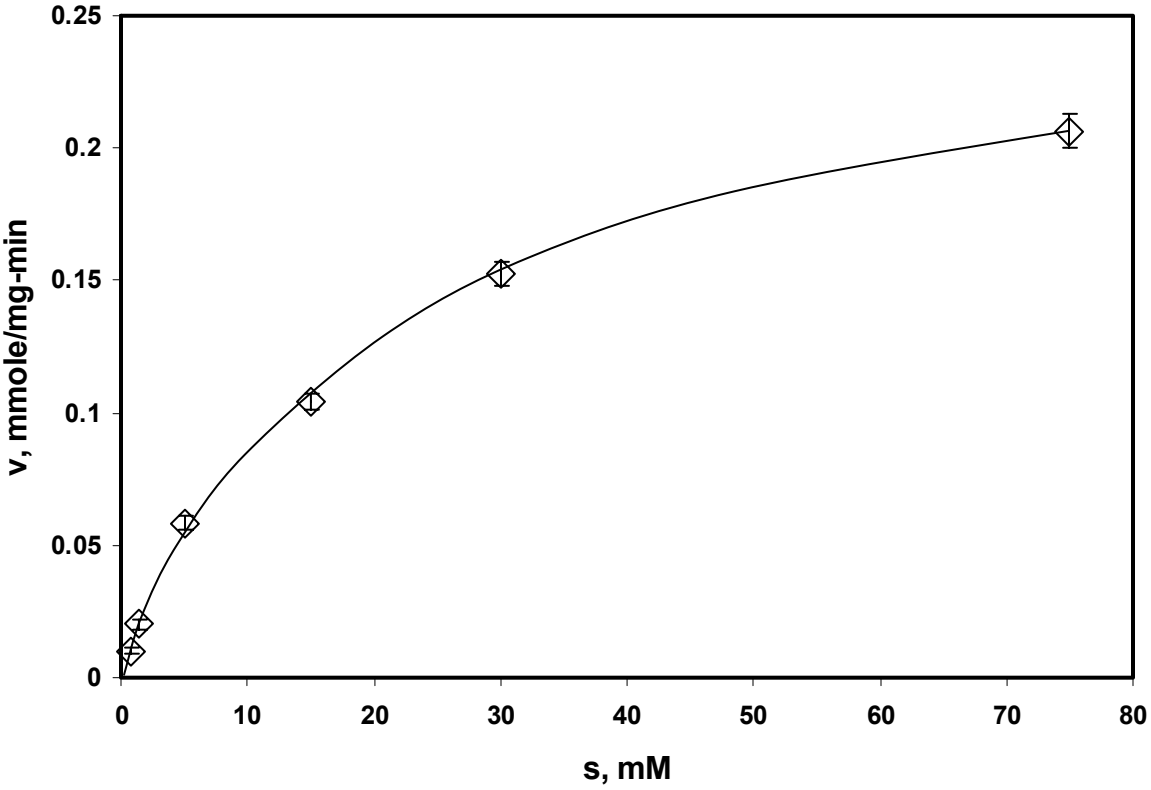

Figure 6.3 Rate (v) vs substrate concentration (s) for free GOX in homogeneous phase batch reaction. Concentration of glucose solution = 0.75 - 75 mM, reactor volume = 25 cm^3, amount of GOX = 0.25 mg, temperature = 25 ^{0}C, pH of NaOAc-HCl buffer = 5.5

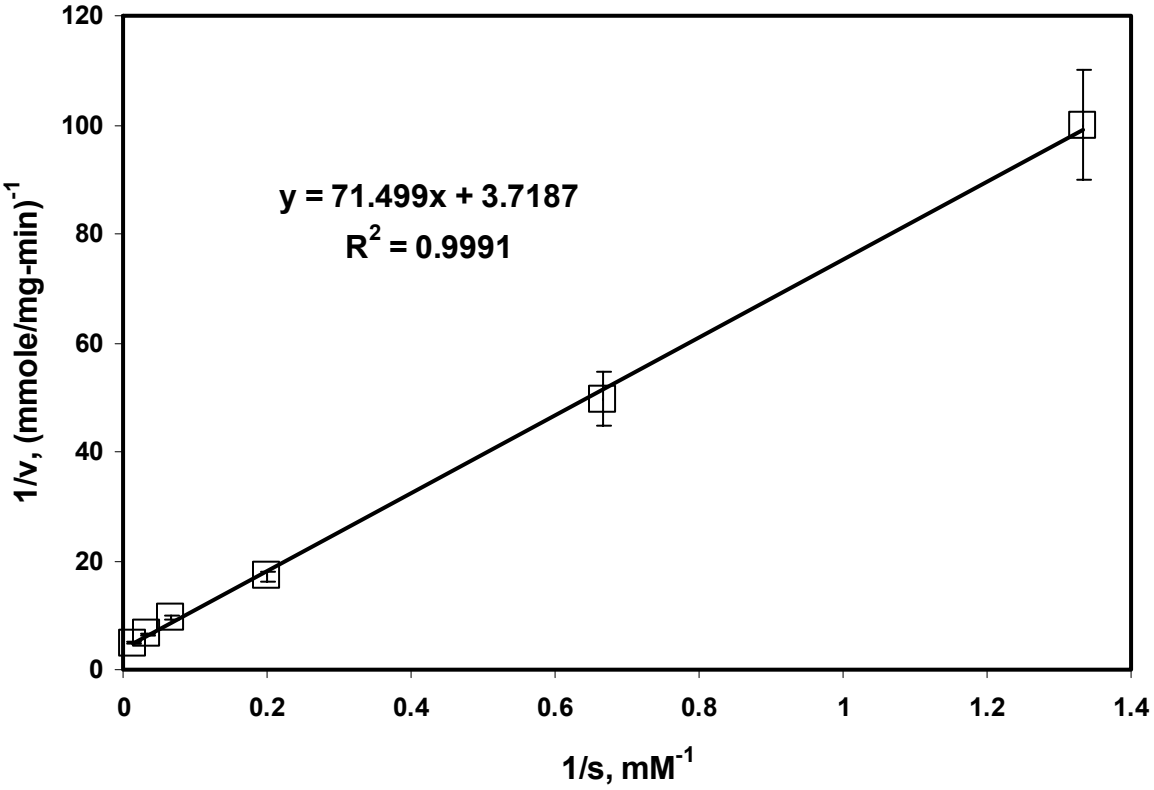

Figure 6.4 Lineweaver-Burke plot for free GOX in homogeneous phase batch reaction. Concentration of glucose solution = 0.75-75 mM (1/s = 1.33 - 0.013 mM^{-1}), reactor volume = 25 cm^3, amount of GOX = 0.25 mg, temperature = 25 ^0C, pH of NaOAc-HCl buffer = 5.5

Nonetheless, in terms of mmole/mg-min the rate is 0.27 for both the cases. However, for the combination of GOX immobilized in membrane and convective flow of glucose solution, the scenario is different and is explained in detail later.

Immobilized phase kinetics: To analyze the rate of reaction for GOX immobilized in a membrane reactor and the substrate solution permeating through it, understanding of hydrodynamics within the reactor is important. Ideally, each molecule of glucose, inside the membrane reactor, should spend equal time in contact with GOX i.e. the residence time, which is the ratio of volume of membrane reactor to volumetric flow rate. Thus, residence time calculation is important to determine the activity of immobilized GOX. Determination of volume of membrane reactor, in this case, is not trivial.

There are two regions inside a membrane pore; polyelectrolyte region, where GOX is immobilized, and a region void of GOX (Figure 6.5). Reaction mixture flows through both the regions. The polyelectrolyte layers were developed from the pore wall toward the pore center. The other region, devoid of GOX, was located near the center of the pore and known as the core region. A fraction of glucose molecules permeating through the core region never interacts with enzyme. This phenomenon is known as core leakage. Core leakage has significant effect in the calculations of enzyme activity (Smuleac et al. 2006). Thus, it is reasonable to consider only the volume of membrane pore containing the enzyme as the effective volume of membrane reactor.

Calculation of effective volume of membrane reactor: For LBL membrane, cumulative thickness of layers after GOX immobilization = 100 nm, pore radius of pure membrane = 225 nm

Therefore, the core region volume = $(225\text{-}100)^2/225^2$) x pore volume = 0.30 x pore volume

Effective membrane reactor volume = 0.7 x pore volume = 0.7 x ε x A_m x l

Where, ε = porosity of the Immunodyne membrane = 0.8, A_m = external area of membrane =13.2 cm^2, l = length of the membrane = 165 x 10^{-4} cm

So, effective membrane reactor volume for LBL membrane = 0.7 x 0.8 x 13.2 x 165 x10^{-4} = 0.122 cm^3.

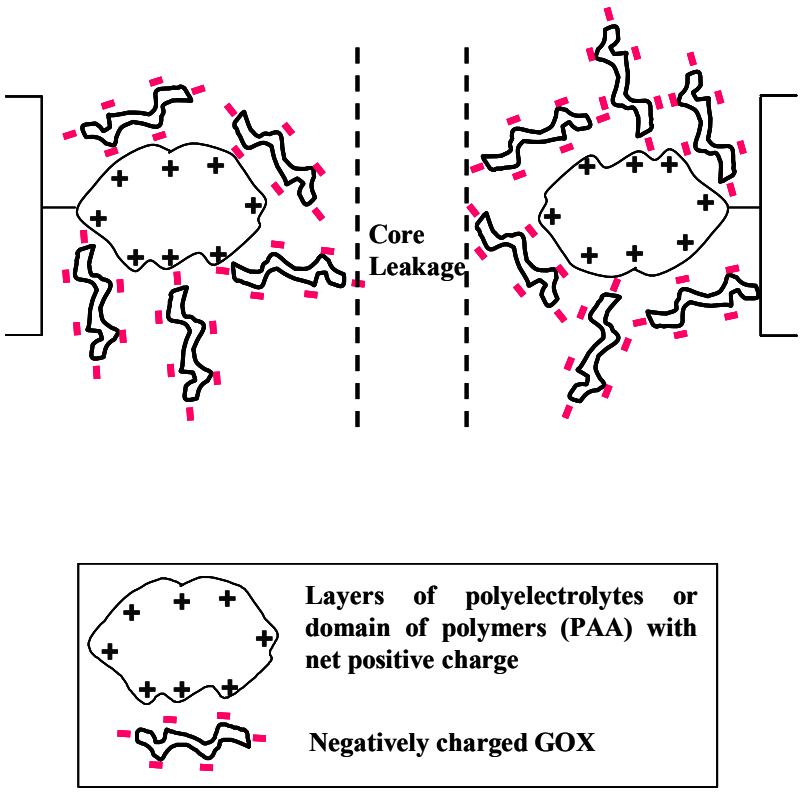

Figure 6.5 Schematic diagram of electrostatically immobilized GOX in polyelectrolyte / polymer domain for both LBL-GOX and PVDF-GOX membranes. There are two distinct regions; one containing GOX and the other devoid of GOX. The first region is responsible for the catalytic action of the membrane, whereas, the latter one is associated with core leakage

Similarly, for PVDF-PAA membrane the effective reactor volume = 0.8 x 0.75 x 13.2 x 125 x 10^{-4} = 0.1 cm^3.

Based on this effective membrane reactor volume, residence time (τ) is calculated for different flow rates. Then, rate for immobilized GOX is calculated as follows.

$$Rate = \frac{C_{P\,H_2O_2}}{\tau \times mg\ enzyme} \tag{6.3}$$

where, $C_{P\,H_2O_2}$ is the concentration of H_2O_2 in permeate

Under steady state condition and for a fixed residence time, the concentration of H_2O_2 produced in permeate is constant, irrespective of volume of the reaction mixture permeated. Hence, it is appropriate to present the rate in terms of mM/mg-min. While comparing the rate of immobilized GOX with free GOX, the conversion of rate unit from mM/mg-min to mmole/mg-min is delicate as it raises the issue of what permeate volume to consider for the conversion. In the author's opinion it would be completely unfair, in this case, to compare the rates between free and immobilized GOX, as hydrodynamics is completely different. Hence, only the rate data obtained for different cases of immobilized GOX are discussed. Similarly, although the units of the K_m values are same, they can not be compared on the basis of different dimensions of rate.

Rate of oxidation of glucose for GOX immobilized both in LBL (LBL-GOX-convective) and PVDF (PVDF-GOX-convective) membranes, with convective flow of reaction mixture, are determined for different substrate concentration using equation (6.3) and plotted in Figure 6.6. As observed from the Figure, at lower s, the rate increases very sharply with s, and then flattens out gradually at higher substrate concentration. For example, the rate increases from 3 mM/mg-min to 10 mM/mg-min as glucose concentration increases from 0.15 mM to 0.75 mM, whereas the rate increases only to 21 mM/mg-min as glucose concentration increases to 75 mM. For comparison, the rate for the same GOX immobilized LBL membrane in soaking mode (LBL-GOX-soaking), and GOX covalently immobilized in an Immunodyne membrane (covalent-GOX-convective), are also presented in Figure 6.6. For soaking mode, the rate is calculated similarly as free GOX in homogeneous phase, whereas, for covalently attached GOX equation (6.3) is used.

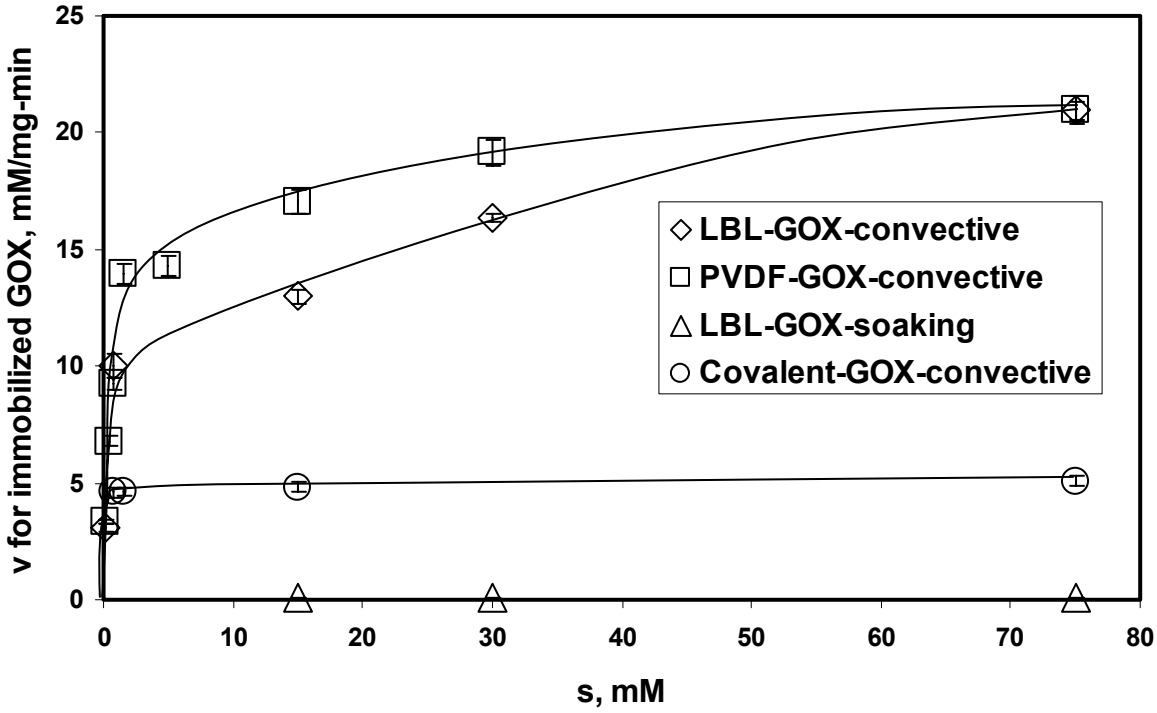

Figure 6.6 Rate of oxidation of glucose as a function of substrate concentration for different GOX immobilization experiments. Amount of GOX immobilized = 1.8 mg, 1.5 mg and 1 mg for PVDF membrane, LBL membrane and covalent immobilization, respectively. Residence time for all experiments were around 0.6 s, temperature = 25 ^{0}C, pH of NaOAc-HCl buffer = 5.5

For 75 mM substrate concentration, the rates are 21, 5 and 0.1 mM/mg-min for LBL-GOX-convective, Covalent-GOX-convective and LBL-GOX-soaking mode, respectively. The residence time was around 0.6 s for all convective flow experiments. Figure 6.6 illustrates that activity of electrostatically immobilized GOX under convective flow of glucose solution is superior to both covalently immobilized GOX under convective flow and electrostatically immobilized GOX under soaking mode. The soaking mode results show that surface immobilization of GOX is negligible and reaction rate is hindered by severe diffusional resistance.

Michaelis-Menten rate equation is again used to describe the immobilized phase reaction kinetics for the substrate concentration range of 0.75 - 75 mM, and it has revealed some interesting facts as explained here. Lineweaver-Burke plot is constructed from the rate data and presented in Figure 6.7. It can be observed that Lineweaver-Burke plots are non-linear for both LBL-GOX-convective and PVDF-GOX-convective. From the non-linear nature of the plots, it can be speculated that Michaelis-Menten rate equation is not effective in predicting the immobilized phase reaction kinetics accurately in the substrate concentration range studied. In other words, for immobilized GOX, the rate of glucose oxidation is not as sensitive to substrate concentration as expected from Michaelis-Menten rate equation in the range of 0.75 - 75 mM (1/s = 1.33 - 0.013 mM^{-1}) glucose solution. This can also be observed by comparing Figures 6.3 and 6.6 for homogeneous and immobilized phase, respectively. Homogeneous phase rate has substantially higher effect of substrate concentration than immobilized phase.

In order to study the behavior of kinetics of immobilized GOX in different regions of substrate concentration, Lineweaver-Burke plots are constructed for both LBL-GOX-convective and PVDF-GOX-convective cases (shown as insert of Figure 6.7) in the substrate concentration range of 15 - 75 mM (1/s = 0.067 - 0.013 mM^{-1}). For both the cases, the straight line plots fit the experimental data extremely well as evident from the R^2 values of > 0.99. v_{max} and K_m values are determined from Lineweaver-Burke plots in this concentration range. v_{max} for LBL-GOX-convective and PVDF-GOX-convective are 24 mM/mg-min and 22 mM/mg-min, respectively. K_m of LBL-GOX-convective is 13 mM and K_m of PVDF-GOX-convective is 4.6 mM.

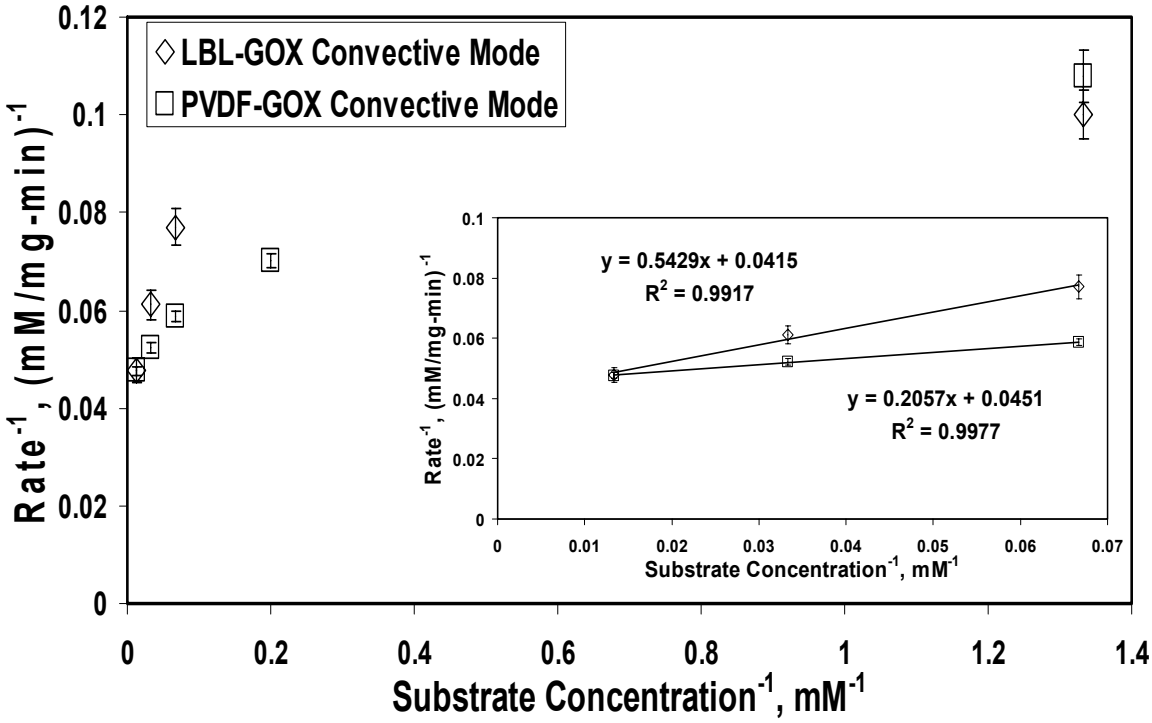

Figure 6.7 Lineweaver-Burke plot for GOX immobilized in functionalized LBL (LBL-GOX-convective) and PVDF (PVDF-GOX-convective) membranes. Concentration of glucose solution = 0.75 - 75 mM (1/s = 1.33 - 013 mM^{-1}), amount of GOX immobilized = 1.5 and 1.8 mg for LBL and PVDF membranes, respectively, temperature = 25 ^{0}C, pH of NaOAc-HCl buffer = 5.5. Inset figure shows Lineweaver-Burke plot for the substrate concentration range of 15 - 75 mM (1/s = 0.067 - 0.013 mM^{-1})

This study suggests that Michaelis-Menten kinetics is valid for immobilized phase GOX in the substrate concentration range of 15-75 mM. However, it fails to explain the rate behavior at lower range. K_m values obtained here are significantly lower than most of the reported K_m values for covalently immobilized GOX in Table 2.1. For covalently immobilized GOX in PAA grafted PVDF membrane (Ying et al.) and soaking mode oxidation of glucose, the value of K_m is 10.5. This again demonstrates the advantage of electrostatic immobilization and covalent flow over covalent immobilization and diffusive flow for an enzyme-substrate system.

6.1.4 Effect of residence time, i.e., flow rate

Effect of residence time on activity and rate of production of H_2O_2 by immobilized GOX in both LBL and PVDF membranes is described considering them as Plug Flow reactor (PFR), i.e., assuming no concentration gradient in radial direction and no mixing in axial direction. Material balance is done within membrane pore and Michaelis-Menten reaction kinetics is incorporated to obtain a mathematical expression for the exit concentration of H_2O_2 in permeate as follows.

$$C_{PH_2O_2} - k_m \ln \frac{\left(s_0 - C_{PH_2O_2}\right)}{s_0} - v_{\max}\tau = 0 \tag{6.4}$$

Then, conversion is calculated as follows.

$$Conversion = \frac{C_{PH_2O_2}}{s_0} \tag{6.5}$$

where, $C_{PH_2O_2}$ is the concentration of H_2O_2 in permeate, s_0 is the initial substrate concentration, and τ is the residence time. K_m and v_{max} for immobilized GOX, determined from the experimental rate values for the immobilized GOX in the substrate concentration range of 15-75 mM, are used for calculations. Equation 6.4 is solved to obtain model predicted concentration of H_2O_2 in permeate for different substrate concentrations and residence times. From the model predicted concentration of H_2O_2 in permeate, conversion and rate are determined using equations (6.5) and (6.3), respectively. The results for 15 mM substrate concentration are represented in Figures 6.8 and 6.9 along with the experimentally obtained values.

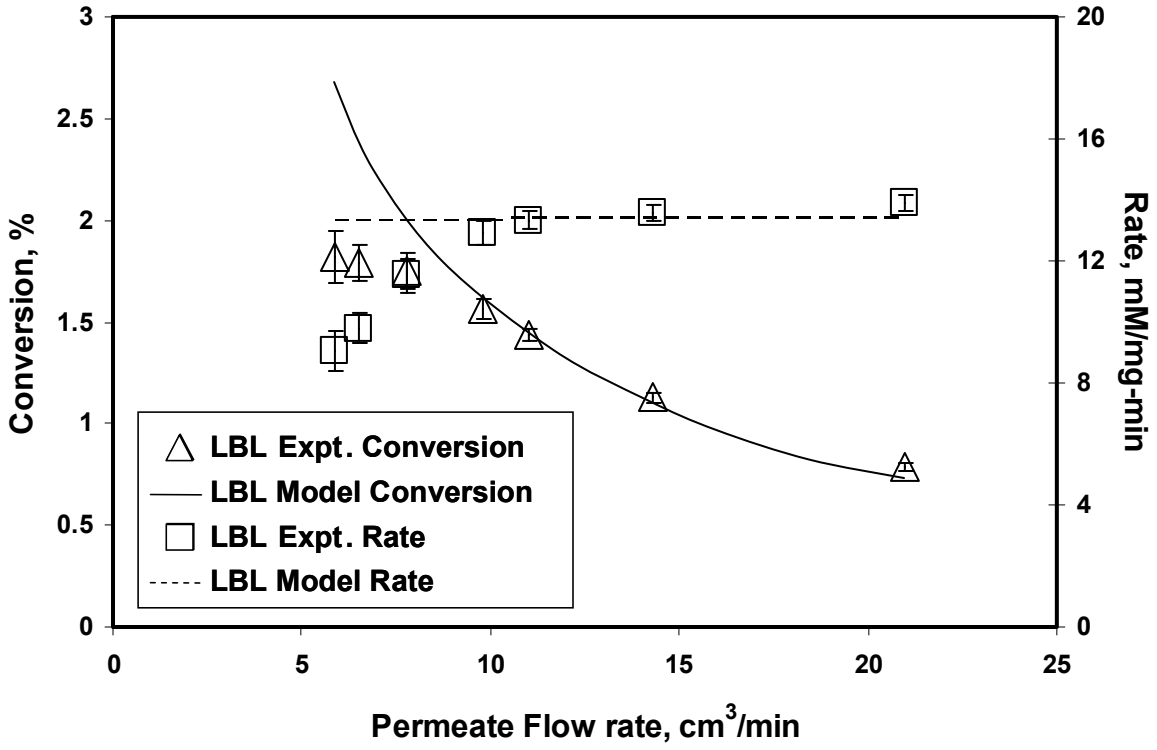

Figure 6.8 Effect of flow rate, i.e. residence time, on conversion of glucose and rate of formation of H_2O_2 for 15 mM glucose solution fed in LBL assembled nylon membrane. Rate and conversions are calculated from equations (6.3) and (6.5). Model values are calculated based on equation of PFR (equation 6.4). Amount of GOX immobilized = 1.5 mg, volume of LBL membrane reactor 0.122 cm^3, pH = 5.5, temperature = 25 ^0C, permeate flux = (75 - 265) x 10^{-4} cm^3/cm^2-s, residence time = 0.4 - 1.25 s

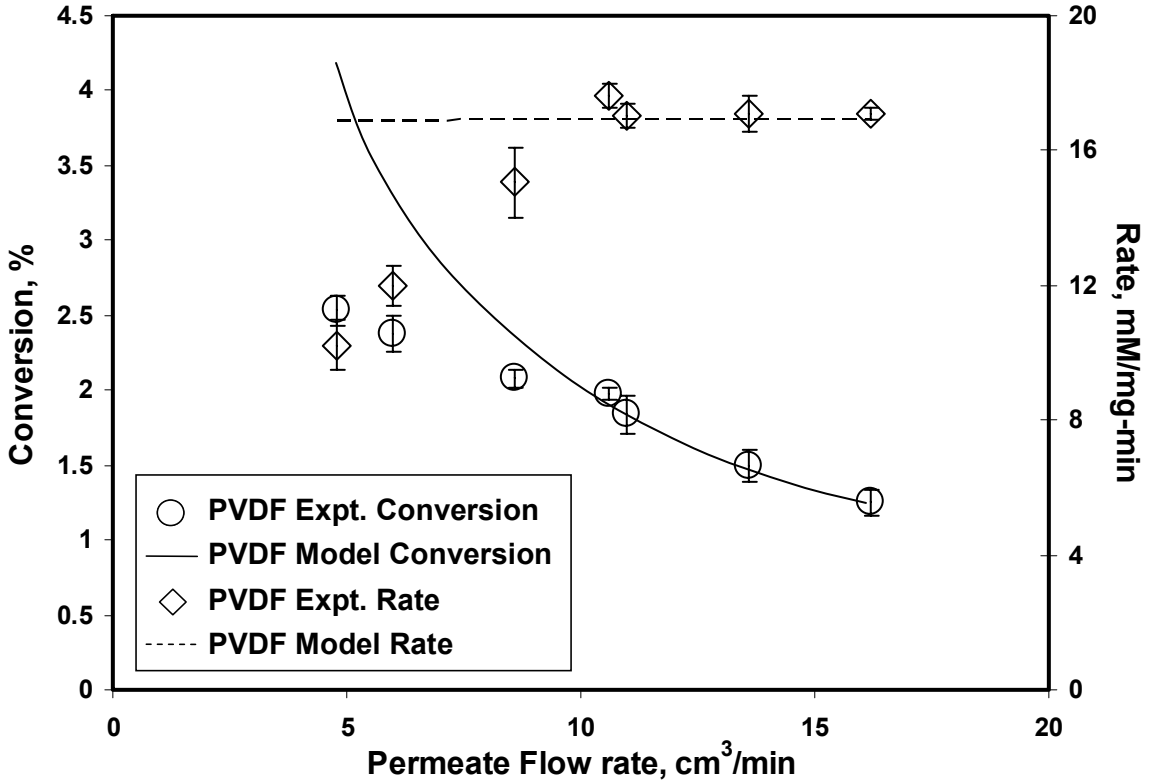

Figure 6.9 Effect of flow rate, i.e. residence time, on conversion of glucose and rate of formation of H_2O_2 for 15 mM glucose solution fed in functionalized PVDF membrane. Rate and conversions are calculated from equations (6.3) and (6.5). Model values are calculated based on equation of PFR (equation 6.4). Amount of GOX immobilized = 1.8 mg, volume of PVDF membrane reactor = 0.1 cm^3, pH = 5.5, temperature = 25 ^{0}C, permeate flux = (60 - 200) x 10^{-4} cm^3/cm^2-s, residence time varied from 0.4 - 1.25 s

Conversion of glucose represents concentration of H_2O_2 in permeates. It can be observed from the Figures 6.8 and 6.9 that as flow rate increases, i.e., residence time decreases, the concentration of H_2O_2 in permeate decreases and hence the conversion. This is because the product formation for a flow reactor is a function of residence time, whereas, rate of product formation is not. That is elucidated by the model predicted values in Figures 6.8 and 6.9. The experimentally obtained values of conversion and rate of glucose oxidation match satisfactorily with the model predicted values at higher flow rates. Discrepancy (over prediction) at lower flow rate is probably due to the resistance in accessibility. Lower flow rate corresponds to lower shear stress, due to which glucose molecules was not able to access all the active sites of immobilized GOX in the domain of polyelectrolytes. As flow rate increases accessibility increases, and eventually after certain flow rate all sites become accessible and reaction rate becomes independent of flow rate. This constant reaction rate for a particular substrate concentration is used for kinetic calculations discussed earlier. The results also demonstrate that the assumption of PFR for both membrane configurations is reasonable and Michaelis-Menten kinetic parameters determined in the higher range of glucose concentrations are acceptable.

6.1.5 Effect of pH

Effect of pH on activity of free GOX has been reported in literature (Chen and Weng 1986; Ozyilmaz et al. 2005). It has been observed that there is a distinct maximum for the activity of free GOX at pH 5.5, and activity decreases dramatically on either side of that pH. For example, in a study by Ozyilmaz and co-workers, the normalized activity (with respect to activity at pH 5.5) for 100 mM glucose solution was reported to be 35 % at pH 4.5 and 50 % at pH 7. Our study for free GOX, covering a range of 0.75 -75 mM of glucose concentration, also exhibited similar trend as shown in Figure 6.10. The effect of pH on activity of LBL-GOX system is also represented in Figure 6.10. It can be observed that although the activity curve goes through a maximum, the range of optimum pH is broad, and the decrease in activity on either side of the optimum pH range is also less. This proves that GOX immobilized in membrane can be operated over a wide range of pH without sacrificing the activity significantly.

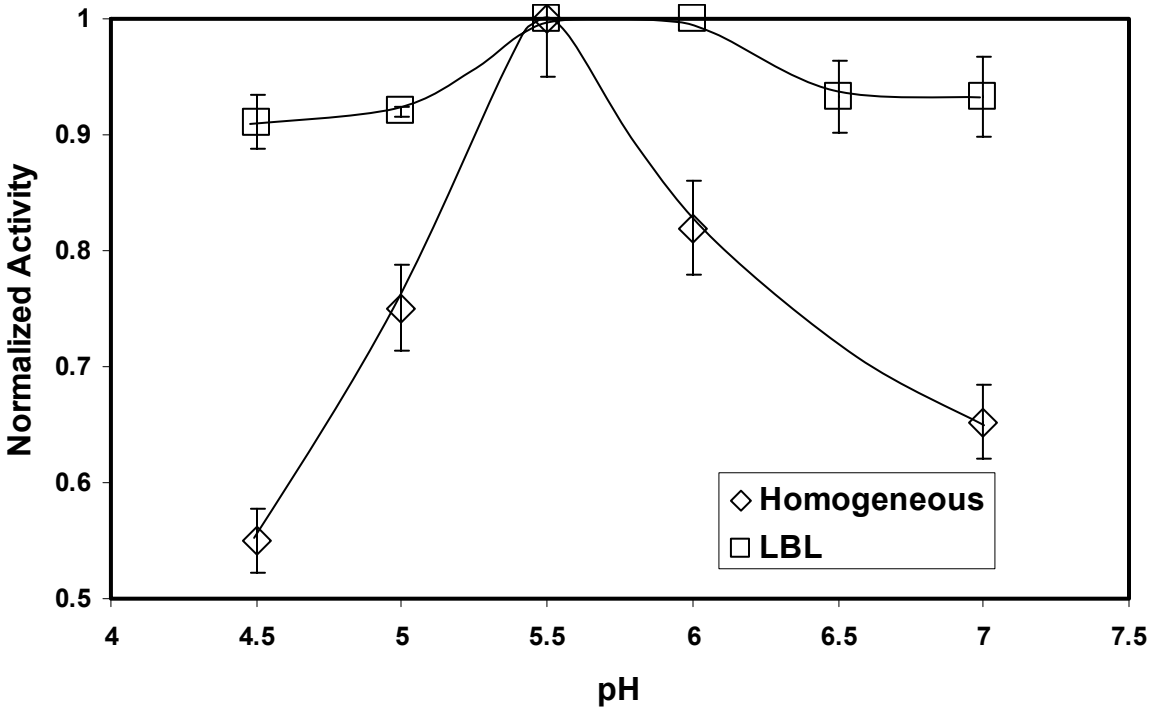

Figure 6.10 Effect of pH on activity for both free GOX and immobilized GOX in LBL assembled membrane. Activity is calculated based on concentration of H_2O_2 in permeate and is normalized by dividing with maximum activity, i.e., $(C_{PH2O2})/ (C_{PH2O2})_{max}$. Amount of GOX immobilized = 1.5 mg, volume of LBL membrane reactor = 0.122 cm^3, permeate flux = 140 x 10^{-4} $cc/cm^2.s$, residence time = 0.6 s, external membrane area = 13.2 cm^2, membrane thickness = 165 μm, pH = 5.5, Temperature = 25 ^0C, concentration of glucose fed = 0.75 - 75 mM

6.1.6 Stability

Figure 6.11 demonstrates the stability of the GOX, immobilized in LBL assembled nylon membrane as well as PVDF-PAA-PAH membrane, as a function of time. It can be observed from Figure 6.11 that after 28 days the activity of immobilized GOX reduced to only 80 % of the initial activity, whereas, according to Ozyilmaz and co-workers (Ozyilmaz et al. 2005), the activity reduced to 25 % after 28 days for free GOX. In another study (Ahuja 2006) the activity was reported to reduce to 30 % after first 7 days. For both the literature studies and our work storage of GOX was carried out at 4 ^{0}C. This shows that immobilized GOX within membrane matrix is well protected and retains its activity over a longer period of time compare to free GOX.

6.1.7 Reusability of membrane matrix by detachment and reattachment of GOX

LBL-GOX membrane: A novel study was carried out on detachment and reattachment of GOX from the polyelectrolyte matrix. After using the GOX immobilized LBL membrane for several times, the GOX was detached from the membrane matrix by lowering the pH. Amount of detached GOX was 90 ± 3 % of the immobilized GOX. It can be hypothesized that the undetached GOX molecules are either situated in such domains of polyelectrolyte layers that they are inaccessible or they are too strongly bound to detach by changing pH alone. The detached GOX was unaffected by the drastic change in pH environment and showed 90 % activity of the fresh GOX in free form as revealed by the homogeneous phase experiments. After the homogeneous phase activity studies, the remaining detached GOX was reattached in the same LBL membrane matrix electrostatically. Activity of the reattached GOX was 90 ± 5 % of the activity prior to the detachment. Same steps of detachment and reattachment were repeated and similar results were obtained. After that, GOX was detached and fresh GOX was attached in the same membrane matrix. The attachment was identical as obtained for the newly made 7-layers LBL membrane. The activity of the immobilized fresh GOX was around 90 % of the activity obtained for fresh GOX in newly made 7-layers LBL membrane. This proves the reusability of the LBL membrane matrix for GOX immobilization.

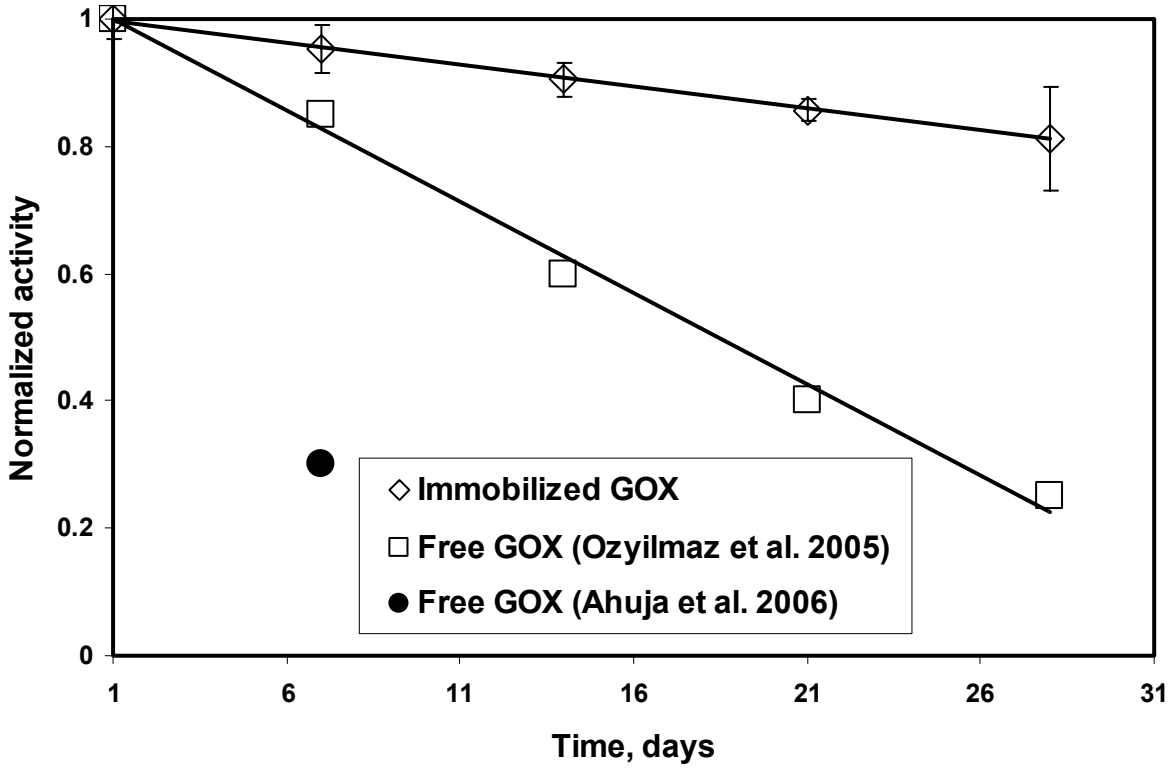

Figure 6.11 Stability of GOX immobilized in LBL assembled nylon membrane as well as PVDF-PAA-PAH membrane based on the change in activity over a period of time. The stability is compared with that reported (Ahuja 2006; Ozyilmaz et al. 2005) for free GOX. Activity is calculated based on concentration of H_2O_2 and is normalized by dividing with the activity on first day of immobilization at pH = 5.5

The immobilization as well as the activity is reproducible after several experiments and pH treatments. Although the current study deals with GOX only, it can potentially be extended for other enzymes as well.

PVDF-GOX membrane: Detachment of GOX, in this case, was different than the GOX-LBL membrane. Since, carboxylic acid groups of PAA have a pK_a of 4.7, at pH 4 the whole PAH-GOX domain dislocates from PVDF-PAA domain. Therefore, each time fresh PAH and GOX were attached in the PVDF-PAA membrane. The amount and activity of fresh GOX attached in the same PVDF-PAA membrane matrix were highly reproducible as observed by multiple studies. This proves that the functionality within the membrane is very consistent and there is no leakage of the components.

6.2 Conclusions

Activity of electrostatically immobilized GOX in two different kinds of charged functionalized membrane domain was studied using glucose as a substrate. In one case, membrane domain was created by electrostatic attachments of polyelectrolytes using LBL technique, and in the other by in-situ polymerization of acrylic acid. Study of homogeneous phase reaction kinetics of free GOX was carried out. Comparative kinetics studies have been presented between free, electrostatically immobilized and covalently immobilized GOX, as well as between convective and soaking mode of glucose solution. Electrostatic immobilization and convective mode were observed to be beneficial than others. Effect of flow rate and pH on activity of GOX was also studied. It was observed that higher flow rate of reaction mixture through the membrane utilizes maximum active sites of the enzyme. It was also demonstrated that GOX immobilized in functionalized membrane has a wide range of operating pH and associated with higher stability compare to free GOX. The potential of reusability of the membrane matrices was one of the most important findings in this research. The reusability of the membrane matrices has been explored with extensive study of the detachment and reattachment of GOX from membrane matrix, along with the activity measurements.

Chapter 7 Oxidative Dechlorination of Trichlorophenol (TCP) by Functionalized 2-Stack Membranes Containing Electrostatically Immobilized GOX and Fe^{+2}

A practical application of enzymatic production of H_2O_2 from glucose, by electrostatically immobilized glucose oxidase (GOX), in functionalized membrane is demonstrated in this chapter. For the first time an attempt has been made to use a 2-stack functionalized membranes system for simultaneous enzymatic production of hydrogen peroxide in first membrane, and oxidative dechlorination of TCP in the second membrane by Fenton reaction.

7.1 Introduction and background studies

In Chapter 6, it was observed that constant production of H_2O_2 can be achieved by GOX based catalytic oxidation of glucose in membranes. It is also well known that H_2O_2 and ferrous iron (Fe^{+2}) react to form very reactive hydroxyl radicals ($OH\cdot$), which has the capability of oxidizing organic molecules (Pignatello et al. 2006). This chapter describes the research study, which combines these two techniques using a unique system of two functionalized membranes, and implements it for the destruction of a chlorinated organic molecule. Two membranes were used so that the immobilized GOX remains separated from the highly reactive hydroxyl radicals. 2, 4, 6-trichlorophenol (TCP) was chosen as the model chloro-compound and PVDF membranes were used for functionalization.

Chlorinated organics are widely used as pesticides, disinfectant, coolant and preservative of woods, and one of the major components of ground water and soil contaminants. Destruction of these compounds is carried out by either reductive or oxidative dechlorination pathways. Reductive dechlorination of different chlorinated organics has been reported in the literature (Ahuja et al. 2004; Schrick et al. 2002; Xu et al. 2005) and out of scope of this study. Fenton reaction is a popular technique for the destruction of chlorinated compounds by oxidative dechlorination (Huston and Pignatello 1999; Li et al. 2005; Pignatello et al. 2006). An enormous number of rate constants for this free radical based reaction has been reported (Ahuja 2006; Buxton et al. 1988).

Fenton (Fenton 1894) was the first researcher to observe the oxidation of tartaric acid by Fe^{+2} and H_2O_2. However, the mechanism and the role of hydroxyl radical was discovered and reported first by Haber and Weiss (Haber and Weiss 1934). The role of additional reactions in determining the fate of free radicals has also been demonstrated (Barb et al. 1949; Barb et al. 1951a, b). For the convenience of understanding, all of the above mentioned reactions are discussed later in experimental section of this chapter. A comprehensive review of the mechanism, important parameters, kinetics and applications of Fenton reaction is available in literature (Pignatello et al. 2006). Although the history of Fenton reaction goes back to 1900, it attracted the attention of academic researchers only around 1990. After that Fenton reaction has been used for the treatment of chlorophenols (Ahuja 2006; De et al. 2006; Watts et al. 1990), trichloroethylene (Xu and Bhattacharyya 2007), polychlorinated bi-phenyls (Aronstine and Rice 1995) and nitroaromatic explosives (Liou and Lu 2007).

Dechlorination of chlorophenols and polychlorinated biphenyls have been extensively studied by our research group. Ahuja and co-workers (Ahuja et al. 2007) have studied the enzymatic production of H_2O_2 and gluconic acid by immobilized GOX in functionalized beads. Then the produced gluconic acid and H_2O_2 was used for homogeneous phase dechlorination of TCP by adding Fe^{+2} extraneously. Effect of gluconate anion as chelate was also studied. Li and co-workers (Li et al. 2007) have studied soaking mode dechlorination of 2, 2'-dichlorobiphenyl (DCB) by Fe^{+2} immobilized in a PAA functionalized PVDF membrane, and adding commercially available H_2O_2 extraneously. However, simultaneous production of H_2O_2 and dechlorination of the chlorinated organics in a solid matrix have never been studied.

7.2 Experimental and analytical procedures

7.2.1 Equipment and materials

Experiments were carried out in a stainless steel membrane cell from Osmonics. The effective external surface area of the membranes in this cell was 13.2 cm^2. Hydrophobic PVDF membrane (pore diameter 0.45 μm, thickness 125 μm, porosity 75 % as supplied by manufacturer) were purchased from Millipore Corporation. The enzyme,

glucose oxidase, from *Aspergillus Niger* (GOX, Product No. G0543, MWt. 160000) and β-D (+) glucose (Product No. G5250, MWt. 180) were purchased from Sigma. 15 % solution of titanium oxysulfate in dilute H_2SO_4 (Product No. 495379), benzoyl peroxide (Product No. 179981), trimethylolpropane triacrylate (TMPTA, Product No. 246808), anhydrous toluene (Product No. 244511), acrylic acid (Product No. 147230, MWt. 72) and 2, 4, 6-trichlorophenol (TCP, Product No. 139481000, MWt. 197.5) were purchased from Aldrich. Tribromophenol (TBP, Product No. CUS-6624) was purchased from Ultra Scientific. The reagents for Bradford assay were purchased from Bio-Rad Laboratories. Unless mentioned otherwise, rest of the chemicals, including the de-ionized ultra filtered water (DIUF), were purchased from Fisher Scientific.

7.2.2 Analytical procedures

All spectrophotometric measurements in the UV and visible range were done by UV-VIS Spectrophotometer (Varian, Cary 300). Analysis of GOX, polyallylamine hydrochloride (PAH) and H_2O_2 were carried out using Bradford Protein Assay, Total Organic Carbon (TOC) analysis and a method reported by Clapp et al. (Clapp et al. 1989), respectively. These analytical procedures are already mentioned in Chapter 3. TCP, Fe, Na and Cl^- analyses were conducted as mentioned below.

Analysis of Na and Fe: Na and Fe analyses were done by Atomic Absorption Spectrometer (Varian 220 Fast Sequential). The measurements were performed at 372 nm wavelength for Fe and at 330.2 nm wave length for Na. The linear range of calibration curve was 1-100 ppm for both of them, with 3-6 % analytical error for Fe and 3-10 % analytical error for Na.

Analysis of TCP: A HPLC (Agilent 1100 Series) method was developed to analyze TCP in an aqueous solution also containing glucose, gluconic acid, H_2O_2 and sodium acetate-acetic acid. A 25:25:1 mixture of methanol, water and acetic acid was used as the mobile phase. TBP was used as internal standard for all the analyses by HPLC. The column used

was purchased from Supelco (LC-8). The retention time for TCP was around 5 min and that for TBP was 6.6 min.

Analysis of Cl^-: Free Cl^- present in permeate after dechlorination reaction was analyzed using Orion 9617 Combination Cl^- electrode along with an Ion Meter from Fisher Scientific (AR 25). The range of calibration curve for Cl^- analysis was 1-10 ppm and analytical error was 3-10 %.

7.2.3 Electrostatic immobilization of GOX in functionalized PVDF membrane

Hydrophobic PVDF membranes were functionalized with polyacrylic acid (PAA), followed by PAH, and then, GOX was electrostatically immobilized in functionalized PVDF membranes as described in Chapter 3. The activity of immobilized GOX was studied using 1 mM glucose solution in sodium acetate-acetic acid (NaOAc-AcOH) buffer of pH 5.5. This GOX immobilized membrane was used as the first membrane in the 2-stack membranes system for dechlorination of TCP.

7.2.4 Immobilization of Fe^{+2} in functionalized PVDF membrane by ion exchange

Fe^{+2} immobilization within PAA-functionalized PVDF membrane was carried out by ion exchange with Na^+. Na^+ was present in the system as counter-ion of carboxylic acid group of PAA. This step was very delicate and needed extra precautions. Fe^{+2} is susceptible to oxidation to Fe^{+3} by any O_2 present in the solution, and Fe^{+3} precipitates at any pH $\geq$ 5. Hence, the ion exchange step was carried out with de-oxygenated water. DIUF water was de-oxygenated by purging N_2 gas. Fe^{+2} also has a tendency to precipitate at any pH $\geq$ 6 and pK_a of carboxylate group of PAA is 4.7. So, the ion exchange step was carried out in a very narrow range of operating pH of 5-5.5 for all the experiments. 100 ml of 750 ppm $FeCl_2.4H_2O$ (MWt. 199) was permeated to immobilize Fe^{+2}. Prior to and after the ion exchange step, membrane matrix was washed with a copious amount of deoxygenated water. Since, Fe^{+2} is prone to oxidation in exposure to air, the Fe^{+2} immobilized membranes were used immediately after functionalization.

7.2.5 Experimental procedure for dechlorination of TCP

In order to carry out Fenton reaction, a reaction mixture containing TCP and glucose was prepared in O_2 saturated NaOAc-AcOH buffer of pH 5.5, and permeated under N_2 atmosphere. Two different concentrations of TCP, 15 ppm (0.07 mM) and 30 ppm (0.14 mM) were studied. Glucose concentration was deliberately kept at a lower value of 1 mM to avoid any potential complexity that might arise from the un-reacted glucose molecules. The flow rate was kept constant through out the reaction. Permeate of the first membrane containing TCP, H_2O_2, gluconic acid, un-reacted glucose and O_2 then enters second membrane.

This reaction is critical in the existing system in terms of presence of oxygen. For maximum H_2O_2 production O_2 saturation is required, whereas, for maximum dechlorination efficiency, absence of O_2 is necessary as it converts Fe^{+2} to Fe^{+3}. From material balance calculation it was confirmed that the amount of Fe^{+2} immobilized in the membrane was such that even if the un-reacted O_2 converts Fe^{+2} to Fe^{+3}, the excess Fe^{+2} would be sufficient to generate hydroxyl radicals and carry out dechlorination. During dechlorination experiments, samples were taken at regular intervals. After dechlorination reaction, the system was washed with DIUF. Then the samples were analyzed for TCP, Cl^- and H_2O_2. The activity of GOX in first membrane was checked after dechlorination.

7.3 Results and discussions

In order to check the reproducibility of the results, all experiments were triplicated. The error bars shown in different figures represent standard deviations.

7.3.1 Electrostatically immobilized GOX in functionalized PVDF membrane

Amount of GOX immobilized electrostatically on the functionalized PVDF membranes was 1 ± 0.1 mg (1.12×10^{-5} mmole). Concentration of H_2O_2 produced by oxidation of 1 mM glucose (pH 5.5) using the GOX immobilized membrane was around 0.1 mM. These membranes were then used as the first membrane in the 2-stack membranes system for different dechlorination experiments.

7.3.2 Fe^{+2} in functionalized PVDF membrane

The amount of Fe^{+2} immobilized into the membranes was 5 ± 0.5 mg (around 0.09 mmole), which corresponds to a positive charge of 0.18 mmole. Fe^{+2} was immobilized by ion exchange with Na^{+} present in PAA-functionalized PVDF membrane in Na-form. To maintain the electro neutrality, 2 moles of Na^{+} should be released from the matrix for each mole of Fe^{+2} immobilized. From the AA analysis of different solutions it was determined that amount of Fe immobilized was 0.09 mole (5 mg), and the amount of Na released was 0.21 mmole (5 mg), which corresponds to a reasonable Fe to Na ratio of 1:2.3. The Fe^{+2} immobilized membranes were then used as the second membrane in the 2-stack membranes system for different dechlorination experiments.

7.3.3 Dechlorination of TCP

Dechlorination of TCP was carried out in a 2-stack membranes system containing GOX-PVDF membrane prior to Fe^{+2}-PVDF membrane as shown in Figure 7.1. The idea was to produce H_2O_2 in the first membrane by enzymatic oxidation of glucose in presence of GOX. TCP remains inert in this membrane. In the second membrane, H_2O_2 reacts with immobilized Fe^{+2} to generate hydroxyl radical ($OH^{\cdot}$). These hydroxyl radicals then participate in Fenton reaction with TCP and dissociate it. The participating reactions are given below.

$$Fe^{+2} + H_2O_2 \rightarrow Fe^{+3} + OH^- + OH\cdot \quad (7.1)$$

$$TCP + OH\cdot \rightarrow I \xrightarrow{OH\cdot} P + Cl^- \quad (7.2)$$

where, I is the intermediate compounds formed and P is the oxidized product of TCP. Other than these two, number of side reactions takes place during oxidative dechlorination of TCP. A detail description of those is beyond the scope of this study. However, the relevant ones are mentioned below.

$$H_2O_2 + OH\cdot \rightarrow H_2O + HO_2\cdot \quad (7.3)$$

$$OH\cdot + OH\cdot \rightarrow H_2O_2 \quad (7.4)$$

$$OH\cdot + Fe^{+2} \rightarrow Fe^{+3} + OH^- \quad (7.5)$$

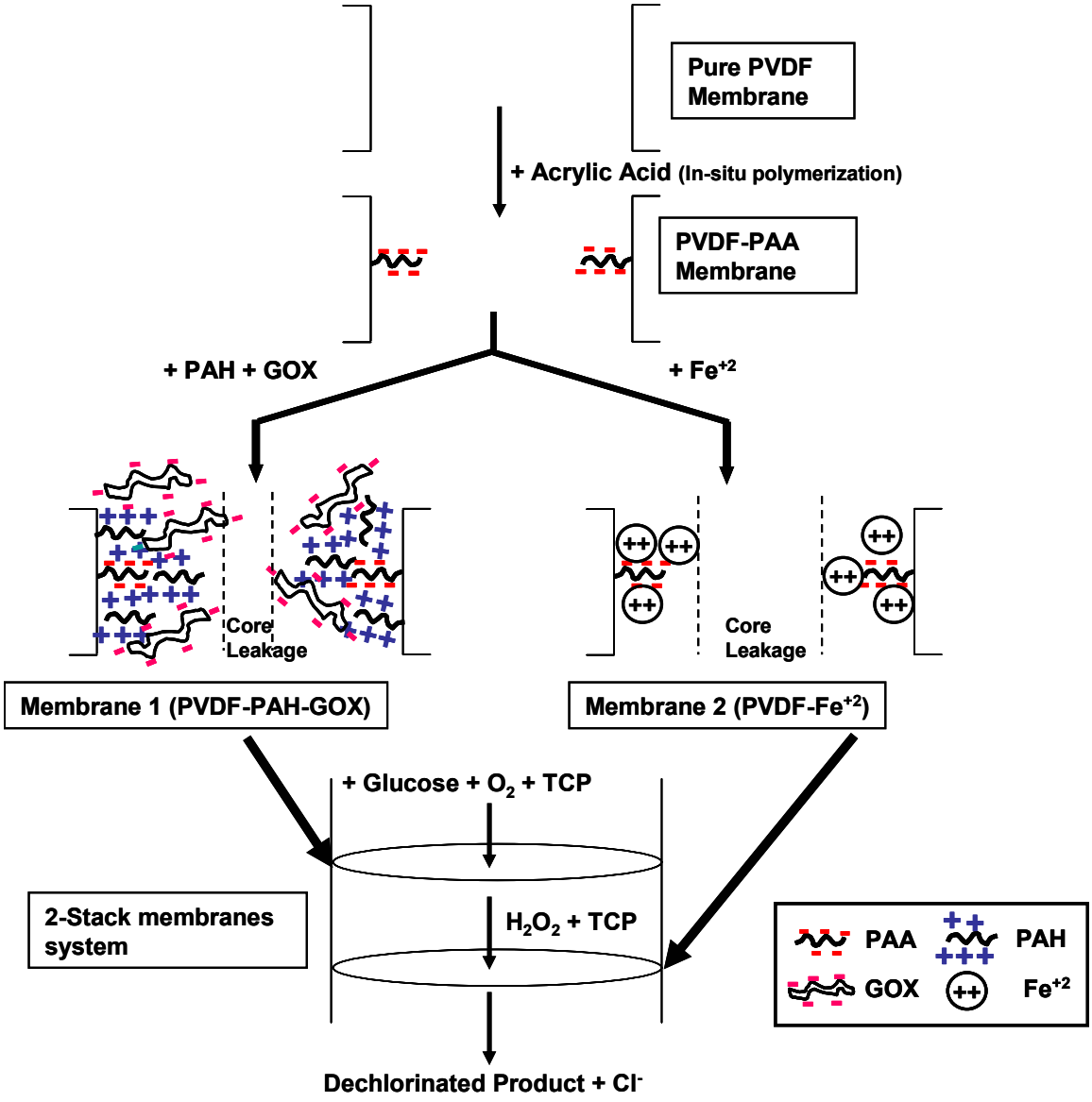

Figure 7.1 Schematic of formation of 2-stack functionalized membranes system for oxidative dechlorination of TCP by Fenton reaction. Membrane 1 and 2 were functionalized with electrostatically immobilized GOX and Fe^{+2}, respectively

The above mentioned side reactions hinder the dechlorination of TCP by consuming both $OH^{\cdot}$ radical and Fe^{+2}.

Concentration of TCP in different solutions was analyzed by reverse phase HPLC. The analyses reveal destruction of TCP inside the 2-stack functionalized membrane system. Blank experiments have been conducted, with 2-stack functionalized PVDF membranes without GOX, to take care of the adsorption of TCP in the system. Dechlorination of TCP results are summarized in Figures 7.2-7.4 for 15 and 30 ppm TCP. Figure 7.2 represents typical breakthrough curves of both H_2O_2 and TCP for 15 ppm (0.07 mM) TCP in feed. Untill around 15 min, the amount of H_2O_2 formed in the first membrane was totally consumed in the second membrane. Then, the concentration of H_2O_2 in permeate gradually increased and a breakthrough is observed. On the other hand, for TCP, the breakthrough is observed at around 5 min. This illustrates the involvement of H_2O_2 in other side reactions, such as Equation (7.3).

Figure 7.3 demonstrates conversion of TCP as a function of cumulative amount of TCP permeated through the system for 15 ppm (0.07 mM) and 30 ppm (0.14 mM) TCP. It can be observed from the figure that simultaneous enzymatic production of H_2O_2 and production of hydroxyl radicals by Fe^{+2} in a 2-stack membranes system is efficient in dechlorination of TCP. Initially, up to 98 % and 85 % conversion of TCP was obtained for 15 ppm and 30 ppm TCP in feed, respectively. However, with time, conversion decreases because of other competitive side reactions, such as Equations (7.1-7.3), which consume the reactants. It is also important to emphasize here that the production of H_2O_2 from the first membrane is under steady state and the concentration of TCP in the permeate of first membrane is constant (the feed concentration of TCP). Hence, if the amount of Fe^{+2} immobilized in the second membrane is in large excess, then ideally conversion of TCP should remain constant. This indicates that further studies are necessary with higher amount of immobilized Fe^{+2} into the membrane to demonstrate the constancy in the conversion. The overall conversion of TCP obtained in this study was 78 % and 70 % for 15 ppm and 30 ppm TCP, respectively. The obtained conversion was significantly higher than the reported value of 40 % conversion for 2, 2'-polychlorinated biphenyl by PVDF-PAA membrane in soaking mode (Li et al. 2007).

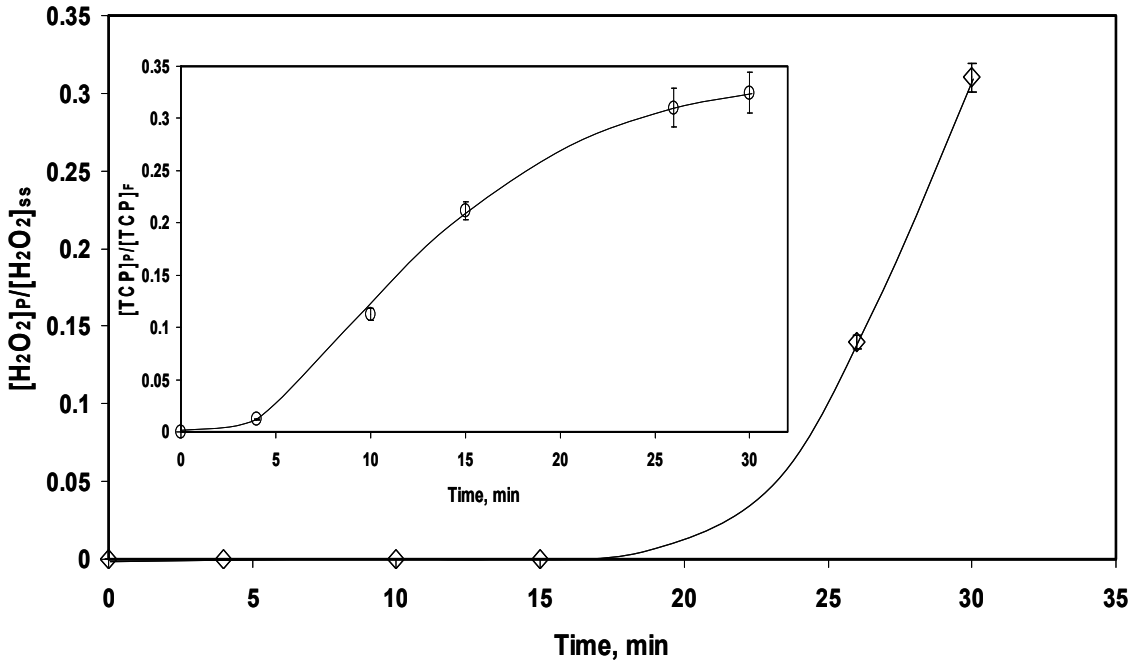

Figure 7.2 Breakthrough curve for H_2O_2 in the permeate of 2-stack functionalized-PVDF membranes system used for dechlorination of TCP. Y-axis represents the ratio of concentration of H_2O_2 in permeate at time t ($[H_2O_2]_P$) to the concentration of H_2O_2 produced in first membrane under steady state condition ($[H_2O_2]_{ss}$). Inset figure represents the breakthrough curve of TCP for the same experiment. Y-axis of inset figure represents the ratio of concentration of TCP in permeate ($[TCP]_P$) at time t to the concentration of TCP in feed ($[TCP]_F$). $[H_2O_2]_{ss}$ = 0.1 mM, $[TCP]_F$ = 0.07 mM (15 ppm), Fe loading = 0.09 mmole, residence time in the first membrane = 2.7 s, residence time in the second membrane = 2 s

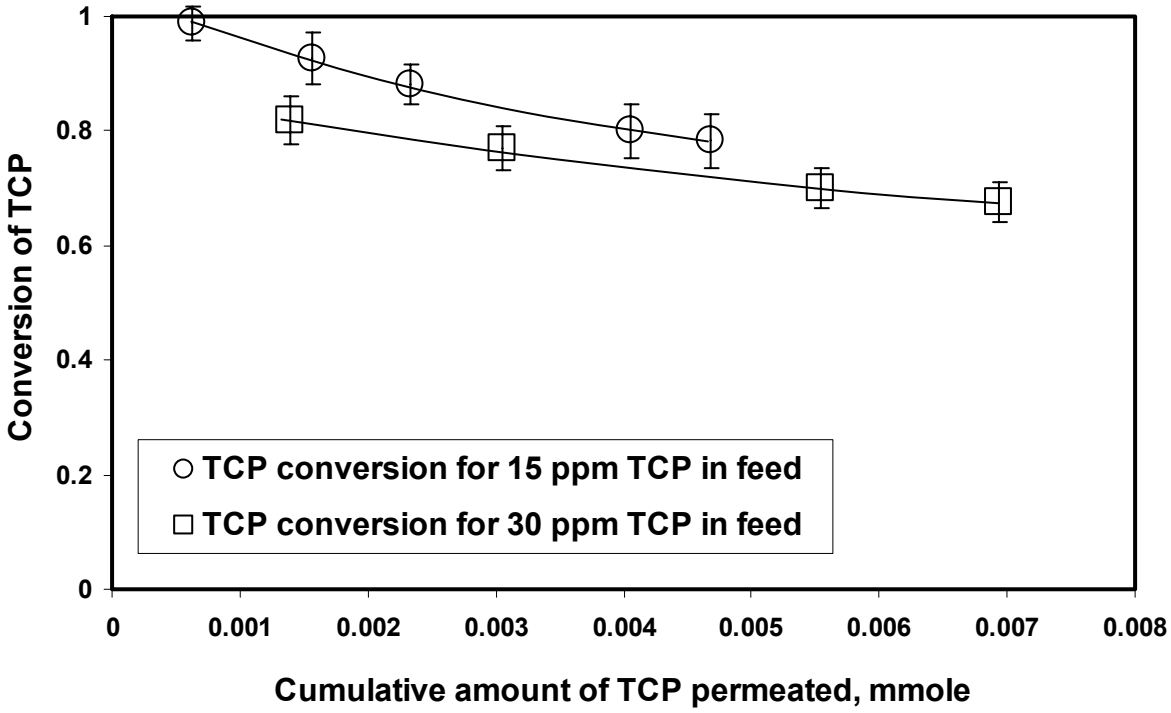

Figure 7.3 The conversion of TCP during the dechlorination reaction as a function of cumulative amount of TCP permeated. Conversion of TCP is the ratio of cumulative amount of TCP dechlorinated at any time to cumulative amount of TCP permeated at that time. Steady state concentration of H_2O_2 from the first membrane is around 0.1 mM, Fe loading = 0.09 mmole, residence time in the first membrane = 2.7 s, residence time in the second membrane = 2 s

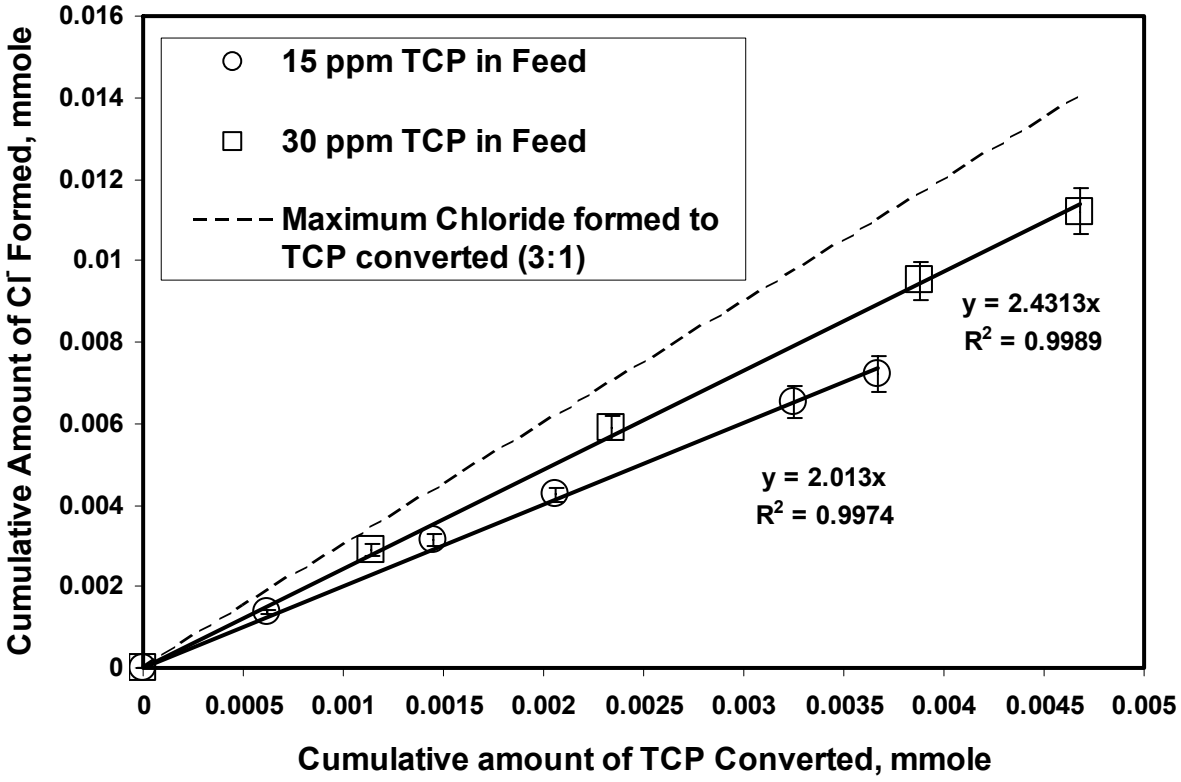

Figure 7.4 Total amount of Cl^- formed as a function of total amount of TCP converted during the dechlorination reaction. The dotted line is constructed by considering 1 mole of TCP conversion corresponds to maximum of 3 mole of chloride formation. Slope of the solid lines represent experimentally obtained ratio of chloride formed to TCP converted. Steady state concentration of H_2O_2 from the first membrane is around 0.1 mM, Fe loading = 0.09 mmole, residence time in the first membrane = 2.7 s, residence time in the second membrane = 2 s

Figure 7.4 represents cumulative amount of Cl^- formed as a function of cumulative amount of TCP converted. For both cases, amount of Cl^- increases with time, because oxidation of TCP ruptures its aromatic ring and liberates free Cl^-. If complete dechlorination takes place then 1 mole of TCP consumption liberates a maximum of 3 moles of Cl^-. It can be observed that the ratio of consumption of TCP to formation of free Cl^- was 2.1 and 2.4 for 15 ppm and 30 ppm TCP in feed, respectively. This again demonstrates satisfactory efficiency of the system to dechlorinate TCP.

After dechlorination experiments, the activity study of GOX in first membrane showed only 3-8 % reduction in activity. This has allowed reusing the membrane for further dechlorination experiments. After several cycles, when the activity of GOX was reduced to less than 60 %, the GOX was detached and fresh GOX was attached as described in Chapter 3. The Fe-immobilized membrane could also be reused by dislodging Fe^{+3} with concentrated nitric acid and reattaching Fe^{+2}. However, for this research work, the Fe-immobilized membranes were not reused.

7.4 Conclusions

Implementation of a 2-stack functionalized PVDF membranes system for simultaneous enzymatic production of hydrogen peroxide in first membrane and oxidative dechlorination of TCP in the second membrane by Fenton reaction has been successful as evident from the results. The initial dechlorination was 98 % and 85 % for two different concentrations of TCP, with an overall dechlorination of 70-80 %. The ratio of Cl^- produced to TCP dechlorinated is more than 2, which re-confirms the efficacy of the technique for oxidative dechlorination. Different process parameters, such as, concentration of glucose in feed, amount of Fe^{+2} and GOX immobilized, need to be tuned to find the optimum operating conditions. If utilized properly this system has the capability of sustaining constant conversion of TCP under continuous mode, which could be very promising for industrial purposes. This technique also provides additional benefit of reusing the same membrane matrices by reattaching fresh GOX and Fe^{+2}.

Chapter 8 Conclusions

The research work discussed in this dissertation was directed towards extensive experimental and theoretical studies of development of functionalized polymeric membranes, critical analysis of interaction between membrane and/or biomolecules, and applications of functionalized membranes for bioseparation and biocatalysis. This chapter summarizes the important findings of the research work.

8.1 Overall scientific and technological advancements

The overall scientific and technological advancements achieved in this research study were,

- Better understanding of the fundamental aspects related to the accessibility of covalently immobilized biomolecules, and the fouling in the membrane structure due to permeation of biomolecules, with proper quantification.

- Isolation of pure monomeric high value protein, with enhanced recovery and lower processing time, using affinity membrane separation.

- Development of high capacity, highly active, stable and reusable enzyme-substrate system based on electrostatic immobilization.

- Development and implementation of a 2-stack functionalized membranes system for simultaneous enzymatic production of hydrogen peroxide in first membrane and oxidative dechlorination of a chloro-organic in the second membrane by Fenton reaction.

8.2 Specific accomplishments

The specific accomplishments for functionalized membrane based bioseparation and biocatalysis research work were as follows.

8.2.1 Functionalized membranes for affinity based bioseparation

- Quantification of the accessibility of covalently immobilized avidin sites by biotin moieties present in different probe molecules. Maximum achievable accessibility of covalently immobilized avidin sites in activated nylon membrane was determined to be 50 % of the accessibility obtained in homogeneous phase.

- Pure monomeric HIV-Tat protein was isolated from a complex fermentation broth (bacterial lysate, BL) using an efficient affinity separation technique based on avidin-biotin interaction in functionalized stacked microfiltration membranes. The membrane purified Tat was superior in quality than conventional column chromatographically purified Tat as demonstrated by different analytical tools, such as, SDS-PAGE, Western Blot and biotin analyses.

- A prefiltration step was effective in enhancing the normalized accessibility of immobilized avidin sites from 20-35 % for unfiltered cases to 50-70 % for pre-filtered cases. It was also able to reduce the fouling of membrane structure from 80 % for unfiltered cases to 10-50 % for pre-filtered cases. The processing time per unit amount of purified Tat isolated was also reduced by 5 times for pre-filtered affinity separation.

- Decrease in permeate flux due to the fouling was mathematically described considering adsorption of protein molecules both inside the pores and on the surface of the membranes for unfiltered BL feed. On the other hand, for pre-filtered BL feed, assumption of protein adsorption only on the pores of the membrane was sufficient to describe the fouling.

8.2.2 Functionalized membranes for biocatalysis

- Development of functionalized membrane domain by Layer-By-Layer (LBL) assembly of polyelectrolytes and by in-situ polymerization of acrylic acid for electrostatic immobilization of Glucose Oxidase (GOX) enzyme.

- Electrostatic immobilization of GOX in functionalized membranes was associated with high capacity (1.5-1.8 mg), activity and stability (20 % reduction in activity after 1 month). The optimum working range of pH for electrostatically immobilized GOX was observed to be broader than free GOX.

- The functionalized membranes developed for GOX immobilization, possess the advantage of regeneration. The attached GOX was successfully detached from the membrane matrix, the activity of detached GOX was examined, and then it was reattached in the same matrix. During this process about 90 % retention of the activity of GOX was observed. Fresh GOX was also attached in the same membrane matrix.

- A 2-stack PAA-functionalized PVDF membranes system was used for simultaneous enzymatic production of hydrogen peroxide in first membrane by electrostatically immobilized GOX, and oxidative dechlorination of 2, 4, 6-trichlorophenol (TCP) in the second membrane by Fenton reaction using electrostatically immobilized Fe^{+2}. The overall conversion of TCP was 70-80 % and the ratio of Cl^- formed to TCP converted was 2-2.4 out of a maximum achievable ratio of 3.

Nomenclature

A_0 Area of avidin immobilized membrane pore at t = 0, cm^2

A_m External surface area of membrane, cm^2

C_f Concentration of biotin in feed, μmole/ml

C_P Concentration of biotin in permeate, μmole/ml

C_{PH2O2} Concentration of H_2O_2 in permeate, mM

J_v Permeate flux at any time t, cm^3/cm^2-s

J_{v0} Initial permeate flux through avidin immobilized membrane, cm^3/cm^2-s

J_w Permeate flux of pure water, cm^3/cm^2-s

K_m Michaelis-Menten kinetic constant, mM

K_S Rate constant of surface protein adsorption, min^{-1}

K_T Rate constant of total protein adsorption, min^{-1}

l Thickness of Immunodyne membrane, cm

L Thickness of 4-stack Immunodyne membranes = 4l, cm

M_S Mass of protein adsorbed on the external surface of the membrane at t, μg

M_S^* Final amount of protein adsorbed on the external surface of the membrane at t, μg

M_T Mass of total protein adsorbed on the membrane (surface + pore) at t, μg

M_T^* Final amount of total protein adsorbed on the membrane (surface + pore), μg

N_P Total number of membrane pores

Q_{w0} Volumetric flow rate of water through bare membrane, cm^3/s

Q_w Volumetric flow rate of water through fouled membrane, cm^3/s

r Radius of membrane pore at time t, cm

r_0 Radius of avidin immobilized membrane pore at t = 0, cm

r_{avidin} Radius of avidin immobilized membrane pore, cm

r_P Radius of fouled membrane pore, cm

R_m Intrinsic membrane resistance, cm^{-1}

R_P Resistance of protein layer in membrane, cm^{-1}

s Substrate concentration, mM

s_0 Initial substrate concentration, mM

v Rate of glucose oxidation by GOX, mmole/mg-min or mM/mg-min

v_{max} Maximum rate in Michaelis-Menten kinetics, mmole/mg-min or mM/mg-min

V Cumulative permeate volume, cm^3

X Volume of total protein adsorbed per unit volume of permeate

Greek letters

ε membrane porosity

δ_{avidin} Effective thickness of covalently immobilized avidin layer, nm

δ_{avidin} Calculated thickness of n-th layer of polyelectrolytes in LBL membrane, nm

δ_P Effective thickness of adsorbed protein layer, nm

δ_T Effective thickness of total protein layer = $\delta_{avidin} + \delta_P$, nm

ρ mass of protein adsorbed in pores per unit volume of adsorbed layer, $\mu g/cm^3$

ΔP Transmembrane pressure drop, bar

τ' Tortuosity of membrane

μ viscosity of water (gm cm^{-1} s^{-1})

τ residence time (s)

Material Abbreviations

PVDF	Polyvinylidene Fluoride
LBL	Layer-By-Layer
GOX	Glucose Oxidase
TCP	2, 4, 6-trichlorophenol
HIV	Human Immunodeficiency Virus
TAT	Trans-Activator of Transcription
BL	Bacterial Lysate
PABA	para-amino benzoic acid
BABA	Biotin-4-amidobenzoic acid
HABA	2-4'-hydroxyazobenzene benzoic acid
BSA	Bovine Serum Albumin
GG	Gamma Globulin
BBSA	Biotinylated Bovine Serum Albumin
RC	Regenerated Cellulose
CDI	1, 1'-carbonyldiimidazole
ECH	Epichlorohydrin
CA	Cellulose Acetate
BDDE	1, 4-butanediol diglycidol ether
PES	Polyether sulfone
PLL	Poly-L-Lysine
PAH	Poly-allylamine hydrochloride

PSS	Poly-sodium, 4-styrene sulfonate
TMPTA	Trimethylolpropane triacrylate
PAA	Poly-acrylic acid
TBP	2, 4, 6-tribromophenol
DIUF	De-Ionized Ultrafiltered Water
RNA	Ribonucleic acid
TAR	Trans-Activating Responsive
DTT	Dithiothreitol
PMSF	Phenylmethyl sulfonyl fluoride
WB 1	Wash Buffer 1
WB 2	Wash Buffer 2
CB	Cleavage Buffer
CC	Column Chromatography
P	Permeate
R	Retentate
F	Feed
E	Tat eluate
UNF BL	Unfiltered bacterial lysate
UF BL	Ultrafiltered bacterial lysate
MF BL	Microfiltered bacterial lysate

Method and Technique Abbreviations

RO	Reverse Osmosis
PV	Pervaporation
NF	Nanofiltration
UF	Ultrafiltration
MF	Microfiltration
ED	Electrodialysis
PI	Isoelectric Point
HPLC	High Performance Liquid Chromatography
MWCO	Molecular Weight Cut-Off
IMAC	Immobilized Metal Affinity Chromatography
SEM	Scanning Electron Microscopy
EDX	Energy Dispersive X-Ray
FTIR	Fourier Transform Infrared
ELISA	Enzyme Linked Immuno Sorbent Assay
SDS-PAGE	Sodium Dodecyl Sulfate-Poly Acrylamide Gel Electrophoresis
TOC	Total Organic Carbon

References

Abu-Amer, Y., Dowdy, S.F., Ross, F.P., Clohisy, J.C., Teitelbaum, S.L., 2001. TAT fusion proteins containing tyrosine 42-deleted IkappaBalpha arrest osteoclastogenesis. The Journal of biological chemistry 276(32), 30499-30503.

Ahuja, D.K., 2006. Degradation of toxic chloroethylenes and chloroaromatics by vitamin B12-based reductive dechlorination and by hydroxyl radical-based oxidative dechlorination reactions. Chemical and Materials Engineering. University of Kentucky, Lexington.

Ahuja, D.K., Bachas, L.G., Bhattacharyya, D., 2007. Modified Fenton reaction for trichlorophenol dechlorination by enzymatically generated H_2O_2 and gluconic acid chelate. Chemosphere 66(11), 2193-2200.

Ahuja, D.K., Gavalas, V.G., Bachas, L.G., Bhattacharyya, D., 2004. Aqueous-Phase Dechlorination of Toxic Chloroethylenes by Vitamin B12 Cobalt Center: Conventional and Polypyrrole Film-Based Electrochemical Studies. Industrial & Engineering Chemistry Research 43(4), 1049-1055.

Amounas, M., Innocent, C., Cosnier, S., Seta, P., 2000. A membrane based reactor with an enzyme immobilized by an avidin-biotin molecular recognition in a polymer matrix. Journal of Membrane Science 176(2), 169-176.

Ariga, K., Hill, J.P., Ji, Q., 2007. Layer-by-layer assembly as a versatile bottom-up nanofabrication technique for exploratory research and realistic application. Phys. Chem. Chem. Phys. 9(19), 2319-2340.

Aronstine, B.N., Rice, L.E., 1995. Biological and integrated chemical-biological treatment of PCB congeners in soil/sediment-containing systems. Journal of Chemical Technology & Biotechnology 63(4), 321-328.

Avramescu, M.-E., Girones, M., Borneman, Z., Wessling, M., 2003. Preparation of mixed matrix adsorber membranes for protein recovery. J. Membr. Sci. 218(1-2), 219-233.

Bao, J., Furumoto, K., Yoshimoto, M., Fukunaga, K., Nakao, K., 2003. Competitive inhibition by hydrogen peroxide produced in glucose oxidation catalyzed by glucose oxidase. Biochemical Engineering Journal 13(1), 69-72.

Barb, W.G., Baxendale, J.H., George, P., Hargrave, K.R., 1949. Reactions of ferrous and ferric ions with hydrogen peroxide. Nature (London, U. K.) 163, 692-694.

Barb, W.G., Baxendale, J.H., George, P., Hargrave, K.R., 1951a. Reactions of ferrous and ferric ions with hydrogen peroxide. I. Ferrous-ion reaction. Transactions of the Faraday Society 47, 462-500.

Barb, W.G., Baxendale, J.H., George, P., Hargrave, K.R., 1951b. Reactions of ferrous and ferric ions with hydrogen peroxide. II. Ferric-ion reaction. Transactions of the Faraday Society 47, 591-616.

Barth, H.G., Jackson, C., Boyes, B.E., 1994. Size Exclusion Chromatography. Analytical Chemistry 66(12), 595R-620R.

Bayer, P., Kraft, M., Ejchart, A., Westendorp, M., Frank, R., Roesch, P., 1995. Structural studies of HIV-1 Tat protein. Journal of Molecular Biology 247(4), 529-535.

Bhardwaj, A., Lee, J., Glauner, K., Ganapathi, S., Bhattacharyya, D., Butterfield, D.A., 1996. Biofunctional membranes: an EPR study of active site structure and stability of papain non-covalently immobilized on the surface of modified poly(ether)sulfone membranes through the avidin-biotin linkage. Journal of Membrane Science 119(2), 241-252.

Bhattacharyya, D., Butterfield, D.A., 2003. New Insights into Membrane Science and Technology: Polymeric and Biofunctional Membranes. [In: Membr. Sci. Technol. Ser., 2003; 8].

Blitz, J.P., Murthy, R.S.S., Leyden, D.E., 1987. Ammonia-catalyzed silylation reactions of Cab-O-Sil with methoxymethylsilanes. Journal of the American Chemical Society 109(23), 7141-7145.

Boi, C., Dimartino, S., Sarti, G.C., 2007. Modelling and simulation of affinity membrane adsorption. J. Chromatogr., A 1162(1), 24-33.

Bowen, W.R., Calvo, J.I., Hernandez, A., 1995. Steps of membrane blocking in flux decline during protein microfiltration. Journal of Membrane Science 101(1-2), 153-165.

Bowen, W.R., Gan, Q., 1991. Properties of microfiltration membranes: flux loss during constant pressure permeation of bovine serum albumin. Biotechnology and Bioengineering 38(7), 688-696.

Bradford, M.M., 1976. A rapid and sensitive method for the quantitation of microgram quantities of protein utilizing the principle of protein-dye binding. Analytical Biochemistry 72(1-2), 248-254.

Brandt, S., Goffe, R.A., Kessler, S.B., O'Connor, J.L., Zale, S.E., 1988. Membrane-based affinity technology for commercial scale purifications. Bio/Technology 6(7), 779-782.

Briefs, K.G., Kula, M.R., 1992. Fast protein chromatography on analytical and preparative scale using modified microporous membranes. Chemical Engineering Science 47(1), 141-149.

Bright, H.J., Appleby, M., 1969. pH dependence of the individual steps in the glucose oxidase reaction. Journal of Biological Chemistry 244(13), 3625-3634.

Brooks, H., Lebleu, B., Vives, E., 2005. Tat peptide-mediated cellular delivery: back to basics. Advanced Drug Delivery Reviews 57(4), 559-577.

Butterfield, D.A., Bhattacharyya, D., 2003. Biofunctional membranes: Site-specifically immobilized enzyme arrays. Membrane Science and Technology Series 8(New Insights into Membrane Science and Technology: Polymeric and Biofunctional Membranes, 2003), 233-240.

Butterfield, D.A., Bhattacharyya, D., Daunert, S., Bachas, L., 2001. Catalytic biofunctional membranes containing site-specifically immobilized enzyme arrays: a review. Journal of Membrane Science 181(1), 29-37.

Buxton, G.V., Greenstock, C.L., Helman, W.P., Ross, A.B., 1988. Critical review of rate constants for reactions of hydrated electrons, hydrogen atoms and hydroxyl radicals (.OH/.O-) in aqueous solution. Journal of Physical and Chemical Reference Data 17(2), 513-886.

Caron, N.J., Torrente, Y., Camirand, G., Bujold, M., Chapdelaine, P., Leriche, K., Bresolin, N., Tremblay, J.P., 2001. Intracellular delivery of a Tat-eGFP fusion protein into muscle cells. Molecular Therapy 3(3), 310-318.

Caruso, F., Caruso, R.A., Moehwald, H., 1998a. Nanoengineering of inorganic and hybrid hollow spheres by colloidal templating. Science (Washington, D. C.) 282(5391), 1111-1114.

Caruso, F., Caruso, R.A., Moehwald, H., 1999. Production of Hollow Microspheres from Nanostructured Composite Particles. Chemistry of Materials 11(11), 3309-3314.

Caruso, F., Furlong, D.N., Ariga, K., Ichinose, I., Kunitake, T., 1998b. Characterization of Polyelectrolyte-Protein Multilayer Films by Atomic Force Microscopy, Scanning Electron Microscopy, and Fourier Transform Infrared Reflection-Absorption Spectroscopy. Langmuir 14(16), 4559-4565.

Chaga, G.S., 2001. Twenty-five years of immobilized metal ion affinity chromatography: past, present and future. J. Biochem. Biophys. Methods 49(1-3), 313-334.

Champluvier, B., Kula, M.R., 1991. Microfiltration membranes as pseudo-affinity adsorbents: modification and comparison with gel beads. Journal of Chromatography 539(2), 315-325.

Chan, R., Chen, V., 2004. Characterization of protein fouling on membranes: opportunities and challenges. J. Membr. Sci. 242(1-2), 169-188.

Charcosset, C., 1998. Purification of proteins by membrane chromatography. Journal of Chemical Technology & Biotechnology 71(2), 95-110.

Chen, T.L., Weng, H.S., 1986. A method for the determinations of the activity and optimal pH of glucose oxidase in an unbuffered solution. Biotechnology and Bioengineering 28(1), 107-109.

Chen, W., McCarthy, T.J., 1997. Layer-by-Layer Deposition: A Tool for Polymer Surface Modification. Macromolecules 30(1), 78-86.

Cheryan M., M.M.A., 1986. Membrane Bioreactors. In: McGregor, W.C. (Ed.), Membrane separations in biotechnology, pp. 255-295. Marcel Dekker, New York.

Chun, K.-Y., Stroeve, P., 2001. External Control of Ion Transport in Nanoporous Membranes with Surfaces Modified with Self-Assembled Monolayers. Langmuir 17(17), 5271-5275.

Clapp, P.A., Evans, D.F., Sheriff, T.S.S., 1989. Spectrophotometric determination of hydrogen peroxide after extraction with ethyl acetate. Analytica Chimica Acta 218(2), 331-334.

Dai, J., Jensen, A.W., Mohanty, D.K., Erndt, J., Bruening, M.L., 2001. Controlling the Permeability of Multilayered Polyelectrolyte Films through Derivatization, Cross-Linking, and Hydrolysis. Langmuir 17(3), 931-937.

Datta, S., Bhattacharyya, D., Ray, P.D., Nath, A., Toborek, M., 2007. Effect of Pre-Filtration on Selective Isolation of Tat Protein by Affinity Membrane Separation: Analysis of Flux, Separation Efficiency, and Processing Time. Separation Science and Technology 42(11), 2451-2471.

Datta, S., Ray, P.D., Nath, A., Bhattacharyya, D., 2006. Recognition based separation of HIV-Tat protein using avidin-biotin interaction in modified microfiltration membranes. Journal of Membrane Science 280(1+2), 298-310.

De, A.K., Dutta, B.K., Bhattacharjee, S., 2006. Reaction kinetics for the degradation of phenol and chlorinated phenols using Fenton's reagent. Environmental Progress 25(1), 64-71.

de Mareuil, J., Carre, M., Barbier, P., Campbell, G.R., Lancelot, S., Opi, S., Esquieu, D., Watkins, J.D., Prevot, C., Braguer, D., Peyrot, V., Loret, E.P., 2005. HIV-1 Tat protein enhances microtubule polymerization. Retrovirology 2, No pp given.

Decher, G., 1997. Fuzzy nanoassemblies: toward layered polymeric multicomposites. Science (Washington, D. C.) 277(5330), 1232-1237.

Decher, G., Hong, J.D., 1991. Buildup of ultrathin multilayer films by a self-assembly process. 1. Consecutive adsorption of anionic and cationic bipolar amphiphiles on charged surfaces. Makromolekulare Chemie, Macromolecular Symposia 46(Eur. Conf. Organ. Org. Thin Films, 3rd, 1990), 321-327.

Decher, G., Lvov, Y., Schmitt, J., 1994. Proof of multilayer structural organization in self-assembled polycation-polyanion molecular films. Thin Solid Films 244(1-2), 772-777.

Degen, P.J., Martin, J.M., Schriefer, J.L., Shirley, B.W., 1986. Concentrating ligands and active membranes used therefor. p. 73 pp. (Pall Corp., USA). Application: EP

Dotzauer, D.M., Dai, J., Sun, L., Bruening, M.L., 2006. Catalytic Membranes Prepared Using Layer-by-Layer Adsorption of Polyelectrolyte/Metal Nanoparticle Films in Porous Supports. Nano Letters 6(10), 2268-2272.

Duke, F.R., Weibel, M., Page, D.S., Bulgrin, V.G., Luthy, J., 1969. Glucose oxidase mechanism. Enzyme activation by substrate. J. Amer. Chem. Soc. 91(14), 3904-3909.

Ekinci, O., Boyukbayram, A.E., Kiralp, S., Toppare, L., Yagci, Y., 2007. Characterization and Potential Applications of Immobilized Glucose Oxidase and Polyphenol Oxidase. Journal of Macromolecular Science, Part A: Pure and Applied Chemistry 44(8), 801-808.

Fausnaugh, J.L., Kennedy, L.A., Regnier, F.E., 1984a. Comparison of hydrophobic-interaction and reversed-phase chromatography of proteins. Journal of Chromatography 317, 141-155.

Fausnaugh, J.L., Pfannkoch, E., Gupta, S., Regnier, F.E., 1984b. High-performance hydrophobic interaction chromatography of proteins. Anal. Biochem. 137(2), 464-472.

Feins, M., Sirkar, K.K., 2004. Highly selective membranes in protein ultrafiltration. Biotechnology and Bioengineering 86(6), 603-611.

Fenton, H.J.H., 1894. Oxidation of tartaric acid in presence of iron. Journal of the Chemical Society, Transactions 65, 899-910.

Fery, A., Schoeler, B., Cassagneau, T., Caruso, F., 2001. Nanoporous Thin Films Formed by Salt-Induced Structural Changes in Multilayers of Poly(acrylic acid) and Poly(allylamine). Langmuir 17(13), 3779-3783.

Fisher, A.G., Feinberg, M.B., Josephs, S.F., Harper, M.E., Marselle, L.M., Reyes, G., Gonda, M.A., Aldovini, A., Debouk, C., Gallo, R.C., 1986. The trans-activator gene of HTLV-III is essential for virus replication. Nature 320(6060), 367-371.

Frankel, A.D., Pabo, C.O., 1988. Cellular uptake of the tat protein from human immunodeficiency virus. Cell 55(6), 1189-1193.

Frederick, K.R., Tung, J., Emerick, R.S., Masiarz, F.R., Chamberlain, S.H., Vasavada, A., Rosenberg, S., Chakraborty, S., Schopfer, L.M., Massey, V., 1990. Glucose oxidase from Aspergillus niger. Cloning, gene sequence, secretion from Saccharomyces cerevisiae and kinetic analysis of a yeast-derived enzyme [Erratum to document cited in CA113(7):53410s]. Journal of Biological Chemistry 265(19), 11405.

Gabriel, E.M., Gillberg, G.E., 1993. In situ modification of microporous membranes. Journal of Applied Polymer Science 48(12), 2081-2090.

Gallo, R.C., 1999. Tat as one key to HIV-induced immune pathogenesis and Pat toxoid as an important component of a vaccine. Proc. Natl. Acad. Sci. U. S. A. 96(15), 8324-8326.

Gibson, Q.H., Swoboda, B.E.P., Massey, V., 1964. Kinetics and mechanism of action of glucose oxidase. Journal of Biological Chemistry 239(11), 3927-3934.

Green, N.M., 1965. A spectrophotometric assay for avidin and biotin based on binding of dyes by avidin. Biochemical Journal 94(3), 23c-24c.

Green, N.M., 1975. Avidin. Advances in Protein Chemistry 29, 85-133.

Grimshaw, P.E., Grodzinsky, A.J., Yarmush, M.L., 1992. Dynamically controlling the transport of a molecule across a polyelectrolyte membrane for separations and drug delivery systems providing controlled drug delivery. pp. 24 pp Cont -in-part of U S Ser No 324,381. (Massachusetts Institute of Technology, USA). Application: US

Grubmuller, H., Heymann, B., Tavan, P., 1996. Ligand binding: molecular mechanics calculation of the streptavidin-biotin rupture force. Science (New York, N.Y.) 271(5251), 997-999.

Gsell, T.C., Salinaro, R.F., Degen, P.J., 1988. A chemically activated medium with low affinity for materials containing peptide groups. p. 17 pp. (Pall Corp., USA). Application: EP

Guo, W., Ruckenstein, E., 2003. Separation and purification of horseradish peroxidase by membrane affinity chromatography. J. Membr. Sci. 211(1), 101-111.

Haber, F., Weiss, J., 1934. The catalytic decomposition of hydrogen peroxide by iron salts. Proc. Roy. Soc. (London) A147, 332-351.

He, P., Hu, N., Rusling, J.F., 2004. Driving forces for layer-by-layer self-assembly of films of SiO2 nanoparticles and heme proteins. Langmuir 20(3), 722-729.

Hearn, M.T., 1987. 1,1'-Carbonyldiimidazole-mediated immobilization of enzymes and affinity ligands. Methods in enzymology 135, 102-117.

Hecht, H.J., Kalisz, H.M., Hendle, J., Schmid, R.D., Schomburg, D., 1993. Crystal structure of glucose oxidase from Aspergillus niger refined at 2.3 .ANG. resolution. Journal of Molecular Biology 229(1), 153-172.

Hendry, R.M., Herrmann, J.E., 1980. Immobilization of antibodies on nylon for use in enzyme-linked immunoassay. Journal of Immunological Methods 35(3-4), 285-296.

Hestekin, J.A., Bachas, L.G., Bhattacharyya, D., 2001. Poly(amino acid)-Functionalized Cellulosic Membranes: Metal Sorption Mechanisms and Results. Industrial & Engineering Chemistry Research 40(12), 2668-2678.

Hlavacek, M., Bouchet, F., 1993. Constant flowrate blocking laws and an example of their application to dead-end microfiltration of protein solutions. Journal of Membrane Science 82(3), 285-295.

Ho, C.-C., Zydney, A.L., 2000. A Combined Pore Blockage and Cake Filtration Model for Protein Fouling during Microfiltration. Journal of Colloid and Interface Science 232(2), 389-399.

Ho, C.-C., Zydney, A.L., 2006. Overview of fouling phenomena and modeling approaches for membrane bioreactors. Sep. Sci. Technol. 41(7), 1231-1251.

Ho, W., Sirkar, K.K. (Eds.), 1992. Membrane Handbook. van Nostrand Reinhold, New York.

Hollman, A.M., Bhattacharyya, D., 2002. Controlled permeability and ion exclusion in microporous membranes functionalized with poly(L-glutamic acid). Langmuir 18(15), 5946-5952.

Hollman, A.M., Bhattacharyya, D., 2004. Pore assembled multilayers of charged polypeptides in microporous membranes for ion separation. Langmuir 20(13), 5418-5424.

Hollman, A.M., Christian, D.A., Ray, P.D., Galey, D., Turchan, J., Nath, A., Bhattacharyya, D., 2005. Selective Isolation and Purification of Tat Protein via Affinity Membrane Separation. Biotechnology Progress 21(2), 451-459.

Hoshi, T., Sagae, N., Daikuhara, K., Takahara, K., Anzai, J.-i., 2007. Multilayer membranes via layer-by-layer deposition of glucose oxidase and Au nanoparticles on a Pt electrode for glucose sensing. Materials Science & Engineering, C: Biomimetic and Supramolecular Systems 27(4), 890-894.

Hou, K.C., Hou, C.J., Roy, S., Zaniewski, R., 1989. Immobilization of protein G on nylon membrane for the removal of IgG from human plasma. Polymeric Materials Science and Engineering 61, 670-674.

Hou, X., Liu, B., Deng, X., Zhang, B., Chen, H., Luo, R., 2007. Covalent immobilization of glucose oxidase onto poly(styrene-co-glycidyl methacrylate) monodisperse fluorescent microspheres synthesized by dispersion polymerization. Anal. Biochem. 368(1), 100-110.

Hout, M.S., Federspiel, W.J., 2003. Mathematical and Experimental Analyses of Antibody Transport in Hollow-Fiber-Based Specific Antibody Filters. Biotechnol. Prog. 19(5), 1553-1561.

Huston, P.L., Pignatello, J.J., 1999. Degradation of selected pesticide active ingredients and commercial formulations in water by the photo-assisted Fenton reaction. Water Research 33(5), 1238-1246.

Ichinose, I., Senzu, H., Kunitake, T., 1996. Stepwise adsorption of metal alkoxides on hydrolyzed surfaces: A surface sol-gel process. Chemistry Letters(10), 831-832.

Iler, R.K., Colloid, J., 1966. Multilayers of colloidal particles. Interface Sci. 21(6), 569-594.

Irvine, G.B., 1997. Size-exclusion high-performance liquid chromatography of peptides: a review. Analytica Chimica Acta 352(1-3), 387-397.

Iwata, H., Saito, K., Furusaki, S., Sugo, T., Okamoto, J., 1991. Adsorption characteristics of an immobilized metal affinity membrane. Biotechnol Prog 7(5), 412-418.

J.-L. Guesdon, T.T., Avrameas S., 1979. The use of avidin biotin interaction in immunoenzymatic techniques. Journal of Histochemistry and Cytochemistry 27, 1131-1139.

Jahraus, A., Tjelle, T.E., Berg, T., Habermann, A., Storrie, B., Ullrich, O., Griffiths, G., 1998. In vitro fusion of phagosomes with different endocytic organelles from J774 macrophages. J. Biol. Chem. 273(46), 30379-30390.

Jain, P., Sun, L., Dai, J., Baker, G.L., Bruening, M.L., 2007. High-Capacity Purification of His-tagged Proteins by Affinity Membranes Containing Functionalized Polymer Brushes. Biomacromolecules 8(10), 3102-3107.

Jeang, K.-T., Xiao, H., Rich, E.A., 1999. Multifaceted activities of the HIV-1 transactivator of transcription, Tat. J. Biol. Chem. 274(41), 28837-28840.

Jin W., T.A., Tieke B, 2003. Use of polyelectrolyte Layer-By-Layer assemblies as nanofiltration and reverse osmosis membranes. Langmuir 19, 2550-2553.

Johnson, K.A., Kroa, B.A., Yourey, T., 2002. Factors affecting reaction kinetics of glucose oxidase. Journal of Chemical Education 79(1), 74-76.

Kelly, S.T., Zydney, A.L., 1995. Mechanisms for BSA fouling during microfiltration. Journal of Membrane Science 107(1-2), 115-127.

Kesting, R.E., 1971. Synthetic Polymeric Membranes.

Khopade, A.J., Caruso, F., 2002. Investigation of the Factors Influencing the Formation of Dendrimer/Polyanion Multilayer Films. Langmuir 18(20), 7669-7676.

Klein, E., 1991. Affinity Membranes. Wiley, New York.

Klein, E., 2000. Affinity membranes: a 10-year review. Journal of Membrane Science 179(1-2), 1-27.

Klein, E., Silva, L.K., 1991. Hydrophilic semipermeable membranes based on copolymers of acrylonitrile and hydroxyalkyl (meth)acrylates. p. 7 pp. (USA). Application: US
US.

Ko, H., Jiang, C., Tsukruk, V.V., 2005. Encapsulating Nanoparticle Arrays into Layer-by-layer Multilayers by Capillary Transfer Lithography. Chemistry of Materials 17(22), 5489-5497.

Kotov, N.A., Dekany, I., Fendler, J.H., 1995. Layer-by-Layer Self-Assembly of Polyelectrolyte-Semiconductor Nanoparticle Composite Films. Journal of Physical Chemistry 99(35), 13065-13069.

Krasemann, L., Tieke, B., 1998. Ultrathin self-assembled polyelectrolyte membranes for pervaporation. Journal of Membrane Science 150(1), 23-30.

Krasemann, L., Toutianoush, A., Tieke, B., 2001. Self-assembled polyelectrolyte multilayer membranes with highly improved pervaporation separation of ethanol/water mixtures. J. Membr. Sci. 181(2), 221-228.

Krass, H., Papastavrou, G., Kurth, D.G., 2003. Layer-by-layer self-assembly of a polyelectrolyte bearing metal ion coordination and electrostatic functionality. Chem. Mater. 15(1), 196-203.

Kugel, K., Moseley, A., Harding, G.B., Klein, E., 1992. Microporous polycaprolactam hollow fibers for therapeutic affinity adsorption. J. Membr. Sci. 74(1-2), 115-129.

Ladhe, A.R., Radomyselski, A., Bhattacharyya, D., 2006. Ethoxylated Nonionic Surfactants in Hydrophobic Solvent: Interaction with Aqueous and Membrane-Immobilized Poly(acrylic acid). Langmuir 22(2), 615-621.

Lechtken, A., Zuendorf, I., Dingermann, T., Firla, B., Steinhilber, D., 2006. Overexpression, refolding, and purification of polyhistidine-tagged human retinoic acid related orphan receptor RORalpha 4. Protein Expression and Purification 49(1), 114-120.

Lehninger, A.L., 1977. Biochemistry. 2nd Ed.

Lensmeyer, G.L., Onsager, C., Carlson, I.H., Wiebe, D.A., 1995. Use of particle-loaded membranes to extract steroids for high-performance liquid chromatographic analyses. Improved analyte stability and detection. J. Chromatogr., A 691(1-2), 239-246.

Leskovac, V., Trivic, S., Wohlfahrt, G., Kandrac, J., Pericin, D., 2005. Glucose oxidase from Aspergillus niger: the mechanism of action with molecular oxygen, quinones, and one-electron acceptors. International Journal of Biochemistry & Cell Biology 37(4), 731-750.

Levison, P.R., 2003. Large-scale ion-exchange column chromatography of proteins. Comparison of different formats. J. Chromatogr., B: Anal. Technol. Biomed. Life Sci. 790(1-2), 17-33.

Lewin, M., Carlesso, N., Tung, C.H., Tang, X.W., Cory, D., Scadden, D.T., Weissleder, R., 2000. Tat peptide-derivatized magnetic nanoparticles allow in vivo tracking and recovery of progenitor cells. Nature biotechnology 18(4), 410-414.

Li, Y., Bachas, L.G., Bhattacharyya, D., 2007. Selected Chloro-Organic Detoxifications by Polychelate (Poly(acrylic acid)) and Citrate-Based Fenton Reaction at Neutral pH Environment. Ind. Eng. Chem. Res. 46(24), 7984-7992.

Li, Y.C., Bachas, L.G., Bhattacharyya, D., 2005. Kinetics Studies of Trichlorophenol Destruction by Chelate-Based Fenton Reaction. Environmental Engineering Science 22(6), 756-771.

Li, Z.F., Kang, E.T., Neoh, K.G., Tan, K.L., 1998. Covalent immobilization of glucose oxidase on the surface of polyaniline films graft copolymerized with acrylic acid. Biomaterials 19(1-3), 45-53.

Lingeman, H., Hoekstra-Oussoren, S.J., 1997. Particle-loaded membranes for sample concentration and/or clean-up in bioanalysis. Journal of chromatography. B, Biomedical sciences and applications 689(1), 221-237.

Liou, M.-J., Lu, M.-C., 2007. Catalytic degradation of nitroaromatic explosives with Fenton's reagent. Journal of Molecular Catalysis A: Chemical 277(1-2), 155-163.

Liu, J., Wang, J., Bachas, L.G., Bhattacharyya, D., 2001. Activity Studies of Immobilized Subtilisin on Functionalized Pure Cellulose-Based Membranes. Biotechnology Progress 17(5), 866-871.

Liu, X., Bruening, M.L., 2004. Size-selective transport of uncharged solutes through multilayer polyelectrolyte membranes. Chemistry of Materials 16(2), 351-357.

Liu, Y.-C., Suen, S.-Y., Huang, C.-W., ChangChien, C.-C., 2005. Effects of spacer arm on penicillin G acylase purification using immobilized metal affinity membranes. J. Membr. Sci. 251(1-2), 201-207.

Livnah, O., Bayer, E.A., Wilchek, M., Sussman, J.L., 1993. Three-dimensional structures of avidin and the avidin-biotin complex. Proc. Natl. Acad. Sci. U. S. A. 90(11), 5076-5080.

Loeb, S., Sourirajan, S., 1964. The preparation of high-flow semi-permeable membranes for separation of water from saline solutions. p. 9 pp. (University of California). Application: US

Lundberg, M., Holmgren, A., Johansson, M., 2006. Human glutaredoxin 2 affinity tag for recombinant peptide and protein purification. Protein Expr Purif FIELD Full Journal Title:Protein expression and purification 45(1), 37-42.

Lvov, Y., Ariga, K., Ichinose, I., Kunitake, T., 1995. Layer-by-layer architectures of concanavalin A by means of electrostatic and biospecific interactions. Journal of the Chemical Society, Chemical Communications(22), 2313-2314.

Lvov, Y., Haas, H., Decher, G., Moehwald, H., Mikhailov, A., Mtchedlishvily, B., Morgunova, E., Vainshtein, B., 1994. Successive Deposition of Alternate Layers of Polyelectrolytes and a Charged Virus. Langmuir 10(11), 4232-4236.

Ma, M., Nath, A., 1997. Molecular determinants for cellular uptake of Tat protein of human immunodeficiency virus type 1 in brain cells. Journal of Virology 71(3), 2495-2499.

Makkuni, A., Varma, R.S., Sikdar, S.K., Bhattacharyya, D., 2007. Vapor Phase Mercury Sorption by Organic Sulfide Modified Bimetallic Iron-Copper Nanoparticle Aggregates. Industrial & Engineering Chemistry Research 46(4), 1305-1315.

Malaisamy, R., Bruening, M.L., 2005. High-Flux Nanofiltration Membranes Prepared by Adsorption of Multilayer Polyelectrolyte Membranes on Polymeric Supports. Langmuir 21(23), 10587-10592.

Mandaro R. M., R.S., Hou K. C., 1987. Filtration supports for affinity separation. Bio/Technology 5, 928-932.

Marshal, A., Munro, P., Tragradh, G., 1993. The effect of protein fouling in microfiltration and ultrafiltration on permeate flux, protein retention and selectivity: A literature review. Desalination 91, 65-108.

Matsuno, H., Nagasaka, Y., Kurita, K., Serizawa, T., 2007. Superior Activities of Enzymes Physically Immobilized on Structurally Regular Poly(methyl methacrylate) Surfaces. Chem. Mater. 19(9), 2174-2179.

McGregor, W.C., Editor, 1986. Bioprocess Technology, Vol. 1: Membrane Separations in Biotechnology.

Mohr C. M., E.D.E., Leeper S. A., Charboneau B. L., 1989. Membrane Applications and Research in Food Processing. Noyes Data Corporation, Park Ridge, NJ, USA.

Mulder, M., 1991. Basic Principles of Membrane Technology Kluwer Academic Publishers, Netherlands.

Muller, D., 1928. Studies on the new enzyme glucoseoxidase. I. Biochemische Zeitschrift 199, 136-170.

Nagai, K., Thøgersen, H.C., 1984. Generation of Beta-globin by sequence-specific proteolysis of a hybrid protein produced in Escherichia coli. Nature 309, 810-812.

Nath, A., Chauhan, A., 2005. Neurology of AIDS. Oxford University Press, USA.

Nath, A., Geiger, J., 1998. Neurobiological aspects of human immunodeficiency virus infection: neurotoxic mechanisms. Progress in Neurobiology (Oxford) 54(1), 19-33.

Nguyen, Q.T., Ping, Z., Nguyen, T., Rigal, P., 2003. Simple method for immobilization of bio-macromolecules onto membranes of different types. J. Membr. Sci. 213(1-2), 85-95.

Nystrom, M., Aimar, P., Luque, S., Kulovaara, M., Metsamuuronen, S., 1998. Fractionation of model proteins using their physiochemical properties. Colloids and Surfaces, A: Physicochemical and Engineering Aspects 138(2-3), 185-205.

Onda, M., Lvov, Y., Ariga, K., Kunitake, T., 1996. Sequential reaction and product separation on molecular films of glucoamylase and glucose oxidase assembled on an ultrafilter. Journal of Fermentation and Bioengineering 82(5), 502-506.

Ozyilmaz, G., Tukel, S.S., Alptekin, O., 2005. Activity and storage stability of immobilized glucose oxidase onto magnesium silicate. Journal of Molecular Catalysis B: Enzymatic 35(4-6), 154-160.

Palacio, L., Ho, C.C., Pradanos, P., Hernandez, A., Zydney, A.L., 2003. Fouling with protein mixtures in microfiltration: BSA-lysozyme and BSA-pepsin. Journal of Membrane Science 222(1-2), 41-51.

Pandey, P., Singh, S.P., Arya, S.K., Gupta, V., Datta, M., Singh, S., Malhotra, B.D., 2007. Application of Thiolated Gold Nanoparticles for the Enhancement of Glucose Oxidase Activity. Langmuir 23(6), 3333-3337.

Parker, J.W., Schwartz, C.S., 1987. Modeling the kinetics of immobilized glucose oxidase. Biotechnology and Bioengineering 30(6), 724-735.

Pemawansa, K.P., 1993. Durable ultrafiltration membranes of polysulfones having optimized molecular weight. p. 10 pp. (Koch Membrane Systems, Inc., USA). Application: EP
EP.

Peterson, E.A., 1978. Ion-exchange displacement chromatography of serum proteins, using carboxymethyldextrans as displacers. Anal. Biochem. 90(2), 767-784.

Pignatello, J.J., Oliveros, E., MacKay, A., 2006. Advanced oxidation processes for organic contaminant destruction based on the Fenton reaction and related chemistry. Critical Reviews in Environmental Science and Technology 36(1), 1-84.

Piramowicz, M.d.O., Czuba, P., Targosz, M., Burda, K., Szymonski, M., 2006. Dynamic force measurements of avidin-biotin and streptavidin-biotin interactions using AFM. Acta Biochimica Polonica 53(1), 93-100.

Polyakov, V., Sharma, V., Dahlheimer, J.L., Pica, C.M., Luker, G.D., Piwnica-Worms, D., 2000. Novel Tat-peptide chelates for direct transduction of technetium-99m and rhenium into human cells for imaging and radiotherapy. Bioconjugate chemistry 11(6), 762-771.

Porath, J., Flodin, P., 1959. Gel filtration: a method for desalting and group separation. Nature (London, United Kingdom) 183, 1657-1659.

Prendergast, M.A., Rogers, D.T., Mulholland, P.J., Littleton, J.M., Wilkins, L.H., Self, R.L., Nath, A., 2002. Neurotoxic effects of the human immunodeficiency virus type-1 transcription factor Tat require function of a polyamine sensitive-site on the N-methyl-D-aspartate receptor. Brain Research 954(2), 300-307.

Ramratnam, B., Mittler, J.E., Zhang, L., Boden, D., Hurley, A., Fang, F., Macken, C.A., Perelson, A.S., Markowitz, M., Ho, D.D., 2000. The decay of the latent reservoir of replication-competent HIV-1 is inversely correlated with the extent of residual viral replication during prolonged anti-retroviral therapy. Nature Medicine (New York) 6(1), 82-85.

Rana, T.M., Jeang, K.-T., 1999. Biochemical and Functional Interactions between HIV-1 Tat Protein and TAR RNA. Archives of Biochemistry and Biophysics 365(2), 175-185.

Ratner, B.D., Hoffman, A.S., Schoen, F.J., Lemons, J.E., Editors, 2004. Biomaterials Science, An Introduction to Materials in Medicine, 2nd Edition.

Rauf, S., Ihsan, A., Akhtar, K., Ghauri, M.A., Rahman, M., Anwar, M.A., Khalid, A.M., 2006. Glucose oxidase immobilization on a novel cellulose acetate-polymethylmethacrylate membrane. Journal of biotechnology 121(3), 351-360.

Regnier, F.E., 1987a. Chromatography of complex protein mixtures. J Chromatogr 418, 115-143.

Regnier, F.E., 1987b. HPLC of biological macromolecules: the first decade. Chromatographia 24, 241-251.

Riggin, A., Regnier, F.E., Sportsman, J.R., 1991. Quantification of antibodies to human growth hormone by high-performance protein G affinity chromatography with fluorescence detection. Anal Chem 63(5), 468-474.

Ritchie, S.M.C., Bachas, L.G., Olin, T., Sikdar, S.K., Bhattacharyya, D., 1999. Surface Modification of Silica- and Cellulose-Based Microfiltration Membranes with Functional Polyamino Acids for Heavy Metal Sorption. Langmuir 15(19), 6346-6357.

Ritter, K., 1991a. Affinity purification of antibodies from sera using polyvinylidenedifluoride (PVDF) membranes as coupling matrices for antigens presented by autoantibodies to triosephosphate isomerase. J Immunol Methods 137(2), 209-215.

Ritter, K., 1991b. Affinity purification of antibodies from sera using polyvinylidenedifluoride (PVDF) membranes as coupling matrixes for antigens. Journal of Immunological Methods 137(2), 209-215.

Rivas, B.L., Jara, M., Pereira, E.D., 2003. Preparation and adsorption properties of the chelating resins containing carboxylic, sulfonic, and imidazole groups. Journal of Applied Polymer Science 89(10), 2852-2856.

Roper, D.K., Lightfoot, E.N., 1995. Separation of biomolecules using adsorptive membranes. J. Chromatogr., A 702(1 + 2), 3-26.

Ruan, G., Agrawal, A., Marcus, A.I., Nie, S., Imaging and Tracking of Tat Peptide-Conjugated Quantum Dots in Living Cells: New Insights into Nanoparticle Uptake, Intracellular Transport, and Vesicle Shedding. Journal of the American Chemical Society, ACS ASAP.

Ruben, S., Perkins, A., Purcell, R., Joung, K., Sia, R., Burghoff, R., Haseltine, W.A., Rosen, C.A., 1989. Structural and functional characterization of human immunodeficiency virus tat protein. J Virol FIELD Full Journal Title:Journal of virology 63(1), 1-8.

Ruckenstein, E., Guo, W., 2004. Cellulose and glass fiber affinity membranes for the chromatographic separation of biomolecules. Biotechnology Progress 20(1), 13-25.

Ruckenstein, E., Zeng, X., 1997. Macroporous chitin affinity membranes for lysozyme separation. Biotechnol. Bioeng. 56(6), 610-617.

Rusnati, M., Coltrini, D., Oreste, P., Zoppetti, G., Albini, A., Noonan, D., Di Fagagna, F.D.a., Giacca, M., Presta, M., 1997. Interaction of HIV-1 Tat protein with heparin. Role of the backbone structure, sulfation, and size. Journal of Biological Chemistry 272(17), 11313-11320.

Saksena, S., Zydney, A.L., 1994. Effect of solution pH and ionic strength on the separation of albumin from immunoglobulins (IgG) by selective filtration. Biotechnology and Bioengineering 43(10), 960-968.

Savage, M.D., 1992. Components of Avidin-Biotin Technology. Avidin-Biotin Chemistry. Pierce Chemical Co.

Schisla, D.K., Carr, P.W., Cussler, E.L., 1995. Hollow Fiber Array Affinity Chromatography. Biotechnol. Prog. 11(6), 651-658.

Schrick, B., Blough, J.L., Jones, A.D., Mallouk, T.E., 2002. Hydrodechlorination of Trichloroethylene to Hydrocarbons Using Bimetallic Nickel-Iron Nanoparticles. Chemistry of Materials 14(12), 5140-5147.

Schwarze, S.R., Ho, A., Vocero-Akbani, A., Dowdy, S.F., 1999. In vivo protein transduction: delivery of a biologically active protein into the mouse. Science (New York, N.Y.) 285(5433), 1569-1572.

Scott, K., 1995. Handbook of Industrial Membranes, First ed. Elsevier, Oxford, UK.

Shang, Z., Zhou, D., Guo, W., Yu, Y., Zhou, L., Pan, M., Zhou, K., 1998. Study on affinity membrane of polyamide used for endotoxin removal. I. Preparation and characterization of affinity membrane. Fenxi Ceshi Xuebao 17(1), 1-4.

Smuleac, V., Butterfield, D.A., Bhattacharyya, D., 2004. Permeability and separation characteristics of polypeptide-functionalized polycarbonate track-etched membranes. Chemistry of Materials 16(14), 2762-2771.

Smuleac, V., Butterfield, D.A., Bhattacharyya, D., 2006. Layer-by-Layer-Assembled Microfiltration Membranes for Biomolecule Immobilization and Enzymatic Catalysis. Langmuir 22(24), 10118-10124.

Smuleac, V., Butterfield, D.A., Sikdar, S.K., Varma, R.S., Bhattacharyya, D., 2005. Polythiol-functionalized alumina membranes for mercury capture. J. Membr. Sci. 251(1-2), 169-178.

Stauber, R.H., Pavlakis, G.N., 1998. Intracellular trafficking and interactions of the HIV-1 Tat protein. Virology 252(1), 126-136.

Stoellner, D., Scheller, F.W., Warsinke, A., 2002. Activation of cellulose membranes with 1,1'-carbonyldiimidazole or 1-cyano-4-dimethylaminopyridinium tetrafluoroborate as a basis for the development of immunosensors. Analytical Biochemistry 304(2), 157-165.

Su, X., Zong, Y., Richter, R., Knoll, W., 2005. Enzyme immobilization on poly(ethylene-co-acrylic acid) films studied by quartz crystal microbalance with dissipation monitoring. Journal of Colloid and Interface Science 287(1), 35-42.

Suen, S.-Y., Lin, S.-Y., Chiu, H.-C., 2000. Effects of spacer arms on Cibacron Blue 3GA immobilization and lysozyme adsorption using regenerated cellulose membrane discs. Ind. Eng. Chem. Res. 39(2), 478-487.

Suen, S.-Y., Liu, Y.-C., Chang, C.-S., 2003. Exploiting immobilized metal affinity membranes for the isolation or purification of therapeutically relevant species. J. Chromatogr., B: Anal. Technol. Biomed. Life Sci. 797(1-2), 305-319.

Suen, S.Y., Etzel, M.R., 1992. A mathematical analysis of affinity membrane bioseparations. Chemical Engineering Science 47(6), 1355-1364.

Suki, A., Fane, A.G., Fell, C.J.D., 1984. Flux decline in protein ultrafiltration. Journal of Membrane Science 21(3), 269-283.

T. Hoshi, J.-I.A., T. Osa, 1995. Controlled deposition of glucose oxidase on platinum electrode based on an avidin/biotin system for the regulation of output current of glucose sensors. Anal. Chem. 63.

Tang, T., Qu, J., Muellen, K., Webber, S.E., 2006. Molecular Layer-by-Layer Self-Assembly of Water-Soluble Perylene Diimides through p-p and Electrostatic Interactions. Langmuir 22(1), 26-28.

Tarvainen, T., Nevalainen, T., Sundell, A., Svarfvar, B., Hyrsyla, J., Paronen, P., Jarvinen, K., 2000. Drug release from poly(acrylic acid) grafted poly(vinylidene fluoride) membrane bags in the gastrointestinal tract in the rat and dog. Journal of Controlled Release 66(1), 19-26.

Tedeschi, C., Caruso, F., Moehwald, H., Kirstein, S., 2000. Adsorption and desorption behavior of an anionic pyrene chromophore in sequentially deposited polyelectrolyte-dye thin films. Journal of the American Chemical Society 122(24), 5841-5848.

Thoemmes, J., Kula, M.R., 1995. Membrane chromatography - an integrative concept in the downstream processing of proteins. Biotechnology Progress 11(4), 357-367.

Tomotani, E.J., Vitolo, M., 2007. Immobilized glucose oxidase as a catalyst to the conversion of glucose into gluconic acid using a membrane reactor. Enzyme and Microbial Technology 40(5), 1020-1025.

Torchilin, V.P., Rammohan, R., Weissig, V., Levchenko, T.S., 2001. TAT peptide on the surface of liposomes affords their efficient intracellular delivery even at low temperature and in the presence of metabolic inhibitors. Proc. Natl. Acad. Sci. U. S. A. 98(15), 8786-8791.

Torres, A.R., Peterson, E.A., 1990. Purification of monoclonal antibodies by complex-displacement chromatography on CM-cellulose. J Chromatogr 499, 47-54.

Toutianoush, A., Jin, W., Deligoez, H., Tieke, B., 2005. Polyelectrolyte multilayer membranes for desalination of aqueous salt solutions and seawater under reverse osmosis conditions. Applied Surface Science 246(4), 437-443.

Tracy, E., Davis, R., 1994. Protein fouling of track-etched polycarbonate microfiltration membranes. J. Colloid Interface Sci 167, 104-116.

Trau, D., Renneberg, R., 2003. Encapsulation of glucose oxidase microparticles within a nanoscale layer-by-layer film: immobilization and biosensor applications. Biosens. Bioelectron. 18(12), 1491-1499.

Ulbricht, M., Riedel, M., 1998. Ultrafiltration membrane surfaces with grafted polymer 'tentacles': preparation, characterization and application for covalent protein binding. Biomaterials 19(14), 1229-1237.

Ulbricht, M., Yang, H., 2005. Porous Polypropylene Membranes with Different Carboxyl Polymer Brush Layers for Reversible Protein Binding via Surface-Initiated Graft Copolymerization. Chemistry of Materials 17(10), 2622-2631.

Urmenyi, A.M., Poot, A.A., Wessling, M., Mulder, M.H.V., 2005. Affinity membranes for hormone removal from aqueous solutions. Journal of Membrane Science 259(1-2), 91-102.

van Eijndhoven, R.H.C.M., Saksena, S., Zydney, A.L., 1995. Protein fractionation using electrostatic interactions in membrane filtration. Biotechnology and Bioengineering 48(4), 406-414.

Varilova, T., Madera, M., Pacakova, V., Stulik, K., 2006. Separation media in affinity chromatography of proteins - a critical review. Current Proteomics 3(1), 55-79.

Velasco, C., Ouammou, M., Calvo, J.I., Hernandez, A., 2003. Protein fouling in microfiltration: deposition mechanism as a function of pressure for different pH. Journal of Colloid and Interface Science 266(1), 148-152.

Voet, D., Pratt, C.W., Voet, J.G., 2004. Fundamentals of Biochemistry, Take Note!, 2nd Edition.

Wadia, J.S., Dowdy, S.F., 2003. Modulation of cellular function by TAT mediated transduction of full length proteins. Current Protein and Peptide Science 4(2), 97-104.

Wadia, J.S., Dowdy, S.F., 2005. Transmembrane delivery of protein and peptide drugs by TAT-mediated transduction in the treatment of cancer. Advanced Drug Delivery Reviews 57(4), 579-596.

Watts, R.J., Udell, M.D., Rauch, P.A., 1990. Treatment of pentachlorophenol-contaminated soils using Fenton's reagent. Hazardous Waste & Hazardous Materials 7(4), 335-345.

Weibel, M.K., Bright, H.J., 1971. Glucose oxidase mechanism. Interpretation of the pH dependence. Journal of Biological Chemistry 246(9), 2734-2744.

Whitaker, J.R., 1994. Principles of Enzymology for the Food Sciences, Second Edition. [In: Food Sci. Technol. (N. Y.), 1994; 61].

Wolpert, S., 1997. Aldehyde activated microporous membranes. J. Membr. Sci. 132(1), 23-32.

Wong, D., Editor, 1995. Food Enzymes: Structure and Mechanism.

Woodward, J., Editor, 1985. Immobilized Cells and Enzymes. A Practical Approach.

Xu, J., Bhattacharyya, D., 2007. Fe/Pd Nanoparticle Immobilization in Microfiltration Membrane Pores: Synthesis, Characterization, and Application in the Dechlorination of Polychlorinated Biphenyls. Ind. Eng. Chem. Res. 46(8), 2348-2359.

Xu, J., Dozier, A., Bhattacharyya, D., 2005. Synthesis of Nanoscale Bimetallic Particles in Polyelectrolyte Membrane Matrix for Reductive Transformation of Halogenated Organic Compounds. Journal of Nanoparticle Research 7(4-5), 449-467.

Yang, H., Viera, C., Fischer, J., Etzel, M.R., 2002. Purification of a large protein using ion-exchange membranes. Industrial & Engineering Chemistry Research 41(6), 1597-1602.

Ying, L., Kang, E.T., Neoh, K.G., 2002. Covalent immobilization of glucose oxidase on microporous membranes prepared from poly(vinylidene fluoride) with grafted poly(acrylic acid) side chains. J. Membr. Sci. 208(1-2), 361-374.

Zeman, L.J., 1983. Adsorption effects in rejection of macromolecules by ultrafiltration membranes. Journal of Membrane Science 15, 213-230.

Zeng, X., Ruckenstein, E., 1998. Crosslinked macroporous chitosan anion-exchange membranes for protein separations. J. Membr. Sci. 148(2), 195-205.

Zeng, X., Ruckenstein, E., 1999. Membrane Chromatography: Preparation and Applications to Protein Separation. Biotechnol. Prog. 15(6), 1003-1019.

Zhang, H., Zhou, Z., Yang, B., Gao, M., 2003. The Influence of Carboxyl Groups on the Photoluminescence of Mercaptocarboxylic Acid-Stabilized CdTe Nanoparticles. Journal of Physical Chemistry B 107(1), 8-13.

Zhao, H., Ju, H., 2006. Multilayer membranes for glucose biosensing via layer-by-layer assembly of multiwall carbon nanotubes and glucose oxidase. Analytical Biochemistry 350(1), 138-144.

Zheng Liu, M.D.A., 2004. FT-IRRAS spectroscopic studies of the interaction of avidin with biotinylated dendrimer surfaces. Colloids and Surfaces B: Biointerfaces 35, 197-203.
Zhou, X., Arnold, M.A., 1995. Internal enzyme fiber-optic biosensors for hydrogen peroxide and glucose. Analytica Chimica Acta 304(2), 147-156.

Zorko, M., Langel, U., 2005. Cell-penetrating peptides: mechanism and kinetics of cargo delivery. Advanced Drug Delivery Reviews 57(4), 529-545.

Zou, H., Luo, Q., Zhou, D., 2001. Affinity membrane chromatography for the analysis and purification of proteins. Journal of Biochemical and Biophysical Methods 49(1-3), 199-240.

Vita

Saurav Datta was born on 19th of April, 1976 in Calcutta, India. He has received his Bachelor of Science degree in Chemistry and Bachelor of Technology degree in Chemical Engineering from University of Calcutta, India in 1997 and 2000, respectively. After that he has pursued in education and obtained Masters of Technology in Chemical Engineering from Indian Institute of Technology, Kanpur, India in 2002. Then, he has continued his career in Indian Institute of Technology, Kanpur as Research Associate till 2003. Then, He has joined Department of Chemical Engineering, University of Kentucky for PhD curriculum.

Awards:

- One of the five recipients of Schering Plough Corporation Research Travel Award for presenting in AIChE 2006
- Recipient of North American Membrane Society Research Travel Award , 2005
- Honorary mention in the 2005 AIChE Separation Division Graduate Student Award in the area of Membranes
- Ranked among the top 15 and received Indian National Merit Scholarship for excellent performance in Bachelor of Science Examination in 1997

Publications:

- **S. Datta**, C. Cecil, D. Bhattacharyya, Enzymatic Production of H_2O_2 with Glucose Oxidase Immobilized in Functionalized Membranes Created by Layer-By-Layer Attachment of Polyelectrolytes and In-Situ Polymerization of Acrylic Acid, to be submitted to the Special centennial issue of *I&EC Res.*
- **S. Datta**, Philip D. Ray, A. Nath, D. Bhattacharyya, Selective separation of HIV-Tat protein using functionalized stacked microfiltration membranes: Enhancement of flux and recovery of protein, Separation Science and Technology 42 (2007) 2451-2471

- **S. Datta**, Philip D. Ray, A. Nath, D. Bhattacharyya, Recognition based separation of HIV-Tat protein using avidin-biotin interaction in modified microfiltration membranes, Journal of Membrane Science 280 (2006) 298-310
- **S. Datta**, P. K. Bhattacharya, N. Verma, Removal of aniline from aqueous solution in a MFR using emulsion liquid membrane, Journal of Membrane Science 226 (2003) 185-201

Presentations:

- **S. Datta**, D. Bhattacharyya, Affinity Based Separation of Proteins using Functionalized Microfiltration Membranes, 2007 Annual Meeting of American Institute of Chemical Engineers, Salt Lake City, UT
- **S. Datta**, D. Bhattacharyya, Functionalized Microfiltration Membranes for Bio-Catalysis and Bio-Separations, 2007 Annual Meeting of American Institute of Chemical Engineers, Salt Lake City, UT
- **S. Datta**, A. Nath, D. Bhattacharyya, Separation and purification of a target protein from mixture of proteins using different membrane separation processes in series, Oral presentation in 2007 Annual Meeting of North American Membrane Society (NAMS), Orlando, FL
- **S. Datta**, D. Bhattacharyya, Development and Applications of Functionalized Microfiltration Membranes, Poster presentation in 2007 Annual Meeting of North American Membrane Society (NAMS), Orlando, FL
- **S. Datta**, P. D. Ray, A. Nath, D. Bhattacharyya, Selective separation of HIV-Tat protein using functionalized microfiltration membranes, Oral presentation in 2006 Annual Meeting of American Institute of Chemical Engineers (AIChE), San Francisco, CA
- **S. Datta**, P. D. Ray, A. Nath, D. Bhattacharyya, Selective separation of high value proteins by functionalized microfiltration membranes, Poster presentation in 2006 Annual Meeting of North American Membrane Society (NAMS), Chicago, IL

- **D. Bhattacharyya,** S. Datta, P. D. Ray, A. Hollman, A. Nath, Selective Isolation and Purification of Genetically Modified Tat Protein by Stacked Affinity Membrane System, Poster presentation in Experimental Biology 2006, San Francisco, CA
- **S. Datta,** P. D. Ray, A. Nath, D. Bhattacharyya, Recognition Based Separation of Proteins Using Avidin-Biotin Interaction in MF Membranes, Oral presentation in 2005 Eastern Regional Chemical Engineering Graduate Symposium organized by University of West Virginia, Morgantown, WV
- **S. Datta**, P. D. Ray, A. Nath, D. Bhattacharyya, Recognition based separation of proteins using avidin-biotin interaction in modified stacked microfiltration membranes, Oral presentation in 2005 Annual Meeting of North American Membrane Society, Providence, RI
- **S. Datta**, A. Nath, D. Bhattacharyya, Recognition based separation of biotinylated-protein using surface modified microfiltration membranes, Poster presentation in 2004 Annual Meeting of American Institute of Chemical Engineers, Austin, TX